

October 2012

Revision 12A

MAGNATRAN

(Modular Advanced Generation
Nuclear All-purpose TRANsport)

MAGNATRAN Submittal

Book 1 of 2

NONPROPRIETARY VERSION

Docket No. 71-9356



November 26, 2012

U.S. Nuclear Regulatory Commission
11555 Rockville Pike
Rockville, MD 20852-2738

Attn: Document Control Desk

Subject: Resubmission of an Application for a NRC Certificate of Compliance (CoC) for the NAC MAGNATRAN Transport Cask

Docket No. 71-9356

- References:
1. Safety Analysis Report for the MAGNATRAN Transport Cask, Revision A10, NAC International, December 2010
 2. Safety Analysis Report for the MAGNATRAN Transport Cask, Revision 12A, NAC International, October 2012
 3. U.S. Nuclear Regulatory Commission (NRC) Certificate of Compliance (CoC) No. 1031 for the NAC International MAGNASTOR Cask System, Amendment No. 2, January 30, 2012
 4. Final Safety Analysis Report (FSAR) for the NAC MAGNASTOR Cask System, Revision 2, NAC International, April 2012
 5. Submission of an Application for the NRC Certificate of Compliance (CoC) for the NAC MAGNATRAN Transport Cask, NAC International, January 19, 2011
 6. Application for the Model No. MAGNATRAN Transport Cask – Supplemental Information Needed, U.S. NRC, April 1, 2011

NAC International (NAC) has developed a transportation cask system for the loaded MAGNASTOR[®] (References 3 and 4) Transportable Storage Canisters (TSCs). The transportation cask system is designated with the model name MAGNATRAN. After submission to the NRC for certification (References 1 and 5), the NRC requested NAC provide supplemental information (Reference 6) prior to accepting the application for technical review. NAC has addressed all Requests for Supplemental Information (RSIs) and General Observations (GOs). All responses and a complete Safety Analysis Report (Reference 2) are enclosed with this letter.

NAC hereby applies for a NRC Certificate of Compliance (CoC) for the MAGNATRAN Transport Cask under the provisions of the Code of Federal Regulations, 10 CFR 71. The package identification requested is USA/9356/B(U)F-96.

US Nuclear Regulatory Commission
November 26, 2012
Page 2 of 4

Reference 2 demonstrates that the MAGNATRAN Transport Cask satisfies all applicable requirements of the Code of Federal Regulations, 10 CFR 71. Reference 2 has been formatted in accordance with the requirements of NRC Regulatory Guide 7.9, Revision 2 and the Standard Review Plan for Transportation Packages for Spent Fuel, NUREG-1617.

The MAGNATRAN Transport Cask is designed to safely transport a TSC containing up to 37 undamaged PWR fuel assemblies in a 37 PWR basket assembly, or up to 87 undamaged BWR fuel assemblies in a 87 BWR basket assembly. The cask is also designed to transport up to four damaged fuel cans (DFC) in the DF Basket Assembly that has four enlarged fuel cells, each of which accommodates a DFC.

The DF Basket Assembly has a capacity of up to 37 undamaged PWR fuel assemblies, including the four DFC locations. Undamaged PWR fuel assemblies may be placed directly into any of the four damaged fuel cells. The MAGNATRAN Transport Cask is also designed to transport a GTCC TSC containing up to 32,000 pounds of Greater than Class C (GTCC) waste in a GTCC waste basket liner.

Primarily based on their lengths, two categories of PWR fuel assemblies and two categories of BWR fuel assemblies have been evaluated for transport. Two lengths of TSCs (long and short) are designed to transport the two categories of PWR and BWR fuel assemblies. The short TSC is also designed to transport damaged fuel in the DF Basket Assembly and GTCC waste. A spacer is used in the MAGNATRAN Transport Cask cavity to axially position the short TSC and limit its potential movement during cask handling and transport.

The principal components of the MAGNATRAN Transport Cask are:

- Transportable Storage Canister
- Transport Cask
- Impact Limiters

US Nuclear Regulatory Commission
November 26, 2012
Page 3 of 4

The MAGNATRAN Transport Cask is described in detail (including materials of construction, design characteristics and authorized contents) and is depicted on the license drawings contained in Chapter 1 of Reference 2 as required by 10 CFR 71.33. Package evaluation is presented in Chapters 2 through 6 per the requirements of 10 CFR 71.35. Chapter 2 of Reference 2 contains the structural evaluation of the MAGNATRAN Transport Cask. Chapters 3 and 4 contain the thermal and containment evaluations, respectively. In Chapters 5 and 6, the shielding and nuclear criticality evaluations are presented. Chapters 7 and 8 contain the package operations and acceptance tests and maintenance program, respectively. In accordance with the requirements of 10 CFR 71.37(a), the NRC-approved NAC International Inc. Quality Assurance Program has been applied to the design and analysis of the MAGNATRAN packaging.

This application package is presented as a full nonproprietary and full proprietary version. The proprietary information described within the affidavit subsequent to this letter, pursuant to 10 CFR 2.390, duly executed by Mr. George Carver, Vice President, Engineering, is provided in a separate sealed package marked "NAC PROPRIETARY INFORMATION." The nonproprietary version of this application package clearly identifies every page where proprietary information has been removed. Each page of the proprietary version is clearly identified as "NAC PROPRIETARY INFORMATION" at the top of the page.

This submittal consists of one hard copy of the nonproprietary and the proprietary versions of this application package, including this cover letter and proprietary affidavit in accordance with 10 CFR 2.390. Enclosed within this package are the proprietary calculations, data input and output files supporting the structural, thermal, shielding and nuclear criticality analyses described in Reference 2. The following is the enclosure structure of the proprietary and nonproprietary packages.

Nonproprietary Package

Submittal¹ Book 1 of 2

- MAGNATRAN Submittal Cover Letter and Affidavit
- Enclosure 1 – RSI Responses
- Enclosure 2 – RSI GO Responses
- Enclosure 3 – RSI and GO Supporting Documents
- Enclosure 4 – Calculations

Submittal Book 2 of 2

- Enclosure 5 – MAGNATRAN SAR Revision 12A

¹ Individual binders associated with the submittal package are referred to as "books" herein.

US Nuclear Regulatory Commission
November 26, 2012
Page 4 of 4

Proprietary Package

Submittal Book 1 of 4

MAGNATRAN Submittal Cover Letter and Affidavit
Enclosure 1 – RSI Responses
Enclosure 2 – RSI GO Responses
Enclosure 3 – RSI and GO Supporting Documents

Submittal Books 2 & 3 of 4

Enclosure 4 – Calculations

Submittal Book 4 of 4


Enclosure 5 – MAGNATRAN SAR Revision 12A

NAC requests that a post-submission presentation meeting be scheduled shortly after the NRC technical review team has been assembled for the MAGNATRAN application. Due to the proprietary nature of part of the application, NAC will request a portion of the post-submission meeting be closed to the public. A separate request for scheduling the public/closed meeting, including appropriate agenda, presentation slides and proprietary affidavit, will be provided in a prompt manner. A draft CoC will be provided to the NRC by March 1, 2013 to support CoC development by the SFST review team.

NAC is submitting this application for the approval of the MAGNATRAN Transport Cask in support of ongoing and anticipated MAGNASTOR storage projects and is requesting that the NRC apply the Focused Review Process for the technical review. Since the MAGNATRAN Transport Cask configuration is similar to another currently licensed NAC transport cask system (i.e., NAC-STC – Docket No. 71-9235), and since all the analytical methods used in the development of the application represent previously accepted methods used in similar applications, NAC hereby requests the NRC to target issuing of a CoC for the MAGNATRAN Transport Cask by December 31, 2013.

If there are any questions and/or comments regarding this application, please contact me on my direct line at 678-328-1274.

Sincerely,

 For
T. Patko

Anthony L Patko
Director, Licensing
Engineering

Enclosures

George Carver (Affiant), Vice President, Engineering, of NAC International, hereinafter referred to as NAC, at 3930 East Jones Bridge Road, Norcross, Georgia 30092, being duly sworn, deposes and says that:

1. Affiant has reviewed the information described in Item 2 and is personally familiar with the trade secrets and privileged information contained therein, and is authorized to request its withholding.
2. The information to be withheld includes the following NAC Proprietary Information that is being provided to support the technical review of NAC's Request for a Certificate of Compliance (CoC) (No. 9356) for the NAC International MAGNATRAN Transport Cask.
 - MAGNATRAN RSI 3-1 - NAC Response
 - MAGNATRAN GO 3-6 - NAC Response Supporting Documents
 - NAC Proprietary Calculations
 - Calculation No. 71160-2007, Structural Evaluation of the Neutron Absorber Retainer, Revision 3, (Data Disk 1 of 1)
 - Calculation No. 71160-2035, Structural Evaluation of PWR Fuel Assembly Spacer for Transportation, Revision 2, (Data Disk 1 of 1)
 - Calculation No. 71160-2101, Structural and Thermal Material Properties – MAGNASTOR/MAGNATRAN Cask System, Revision 6, (Data Disk 1 of 1)
 - Calculation No. 71160-2108, Transport Cask Structural Evaluation, Revision 2, (Data Disk 1 of 1)
 - Calculation No. 71160-2110, MAGNATRAN Transport Cask Lifting Trunnion Structural Analysis, Revision 1, (Data Disk 1 of 1)
 - Calculation No. 71160-2113, Transport Cask Neutron Shielding Structural Evaluation, Revision 2, (Data Disk 1 of 1)
 - Calculation No. 71160-2116, Structural Evaluation of MAGNATRAN Canister, Revision 1, (Data Disk 1 of 1)
 - Calculation No. 71160-2117, PWR Basket Structural Evaluation – Transport, Revision 1, (Data Disk 1 thru 5 of 5)
 - Calculation No. 71160-2118, BWR Basket Structural Evaluation – Transport, Revision 1, (Data Disk 1 thru 7 of 7)
 - Calculation No. 71160-2119, BWR Basket Stability Evaluation – Transport, Revision 1, (Data Disk 1 thru 4 of 4)
 - Calculation No. 71160-2120, Canister Spacer Structural Evaluation – Transport, Revision 1, (Data Disk 1 of 1)
 - Calculation No. 71160-2126, Fuel Rod Accident Evaluation, Revision 1, (Data Disk 1 of 1)
 - Calculation No. 71160-2127, PWR DFC Basket Structural Evaluation – Transport, Revision 1, (Data Disk 1 thru 4 of 4)
 - Calculation No. 71160-2132, Structural Evaluation of MAGNATRAN TSC3 and TSC4, Revision 1, (Data Disk 1 of 1)
 - Calculation No. 71160-2138, MAGNATRAN Balsa-Redwood Impact Limiter Free Drop Structural Evaluation, Revision 3, (Data Disk 1 thru 6 of 6)

- Calculation No. 71160-2145, PWR Basket Stability Evaluation – Transport, Revision 5, (Data Disk 1 thru 5 of 5)
- Calculation No. 71160-2155, BWR Fuel Assembly Impact Calculation, Revision 0, (Data Disk 1 of 1)
- Calculation No. 71160-3011, Effective Property Calculation of PWR/BWR Fuel Assembly and Poison Plate for Transport Condition of the NAC MAGNATRAN System, Revision 0, (Data Disk 1 of 1)
- Calculation No. 71160-3013, Thermal Evaluation of MAGNATRAN Transport Cask/BWR Canister, Revision 0, (Data Disk 1 of 1)
- Calculation No. 71160-3014, Thermal Evaluation of NEWGEN Transport Cask/PWR Canister, Revision 2, (Data Disk 1 of 1)
- Calculation No. 71160-3015, MAGNATRAN PWR/BWR Cask/Basket Hypothetical Fire Accident Analyses, Revision 1, (Data Disk 1 of 1)
- Calculation No. 71160-3045, Evaluation of the Convection Film Coefficient for the MAGNATRAN Cask Surface, Revision 0, (Data Disk 1 of 1)
- Calculation No. 630073-2140, Structural Evaluation of MAGNATRAN GTCC TSC, Revision 2, (Data Disk 1 thru 3 of 3)
- MAGNATRAN Shielding Sample Data Files, (Data Disk 1 of 1)
- MAGNATRAN Criticality Sample Data Files, (Data Disk 1 of 1)
- MAGNATRAN SAR, Revision 12A, – Proprietary Version, including:
- NAC International Proprietary License Drawings
 - 71160-500, Revision 3P - Shipping Configuration, Transport Cask, MAGNATRAN
 - 71160-502, Revision 2P - Transport Cask Body, MAGNATRAN
 - 71160-505, Revision 3P - Lid Assembly, Transport Cask, MAGNATRAN
 - 71160-531, Revision 1P - Impact Limiter, Transport Cask, MAGNATRAN
 - 71160-551, Revision 10P - Fuel Tube Assembly, MAGNASTOR – 37 PWR
 - 71160-575, Revision 11P - Basket Assembly, MAGNASTOR – 37 PWR
 - 71160-591, Revision 6P - Fuel Tube Assembly, MAGNASTOR – 87 BWR
 - 71160-598, Revision 5P - Basket Support Weldments, MAGNASTOR – 87 BWR
 - 71160-599, Revision 6P - Basket Assembly, MAGNASTOR – 87 BWR
 - 71160-600, Revision 4P - Basket Assembly, MAGNASTOR – 82 BWR
 - 71160-620, Revision 1P - Top Fuel Spacer, MAGNASTOR
 - 71160-674, Revision 3P - DF Corner Weldment, MAGNASTOR
 - 71160-675, Revision 3P - DF Basket Assembly, 37 Assembly PWR, MAGNASTOR

NAC is the owner of the information contained in the above documents. Thus, all of the above identified information is considered NAC Proprietary Information.

3. NAC makes this application for withholding of proprietary information based upon the exemption from disclosure set forth in: the Freedom of Information Act (“FOIA”); 5 USC Sec. 552(b)(4) and the Trade Secrets Act; 18 USC Sec. 1905; and NRC Regulations 10 CFR Part 9.17(a)(4), 2.390(a)(4), and 2.390(b)(1) for “trade secrets and commercial financial information obtained from a person, and privileged or confidential” (Exemption 4). The information for which exemption from disclosure is herein sought is all “confidential commercial information,” and some portions may also qualify under

the narrower definition of “trade secret,” within the meanings assigned to those terms for purposes of FOIA Exemption 4.

4. Examples of categories of information that fit into the definition of proprietary information are:
 - a. Information that discloses a process, method, or apparatus, including supporting data and analyses, where prevention of its use by competitors of NAC, without license from NAC, constitutes a competitive economic advantage over other companies.
 - b. Information that, if used by a competitor, would reduce their expenditure of resources or improve their competitive position in the design, manufacture, shipment, installation, assurance of quality or licensing of a similar product.
 - c. Information that reveals cost or price information, production capacities, budget levels or commercial strategies of NAC, its customers, or its suppliers.
 - d. Information that reveals aspects of past, present or future NAC customer-funded development plans and programs of potential commercial value to NAC.
 - e. Information that discloses patentable subject matter for which it may be desirable to obtain patent protection.

The information that is sought to be withheld is considered to be proprietary for the reasons set forth in Items 4.a, 4.b, and 4.d.

5. The information to be withheld is being transmitted to the NRC in confidence.
6. The information sought to be withheld, including that compiled from many sources, is of a sort customarily held in confidence by NAC, and is, in fact, so held. This information has, to the best of my knowledge and belief, consistently been held in confidence by NAC. No public disclosure has been made, and it is not available in public sources. All disclosures to third parties, including any required transmittals to the NRC, have been made, or must be made, pursuant to regulatory provisions or proprietary agreements, which provide for maintenance of the information in confidence. Its initial designation as proprietary information and the subsequent steps taken to prevent its unauthorized disclosure are as set forth in Items 7 and 8 following.
7. Initial approval of proprietary treatment of a document/information is made by the Vice President, Engineering, the Project Manager, the Licensing Specialist, or the Director, Licensing – the persons most likely to know the value and sensitivity of the information in relation to industry knowledge. Access to proprietary documents within NAC is limited via “controlled distribution” to individuals on a “need to know” basis. The procedure for external release of NAC proprietary documents typically requires the approval of the Project Manager based on a review of the documents for technical content, competitive effect and accuracy of the proprietary designation. Disclosures of proprietary documents outside of NAC are limited to regulatory agencies, customers and potential customers and their agents, suppliers, licensees and contractors with a legitimate need for the information, and then only in accordance with appropriate regulatory provisions or proprietary agreements.
8. NAC has invested a significant amount of time and money in the research, development, engineering and analytical costs to develop the information that is sought to be withheld as proprietary. This information is considered to be proprietary because it contains detailed descriptions of analytical approaches, methodologies, technical data and/or evaluation results not available elsewhere. The

precise value of the expertise required to develop the proprietary information is difficult to quantify, but it is clearly substantial.


9. Public disclosure of the information to be withheld is likely to cause substantial harm to the competitive position of NAC, as the owner of the information, and reduce or eliminate the availability of profit-making opportunities. The proprietary information is part of NAC's comprehensive spent fuel storage and transport technology base, and its commercial value extends beyond the original development cost to include the development of the expertise to determine and apply the appropriate evaluation process. The value of this proprietary information and the competitive advantage that it provides to NAC would be lost if the information were disclosed to the public. Making such information available to other parties, including competitors, without their having to make similar investments of time, labor and money would provide competitors with an unfair advantage and deprive NAC of the opportunity to seek an adequate return on its large investment.

STATE OF GEORGIA, COUNTY OF GWINNETT

Mr. George Carver, being duly sworn, deposes and says:

That he has read the foregoing affidavit and the matters stated herein are true and correct to the best of his knowledge, information and belief.

Executed at Norcross, Georgia, this 26TH day of NOVEMBER, 2012.

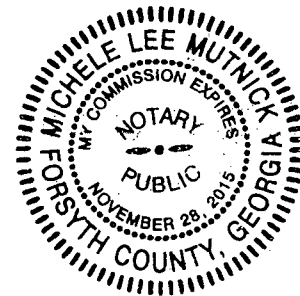


George Carver
Vice President, Engineering
NAC International

Subscribed and sworn before me this 26th day of November, 2012.



Notary Public



NAC INTERNATIONAL
RESPONSE TO THE
UNITED STATES
NUCLEAR REGULATORY COMMISSION
REQUEST FOR SUPPLEMENTAL INFORMATION
APRIL 1, 2011

FOR MAGNATRAN TRANSPORT CASK LICENSE APPLICATION

**(DOCKET NO. 71-9356,
TAC NO. L24511)**

October 2012

TABLE OF CONTENTS

	<u>Page</u>
REQUEST FOR SUPPLEMENTAL INFORMATION	
1.0 GENERAL INFORMATION	3
2.0 STRUCTURAL AND MATERIALS EVALUATION	9
3.0 THERMAL EVALUATION.....	16
5.0 SHIELDING EVALUATION.....	29
6.0 CRITICALITY EVALUTION.....	33
7.0 OPERATING PROCEDURES EVALUATION	38
8.0 ACCEPTANCE TESTS AND MAINTENANCE EVALUATION	39

**NAC INTERNATIONAL RESPONSE
TO
REQUEST FOR SUPPLEMENTAL INFORMATION**

1.0 GENERAL INFORMATION

- 1-1 Provide a table that clearly identifies the Transportable Storage Canister (TSC) and the allowable fuel assembly types for each.

It is unclear what assemblies are allowed in each type of TSC.

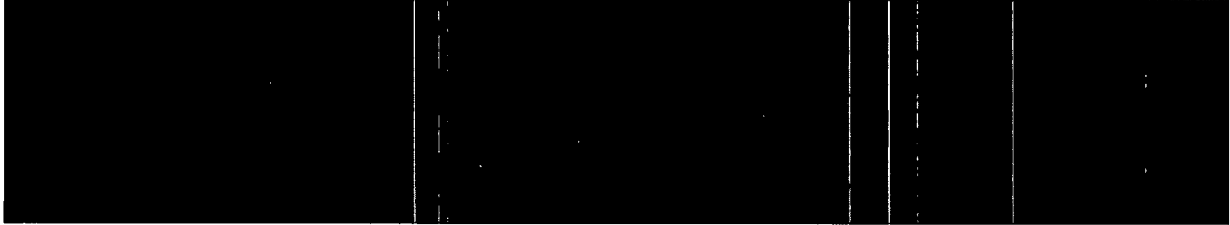
This information is needed to satisfy regulation 10 CFR 71.33(b).

NAC International Response to RSI 1-1

See below for a table correlating fuel type to TSC.

TSC	Nominal Cavity	Content
PWR (Long)	180 inches	All PWR assemblies requested for approval.
PWR (Short)	173 inches	All PWR assemblies requested for approval. (Exception: The System 80 16x16 fuel assembly is physically taller than the cask cavity and therefore must be loaded into the long TSC.)
BWR (Long)	180 inches	BWR/4-6 fuel assemblies with a fuel assembly length of approximately 176 inches (typical active fuel length 150 inches)
BWR (Short)	173 inches	BWR/2/3 fuel assemblies with a fuel assembly length of approximately 171 inches (typical active fuel length < 150 inches)

NAC International Response to RSI 1-1 (cont'd)



**NAC INTERNATIONAL RESPONSE
TO
REQUEST FOR SUPPLEMENTAL INFORMATION**

1.0 GENERAL INFORMATION

1-2 Clarify the contents to be transported in the MAGNATRAN.

The acronyms used to describe the allowed fuel assemblies in Tables 1.3-6, 1.3-7, 1.3-19, and 1.3-20 are not clearly defined or consistent throughout the application.

This information is needed to satisfy the requirements of 10 CFR 71.33(b) which gives specific requirements for specifying the contents of the package.

NAC International Response to RSI 1-2

In order to accommodate as many fuel assembly designs as possible without analyzing each one, NAC has defined specific bounding parameters for radiation shielding, criticality, thermal, and structural loading. For example, this approach for PWR fuel is discussed on SAR page 1.3-22 under "PWR Fuel."

Fuel assemblies are initially divided into categories by fuel rod array configuration. PWR fuel assemblies are therefore divided into 14x14 to 17x17 array groupings with BWR fuel assemblies divided into 7x7 to 10x10 array groupings. This terminology is used in Tables 1.3-6 and 1.3-19, as these tables apply broad assembly definitions. Within a given array size, assemblies may contain significant geometry variations that require individual analysis. The FSAR differentiates between the variations by assigning a letter designator to the array by a baseline assembly and/or nuclear steam supply system or core vendor (e.g, for PWR NSSS designed by Westinghouse for a 14x14 fuel assembly, the designation WE14 or WE14x14 ("WE" or "W") is used; for a General Electric BWR 7x7, the designator B7 is used). Where applicable, in particular for criticality analysis, further subdivisions in a group are made by either adding "Hx" for PWR assemblies or "_XXY" for BWR assemblies. The "Hx" is the designator for hybrid assembly, the term used for an assembly constructed from characteristics bounding one or more assemblies, with "x" being an incremented counter dependent on the number of subgroups. For BWR assemblies the designator relates to the number of fuel rods in the lattice ("XX") followed by an incremental subgroup indicated "Y", which is either "A" or "B" as at most two subgroupings are

NAC International Response to RSI 1-2 (cont'd)

established. As noted in the footnotes to Table 1.3-6 and Table 1.3-19, specific vendor assemblies are allowed to be loaded provided they meet key characteristics in the tables (e.g., AREVA and B&W replacement assemblies for WE cores would be acceptable based on meeting the appropriate WEXX assembly characteristic).

For example, the Westinghouse 17x17 OFA assembly characteristics place it in the WE17H2 hybrid (Table 1.3-7) subgroup. The WE17H2 hybrid is part of, and bounded by, the WE17 or WE17x17 group (Tables 1.3-9 through 1.3-10, Tables 1.3-12 through 1.3-14, and Table 1.3-16 through 1.3-18). The WE17x17 group in turn is part of, and bounded by, the 17x17 designator in Table 1.3-6. BWR assemblies are similarly grouped.

This grouping approach for PWR fuel is discussed on SAR page 1.3-22 under "PWR Fuel" and states:

"The bounding fuel assembly values are established based primarily on how the principal parameters are combined, and on the loading conditions (or restrictions) established for a group of fuel assemblies based on its parameters."

This type of terminology for fuel assembly classification is used throughout SAR Chapters 1, 5 and 6. Therefore, NAC will incorporate new definitions in the terminology section of the SAR for fuel assemblies. The following are the proposed definitions.

Fuel Assembly

The mechanical arrangement of nuclear fuel rods that is typically based on a square lattice structure. For many tables that list fuel assemblies within the MAGNATRAN Safety Analysis Report (SAR), the following naming methodology is typically used. Note this is not an exhaustive list.

"Y"x"Y"

Indicates the fuel assembly lattice size (square). For example, 14x14 indicates a square lattice fuel assembly containing a 14x14 array. The number of fuel rods and guide tubes within the array may vary and oversize tubes/rods may be present (e.g., BWR water rods or CE oversize guide tubes).

NAC International Response to RSI 1-2 (cont'd)

“X”“Y”

A subgroup below lattice size. Letter indicator (“X”) defines the base assembly/nuclear steam supply system/core vendor used to define the assembly type followed by the lattice size (“Y”). For example W14, WE14, or WE14x14 all indicate a Westinghouse type 14x14 fuel assembly type that is part of the 14x14 lattice size grouping. Provided a fuel assembly meets the fuel assembly characteristics required, no restriction on assembly vendor is applied. BWR uses the simple “B” designator.

“X”“Y”“Z”

A subgroup below the “X”“Y” level of array and primary fuel/NSSS/core vendor. These subcategories are used to separate fuel assemblies within a group by key physical characteristics. For PWR assemblies, for example, the Westinghouse 17x17 standard (WE17H1) assembly is separated from 17x17 OFA fuel (WE17H2). GE fuel assemblies are separated by the number of fuel rods in the array followed by a hybrid indicator (e.g., “A”, “B”). BWR fuel types may also be addressed within the SAR by reactor containment type (i.e., BWR/2-3 for typical 171-inch fuel assembly length and BWR/4-6 for typical 176-inch fuel assembly length).

**NAC INTERNATIONAL RESPONSE
TO
REQUEST FOR SUPPLEMENTAL INFORMATION**

1.0 GENERAL INFORMATION

- 1-3 Clarify if this system is being licensed for Pu shipments or to transport MOX? (SAR page 6.8.1-5)

SAR Section 1.3.3 has a special requirement for shipping Pu. It is noted that Chapter 6.0 references MOX fuel critical experiments to cover actinides burnup credit for benchmarking purposes; however, this is not a comprehensive criticality safety evaluation for MOX fuel.

This information is needed to satisfy regulation 10 CFR 71.33(b), and 71.63.

NAC International Response to RSI 1-3

The application is for transport of uranium oxide-based PWR and BWR fuel assemblies. As described in Chapter 6, the MOX material is addressed in the context of criticality code bias of spent (used) fuel, which resembles MOX material closer than the uranium oxide composition of fresh fuel. No indication of MOX material is included in the Chapter 1 content description. NAC is revising Chapter 1, Section 1.3.2 to use the term applied in the MAGNASTOR technical specification referring to "uranium" fuel assemblies. Note that this wording applies to the material in its unirradiated state and that the recognition must be made that spent fuel contains a significant amount of plutonium.

**NAC INTERNATIONAL RESPONSE
TO
REQUEST FOR SUPPLEMENTAL INFORMATION**

2.0 STRUCTURAL AND MATERIALS EVALUATION

MATERIALS EVALUATION

- 2-1 Revise the SAR to add, and by reference in the proposed Certificate of Compliance (CoC), a plan to ensure, that for any TSC that has spent time in storage, that the contents and TSC itself meet all the requirements in the CoC. This plan should include inspections to obtain data, or analysis to support that the: 1) mechanical and thermal properties of the components of the TSCs related to safety, and 2) contents, have not degraded during the storage period. Provide evidence that removal of the TSC from the storage overpack will not damage the TSC, and impact safety.

All the mechanical and thermal properties of the materials of construction of the TSC used in this part 71 analysis are for pristine materials. Dry loaded (SAR page 7.1-4) canisters will have previously been in storage for some time and have been on a storage pad for a considerable number of years. The materials properties used for the evaluation of the safety systems and contents of the TSCs that have already been in storage service must be representative of the conditions at the time of transport, not at the time of the loading of the TSC. No evidence was presented to indicate that the thermal and mechanical properties of the TSCs, or contents have not degraded during storage and are still applicable to the transportation evaluation. No consideration has been given in the SAR to the potential damage that may occur to the TSC during its removal from the storage overpack.

This information is needed to meet any thermal, shielding, criticality or structural requirements of 10 CFR 71 where the materials properties are integral to the response of the system.

NAC International Response to RSI 2-1

Chapter 7, Section 7.1.2 of the MAGNATRAN SAR describes the activities associated with loading of contents for the MAGNATRAN system. Page 7.1-4 addresses canisters that have been used for on-site storage and states, in general, that canisters used for storage will be

NAC International Response to RSI 2-1 (cont'd)

evaluated to ensure they meet the functional and performance requirements of the MAGNATRAN packaging certified content conditions.

Continuation of this description onto the following page, 7.1-5, details evaluations for canisters that experienced normal or off-normal events. These canisters need only be evaluated for potential corrosion at the welds and any damage caused by removal of the canister from the storage overpack. Those canisters that experience accident or natural phenomena events will be evaluated for potential degradation of the fuel, basket, and neutron absorbers. In addition, the first paragraph of Section 7.1 states, in short, that for the transport of loaded TSCs, the contents will be verified to be in compliance with the applicable content conditions of the CoC. These additions to the MAGNATRAN SAR are consistent with those associated with the NAC-STC SAR where this same question was addressed and resolved in a 2010 RAI (TAC No. L24408, Response dated June 3, 2010).

The structural characteristics of the TSC are based on the ASME Boiler and Pressure Vessel Code, Section III, Subsection NB. These structural code requirements are used in currently operating nuclear power plants for an initial 40 years and, in many cases, an additional 20 years of licensed operation. This licensed operation subjects these materials to temperatures, pressures, and radiation levels significantly greater than those seen during dry storage. Based on this comparison, there is reasonable assurance that the TSC will not degrade and will maintain material properties that meet the design performance criteria for many years. This justification is consistent with those associated with the NAC-STC SAR where this same question was addressed and resolved in a 2010 RAI.

For those canisters that have been used for an extended period of time (i.e., a license renewal has been approved), an aging management program will have been implemented for those SSCs where aging effects need to be managed. This provides reasonable assurance that components requiring aging management have not degraded during the storage time. Should NAC pursue a license renewal in the future, the application will address the effects of aging as required by the regulations.

With respect to canister contents, NUREG\CR-6745 and NUREG\CR-6831 demonstrate that spent fuel maintained in a dry storage environment, similar to the MAGNATRAN and MAGNASTOR TSCs, does not result in any significant fuel degradation. This work was

NAC International Response to RSI 2-1 (cont'd)

performed by Idaho and Argonne National Labs in the early 2000s on spent fuel from Surry that had been in dry storage for 14 years and was 18 years old. No significant mechanical or thermal degradations were identified at Idaho when the fuel was extracted and visually examined, nor was any degradation identified at Argonne when the fuel was destructively, nondestructively, and physically examined.

The request to provide evidence that removal of the TSC from the storage overpack will not damage the TSC and impact safety is provided as part of the MAGNASTOR 10 CFR 72 CoC, Technical Specification, Appendix A, Section 5.8, Preoperational Testing and Training Exercises. The procedure demonstrated as part of the 10 CFR 72 dry run is identical to the procedure that is used to move the TSC from the storage overpack for off-site transport. This procedure for retrieving the loaded TSC from the concrete overpack has been performed several times during normal loading operations for the similar UMS[®] system. Therefore, current 10 CFR 72 CoC and operational history provide adequate evidence that removal of the TSC from the storage overpack will not damage the TSC and impact safety. This justification is consistent with those associated with the NAC-STC SAR where this same question was addressed and resolved as referenced previously.

**NAC INTERNATIONAL RESPONSE
TO
REQUEST FOR SUPPLEMENTAL INFORMATION**

2.0 STRUCTURAL AND MATERIALS EVALUATION

STRUCTURAL EVALUATION

2-2 Structural Capability of for Nonfuel Hardware

Page 1.1-6. For the nonfuel hardware contents cited, identify those with potential structural functions for maintaining the as analyzed geometry of a fuel assembly and its ancillaries for the criticality safety evaluation. Provide a structural evaluation of the hardware, including the rod cluster control assembly (RCCA), to demonstrate acceptable stress, stiffness, and stability capabilities for the cask free drops associated with normal conditions of transport (NCT) and hypothetical accident conditions (HAC).

It is understood by the staff that some hardware, such as RCCAs, are to be used to control reactivity of an under-burned fuel assembly in a loaded cask. Given the fact that the fuel assemblies with RCCA nozzles will need extra axial space in comparison to the ones without, the additional space may exacerbate the secondary impact effects under the 30-foot drop test. This may cause the fuel assemblies without RCCAs to slide out of the fuel cells and cause an increase in reactivity. If the structural analysis cannot demonstrate this scenario is not plausible, the applicant may need a criticality safety analysis to demonstrate that the package design meets the criticality safety requirements of 10 CFR 71.55.

Structural capabilities for the nonfuel hardware must, therefore, be identified and evaluated to meet the 10 CFR Part 71 requirements, including 10 CFR 71.55, 71.71(c)(7), and 71.73(c)(1).

NAC International Response to RSI 2-2

As the following details, the full length rod cluster control assembly is the only nonfuel hardware contents credited in the criticality evaluation. As such, no other nonfuel hardware is used for maintaining the as analyzed geometry of a fuel assembly and its ancillaries for the criticality safety evaluation.

NAC International Response to RSI 2-2 (cont'd)

For low burnup Westinghouse PWR 15x15 fuel assemblies, full length rod cluster control assemblies (F/L RCCAs) are used to limit system reactivity. The criticality evaluation demonstrates the acceptability of the system configuration is maintained if extraction of the F/L RCCA, from the fuel assembly, is limited to a maximum of 5 inches. Top spacers are used to provide positional control of the F/L RCCA and to limit the gap between the fuel assembly and TSC. The top spacer consists of four legs that interface with the top nozzle of the fuel assembly and a reinforced plate, welded to the legs, which limits the motion of the F/L RCCA. The top spacer is designed such that the F/L RCCA supports only its self-weight, as the weight of the fuel assembly is transferred to the TSC lid through the legs of the spacer. The top spacer and F/L RCCA spider body are analyzed for the 30-foot top end drop accident which bounds all conditions of transport (see SAR Section 2.11.3). Qualification of the top spacer is provided by evaluating the total deformation of the spacer and F/L RCCA spider body as well as ensuring loading will not exceed 0.7 times the plastic limit collapse load, per ASME Appendix F subsection F-1341.4. Accordingly, the top spacer evaluation demonstrates that proper positional control of the F/L RCCA is maintained consistent with the criticality evaluation.

**NAC INTERNATIONAL RESPONSE
TO
REQUEST FOR SUPPLEMENTAL INFORMATION**

2.0 STRUCTURAL AND MATERIALS EVALUATION

STRUCTURAL EVALUATION

2-3 Design, Modeling, and Qualification of Impact Limiters

1. Drawing 71160-531. Add sufficient details to the proprietary drawings on the impact limiter design to ensure that the use of balsa wood to aid in mitigating end impact effects can properly be modeled and accounted for in both the end- and corner-drop tests in the LS-DYNA cask response simulation analysis.
2. Section 2.12.2.3, Benchmarking of LS-DYNA Impact Limiter Analysis Methodology. Provide scale model testing data of the impact limiter to demonstrate benchmarking of LS-DYNA. Expand the sensitivity analyses, or parametric studies, to identify drop orientations for which maximum damages to the cask are expected by including also the slapdown drop effects associated with landing the balsa center section tip onto an unyielding surface. In the expanded sensitivity analyses, bounding conditions of zero coefficient of friction between the target and the impact limiter must also be considered or otherwise justified.

The drop orientation parametric studies address the NAC-STC equivalent cask system geometry, which, without additional evaluation, are inconclusive for the MAGNATRAN in that the balsa center section may land on the target to introduce large rotational motion and corresponding secondary impact to the cask. Additional drop orientations must, therefore, be examined before concluding that decelerations associated with the side drop will govern the structural evaluation of the cask system.

The impact limiter capabilities must be evaluated to meet the requirements of 10 CFR 71.73.

NAC International Response to RSI 2-3

1. The MAGNATRAN impact limiter has been revised to have the same shape as the currently licensed NAC-STC balsa (CY MPC configuration) impact limiter. The revised design is sufficiently detailed in the NAC Proprietary Drawings for the impact limiter in the MAGNATRAN design. The drawings include the wood grain orientation,

NAC International Response to RSI 2-3 (cont'd)

dimensions and material definitions. Drawing details are sufficient to generate the model used in the evaluation of the impact limiter performance.

2. The revised impact limiter for MAGNATRAN has the same shape as the impact limiter used in the quarter scaled drop tests for the NAC-STC balsa impact limiter, which were performed at the Sandia National Laboratory. The benchmarking of the LS-DYNA Impact Limiter analysis methodology is contained in Section 2.12.2.3. The drop test program was comprised of a side drop, corner drop, and end drop. The side drop results in the maximum damage to the redwood segments. The end drop results in the maximum uniform crushing of the balsa wood segments at the impact limiter axial end. The corner drop effectively prevents the cask from rotation and results in the maximum crush depth of the balsa segment of the impact limiter. The crush depths of the analytical model are summarized in Table 2.6.7-37. Cask drop orientations between the corner and side drop would result in cask rotation. Cask rotation would increase the volume of wood to be involved in the absorption of energy without any alteration of the load path which was possible with the previous configuration. This eliminates the need to examine intermediate drop angles as suggested for the previous impact limiter design. Section 2.12.2.3.14 is revised to contain a parametric study of the cask shallow drop as well as the effect of the friction on the shallow angle drop condition.

**NAC INTERNATIONAL RESPONSE
TO
REQUEST FOR SUPPLEMENTAL INFORMATION**

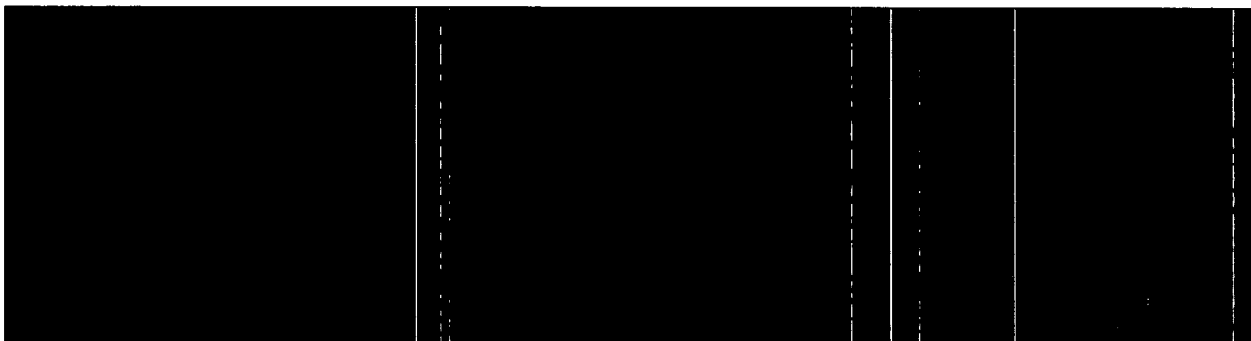
3.0 THERMAL EVALUATION

3-1 Provide further details on the design and effectiveness of the fins that are used to aid heat transfer during NCT and HAC.

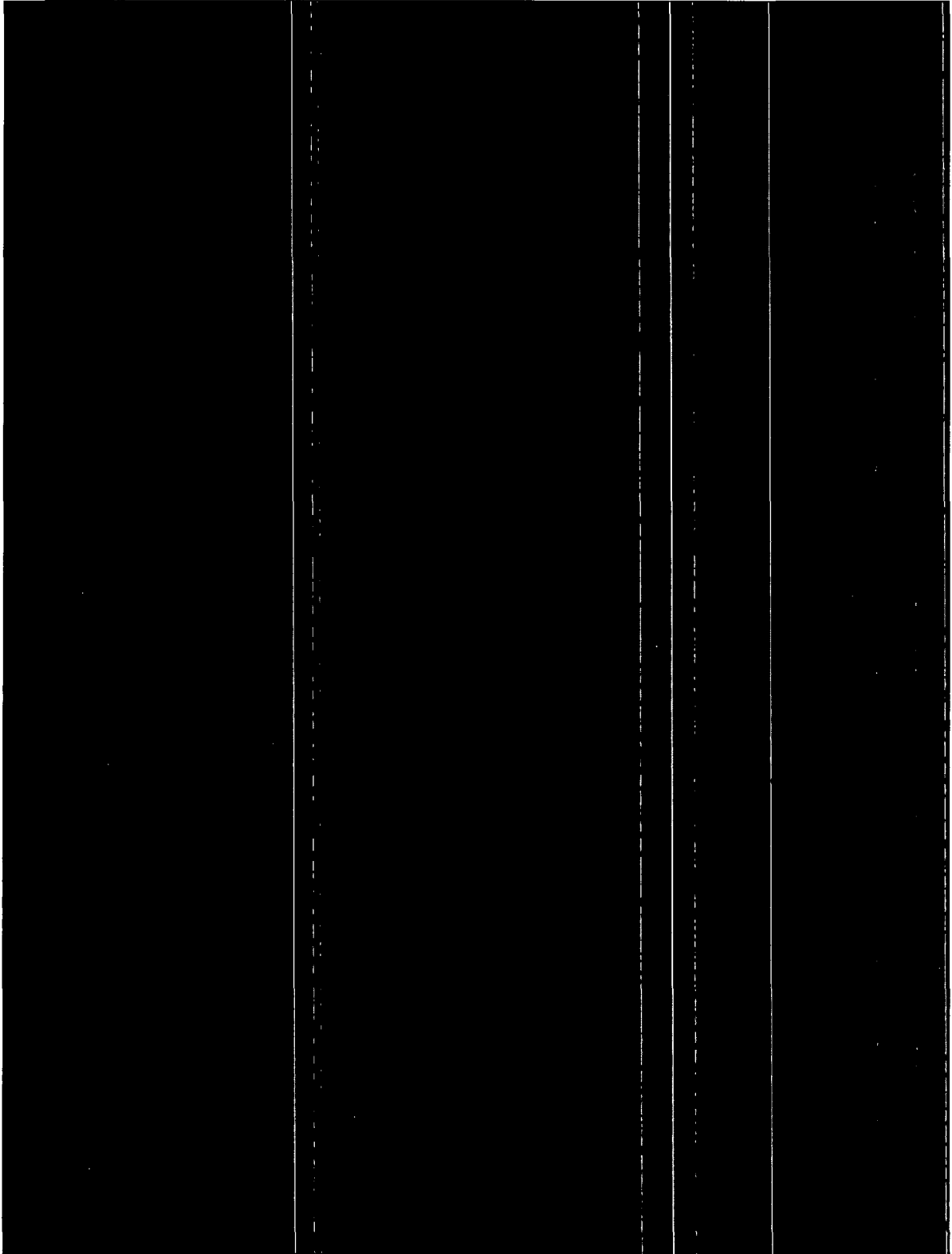
1. Further explanation of the fins, in terms of design and effectiveness, are needed in order to determine the adequacy in removing thermal energy from the package during NCT and HAC. Issues to address in the text include general fin layout and design; sketches would also be helpful.
2. What is the effect on package component temperatures if there is some loss of fin effectiveness due to breakage, fouling, etc.? This should be quantified in some way; heat exchangers, for example, use fin effectiveness and overall surface efficiency.
3. The need to check the conditions of the fins (the number attached to the package, confirm the adequacy of their attachment to the package, fouling conditions, etc.) should be explicitly stated in Chapter 7.
4. What is the effectiveness of the fins during hypothetical accident fire conditions, where temperatures can reach 1475°F? Page 1.3-3 indicates that the fins are constructed of aluminum, which has a melting point of 1220°F. Do the fins survive the fire intact? If not, their loss must be accounted for during the fire and post fire. Likewise, it is important to consider the eutectic temperatures of dissimilar materials in contact.

This information is needed to determine compliance with 10 CFR 71 (71.43, 71.71, 71.73).

NAC International Response to RSI 3-1



NAC International Response to RSI 3-1 (cont'd)



NAC International Response to RSI 3-1 (cont'd)



**NAC INTERNATIONAL RESPONSE
TO
REQUEST FOR SUPPLEMENTAL INFORMATION**

3.0 THERMAL EVALUATION

3-2 Provide further explanation concerning the effect of the personnel barrier on thermal performance.

1. The thermal description should clearly state the effect of the personnel barrier, if any, on the analyses considered in Chapter 3 and 7 of the SAR. This may require additional analysis to determine the bounding condition.
2. The effect of the personnel barrier on natural convection (Rayleigh number, etc.) and the boundary conditions modeled should be mentioned. The relation to Document No. 71160-3045, if any, should be clarified.
3. Do Table 3.4-1 and Table 3.5-1, 3.5-2 include the effect of the personnel barrier?
4. Clarify the effect of the personnel barrier during HAC.

This information is needed to determine compliance with 10 CFR 71.43, 71.71 and 71.73.

NAC International Response to RSI 3-2

1. The personnel barrier is fabricated from aluminum mesh, which allows free flow of the air through the aluminum mesh. Due to the small surface area of the mesh and the low emissivity of aluminum (0.22), the personnel barrier absorbs an insignificant amount of solar energy or radiant energy from the transport cask. Therefore, the effect of the personnel barrier on the MAGNATRAN transport thermal performance is insignificant and the personal barrier does not need to be included in the thermal analysis of the system. The following justification is added to Section 3.4.1.3.

“The personnel barrier is made from aluminum mesh with a large ratio of open area. Due to the small surface area of the aluminum mesh and the low emissivity of aluminum (0.22), the personnel barrier absorbs an insignificant amount of solar energy. The high percentage of open area allows free flow of the air through the aluminum mesh. Therefore, natural convection is not affected by the personnel barrier. The thermal effect of the personnel barrier on the transport thermal performance is insignificant; therefore, the personal barrier is not explicitly included in the CFD thermal model.”

NAC International Response to RSI 3-2 (cont'd)

2. The justification in Item 1 to be included in Section 3.4.1.3 will include a discussion regarding the effect on natural convection (Raleigh number, etc.).
3. Tables 3.4-1, 3.5-1, and 3.5-2 are acceptable as written as the justification included as a response to Item 1 dispositions the barrier to have an insignificant effect on system thermal performance (both normal and HAC).
4. For the fire accident condition, the convection representing the fire is applied directly to the package surface, and therefore neglects any effect of the personnel barrier on the fire condition. In addition, the fire accident condition is expected to eliminate the aluminum personnel barrier by melting due to the fire temperature exceeding aluminum's melting point.

**NAC INTERNATIONAL RESPONSE
TO
REQUEST FOR SUPPLEMENTAL INFORMATION**

3.0 THERMAL EVALUATION

3-3 Provide the two-dimensional and three-dimensional ANSYS and FLUENT computational models discussed in Chapter 3 and 7.

1. Some of the thermal models were provided as part of the initial application (Document No. 71660-3013, 3014, 3015, 3045). Provide the two-dimensional and three-dimensional ANSYS and FLUENT computational models (input and output files) described in Chapter 3 and 7, including the three ANSYS models described on page 3.4-4, the four ANSYS models described on page 3.4-10, the HAC models, the models that show the 41 hour time limit on page 7.1-5, and the models that show the six hour time limit on page 7.2-3.
 - a. For the models mentioned in Section 7, additional discussion should be provided that describes the models, boundary conditions, assumptions, transient conditions, etc.
 - b. Additional discussion should be provided for the two-dimensional and three-dimensional k-effective models, such as the geometric extent of the “average” area, level of detail, boundary conditions, etc.
 - c. Provide an overall sketch of the computational models. Note: It is difficult to grasp the extent of the models, even with the general descriptions provided (example, page 7 of 37 of Document 71160-3014).
2. At the appropriate places in the SAR, provide references to the specific documents (71660-3013, 3014, 3015, 3045) so that the staff can relate the SAR discussion with the descriptions in the individual documents.

This information is needed to determine compliance with 10 CFR 71.43, 71.71, and 71.73.

NAC International Response to RSI 3-3

1. All two-dimensional and three-dimensional ANSYS and FLUENT computational models (input and output files) described in Chapter 3, including the three ANSYS models described on page 3.4-4, the four ANSYS models described on page 3.4-10, and the HAC models, are

NAC International Response to RSI 3-3 (cont'd)

provided in NAC calculations 71160-3011, 71160-3013, 71160-3014, 71160-3015I, and 71160-3045.

The model that shows the 41-hour time limit on page 7.1-5 and the six-hour time limit on page 7.2-3 is contained in NAC calculation 71160-3020 in Appendix O, which is being transmitted to the NRC. The calculation package contains the description of the FLUENT model, as well as the FLUENT model input used in the evaluation.

- 1a) Section 7 describes the operational steps for loading the transport cask from the MAGNASTOR transfer cask. The MAGNASTOR transfer cask has been licensed for storage operations under Part 72. These operations include movement of fuel to and from the concrete cask for long-term storage conditions (NAC calculation 71160-2028).
 - 1b) & 1c) The discussion for the extent of the PWR fuel assembly and absorber is contained in SAR Section 3.4.1.1.2 and Section 3.4.1.1.3, which reference figures for the PWR effective property model definitions. The discussion for the extent of the BWR fuel assembly and absorber is contained in SAR Section 3.4.1.2.2 and Section 3.4.1.2.3, which reference figures for the BWR effective properties model definitions. These sections also contain boundary condition definitions in terms of temperature constraints, heat fluxes, and heat generations. NAC calculation 71160-3011 is the calculation for the effective property determination. This calculation contains the macros used to generate the material property input for the ANSYS cask model. These macros can be imported directly into ANSYS for model generation and properties. NAC calculation 71160-3011 references two other calculations containing model details, which are in the above-referenced SAR sections. These are NAC calculations 71160-3001 and 71160-3002 for the PWR and BWR effective model properties, respectively. These calculations are being submitted with RSI 3-3.
2. Calculation titles can be used in conjunction with the SAR section titles to determine which calculations are appropriate for the SAR section of interest.

**NAC INTERNATIONAL RESPONSE
TO
REQUEST FOR SUPPLEMENTAL INFORMATION**

3.0 THERMAL EVALUATION

3-4 Quantify the uncertainty in the cladding temperatures of the analyses.

The uncertainty in cladding temperature during NCT and HAC should be provided considering that there is only a 26°F temperature difference between the computational value of 726°F and the 752°F storage temperature limit.

This information is needed to determine compliance with 10 CFR 71.43, 71.71, 71.73.

NAC International Response to RSI 3-4

Thermal evaluations contained in the NAC MAGNATRAN SAR for the normal condition of transport provide bounding component temperatures. Conservatisms contained in the analyses are:

- A conservative convective film coefficient
- Adiabatic boundary conditions to the cask area covered by the impact limiter
- A conservative fuel thermal conductivity
- No credit for tube to tube contact in the horizontal transport configuration

The conservatisms are described in further detail as follows. While, with the exception of the film coefficient, the individual conservatisms are not quantified, they assure that the overall result is conservative and therefore does not require quantification to its uncertainty.

1. In the analyses for transport cask normal condition, a uniform, conservative, convection film coefficient is applied to cask surface area between top and bottom impact limiters. The portion of the cask covered by the impact limiter is modeled as adiabatic. Appendix E of NAC calculation 71160-3014 compared maximum clad temperature calculated by the use of a three-dimensional MAGNATRAN CFD determined film coefficient (NAC calculation 71160-3045) to the results obtained from the licensing basis film coefficient. The results of Appendix E confirmed that the clad temperatures reported in the SAR are conservative and are 12°F higher than the evaluation using the actual film coefficient from NAC calculation 71160-3045.

NAC International Response to RSI 3-4 (cont'd)

2. NRC Information Notice 2009-23 reports a degradation of approximately 5% to 7% of UO₂ thermal conductivities for every 10,000 MWd/MTU of fuel rod burnup. A degradation in thermal conductivity of approximately 22 to 32% is therefore to be accounted for based on the 45 GWd/MTU fuel requested for approval within the MAGNATRAN SAR (PWR may be loaded up to 60 GWD/MTU but is restricted to four DFC locations out of a total payload of 37 assemblies; this would affect the average potential degradation by < 1%). To ensure that a bounding condition of the fuel rod properties is used in the evaluation, the UO₂ thermal conductivity for all the assemblies is conservatively reduced by 40%.
3. During transport, the cask is in the horizontal position, which results in the closure of all gaps between adjacent basket fuel tubes. However, the thermal finite element model for this condition contains a 0.010-inch gap (modeled as helium) between each fuel tube. Similarly, no contact is considered for the poison plate and the adjacent components (there is a helium gap modeled on both sides of the poison plate). The fuel assembly is also conservatively assumed to be located in the center of the cell and there is no contact between the fuel assembly and the fuel tube walls. The imposition of these gaps in the model results in an additional conservatism for the reported maximum fuel clad temperature.

These considerations confirm that the actual maximum clad temperature reported in the MAGNATRAN SAR has greater than 12°F conservatism for the normal condition of transport.

The summary of the maximum component temperatures for the fire hypothetical accident condition (HAC) is reported in Table 3.5-1. This table reports a maximum fuel clad temperature of 893°F. The allowable clad temperature for the HAC is specified to be 1,058°F. This corresponds to a temperature margin of 165°F, which is significantly larger than the 26°F margin for the normal condition of transport. For the thermal evaluation of the 30-minute fire accident condition reported in MAGNASTOR SAR Section 3.5, a film coefficient is applied to the cask surface to simulate the fire accident boundary condition. The film coefficient applied to the surface of the model incorporates both radiation and convection (associated with the flame). The convection coefficient used in the thermal analyses is 50% larger than the film coefficient provided in the PATRAM '95 paper (Reference 11 in SAR Section 3.6). A larger convection film coefficient is conservative since it transfers more heat into the cask during the 30-minute period of the fire.

Therefore, the temperature margin for the fuel clad is greater than the 165°F margin reported in SAR Section 3.5 for the accident condition.

**NAC INTERNATIONAL RESPONSE
TO
REQUEST FOR SUPPLEMENTAL INFORMATION**

3.0 THERMAL EVALUATION

3-5 Clarify the maximum pressure within the cask during accident conditions.

Page 3.5-4 states that "TSC and cask pressures are determined for two accident scenarios, 100% fuel failure **OR** the maximum temperature accident." Maximum pressure within the cask under accident conditions should assume maximum temperature **AND** 100% fuel failure. The maximum pressure within the cask during accident conditions should be updated.

This information is needed to determine compliance with 10 CFR 71.43, 71.71, and 71.73.

NAC International Response to RSI 3-5

Section 3.5.4, Maximum Internal Pressures, and Table 3.5-3 are revised to contain the system results under accident conditions at the maximum fire accident temperature in combination with 100% fuel rod failure.

**NAC INTERNATIONAL RESPONSE
TO
REQUEST FOR SUPPLEMENTAL INFORMATION**

3.0 THERMAL EVALUATION

- 3-6 Provide the maximum thermal stresses and interferences during HAC in order to ensure structural integrity.

Page 3.5-4 does not address thermal stresses. The maximum thermal stresses and interferences during HAC should be discussed to ensure structural integrity.

This information is needed to determine compliance with 10 CFR 71.43, 71.71, and 71.73.

NAC International Response to RSI 3-6

The stresses developed during the HAC due to thermal gradients are defined to be secondary stresses. The evaluation of containment boundary structural integrity for accident conditions does not consider secondary stresses. The only primary loading affected by the HAC is the effect on pressure due to an increase in gas temperature. These pressures used in the evaluations bound the pressures developed during the HAC.

During the fire accident condition, the cask shells have a significantly higher temperature than the basket, which would allow the gap between the basket and canister and cask body to increase.

**NAC INTERNATIONAL RESPONSE
TO
REQUEST FOR SUPPLEMENTAL INFORMATION**

3.0 THERMAL EVALUATION

- 3-7 Provide the references listed in the MAGNATRAN analyses documents to support confirmatory analysis.

The following references listed in the MAGNATRAN analyses documents should be provided to support confirmatory analysis:

Document 71160-3015, Rev. 1: reference 6

Document 71160-3013, Rev. 0: references 1, 2 (confirm if the drawings listed in the SAR are the equivalent drawings), 3, 5, and 6

Document 71160-3014, Rev. 0: references 10, 2 (confirm if the drawings listed in the SAR are the equivalent drawings)

Document 71160-3045, Rev. 0: references 4 and 7

This information is needed to determine compliance with 10 CFR 71.43, 71.71, and 71.73.

NAC International Response to RSI 3-7

Document 71160-3015, reference 6 is the paper by Wix (“Convective Effects in a Regulatory and Proposed Fire Model”) presented at the 1995 PATRAM International Conference, which is included in this submittal in response to RSI 3-7.

Document 71160-3013, reference 1 is the NAC Specification that defines the design basis heat load. The design basis heat load is listed on the cover sheet of the calculation. Submitting the NAC Specification is not required for calculation review.

Document 71160-3013, reference 2; Document 71160-3014, reference 2; and Document 71160-3045, reference 4 correspond to NAC Proprietary engineering drawings. The license drawings provided with the MAGNATRAN SAR contain sufficient information to define the cask geometry.

NAC International Response to RSI 3-7 (cont'd)

Document 71160-3014, reference 10 is the specification of the film coefficient for the cask surface. The expression for the cask surface film coefficient is listed along with its source in MAGNATRAN SAR Section 3.2.3.

Per Section 4 of Document 71160-3045, reference 4 and reference 7 are for the definitions of the heat load and peaking factor (for BWR and PWR fuel assemblies). The references are not required for SAR analysis review as the design basis heat load and the power distribution are defined in the SAR. Section 3.1 lists PWR and BWR assembly and cask maximum heat loads. Figure 3.4-3 and Figure 3.4-7 illustrate the PWR and BWR axial heat load profiles, respectively. Further information on the axial profile may be found in Section 5.3.

**NAC INTERNATIONAL RESPONSE
TO
REQUEST FOR SUPPLEMENTAL INFORMATION**

5.0 SHIELDING EVALUATION

- 5-1 (See RSI 5-1 of Amendment 3 of the MAGNASTOR System Docket No. 72-1031, ML103060029) Provide additional information demonstrating that the gamma and neutron source terms with fuel burnup up to 70 GWd/MTU are accurate or conservative.

The applicant requests that the allowable contents in the MAGNATRAN have a maximum burnup of 70 GWd/MTU. This exceeds the burnup level the staff has previously approved using the method described in the MAGNATRAN SAR. The SAS2H code of the SCALE 4.4 package used in the source term calculations has not been validated to 70 GWd/MTU and because of this, the staff does not find that the application has enough information to justify that the source terms up to this burnup level are either accurate or conservative. The staff also notes that some of the SAR licensing calculations do not have any margin in meeting regulatory limits with respect to calculated dose rates.

The staff does not find NUREG/CR-7012 and NUREG/CR-7013 (these documents were cited in response to RSI 5-1 for the MAGNASTOR Amendment 3 application, Docket No. 72-1031) provide an adequate basis for use in shielding applications for high burnup fuel since these documents were written for use in burnup credit applications. These reports document the use of the TRITON code (versus SAS2H) and the nuclides important for burnup credit analyses are not the same as those used for shielding analyses.

The staff requests that the applicant provide technical information justifying the gamma and neutron source terms with fuel burnup up to 70 GWd/MTU are accurate or conservative. The staff finds that with little to no margin to meeting regulatory limits that all uncertainties should also be justified.

This information is needed to verify that the applicant has satisfied the dose rate requirements in 10 CFR 71.47 and 10 CFR 71.51.

NAC International Response to RSI 5-1

In order to minimize review time of the MAGNATRAN application, the maximum burnup for PWR fuel is reduced to an assembly average of 60 GWd/MTU consistent with the MAGNASTOR[®] FSAR, Revision 0, Amendment 1 and Amendment 2 configurations. BWR fuel is reduced to 45 GWd/MTU.

NAC International Response to RSI 5-1 (cont'd)

A 5% reduction in allowed heat load for fuel above 45 GWd/MTU (assembly average) is documented within the MAGNASTOR system SER to be acceptable to cover uncertainties of the burnup extrapolation. The relevant section of the SER is replicated below.

“Recognizing that the SAS2H depletion analysis code is only benchmarked to 46.6 GWd/MTU for PWR fuel assemblies and to 57 GWd/MTU for BWR fuel assemblies, the applicant added an extra 5% safety margin to the calculated source terms for the proposed loading of spent fuel assemblies with burnup ranging from 46 GWd/MTU to 60 GWd/MTU for PWR fuels, and 57 to 60 GWd/MTU for BWR fuels. The staff considers this extra safety margin sufficient to account for the uncertainties involved in the burnup extrapolation, based on various publications such as NUREG/CR-6701, NUREG/CR-6801, and NUREG/CR-6802.”

The same 5% value is applied in the MAGNATRAN transport application. The source terms for the transport application are directly extracted from the storage calculations.

**NAC INTERNATIONAL RESPONSE
TO
REQUEST FOR SUPPLEMENTAL INFORMATION**

5.0 SHIELDING EVALUATION

5-2 Provide additional information on the shielding analysis for GTCC.

The staff finds that the information in Section 5.8.11 of the SAR describing the shielding evaluation for GTCC waste is incomplete. The applicant should submit additional information including the same (and applicable) components as the spent fuel storage evaluations. This should include at a minimum a description and justification for material, geometry, energy spectra, and activity, as well as any methods used to generate the aforementioned. The applicant should include a description of and a justification for the differences between NCT and HAC. The location of the detectors for evaluating dose rates should be discussed and justified. Streaming paths should be identified and discussed.

This information is needed to meet the requirements of 10 CFR 71.31 which provides requirements for the contents of a package application.

NAC International Response to RSI 5-2

The requested information has been added to Chapter 5, Section 5.8.11 in the form of additional text, figures, tables, and references to the fuel analysis sections where appropriate.

**NAC INTERNATIONAL RESPONSE
TO
REQUEST FOR SUPPLEMENTAL INFORMATION**

5.0 SHIELDING EVALUATION

- 5-3 Correct inconsistent information throughout SAR when referencing maximum burnup requested for BWR assemblies.

Table 1.3-19 indicates that the maximum burnup for BWR fuel assemblies is 45,000 MWd/MTU. Chapter 5 indicates that the maximum burnup for BWR fuel is 60 GWd/MTU (see pages 5.3-1, 5.8.2-3, 5.8.4-3, 5.8.5-2 and Tables 5.8.4-6, 5.8.8-5).

This information is needed to satisfy the requirements of 10 CFR 71.33(b) which gives specific requirements for specifying the contents of the package.

NAC International Response to RSI 5-3

Chapter 5 was revised throughout to limit information presented to 45 GWd/MTU burnup.

**NAC INTERNATIONAL RESPONSE
TO
REQUEST FOR SUPPLEMENTAL INFORMATION**

6.0 CRITICALITY EVALUATION

6-1 Provide the following detailed information on the benchmark analysis for the fuel depletion analysis code:

1. List of sample identifications and isotopes included in each of the chemical assay samples that were used in the benchmarking analysis.
2. Method used in calculating the bias and bias uncertainty that were used to adjust the calculated cask k_{eff} with consideration that some of the chemical assay measurement data do not include all isotopes for which burnup credit are sought.
3. Technical basis and justification for the approach used to determine the biases and bias uncertainties of the depletion code.
4. Input files for the models for all chemical assay samples that were used in the code benchmark analysis.

The applicant takes burnup credit for some actinides in its criticality safety analysis for the MAGNATRAN PWR spent fuel transportation package. In Section 6.8.2.2 of the SAR, the applicant lists the chemical assay data used in the depletion code benchmarking analysis. However, a survey of the relevant publications indicates that some of the chemical assay data do not include measurements for all actinides for which burnup credit is sought. The applicant is requested to provide information as listed above and justification for the applicability of each of the measured data to the MAGNATRAN package safety analysis.

In addition, the SAR indicates that an approach not consistent with NUREG/CR-6811 was developed for calculating the bias and bias uncertainty of the depletion code. It is not clear (1) how the bias and bias uncertainty were calculated using the MCNP code (in reference to the proprietary information), and (2) why this approach is appropriate for a finite system like the MAGNATRAN. The applicant is requested to provide information on the rational and technical basis for the chosen approach.

This information is needed based on 10 CFR 71.35 and to enable the reviewer to confirm compliance with 10 CFR 71.55 and 71.59.

NAC International Response to RSI 6-1

MAGNATRAN SAR Section 6.8 was revised to address a number of items included within this RSI. Also included in the RSI response is a copy of the bias calculation. This NAC proprietary information is transmitted with all input and output files that were used in the generation of the code bias in a separate, sealed envelope marked NAC PROPRIETARY INFORMATION.

SAR Section 6.8 was modified to add Table 6.8.2-1 containing the fuel isotopes used in the calculation including nuclide IDs and cross-sections. A table listing the available isotopes in each of the reactor sets was also added. The input section of the proprietary calculation contains the detailed information of available isotopes in each radiochemical assay (RCA).

SAR Section 6.8 was further modified to include a brief discussion on the isotope correction factor used to generate data for the missing isotopes in the RCA sets. Additional detail on the correction factor is included in the proprietary calculation.

The write-up in Section 6.8 was augmented to better describe the "direct difference" approach being applied and to include the method used in generating missing isotope data in the RCAs (using an "f" correction factor on the TRITON-generated data for insertion into the RCA data set). Also, the section replaces the k-infinity calculation with a MAGNATRAN k_{eff} calculation to ensure applicability of the bias to the finite MAGNATRAN system.

The provided proprietary calculation includes input and output files for all the RCAs evaluated in support of the MAGNATRAN burnup credit application.

The previously reviewed version of Section 6.8 was also modified to remove the Mihama reactor data set. While addressing the adjustment for missing isotopes in the chemical assay, the Mihama set was reviewed again for applicability. As observed in ORNL/M-6121, the Mihama set contains incomplete documentation of fuel assembly design and operating parameters. The Mihama data set also included large variations in the results for the measured-to-calculated ratios for different axial locations in a single fuel pin and was, therefore, not recommended for use in determining the isotopic bias and uncertainty.

**NAC INTERNATIONAL RESPONSE
TO
REQUEST FOR SUPPLEMENTAL INFORMATION**

6.0 CRITICALITY EVALUATION

- 6-2 Provide information on misload analysis with consideration of the complicated zoned loading patterns of the MAGNATRAN fuel baskets.

The applicant provided misload analyses in the Safety Analysis Report of the MAGNATRAN and concluded that misload is not a credible event based on an EPRI study. However, review of the EPRI report indicates that the conclusion of the report was drawn not based on complete data of misload events. In addition, the EPRI report does not include consideration of the complex loading patterns as required in the MAGNATRAN license application. The applicant is requested to provide its own misload analysis based on the up-to-date misload events and specific data with consideration of the loading patterns of the fuel baskets to be transported by MAGNATRAN.

This information is needed based on 10 CFR 71.43 and to enable the reviewer to confirm compliance with 10 CFR 71.55 and 71.59.

NAC International Response to RSI 6-2

With the exception of allowing very low burnup assemblies in the basket center nine locations and damaged fuel cans in four corner locations, no other zone loadings are employed within the MAGNATRAN system. Damaged fuel cans are clearly differentiated visually from undamaged fuel and are designed to be located in oversize basket openings only available in the corners of the damaged fuel basket. The low burnup assemblies are required to be loaded using rod cluster control assemblies (RCCAs) that are clearly differentiated visually from those not containing RCCAs (Note: A maximum of nine RCCA assemblies may be loaded in MAGNATRAN). From a reactivity standpoint, any number of RCCAs containing assemblies could be loaded, anywhere in the basket, without a positive reactivity effect on the system (i.e., RCCAs containing assemblies are lower in reactivity than other assemblies meeting the burnup curve requirements). The loading limitation is based on shielding limitations associated with the RCCA activated materials source.

NAC International Response to RSI 6-2 (cont'd)

To address misloads, SAR Section 6.10.1.10 was rewritten to focus on the misload analysis performed for the MAGNATRAN system rather than the previous focus on probability analysis, backed up by a misload analysis.

**NAC INTERNATIONAL RESPONSE
TO
REQUEST FOR SUPPLEMENTAL INFORMATION**

6.0 CRITICALITY EVALUATION

6-3 Clarify the maximum burnup of the fuels to be shipped by MAGNATRAN.

The applicant indicates in Table 1.3-6 of the SAR that the maximum burnup of the fuels is 70 GWd/MTU. Page 6.8.2-1, however, indicates that the maximum burnup is 46.46 GWd/MTU. The maximum burnup for the spent fuel to be transported is not clear.

In addition, on pages 1.3-26 and 1.3-35, the applicant indicates that all fuels with burnup greater than 45 GWd/MTU must be placed in the damaged fuel cans, which are at the four corner locations of the fuel basket. This loading pattern could create a challenge to the shielding design. Although Chapter 5 of the SAR presents some information on dose rate calculations, it was not clear what loading pattern was used in the dose rate calculation for the baskets having the damaged fuel can loaded with high burnup fuels.

This information is needed based on 10 CFR 71.43 and to enable the reviewer to confirm compliance with 10 CFR 71.47, 71.55 and 71.59.

NAC International Response to RSI 6-3

The maximum 46.46 GWd/MTU value in Chapter 6 is listed within the subsection dealing with actinide-only burnup credit benchmarking. It is not a limit on system operations, rather a limit on the benchmark for burnup credit and, therefore, may be considered as an implicit limit on the amount of burnup credit that can be taken, not the maximum burnup of fuel placed into transport. At a given enrichment level, increasing the burnup level beyond 46.46 GWd/MTU will clearly result in a decreasing reactivity level. Thus, an analysis (and benchmark) at the 46.46 GWd/MTU burnup level will clearly bound assemblies with higher burnup levels (up to 60 GWd/MTU).

Undamaged fuel and damaged fuel were evaluated within Chapter 5 for maximum 70 GWd/MTU. (Note: As stated in the RSI 5-3 response, the Chapter 5 maximum burnup has been decreased to 60 GWd/MTU.) Damaged fuel is evaluated in an identical manner to that submitted in the MAGNASTOR Amendment 3 application with damaged fuel being allowed to migrate into the non-fuel hardware regions (i.e., into top and bottom plenum/nozzle regions of the assembly, top and bottom of the damaged fuel can) and it is allowed to concentrate in the active fuel region (up to 100% of the volume occupied). The licensing analyses evaluated casks with > 45 GWd/MTU fuel in every location (including the corners), which clearly covers casks that contain such high burnup fuel in only four of the locations.

**NAC INTERNATIONAL RESPONSE
TO
REQUEST FOR SUPPLEMENTAL INFORMATION**

7.0 OPERATING PROCEDURES EVALUATION

- 7-1 Add a more complete description for the drying process to the operating procedure in SAR Section 7.1.4 Step 11.

Currently SAR Section 7.1.4 step 11 states; "Vacuum dry the TSC and verify dryness." Since there can be direct transfer of a TSC from the pool to the overpack (SAR Section 7.1.4 Step 17), this is insufficient. Steps including isolation of the pump, and criteria such as hold times and pressures should be included.

This information is needed to satisfy regulation 10 CFR 71.43(d).

NAC International Response to RSI 7-1

SAR Section 7.1.4, step 11 and step 12 have been revised to incorporate additional information on the vacuum drying process, including vacuum pump isolation, dryness verification hold times, and acceptance pressure criterion in accordance with the standard vacuum drying process from the MAGNASTOR[®] FSAR.

**NAC INTERNATIONAL RESPONSE
TO
REQUEST FOR SUPPLEMENTAL INFORMATION**

8.0 ACCEPTANCE TESTS AND MAINTENANCE EVALUATION

8-1 Additional details of the thermal acceptance test must be provided in order to determine the effectiveness of the test.

1. There should be additional discussion of the thermal acceptance test provided on pages 8.1-24 through 8.1-26. It is unclear how the results can be used for acceptance, especially the concept of heat rejection capability by measuring condensate flow rate. In addition, provide mass and thermal energy balances to validate the concept.
2. Discuss the test implementation: where the steam enters, where the steam exits, where/how the condensate is collected, specifically where are the thermocouples located and which temperature gradients are to be measured.
3. There should be a corresponding numerical thermal analysis of the proposed test conditions (i.e., no insolation, ambient temperature, steam entering in/out) provided in Chapter 3 in order to determine the appropriateness of the measured temperature and temperature gradients.
4. Is this test to be performed at time intervals throughout the package lifetime in order to confirm the continued effectiveness of the packaging (i.e., gap dimensions remain, etc.)?

This information is needed to determine compliance with 10 CFR 71 (71.43, 71.71, 71.73).

NAC International Response to RSI 8-1

- 1) When thermal equilibrium is established, the total energy input by the dry steam is divided into two parts, one (Q_{c_out}) is the energy transferred out through the cask surface, and two (Q_{cond_out}) is the energy carried away by the condensate water. The energy transferred out through the cask surface represents the cask capability to dissipate heat out of the cask, which should be equal to (or larger than) the cask design heat load. Therefore, the thermal test acceptance criteria for energy balance is specified as the total heat rejection rate is equal to, or greater than, the cask design basis heat rejection rate.

NAC International Response to RSI 8-1 (cont'd)

When thermal equilibrium is established, the mass of the dry steam input (m_s) at inlets must be equal to the mass of the condensate water (m_{cond_out}).

Enthalpy is the total energy of matter in a state that includes the internal energy (temperature related) and pressure work (pressure specific volume product). The input of the total dry steam (m_s) with a temperature of 212°F and a pressure of 14.7 psi (or other pressure) defines the total energy input into the cask. The energy carried away by the condensate water (Q_{cond_out}) is represented by total mass of the condensate water (m_{cond_out}) times enthalpy of the water at its state (water temperature is measured, ambient pressure) flowing out of the cask.

For example, the enthalpy for saturated steam and saturated water under a pressure of 1.0 atm (14.7 psi) and 212°F is 2676 kJ/kg and 419 kJ/kg, respectively. The energy released from dry steam (2676 kJ/kg) to saturated water (419 kJ/kg) is 2257 kJ/kg. The mass flow rate needed for a 23kW heat source is 81 lbs/hour [1.0191×10^{-2} kg/sec, $23(\text{kJ/sec.})/2257(\text{kJ/kg})$]. A discussion of the energy balance is contained in Section 8.1.7.1.

- 2) A special cask lid will be designed to have inlet for steam coming in and outlet for the condensate water exiting. The outlet will be positioned at the lower elevation to ensure the discharge of the condensate water. Guide pipes for steam flow will be implemented to ensure the uniform distribution of the dry steam. The cask will be slightly tilted along the cask axial to provide discharge of the condensate water. A guide pipe on the cask test lid will be designed as an outlet guiding the flow of the condensate water.
- 3) A new section (Section 8.1.7.3) is added to the SAR presenting steady state analysis and transient analyses simulating the MAGNATRAN cask thermal test.
- 4) This thermal test is performed as an acceptance test validating performance of the as-fabricated hardware. Periodic life cycle testing is not performed since there is no significant change in material properties and design gaps throughout the package lifetime, therefore, the continued effectiveness of the packaging cask design is ensured.

NAC INTERNATIONAL
RESPONSE TO THE
UNITED STATES
NUCLEAR REGULATORY COMMISSION
REQUEST FOR SUPPLEMENTAL INFORMATION
OBSERVATIONS
APRIL 1, 2011

FOR MAGNATRAN TRANSPORT CASK LICENSE APPLICATION

**(DOCKET NO. 71-9356,
TAC NO. L24511)**

October 2012

TABLE OF CONTENTS

	<u>Page</u>
REQUEST FOR SUPPLEMENTAL INFORMATION – OBSERVATIONS	
1.0 GENERAL INFORMATION	3
2.0 STRUCTURAL AND MATERIALS EVALUATION	4
3.0 THERMAL EVALUATION.....	25
4.0 CONTAINMENT EVALUATION.....	31
5.0 SHIELDING EVALUATION.....	32
8.0 ACCEPTANCE TESTS AND MAINTENANCE EVALUATION	36

**NAC INTERNATIONAL RESPONSE
TO
REQUEST FOR SUPPLEMENTAL INFORMATION**

OBSERVATIONS

1.0 GENERAL INFORMATION

1-1 Provide non-proprietary versions of all drawings.

The drawings in the non-proprietary version and proprietary version of the SAR do not match. The proprietary version contains drawings 71160-531 and 71160-618. The non-proprietary version does not list or contain these drawings in Section 1.4.3.

NAC International Response to RSI 1-1

NAC has updated the list of drawings to reflect the current list of license drawings for both the proprietary and non-proprietary versions of the SAR. Drawing 71160-618 has been removed from the application and is no longer listed. Drawing 71160-531 is proprietary in its entirety. Since the drawing is proprietary in its entirety, the list of drawings in the non-proprietary version of the SAR has a note indicating that even though the drawing is listed it is being withheld completely via 10 CFR 2.390.

**NAC INTERNATIONAL RESPONSE
TO
REQUEST FOR SUPPLEMENTAL INFORMATION**

OBSERVATIONS

2.0 STRUCTURAL AND MATERIALS EVALUATION

MATERIALS EVALUATION

2-1 Provide precise references (document, page) on all the tables for materials properties.

In the case of obscure references, copies of the applicable pages of the reference should be submitted with the SAR.

Currently there are no references on any of the tables for the sources of the material properties. References are only given at the end of the Chapter.

NAC International Response to RSI 2-1

The material property tables from Chapter 2 are provided with detail references. Note that the reference numbers are unique to this general observation response document and do not match the reference numbers used in the SAR. A copy of all references except for Reference 1 (ASME Boiler and Pressure Vessel Code) is provided for clarification.

Table 2.2.1-1 Mechanical Properties of SA-240, Type 304 Stainless Steel

Property (units)	Value at Temperature (°F)									
	-40	-20	70	200	300	400	500	650	800	900
Ultimate Tensile Strength ^a , S _u (ksi)	75.0	75.0	75.0	71.0	66.2	64.0	63.4	63.4	62.8	60.8
Yield Strength ^a , S _y (ksi)	30.0	30.0	30.0	25.0	22.4	20.7	19.4	18.0	16.9	16.2
Design Stress Intensity ^a , S _m (ksi)	20.0	20.0	20.0	20.0	20.0	18.6	17.5	16.2	15.2	-
Modulus of Elasticity ^a , E (10 ⁶ psi)	28.8	28.7	28.3	27.6	27.0	26.5	25.8	25.1	24.1	23.5
Coefficient of Thermal Expansion ^a , α (10 ⁻⁶ in/in/°F)	8.13 ^c	8.2 ^c	8.5	8.9	9.2	9.5	9.7	9.9	10.1	10.2
Poisson's Ratio ^a	0.31									
Density ^b , (lb/in ³)	0.29									

Notes:

- ^a Ref. 1, Ultimate Tensile Strength: Table U, Page 452, Line 10. Yield Strength: Table Y-1, Page 556, Line.14. Design Stress Intensity: Table 2A, Page 316, Line 3. Modulus of Elasticity: Material Group G in Table TM-1, Page 671. Coefficient of Thermal Expansion: Material Group 3 in Table TE-1, Page 651. Poisson's Ratio: Material Group Cr-Ni-Fe-Mo-Cu-Cb in Table NF-1, Page 677.
- ^b Ref. 2, Metals Handbook, Density: 17-4PH in Page 1-49.
- ^c Extrapolated.

Table 2.2.1-2 Mechanical Properties of SA-336, Type F304 Stainless Steel

Property (units)	Value at Temperature (°F)						
	-40	70	200	300	400	500	750
Ultimate Tensile Strength, S_u (ksi)	70.0	70.0	66.3	61.8	59.7	59.2	59.0
Yield Strength, S_y (ksi)	30.0	30.0	25.0	22.4	20.7	19.4	17.2
Design Stress Intensity, S_m (ksi)	20.0	20.0	20.0	20.0	18.6	17.5	15.5
Modulus of Elasticity, E (10^6 psi)	28.8	28.3	27.6	27.0	26.5	25.8	24.4
Coefficient of Thermal Expansion, α (10^{-6} in/in/ °F)	8.5	8.5	8.9	9.2	9.5	9.7	10.0
Poisson's Ratio	0.31						
Density (lb/in ³)	0.291						

Notes:

Ref. 1, Ultimate Tensile Strength: Table U, Page 420. Yield Strength: Table Y-1, Page 492. Design Stress Intensity: Table 2A, Page 256. Modulus of Elasticity: Table TM-1, Page 671. Coefficient of Thermal Expansion: Table TE-1, Page 648. Poisson's Ratio: Table NF-1, Page 677. Density: Table NF-2, Material Cr-Ni-Fe-Mo-Cu-Cb, Page 679.

Table 2.2.1-3 Mechanical Properties of SA-479, Type 304 Stainless Steel

Property (units)	Value at Temperature (°F)						
	-40	70	200	300	400	500	750
Ultimate Tensile Strength ^a , S _u (ksi)	75.0	75.0	71.0	66.2	64.0	63.4	63.3
Yield Strength ^a , S _y (ksi)	30.0	30.0	25.0	22.4	20.7	19.4	17.2
Design Stress Intensity ^a , S _m (ksi)	20.0	20.0	20.0	20.0	18.6	17.5	15.5
Modulus of Elasticity ^a , E (10 ⁶ psi)	28.8	28.3	27.6	27.0	26.5	25.8	24.4
Coefficient of Thermal Expansion ^a , α (10 ⁻⁶ in/in/ °F)	8.1 ^b	8.5	8.9	9.2	9.5	9.7	10.0
Poisson's Ratio ^a	0.31						
Density ^a (lb/in ³)	0.291						

Notes:

^a Ref. 1, Ultimate Tensile Strength: Table U, Page 452. Yield Strength: Table Y-1, Page 556. Design Stress Intensity: Table 2A, Page 316. Modulus of Elasticity: Table TM-1, Page 671. Coefficient of Thermal Expansion: Table TE-1, Page 648. Poisson's Ratio: Material Cr-Ni-Fe-Mo-Cu-Cb in Table NF-1, Page 677. Density: Table NF-2, Material Cr-Ni-Fe-Mo-Cu-Cb, Page 679.

^b Extrapolated.

Table 2.2.1-4 Mechanical Properties of SA-240 Type XM-19 Stainless Steel

Property (units)	Value at Temperature (°F)								
	-40	70	200	300	400	500	750	800	900
Ultimate Tensile Strength, S_u (ksi)	100.0	100.0	99.4	94.2	91.1	89.1	85.6	84.8	82.6
Yield Strength, S_y (ksi)	55.0	55.0	47.1	43.3	40.7	38.8	35.8	35.3	34.5
Design Stress Intensity, S_m (ksi)	33.3	33.3	33.1	31.4	30.4	29.7	28.5	28.3	-
Modulus of Elasticity, E (10^6 psi)	28.8	28.3	27.6	27.0	26.5	25.8	24.4	24.1	23.5
Coefficient of Thermal Expansion, α (10^{-6} in/in/°F)	8.2	8.2	8.5	8.8	8.9	9.1	9.3	9.4	9.5
Poisson's Ratio	0.31								
Density (lb/in ³)	0.291								

Notes:

Ref. 1, Ultimate Tensile Strength: Table U, Page 462, Line 16. Yield Strength: Table Y-1, Page 576, Line 16. Design Stress Intensity: Table 2A, Page 340, Line 2. Modulus of Elasticity: Table TM-1, Group G, Page 671. Coefficient of Thermal Expansion: Table TE-1, Page 648. Poisson's Ratio: Table NF-1, Material Cr-Ni-Fe-Mo-Cu-Cb, Page 677. Density: Table NF-2, Material Cr-Ni-Fe-Mo-Cu-Cb, Page 679.

**Table 2.2.1-5 Mechanical Properties of SA-564/SA-693/SA-705, Type 630 (17-4 PH)
Stainless Steel**

Property (units)	Value at Temperature (°F)							
	-40	70	200	300	400	500	600	700
Ultimate Strength ^a , S _u (ksi)	135.0	135.0	135.0	135.0	131.2	128.6	126.7	123.8
Yield Strength ^a , S _y (ksi)	105.0	105.0	97.1	93.0	89.7	87.0	84.7	82.5
Design Stress Intensity ^a , S _m (ksi)	45.0	45.0	45.0	45.0	43.7	42.9	42.2	-
Modulus of Elasticity ^a , E (× 10 ⁶ psi)	29.4	28.5	27.8	27.2	26.6	26.1	25.5	24.9
Coefficient of Thermal Expansion ^a , α (×10 ⁻⁶ in/in/°F)	5.9							
Poisson's Ratio ^a	0.31							
Density ^b (lb/in ³)	0.28							

Notes:

^a Ref. 1, Ultimate Tensile Strength: Table U, Page 438, Line 15 (bounds Lines 16-23). Yield Strength: Table Y-1, Page 528, Line 16 (bounds Lines 17-24). Design Stress Intensity: Table 2A, Page 288, Line 5 (bounds lines 6-13). Modulus of Elasticity: Table TM-1, Material S17400, Page 671. Coefficient of Thermal Expansion: Material Group 17Cr-4Ni-4Cu in Table TE-1, Page 652. Poisson's Ratio: Table NF-1, Material Cr-Ni-Fe-Mo-Cu-Cb, Page 677.

^b Ref. 2, Metals Handbook, Density: 17-4PH in Page 1-49

Table 2.2.1-6 Mechanical Properties of SA-537, Class 1, Carbon Steel

Property (units)	Value at Temperature (°F)							
	-40	70	200	300	400	500	700	800
Ultimate Strength ^a , S _u (ksi)	70.0	70.0	70.0	69.1	68.4	68.4	68.4	65.4
Yield Strength ^a , S _y (ksi)	54.9	50.0	44.2	40.5	37.6	35.4	32.3	30.5
Design Stress Intensity ^a , S _m (ksi)	23.3	23.3	23.3	22.8	22.7	22.7	21.4	20.3 ^c
Modulus of Elasticity ^a , E (× 10 ⁶ psi)	30.0	29.5	28.8	28.3	27.7	27.3	25.5	24.2
Coefficient of Thermal Expansion ^a , α (× 10 ⁻⁶ in/in/°F)	6.1	6.4	6.7	6.9	7.1	7.3	7.6	7.8
Poisson's Ratio ^a	0.31							
Density ^b (lb/in ³) ^b	0.284							

Notes:

- ^a Ref. 1, Ultimate Tensile Strength: Table U, Page 426, Line 24. Yield Strength: Table Y-1, Page 504, Line 24. Design Stress Intensity: Table 2A, Page 264, Line 30. Modulus of Elasticity: Material: Carbon steel with C<0.3% in TM-1, Page 671. Coefficient of Thermal Expansion: Material Group 1 in Table TE-1, Page 648. Thermal Conductivity: Material Group B in Table TCD, Page 662. Poisson's Ratio: Material Cr-Ni-Fe-Mo-Cu-Cb in Table NF-1, Page 677.
- ^b Ref. 2, Metals Handbook, Density: 0.23% Carbon Steel in Page 1-49.
- ^c Ref. 3, ASME Code Case N-707, Table 1.

Table 2.2.1-7 Mechanical Properties of SA-695, Type B, Grade 40, and SA-696, Type C, Carbon Steel

Property (units)	Value at Temperature (°F)							
	-40	70	200	300	400	500	700	800
Ultimate Strength ^a , S _u (ksi)	70.0	70.0	70.0	70.0	70.0	70.0	70.0	64.3
Yield Strength ^a , S _y (ksi)	40.0	40.0	36.6	35.4	34.2	32.6	28.6	26.8
Design Stress Intensity ^a , S _m (ksi)	23.3	23.3	23.3	23.3	22.8	21.7	19.2	--
Modulus of Elasticity ^a , E (× 10 ⁶ psi)	29.8	29.3	28.6	28.1	27.5	27.1	25.3	24.0
Coefficient of Thermal Expansion ^a , α (×10 ⁻⁶ in/in/°F)	6.13	6.4	6.7	6.9	7.1	7.3	7.6	7.8
Poisson's Ratio ^a	0.31							
Density (lb/in ³) ^b	0.284							

Notes:

^a SA-695, Type B, Grade 40: Ref. 1, Ultimate Tensile Strength: Table U, Page 426, Line 18. Yield Strength: Table Y-1, Page 504, Line 18. Design Stress Intensity: Table 2A, Page 264, Line 25. Modulus of Elasticity: Material: Carbon steel with C>0.3% in TM-1, Page 671. Coefficient of Thermal Expansion: Material Group 1 in Table TE-1, Page 648. Poisson's Ratio: Material Cr-Ni-Fe-Mo-Cu-Cb in Table NF-1, Page 677.

SA696, Type C: Ref. 1, Ultimate Tensile Strength: Table U, Page 426, Line 19. Yield Strength: Table Y-1, Page 504, Line 19. Design Stress Intensity: Table 2A, Page 264, Line 26. Modulus of Elasticity: Material: Carbon steel with C>0.3% in TM-1, Page 671. Coefficient of Thermal Expansion: Material Group 1 in Table TE-1, Page 648. Poisson's Ratio: Material Cr-Ni-Fe-Mo-Cu-Cb in Table NF-1, Page 677.

^b Ref. 2, Metals Handbook, Density: 0.23% Carbon Steel in Page 1-49.

Table 2.2.1-8 Mechanical Properties of SA-193, Grade B6, High Alloy Bolting Steel

Property (units)	Value at Temperature (°F)							
	-40	-20	70	200	300	400	500	700
Ultimate Strength ^a , S _u (ksi)	110.0	110.0	110.0	104.9	101.4	98.3	95.6	90.6
Yield Strength ^a , S _y (ksi)	85.0	85.0	85.0	81.1	78.4	76.0	73.9	70.0
Design Stress Intensity ^b , S _m (ksi)	28.3	28.3	28.3	27.0	26.1	25.3	24.6	23.3
Bolt Stress Intensity ^b , S _{mbm} (ksi)	21.2	21.2	21.2	21.2	21.2	21.2	21.2	21.2
Modulus of Elasticity ^b , E (× 10 ⁶ psi)	29.8	29.7	29.2	28.5	27.9	27.3	26.7	25.6
Coefficient of Thermal Expansion ^b , α (× 10 ⁻⁶ in/in/°F)	5.65 ^d	5.69 ^d	5.90	6.20	6.30	6.40	6.50	6.60
Poisson's Ratio ^b	0.31							
Density (lb/in ³) ^c	0.28							

Notes:

^a Calculated based on Design Stress Intensity, e.g., $\frac{S_{mtemp}}{S_{m70°F}}(S_{u70°F}) = S_{temp}$

^b Ref. 1, Design Stress Intensity: Table 4, Page 412, Line 26. Modulus of Elasticity: Material Group F in Table TM-1, Page 671. Coefficient of Thermal Expansion: Material 12Cr in Table TE-1, Page 650. Poisson's Ratio: Material Cr-Ni-Fe-Mo-Cu-Cb in Table NF-1, Page 677.

^c Ref. 2, Metals Handbook, Density: Stainless Steel Type 410 in Page 1-49.

^d Extrapolated.

Table 2.2.1-9 Mechanical Properties of SA-193, Grade B8, Bolting Steel

Property (units)	Value at Temperature (°F)							
	-40	70	200	300	400	500	700	800
Ultimate Strength ^a , S _u (ksi)	75.0	75.0	71.0	66.2	64.0	63.4	63.4	62.8
Yield Strength ^a , S _y (ksi)	30.0	30.0	25.0	22.4	20.7	19.4	17.6	16.9
Design Stress Intensity ^a , S _m (ksi) (Bolt Material)	10.0	10.0	8.3	7.5	6.9	6.5	5.9	5.6
Modulus of Elasticity ^a , E (× 10 ⁶ psi)	28.8	28.3	27.6	27.0	26.5	25.8	24.8	24.1
Coefficient of Thermal Expansion ^a , α (×10 ⁻⁶ in/in/°F)	8.13 ^c	8.5	8.9	9.2	9.5	9.7	10.0	10.1
Poisson's Ratio ^a	0.31							
Density ^b (lb/in ³)	0.29							

Notes:

- ^a Ref. 1, Ultimate Tensile Strength: Table U, Page 452, Line 6. Yield Strength: Table Y-1, Page 556, Line.10.
Design Stress Intensity Bolt Material: Table 4, Page 416, Line 10. Modulus of Elasticity: Material Group G in
Table TM-1, Page 671. Coefficient of Thermal Expansion: Material Group 3 in Table TE-1, Page 651.
Poisson's Ratio: Material Group Cr-Ni-Fe-Mo-Cu-Cb in Table NF-1, Page 677.
- ^b Ref. 2, Metals Handbook, Density: Stainless Steel Type 304 in Page 1-49.
- ^c Extrapolated.

Table 2.2.1-10 Mechanical Properties of SA-193, Grade B8S, Bolting Steel

Property (units)	Value at Temperature (°F)							
	-40	70	200	300	400	500	700	800
Ultimate Strength ^a , S _u (ksi)	95.0	95.0	74.0	62.6	56.3	52.3	48.4	47.8
Yield Strength ^a , S _y (ksi)	50.0	50.0	38.9	32.9	29.6	27.5	25.4	25.1
Design Stress Intensity ^b , S _m (ksi)	16.7	16.7	13.0	11.0	9.9	9.2	8.5	8.4
Bolt Stress Intensity ^b , S _{mbm} (ksi)	28.8	28.3	27.6	27.0	26.5	25.8	25.1	24.1
Modulus of Elasticity ^b , E (× 10 ⁶ psi)	28.8	28.3	27.6	27.0	26.5	25.8	24.8	24.1
Coefficient of Thermal Expansion ^b , α (× 10 ⁻⁶ in/in/°F)	8.13 ^d	8.5	8.9	9.2	9.5	9.7	10.0	10.1
Poisson's Ratio ^b	0.31							
Density (lb/in ³) ^c	0.29							

Notes:

^a Calculated based on Design Stress Intensity, e.g., $\frac{S_{mtemp}}{S_{m70°F}}(S_{u70°F}) = S_{mtemp}$

^b Ref. 1, Design Stress Intensity: Table 4, Page 416, Line 12. Modulus of Elasticity: Material Group G in Table TM-1, Page 671. Coefficient of Thermal Expansion: Material Group 3 in Table TE-1, Page 651. Poisson's Ratio: Material Group Cr-Ni-Fe-Mo-Cu-Cb in Table NF-1, Page 677.

^c Ref. 2, Metals Handbook, Density: Stainless Steel Type 304 in Page 1-49.

^d Extrapolated.

Table 2.2.1-11 Mechanical Properties of SB-637, Grade N07718, Nickel Alloy Bolting Steel

Property (units)	Value at Temperature (°F)						
	-40	70	200	300	400	500	700
Ultimate Strength ^a , S _u (ksi)	185.0	185.0	177.6	173.5	170.6	168.7	165.8
Yield Strength ^a , S _y (ksi)	150.0	150.0	144.0	140.7	138.3	136.8	134.4
Design Stress Intensity ^b , S _m (ksi)	50.0	50.0	48.0	46.9	46.1	45.6	44.8
Modulus of Elasticity ^b , E (× 10 ⁶ psi)	29.6	29.0	28.3	27.8	27.6	27.1	26.4
Coefficient of Thermal Expansion ^b , α (×10 ⁻⁶ in/in/°F)	7.0 ^c	7.1	7.2	7.3	7.5	7.6	7.8
Poisson's Ratio ^b	0.31						
Density ^b (lb/in ³)	0.297						

Notes:

^a Calculated based on Design Stress Intensity, e.g., $\frac{S_{mtemp}}{S_{m70°F}}(S_{u70°F}) = S_{uemp}$

^b Ref. 1, Design Stress Intensity: Table 4, Page 416, Line 33, Modulus of Elasticity, Material Group B Nickel Steel in Table TM-4, Page 675, Coefficient of Thermal Expansion: Material N07718 in Table TE-4, Page 660, Poisson's Ratio: Material Cr-Ni-Fe-Mo-Cu-Cb in Table NF-1, Page 677, Density: Table NF-2, Material Alloy 718 in Page 679.

^c Extrapolated

Table 2.2.1-12 Mechanical Properties of Chemical Copper Grade Lead

Property (units)	Value at Temperature (°F)					
	-40	-20	70	200	300	600
Tensile Yield Strength ^a , S _y (psi)	720 ^b	700 ^b	610 ^b	500	370	-
Modulus of Elasticity ^c , E (× 10 ⁶ psi)	2.45	2.42	2.28	2.06	1.94	1.5
Coefficient of Thermal Expansion ^c , α (×10 ⁻⁶ in/in/°F)	15.6	15.7	16.1	16.7	17.3	20.2
Poisson's Ratio ^d	0.4					
Density (lb/in ³) ^d	0.41					

Notes:

- ^a Ref. 4, Determination of the Mechanical Properties of High Purity Lead and a 0.05% Copper-Lead Alloy, values extrapolated and interpolated from copperized lead data, p. 21.
- ^b Extrapolated.
- ^c Ref. 5, NUREG/CR-0481, coefficient of thermal expansion from p. 56, modulus of elasticity from p.66.
- ^d Ref. 6, Standard Handbook for Mechanical Engineers, Poisson's Ratio and Density: Basic Properties of Several Metals, p. 6-11.

Table 2.2.1-13 Mechanical Properties of NS-4-FR

Property (units)	Value at Temperature (°F)			
	108	158	212	302
Coefficient of Thermal Expansion ^a ($\times 10^{-6}$ in/in/°F)	51.8	57.9	57.4	58.9
Compressive Modulus of Elasticity ^b (ksi)	561			
Density ^b (lbm/in ³)	0.0607			

Notes:

^a Ref. 7, GESC Shield Materials Technical Report.

^b Ref. 8, GESC Shield Materials Product Data. Density calculated from specific gravity.

Table 2.2.1-14 Mechanical Properties of 1100-O Aluminum Alloy

Property (units)	Value at Temperature (°F)								
	-40	70	200	212	300	400	500	600	700
Ultimate Tensile Strength ^a , S _u (ksi)	14.2	13.1	10.3	10.0	8.0	6.0	4.0	2.9	2.1
Yield Strength ^a , S _y (ksi)	5.1	5.0	4.6	4.6	4.2	3.5	2.6	2.0	1.6
Modulus of Elasticity ^b , E (10 ⁶ psi)	10.3	10.0	9.6	9.6	9.2	8.7	8.1	-	-
Coefficient of Thermal Expansion ^b , α , (10 ⁻⁶ in/in/°F)	12.1	12.1	13.0	13.0	13.3	13.6	13.9	14.2	-
Poisson's Ratio ^b	0.33								
Density ^b (lb/in ³)	0.098								

Notes:

^a Required 13.1 ksi minimum ultimate strength and 5.0 ksi minimum yield strength at 70°F. Ultimate and Yield Strengths at other temperatures extrapolated using corresponding property change/temperature change ratios from Ref. 9 (Table 2.2, Alloy and Temper 1100-O, Page 2-5).

^b ASME Boiler and Pressure Vessel Code

REFERENCES

1. *ASME Boiler and Pressure Vessel Code, Section II, Part D – Properties*, The American Society of Mechanical Engineers, New York, 2001 Edition with 2003 Addenda, July 1, 2003.
2. Boyer, Howard E., *Metals Handbook Desk Edition*, American Society for Metals, Metals Park, Ohio, 1985.
3. *ASME Boiler and Pressure Vessel Code, Case N-707, Use of SA-537, Class 1 Plate for Spent-Fuel containment Internals in Non-pressure retaining Application above 700°F (370°C)*, Section III, Division 3, The American Society of Mechanical Engineers, New York, 2004.
4. Tietz, T.E., “Determination of the Mechanical Properties of High Purity Lead and a 0.05% Copper-Lead Alloy,” WADC Technical Report 57-695, ASTIA Document Number 151165, Stanford Research Institute, Menlo Park, CA, April 1958.
5. SAND77-1872, Rack, H.J., Knorovsky, G.A., *An Assessment of Stress-Strain Data Suitable for Finite-Element Elastic Plastic Analysis of Shipping Containers*, NUREG/CR-0481, September 1978.
6. Avallone, E., A., Baumeister III, T., *Marks' Standard Handbook for Mechanical Engineers*, 9th Edition, New York, McGraw-Hill Book Co., 1987.
7. “NS-4-FR with 0.6WT% Boron Carbide for Consolidated Fuel Storage Cask Application,” Technical Report No. NS-4-025 Rev. 0, GESC Shield Materials, January 8, 1988.
8. “NS-4-FR Fire Resistant Neutron and/or Gamma Shielding Material,” Technical Data, GESC Shield Materials.
9. “Aluminum Standards and Data,” The Aluminum Association Incorporated, 900 19th Street NW Washington, DC, 1997.

**NAC INTERNATIONAL RESPONSE
TO
REQUEST FOR SUPPLEMENTAL INFORMATION**

OBSERVATIONS

2.0 STRUCTURAL AND MATERIALS EVALUATION

STRUCTURAL EVALUATION

2-2 Design, Modeling, and Qualification of Impact Limiters

1. Section 2.6.7.5, Impact Limiter. Provide sufficient physical attribute details, including wood block grain orientation and associated gusset partitioning, if any, for the impact limiter balsa sleeve and center sections. It is unclear how the two large pieces of balsa wood center and sleeve sections can be produced and assembled without sufficient drawing details, including gusset partitioning. Sufficient design details are needed to ensure proper implementation of a LS-DYNA impact limiter finite element model in calculating free drop cask response.
2. Section 2.6.7.5.1, Impact Limiter Evaluation. For the eight HAC drops, conditions cold and hot included, provide bounding hard copy LS-DYNA impact limiter part deformation plots, with sufficient annotations, to delineate the crush depths corresponding to those reported in Table 2.6.7-38.

The reported crush depths suggest various degrees of material lock ups of the wood impact limiter. This information is needed to facilitate staff review of the benchmarking and performance of the impact limiter finite element model.

3. Table 2.6.7-38. For the same 30-ft HAC oblique drop, explain why a larger crush depth is calculated for the condition cold than for the hot. Explain also the seemingly inconsistent acceleration values, which are considered for selecting the baseline decelerations for evaluating the cask system and components.

NAC International Response to RSI 2-2

1. The MAGNATRAN impact limiter was revised to simplify the design and Section 2.6.7.5 has been revised to include figures showing a cut away view of the revised impact limiter and the materials. Figures are included which define the grain orientation of the individual sections of the impact limiter and dimensions associated with the design. These details and the dimensions are sufficient to generate a finite element model.
2. Deformation plots of the impact limiters have been included in the NAC Proprietary calculation 71160-2138. A separate table has been provided in SAR (e.g. Table 2.6.7-37) and the calculation to define the bounding case. Since the plots contained in the calculation show the deformation and the tables define the numerical values, the figures themselves do not need to show the actual values of crush in the figure.

Table 2.6.7-37 reports the crush depth as well as the percent of volumetric change, which is consistent with the LS-DYNA input for material models used in the impact limiter evaluation. The maximum crush reported is for the side drop and is 65%. This occurs in only one of the six radial segments of each impact limiter being crushed in the side drop. The 65% strain does not occur in the other radial segments of the impact limiter. It is noted that this occurs for the hot condition, in which the crush properties have been reduced by an additional 10% for all the redwood segments in the impact limiter for the side drop. The end drop represents a condition in which the impact limiter is uniformly crushed, and the strain reported in Table 2.6.7-37 shows a maximum value of 54%, which also includes a 10% reduction in all the balsa wood properties. Table 2.6.7-33 contains the balsa wood properties and at this strain level. Lock up of the material is not being experienced. The maximum strain contained in this table is 60%, which also does not reflect a lock up condition, since the final value is only a 14% increase of the 50% strain value. Further stress-strain data beyond 60% is not required for the evaluations.

3. The MAGNATRAN impact limiter was revised to be similar to the previous impact limiters tested in a quarter scale test by NAC International. In the quarter scale test program only the end drop and the corner drops were performed to assess the behavior of the balsa wood impact limiter. The end drop and corner drop orientations have been evaluated and the results are shown in Table 2.6.7-37. The oblique drop for the revised design was not required due to the design revision. Table 2.6.7-37 shows that for all orientations, the crush depths and associated strains are larger for the hot condition as compared to the cold condition.

**NAC INTERNATIONAL RESPONSE
TO
REQUEST FOR SUPPLEMENTAL INFORMATION**

OBSERVATIONS

2.0 STRUCTURAL AND MATERIALS EVALUATION

STRUCTURAL EVALUATION

2-3 Stress Acceptance Criteria for the Closure Lid Bolt Subject to Secondary Impact

Table 2.1.2-2, Allowable Stress Limits for Containment Structures. Revise the table by adding stress allowable for the closure lid bolts. Provide justification for considering only the maximum axial stress for the bolts subject to the end-drop secondary impact, as evaluated in Section 2.6.7.6.2 and 2.7.1.7.2 for the NCT and HAC cask free end drops, respectively.

It's unclear why the bolts are not evaluated also for other stress performance criteria, including the primary membrane-plus-bending category at the periphery of the bolt cross section resulting from prying action produced by deformation of the connected parts, per ASME, Section III, Appendix F, Section F-1335.1.

NAC International Response to RSI 2-3

Section 2.6.7.6 and Section 2.7.1.7.1 present the evaluations of the cask closure lid for the normal conditions and accident conditions of transport. In both of these sections, it is stated that the criteria for evaluation are contained in NUREG/CR-6007. Since the evaluation by NUREG/CR-6607 involves interaction equations and it is specifically used for the closure bolts, these are not included in the general stress criteria in Table 2.1.2-2.

A recent decision by the USNRC staff has led to the removal of the secondary impact evaluations for the impact limiter and for the closure lid. Further evaluations for the closure bolts for this loading condition have not been included.

**NAC INTERNATIONAL RESPONSE
TO
REQUEST FOR SUPPLEMENTAL INFORMATION

OBSERVATIONS**

2.0 STRUCTURAL AND MATERIALS EVALUATION

STRUCTURAL EVALUATION

2-4 Factor of Safety for PWR Basket Geometric Instability

Section 2.7.13.1, PWR Basket Stability. Re-evaluate geometric instability potential of the PWR basket for an acceptable factor of safety, per the ASME Code Section III, Appendix F, Section F-1341.4 provisions. For the design weight multiplier selection, as described in the top paragraph of page 2.7.13.1-5, the basket weight must also be considered in addition to the fuel assemblies.

The collapse load analysis as called out, per Section F-1341.3, applies to the load determined by a "limit analysis" rather than the kinematically strain hardening analysis considered in the application. The staff considers the Section F-1341.4 provisions acceptable for which the applied load shall not exceed 0.7 PI, in determining the minimum factor of safety for the basket geometric instability evaluation.

NAC International Response to RSI 2-4

As per ASME Section III, Appendix F, Subsection F-1341.4, the minimum factor of safety for the basket stability evaluation is 1.4 (i.e., $1/0.7$). In the PWR Basket stability evaluation, inertial loading applied to the basket is due to the deceleration of the cask due to the impact limiters. A factor of 1.2 was applied to the acceleration time history, which applied the inertial loading to the basket. There is also a factor of 1.2 applied to the mass of the basket assembly. This extra mass is lumped with the mass of the fuel elements representing the fuel assemblies. Therefore, the increase in mass and acceleration results in a combined factor of 1.44 applied to the inertial load on the basket assembly. It is concluded that the factor of safety for the PWR basket stability evaluation for the cask side drop accident is greater than 1.4. This method is also applied to the BWR basket stability evaluation. This discussion is added to Sections 2.7.13.1 and 2.7.13.2 for the side drop stability evaluation for the PWR and BWR basket designs, respectively.

**NAC INTERNATIONAL RESPONSE
TO
REQUEST FOR SUPPLEMENTAL INFORMATION
OBSERVATIONS**

2.0 STRUCTURAL AND MATERIALS EVALUATION

STRUCTURAL EVALUATION

2-5 Figures 2.6.13-3 and 2.6.13-4. Explain why two different element discretization schemes are used for the "pin" in analyzing the same PWR baskets but for different drop orientations.

NAC International Response to RSI 2-5

Figures 2.6.13-3 and 2.6.13-4 show two different finite element models. The 45° model is not generated from the 0° model. A different meshing scheme at the pin was required since the symmetry plane cuts through the actual pin itself in a different manner between the 0° model and the 45° model. The pin shown in Figure 2.6.13-3 for the 0° model cannot be divided along the diagonal. While this would only affect the pins at the plane of symmetry, the model was generated such that the pin mesh would be the same whether the pin model was at the plane of symmetry or away from the plane of symmetry. As a result, the two meshes will have a different appearance in the pin region.

**NAC INTERNATIONAL RESPONSE
TO
REQUEST FOR SUPPLEMENTAL INFORMATION**

OBSERVATIONS

2.0 STRUCTURAL AND MATERIALS EVALUATION

STRUCTURAL EVALUATION

2-6 Table 2.6.14-9. Verify that the maximum stresses are correctly reported for fuel tubes.

Tube No. 12 for which all maximum stresses are reported is not delineated in Figure 2.6.14-4 for the 45° side-drop basket orientation.

NAC International Response to RSI 2-6

Figure 2.6.14-4 states in the note on the figure, "Note: Tube numbers 1, 8, and 12 are omitted." Tube 12 (and tubes 1 and 8) are the DF slot locations and are shown on Figure 2.6.14-6. The reference in Table 2.6.14-9 was altered to reference Figure 2.6.14-4, which shows Tubes referenced in Table 2.6.14-9. An additional note was added to Figure 2.6.14-4: "Tube numbers 1, 8 and 12 are shown in Figure 2.6.14-6," and in addition, labels were added to Figure 2.6.14-6 that clearly identify which tube is 1, 8 and 12.

A similar situation exists for Figure 2.6.14-3. This figure has the following note: "Note: Tube numbers 3 and 11 are omitted." An additional note was added to Figure 2.6.14-3: "Tube numbers 3 and 11 are shown in Figure 2.6.14-5." In addition, labels were added to Figure 2.6.14-5 that clearly identify which tube is 3 and which tube is 11.

All stress tables for the PWR, PWR DF and BWR basket evaluations were reviewed to confirm that the stresses for both normal and accident conditions of transport are reported correctly.

**NAC INTERNATIONAL RESPONSE
TO
REQUEST FOR SUPPLEMENTAL INFORMATION**

OBSERVATIONS

3.0 THERMAL EVALUATION

3-1 It is stated that some portions of the outer package, such as the fins, are made of aluminum. Confirm that the aluminum will not reach an ignition temperature.

NAC International Response to RSI 3-1

The cask fins are made of copper, while the cover plate for cooling fin-B is made of aluminum. The maximum cask surface temperature for PWR and BWR configurations is 246°F and 238°F (Table 3.4-1 of the SAR) for normal condition, respectively. Those temperatures are well below the aluminum melting temperature.

During the fire accident, the maximum cask surface temperature is 1443°F for both PWR and BWR configurations. This exceeds the aluminum ignition temperature of 1440°F for layer. The ignition temperature of 1440°F was obtained from the website:

http://www.ccohs.ca/oshanswers/chemicals/chem_profiles/aluminum_powder/working_alu.html

In the fire accident analyses, the aluminum cover plate's temperature will exceed its melting point before the ignition temperature is reached. Since the cover plates are on the exterior surface of the cask, and would not be restrained by any component of the cask, the cover plates will leave the cask surface. Therefore in the fire accident evaluation, the cover plates are assumed to be removed at the initiation of the fire accident condition.

**NAC INTERNATIONAL RESPONSE
TO
REQUEST FOR SUPPLEMENTAL INFORMATION**

OBSERVATIONS

3.0 THERMAL EVALUATION

- 3-2 It does not appear that the allowable pressure of the containment boundary is explicitly mentioned in Chapter 3, such as in Table 3.4-3; this information should be provided.

NAC International Response to RSI 3-2

The applicable allowable pressure of the containment boundary is added as shown in Table 3.4-3 for the normal condition and in Table 3.5-3 for the accident condition.

**NAC INTERNATIONAL RESPONSE
TO
REQUEST FOR SUPPLEMENTAL INFORMATION
OBSERVATIONS**

3.0 THERMAL EVALUATION

3-3 Page 3.5-2 states that the NS-4-FR neutron shield does not withstand the fire and is replaced with air during the post fire analysis. Does the material reach a temperature where it no longer acts as a barrier during the fire? If so, the air void should replace the shield before the 30 minute fire ends; this would be more conservative during the fire.

NAC International Response to RSI 3-3

In the fire accident analyses for both PWR and BWR configurations, the NS-4-FR neutron shield remains functional during the 30-minute fire and is replaced by air after the fire accident. 1) The functional NS-4-FR allows more heat to enter into the cask since it has higher thermal conductivities than air. 2) The air replacing the NS-4-FR right after the fire traps more heat inside the cask after the fire.

Both 1) and 2) are conservative and result in higher calculated component temperatures for the fire accident than what will actually be developed in the physical hardware.

If the air void replaces the shield before the 30-minute fire ends, this would not be a conservative assumption during the fire.

**NAC INTERNATIONAL RESPONSE
TO
REQUEST FOR SUPPLEMENTAL INFORMATION
OBSERVATIONS**

3.0 THERMAL EVALUATION

- 3-4 The allowable temperatures for the components should be listed in Table 3.5-1 and Table 3.5-2; the blanks in the tables should be filled with appropriate values.

NAC International Response to RSI 3-4

The blanks in Table 3.5-1 and Table 3.5-2 for component allowable temperatures have been filled with appropriate values.

**NAC INTERNATIONAL RESPONSE
TO
REQUEST FOR SUPPLEMENTAL INFORMATION
OBSERVATIONS**

3.0 THERMAL EVALUATION

3-5 Document 71160-3014 mentions a transport cask that is not MAGNATRAN. Confirm that the analyses are in fact for MAGNATRAN.

NAC International Response to RSI 3-5

In calculation 71160-3014, NAC-NEWGEN is used for the cask name, which was the original name of the MAGNATRAN cask. Therefore, the analyses are in fact for MAGNATRAN.

**NAC INTERNATIONAL RESPONSE
TO
REQUEST FOR SUPPLEMENTAL INFORMATION
OBSERVATIONS**

3.0 THERMAL EVALUATION

3-6 Color temperature contour plots should be provided in Document No. 71160-3045.

NAC International Response to RSI 3-6

All supporting calculations are being provided in color as part of the resubmittal of the MAGNATRAN application.

**NAC INTERNATIONAL RESPONSE
TO
REQUEST FOR SUPPLEMENTAL INFORMATION

OBSERVATIONS**

4.0 CONTAINMENT EVALUATION

- 4-1 Page 4-1 states that "No normal condition of transport or hypothetical accident condition results in releases of the TSC contents into the cask cavity or releases from the MAGNATRAN cask containment boundary into the atmosphere." Similar statements are made on pages 4.2-1 and 4.3-1. Considering the potential for long term storage, the basis for concluding that TSC contents cannot be released into the MAGNATRAN cask during NCT and HAC should be provided.

NAC International Response to RSI 4-1

As the MAGNATRAN transport cask provides 10 CFR 71 containment of the contents, the statements regarding TSC integrity under all conditions are removed from Chapter 4. The wording is revised to a more general description indicating that a typical load is expected to be a sealed TSC. A sealed TSC load is a conservative configuration as the TSC would have retained its high pressure helium backfill, which then can be released into the cask cavity. Both normal and HAC pressures shown in Chapter 3 are based on a TSC content release after loading into the transport cask.

**NAC INTERNATIONAL RESPONSE
TO
REQUEST FOR SUPPLEMENTAL INFORMATION**

OBSERVATIONS

5.0 SHIELDING EVALUATION

- 5-1 The staff finds that more justification and possibly a CoC condition for verifying the peaking factors and the burnup profiles for the shielding analysis are required. The staff does not find adequate justification that those used for PWR and BWR fuel are bounding for all fuel assemblies that are to be transported in the MAGNATRAN. In its review of MAGNASTOR (Docket No. 72-1031, reference the staff's SER on MAGNASTOR, Rev. 0, ML090350589) the staff discusses that the use of 1.08 for PWR fuel is not consistent with the guidance in NUREG/CR-6801.

NAC International Response to RSI 5-1

NAC acknowledges that the NRC review staff has indicated that the NUREG/CR-6801 peaking factor of 1.108 should be applied for generic PWR shielding analyses (NRC staff SER on MAGNASTOR). The cited NUREG is a burnup credit guidance document that NAC does not consider an appropriate reference for shielding guidance. It is specifically designed to produce underburned ends which are controlling for burnup credit applications, not necessarily conservative or appropriate for a shielding analysis.

The two primary references forming the input basis to NUREG/CR-6801 are the DLC-201 database ("Axial Burnup Profile Database for Pressurized Water Reactors", YAEC-1937) and Parish and C.H. Chen (Bounding Axial Profile Analysis for the Topical Report Database). The Parish and Chen report in turn references an earlier YAEC report for data (YAEC-1918). NAC's MAGNATRAN SAR Section 5.3.1 bases its 1.08 shape on the earlier, more plant limited, YAEC data. The SAR then follows the initial discussion with Figure 5.3-5, which demonstrates that the chosen shape is applicable to the more encompassing data set in YAEC-1937.

It should be noted that within the profile section of the SAR (Section 5.3) NAC justifies that significantly higher peaked values are acceptable for lower burned fuel.

In the context of the shielding analysis for the MAGNATRAN cask, a difference of ~3% between the NRC proposed and the NAC peak profile does not justify a CoC limitation as the suggested

NAC International Response to RSI 5-1 (cont'd)

profile change does not have a significant safety impact. The change if applied would not result in an increase in the limiting reported maximum dose rates. Further detail on this statement is provided below:

- Dose effect at peak burnup profile location – Applying a fourth power relationship between neutron source and burnup, and a 1.08 to 1.108 burnup peak change, would result in a localized increase in source of approximately 10%. For a pure neutron dose driven peak this would result in 1 mrem/hr change for an at limit 10 mrem/hr calculated design basis condition. This potential increase would be reduced as total dose contains a significant fuel gamma component (affected proportional to the 3% change in profile peak), fuel hardware component (not impacted based on analysis method), and non-fuel hardware component (not affected by analysis method), and a smearing out of the localized peak at the bounding 2 meter dose location. To achieve any resolvable change in calculated dose a significant number of the assemblies on the periphery of the cask would need to be at the higher peak, an unlikely scenario based on the fuel profile database used in the analysis. Overall, the effect at the mid-plane of a higher peaked payload is therefore expected to be minor. As discussed in the next bullet, the location of the peak profile is not the location of the maximum system dose.
- Maximum dose location and profile effect – The maximum dose location for both PWR and BWR systems (see Figure 5.8-13, PWR, and Figure 5.8-25, BWR) is not at the burnup profile peak location. The peak dose is associated with reduced shielding near the top of the cask cavity. The majority of the peak dose is hardware fuel assembly and non-fuel hardware driven with the remaining dose associated with fuel source near the fuel ends. There is no impact on maximum dose of a postulated burnup peak in either PWR or BWR systems.

Based on the arguments provided above, NAC believes the profiles used in the MAGNATRAN application provide reasonable assurance that cask dose limits will be met and that a CoC limitation on profile peak is not appropriate.

**NAC INTERNATIONAL RESPONSE
TO
REQUEST FOR SUPPLEMENTAL INFORMATION

OBSERVATIONS**

5.0 SHIELDING EVALUATION

5-2 (See Observation 1 of Amendment 3 of the MAGNASTOR System Docket No. 72-1031, ML103060029). The source spectra for gamma and neutron source terms for the shielding analysis for high burnup fuels were not included in the SAR. In general, the source spectra are necessary information for the staff to determine if the application meets the regulatory requirements of the cask shielding design. This information is missing in the SAR.

NAC International Response to RSI 5-2

Section 5.2 (subsection 5.2.3) contains source terms producing the limiting dose, in this case for the cases producing maximum cask surface dose while maintaining the radial 2 meter dose maximum at or below 10 mrem/hr. Under these conditions maximum dose is obtained from lower burnup source configurations. Cask radial maximum dose rates are produced near the top of the cask cavity where hardware activation and decay are the controlling mechanism. High burnup fuels require extended cool times which reduce this phenomenon. As documented in Section 5.1, maximum dose rates for axial detectors are produced by high burnup fuel. Section 5.2.3 was revised to include the top axial source term from the 14b hybrid assembly type.

**NAC INTERNATIONAL RESPONSE
TO
REQUEST FOR SUPPLEMENTAL INFORMATION**

OBSERVATIONS

5.0 SHIELDING EVALUATION

- 5-3 The staff finds that the description of the damaged fuel evaluations for the shielding analysis is not clear. The SAR states that there are two modeling strategies for damaged fuel. Presumably the one that produces higher dose rates is used in the dose rate calculations, but the staff did not see this explicitly stated. In addition, the staff is not clear on the modeling of the damaged fuel within the MCNP shielding calculation.

NAC International Response to RSI 5-3

The SAR was revised in all applicable sections (starting in Section 5.1.2.2) to clarify that two scenarios (strategies) for fuel redistribution were evaluated and that the reported dose rates are obtained from the bounding scenario (the one producing maximum dose rates).

The “active fuel region” scenario was previously stated to not increase dose rates over that of the undamaged fuel configuration. “Non-fuel hardware region” shifts were indicated to increase dose rates. The NRC requested statement clarifies that the analysis results represented the maximum dose, bounding, non-fuel hardware scenario and has been added.

**NAC INTERNATIONAL RESPONSE
TO
REQUEST FOR SUPPLEMENTAL INFORMATION**

OBSERVATIONS

8.0 ACCEPTANCE TESTS AND MAINTENANCE EVALUATION

8-1 There is only 36°F margin between neutron shield temperature and its allowable temperature. Considering that the neutron shield is made of polymer, which can degrade over time due to radiation and temperature, confirm that the NS-4-FR shield will retain its thermal properties throughout the package lifetime. Periodic acceptance tests may have to be performed to confirm consistent thermal properties.

NAC International Response to RSI 8-1

The original material formulation owner/developer, Dow and Bisco Products, has published material specification technical data information stating that NS-4-FR retains long term functional stability at temperatures from -40°F to 300°F. In addition to this specific data, Bisco Products has performed thermal tests showing stability of the material through temperatures as high as 338°F. Beyond this data developed by Bisco Products, over the past ten years or more several organizations associated with the current owner of the NS-4-FR technology have performed independent investigations of off gassing and material loss when NS-4-FR is confined in different configurations and exposed to temperature both less than and greater than 300°F. The following reports are enclosed herewith:

- 1) Experimental Studies on Long-term Thermal Degradation of Enclosed Neutron Shielding Resin, R. Asano and N. Niomura.
- 2) Evaluation Test on the Thermal Stability of Resin as Neutron Shielding Material for Spent Fuel Transport Cask, Y. Momma, M. Matsumoto, M. Takani, et. al.

In summary, these reports document material stability under a number of different conditions and temperatures ranging from 125°C (257°F) through 200°C (392°F). Both tests demonstrate that NS-4-FR is a stable material without any observed failures in the form of cracks at prolonged exposure to temperatures above the published specification limit of 300°F. Based on these test results demonstrating NS-4-FR material stability at temperatures above the identified design limits defined in the MAGNATRAN design application, periodic acceptance testing is not required.

RSI and RSI Observations Supporting Documents

RSI 3-7:

- Wix, S.D., G.F. Hohnstreiter, "Convective Effects in a Regulatory and Proposed Fire Model," PATRAM '95, December 1995.

RSI Observation 2-1:

- Reference 2: Boyer, Howard E., *Metals Handbook Desk Edition*, American Society for Metals, Metals Park, Ohio, 1985.
- Reference 3: *ASME Boiler and Pressure Vessel Code, Case N-707*, Use of SA-537, Class 1 Plate for Spent-Fuel containment Internals in Non-pressure retaining Application above 700°F (370°C), Section III, Division 3, The American Society of Mechanical Engineers, New York, 2004.
- Reference 4: Tietz, T.E., "Determination of the Mechanical Properties of High Purity Lead and a 0.05% Copper-Lead Alloy," WADC Technical Report 57-695, ASTIA Document Number 151165, Stanford Research Institute, Menlo Park, CA, April 1958.
- Reference 5: SAND77-1872, Rack, H.J., Knorovsky, G.A., *An Assessment of Stress-Strain Data Suitable for Finite-Element Elastic Plastic Analysis of Shipping Containers*, NUREG/CR-0481, September 1978.
- Reference 6: Avallone, E., A., Baumeister III, T., *Marks' Standard Handbook for Mechanical Engineers*, 9th Edition, New York, McGraw-Hill Book Co., 1987.
- Reference 7: "NS-4-FR with 0.6WT% Boron Carbide for Consolidated Fuel Storage Cask Application," Technical Report No. NS-4-025 Rev. 0, GESC Shield Materials, January 8, 1988.
- Reference 8: "NS-4-FR Fire Resistant Neutron and/or Gamma Shielding Material," Technical Data, GESC Shield Materials.
- Reference 9: "Aluminum Standards and Data," The Aluminum Association Incorporated, 900 19th Street NW Washington, DC, 1997

RSI Observation 3-6:

- Color Temperature Contour Plots

RSI Observation 8-1:

- "Experimental Studies on Long-term Thermal Degradation of Enclosed Neutron Shielding Resin," R. Asano and N. Niomura.
- "Evaluation Test on the Thermal Stability of Resin as Neutron Shielding Material for Spent Fuel Transport Cask," Y. Momma, M. Matsumoto, M. Takani, et. al

Proceedings

Volume II



PATRAM'95

Packaging and Transportation of Radioactive Materials

The 11th International
Conference on the Packaging
and Transportation of Radioactive
Materials (PATRAM '95)

December 3-8, 1995
Las Vegas, Nevada, USA

Convective Effects in a Regulatory and Proposed Fire Model¹

*S.D. Wix
GRAM, Inc.*

*G.F. Hohnstreiter
Sandia National Laboratories*

INTRODUCTION

Radiation is the dominant mode of heat transfer in large fires. However, convection can be as much as 10 to 20 percent of the total heat transfer to an object in a large fire. The current radioactive material transportation packaging regulations include convection as a mode of heat transfer in the accident condition scenario. The current International Atomic Energy Agency (IAEA) Safety Series 6 packaging regulation states, "the convection coefficient shall be that value which the designer can justify if the package were exposed to the specified fire." The current Title 10, Code of Federal Regulations, Part 71 (10 CFR 71) packaging regulation states "when significant, convection heat input must be included on the basis of still, ambient air at 800°C (1475°F)." Two questions that can arise in an analyst's mind from an examination of the packaging regulations are whether convection is significant and whether convection should be included in the design analysis of a radioactive materials transportation container. The objective of this study is to examine the convective effects on an actual radioactive materials transportation package using a regulatory and a proposed thermal boundary condition.

A single thermal model with six thermal boundary conditions was used in this analysis. The thermal boundary conditions were the regulatory thermal environment with and without convective effects, and a proposed thermal environment with and without convection. The proposed thermal environment is from a paper presented at PATRAM'92 by Chris Fry (1992).

The proposed thermal environment was designed for modeling two types of transportation casks. The first type contains low activity material which generates negligible heat and thermal protection provided by an insulating layer on the container exterior. The second type contains highly active materials and thermal protection is based on high thermal capacitance of the transportation cask.

The thermal model developed for this study is based on the Beneficial Uses Shipping System (BUSS) cask. The BUSS cask is a Type B shipping container used for non fissile

¹ This work was supported by the U.S. Department of Energy under Contract DE-AC04-4 AL85000

radioactive materials shipment. The dimensions of the BUSS cask body are 1.24 m long by an outer diameter of 1.38 m. The BUSS cask body weight is 9,300 kg.

THERMAL MODEL DESCRIPTION

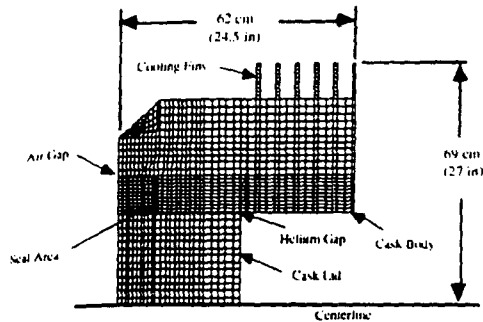


Figure 1. Thermal Model

The thermal model is a two-dimensional axisymmetric representation of the cask. Another simplifying assumption is that half the length of the cask was modeled. The model consists of 1,457 nodes and 1,319 elements. PATRAN was used for pre- and postprocessing of the analysis, while P/THERMAL was used as the thermal solver. Temperature-dependent material properties were used in the analysis. Figure 1 presents the thermal model.

The materials in the cask, and simulated in the thermal model, were stainless steel, air, helium, and silicone rubber. The cask lid and body material were stainless steel. The gap between the cask lid and body was filled with air on the outside of the seal and helium on the inside of the seal. The seal material was silicone. Temperature-dependent thermal conductivity was used for the stainless steel, air, and helium, while the silicone thermal conductivity was constant. Table 1 presents the material thermal transport properties used in the model. All material properties presented in Table 1 are at 25°C.

Material	Thermal Conductivity (W/m-K)	Density (kg/m ³)	Specific Heat (J/kg-K)
Stainless Steel	13.4	7920	502
Air	0.0242	0.177	5191
Helium	0.141	1.29	992
Silicone	0.138	1300	1256

Table 1. Material Properties used in the Thermal Model

THERMAL BOUNDARY CONDITIONS

Six different thermal boundary conditions were applied to the cask thermal model. The first set of three thermal boundary conditions was based on the IAEA Safety Series No. 6 regulations. The second set of three thermal boundary conditions was based on the proposed thermal environment.

The IAEA Safety Series No. 6 boundary conditions consist of an 800°C environment temperature with an emissivity of 0.9, and a package surface emissivity of 0.8 for 30 minutes. After 30 minutes, the ambient temperature drops to 38°C for the subsequent cool down period. Convection was included in two of the thermal boundary conditions, and the convection coefficients used were 5 and 10 W/m². These convective coefficient values are typical for natural convection.

The proposed thermal environment is a modification of the IAEA Safety Series 6 regulatory thermal environment. The modifications are raising the environmental temperature to 1100°C and including a reduction factor of 0.3. The reduction factor is equivalent to a flame emissivity but physically represents a reduced effective flame temperature adjacent to the container surface and ensures the heat flux specified in the IAEA regulations is met. The thermal environment is modeled with the following equation.

$$Q = 0.3\epsilon\sigma\left[(1100 + 273)^4 - (T_s + 273)^4\right] + h(1100 - T_s)$$

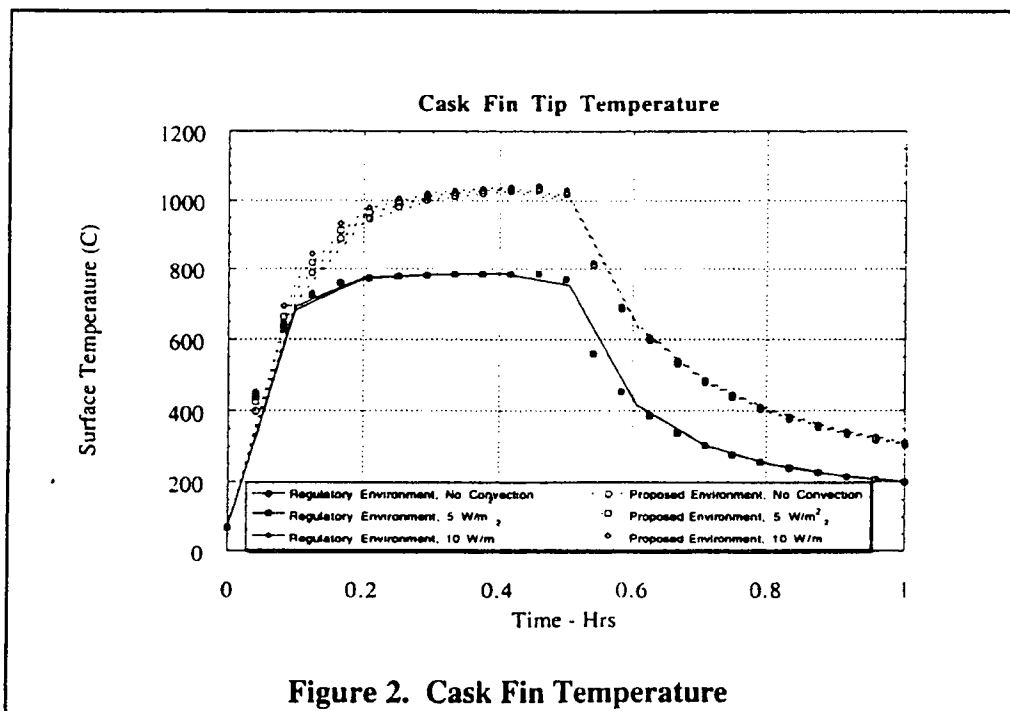
where,

ϵ is the emissivity of the container surface,

σ is the Stefan-Boltzman constant,

T_s is container surface temperature (°C), and,

h is the convection coefficient.



The package surface emissivity was not specified in the proposed thermal boundary conditions, so the IAEA regulation package surface emissivity of 0.8 was used. The duration of the proposed thermal environment is 30 minutes, after which the environmental temperature drops to 38°C for the subsequent cool down period. Convection was included in two of the thermal boundary conditions and the convection coefficients used were 5 and 10 W/m².

RESULTS

Figures 2 and 3 present time-temperature plots of the cask fin tip temperature and the cask seal area temperature, respectively. The cask fin tip is where the highest temperature on the cask occurred. The cask fin tip temperature difference due to convection for the regulatory environment is small when compared to the proposed environment. The larger cask fin tip temperature difference in the proposed environment is due to the greater sensitivity to convection.

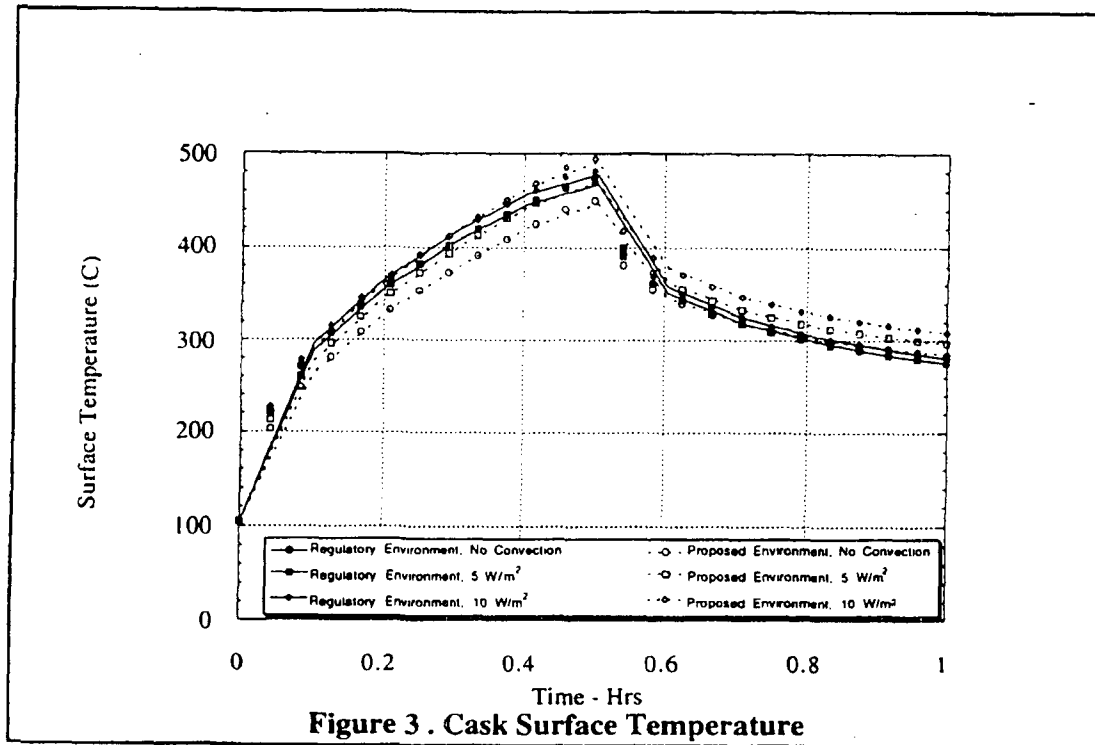


Figure 3 shows that adding convection does not dramatically increase the seal temperature for this model. For the regulatory environment, the increase in seal area temperature due to convection is between 5 and 10 °C. For the proposed environment, the increase in seal area temperature is between 10 and 20° C. Again these results point to the greater sensitivity to convection for the proposed environment.

Figure 4 presents the total calculated surface heat flux for all thermal boundary conditions. The total surface heat flux was calculated using two methods. The first method was for the regulatory environment and used the following equation.

$$Q = \epsilon_s \sigma \left[\epsilon_f (800 + 273)^4 - (T_s + 273)^4 \right] + h(800 - T_s)$$

where,

ϵ_s is the emissivity of the container surface, and,
 ϵ_f is the emissivity of the flame.

The second method was for the proposed environment and used the equation that defined the proposed environment. Since the cask surface temperature was known from the calculations, the total heat surface heat flux for both environments was calculated.

The maximum surface heat fluxes for the regulatory environment were 51.3 W/m², 53.9 W/m², and 56.4 W/m² for no convection and convection coefficients of 5 W/m² and 10 W/m², respectively.

The maximum surface heat fluxes for the proposed environment were 47.6 W/m², 51.8 W/m², and 56.0 W/m² for no convection and convection coefficients of 5 W/m² and 10 W/m², respectively.

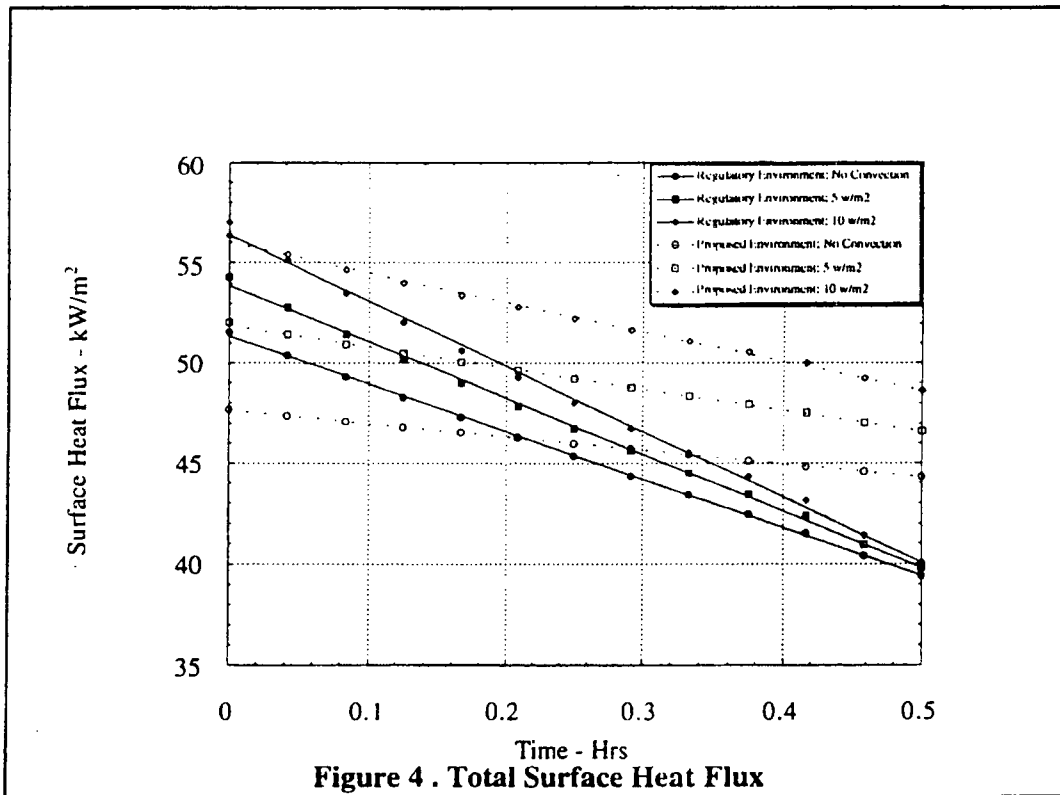


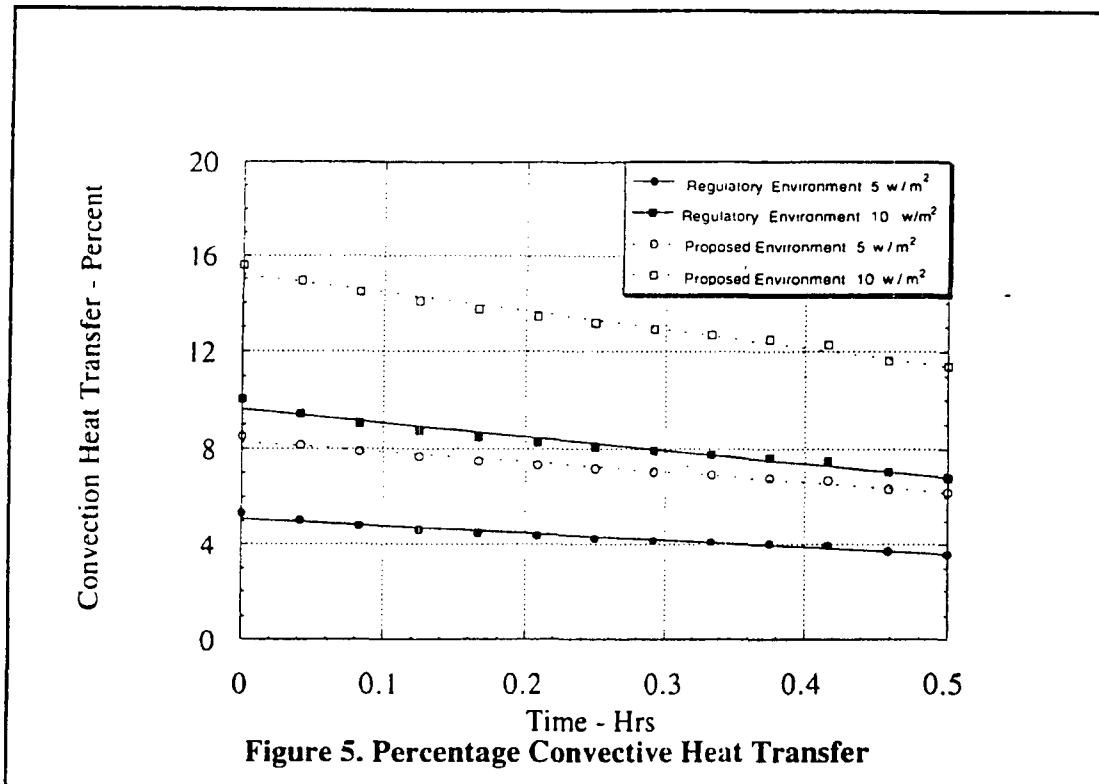
Figure 5 presents the percentage amount of convective heat transfer for both thermal environments. The percentage of convective heat transfer, when compared to the total heat transfer, for the regulatory environment was 5.1 for 5 W/m² and 9.6 for 10 W/m².

For the proposed environment, the percentage of convective heat transfer was 9.3 for 5 W/m² and 15.2 for 10 W/m². Again Figure 5 shows the increased sensitivity to convective heat transfer for the proposed environment.

CONCLUSIONS

Convection contributes between 5 and 9 percent of the total heat flux for the regulatory fire, assuming a range of between 5 and 10 W/m² for the convective heat transfer coefficient. Again assuming a range of 5 to 10 W/m² for a convective heat transfer

coefficient, the convective heat transfer loading is between 9 and 15 percent for the proposed thermal environment.



An equivalent maximum heat flux between the regulatory and proposed thermal environment can occur by including convection as a heat transfer mechanism. To make the environments approximately equivalent for the maximum surface heat flux, a convection coefficient of 5 W/m² for the proposed environment and no convection for the regulatory environment can be used. Of course there exist an infinite number of combinations between the regulatory and proposed environments to make the maximum surface heat flux equivalent.

Experimental data indicate that convection contributes between 10 and 20 percent toward the total surface heat flux. Therefore, a minimum heat transfer coefficient of 10 W/m² is recommended.

Including convection doesn't greatly affect seal temperature in this case due to the massive size and amount of thermal capacitance. However, the convection component will affect thin, low-capacitance components, such as fins.

REFERENCES

IAEA Safety Series 6. *Regulations for the Safe Transport of Radioactive Material*, 1985 Edition as amended in 1990 (1990).

Title 10, Code of Federal Regulations, Part 71, Nuclear Regulatory Commission, Washington, D.C., (January 1991).

Nakos, J. T., and Keltner, N.T., *The Radiative-Convective Partitioning of Heat Transfer to Structures in Large Pool Fires*, Heat Transfer Phenomena in Radiation, Combustion, and Fires, The American Society of Mechanical Engineers (1989).

Fry, C. J., *An Experimental Examination of the IAEA Fire Test Parameters*, Proc., 10th International Symposium on the Packaging and Transportation of Radioactive Materials, (PATRAM'92), Yokohama Japan (August 1992).

PATTRAN 2.5 Users Manual, PDA Engineering, Costa Mesa, Ca (1991).

P/THERMAL Users Guide, PDA Engineering, Costa Mesa, Ca (1991).

METALS HANDBOOK®

Desk Edition

Edited by
Howard E. Boyer
Timothy L. Gall



AMERICAN SOCIETY FOR METALS
Metals Park, Ohio 44073

Copyright © 1985
by the
AMERICAN SOCIETY FOR METALS
All rights reserved

First printing, November 1984

No part of this book may be reproduced, stored in a retrieval system, or transmitted, in any form or by any means, electronic, mechanical, photocopying, recording, or otherwise, without the written permission of the copyright owner.

Metals Handbook is a collective effort involving thousands of technical specialists. It brings together in one book a wealth of information from world-wide sources to help scientists, engineers, and technicians solve current and long-range problems.

Great care is taken in the compilation and production of this volume, but it should be made clear that no warranties, express or implied, are given in connection with the accuracy or completeness of this publication, and no responsibility can be taken for any claims that may arise.

Nothing contained in the Metals Handbook shall be construed as a grant of any right of manufacture, sale, use, or reproduction, in connection with any method, process, apparatus, product, composition, or system, whether or not covered by letters patent, copyright, or trademark, and nothing contained in the Metals Handbook shall be construed as a defense against any alleged infringement of letters patent, copyright, or trademark, or as a defense against any liability for such infringement.

Comments, criticisms, and suggestions are invited, and should be forwarded to the American Society for Metals, Metals Park, Ohio 44073.

Library of Congress Catalog Card Number: 84-71465
ISBN: 0-87170-188-X
SAN: 204-7586

Project Director: Timothy L. Gall
ASM Staff Assistants: Joan L. Tomsic and Judith S. Gibbs
Editorial and production coordination by Carnes Publication Services, Inc.
President: William J. Carnes
Project Manager: Craig W. Kirkpatrick

PRINTED IN THE UNITED STATES OF AMERICA

Approval Date: November 2, 2004

The ASME Boiler and Pressure Vessel Standards Committee took action to eliminate Code Case expiration dates effective March 11, 2005. This means that all Code Cases listed in this Supplement and beyond will remain available for use until annulled by the ASME Boiler and Pressure Vessel Standards Committee.

Case N-707
Use of SA-537, Class 1 Plate Material for Spent-Fuel Containment Internals in Non-pressure Retaining Applications Above 700°F (370°C)
Section III, Division 3

Inquiry: Until such time as Section III, Division 3, incorporates rules for internals, may plate material conforming to the requirements of SA-537, Class 1, ≤ 1 in. (25 mm) thickness, normalized condition, be used at temperatures above 700° (370°C), but not exceeding 850°F (455°C), for spent-fuel containment internals in non-pressure retaining applications?

Reply: It is the opinion of the Committee that, until such time as Section III, Division 3, incorporates rules

for internals, plate material conforming to the requirements of SA-537, Class 1, ≤ 1 in. (25 mm) thickness, normalized condition, may be used at temperatures above 700°F (370°C), but not exceeding 850°F (455°C), for spent-fuel containment internals in non-pressure retaining applications, provided that the ultimate tensile strength, yield strength, and design stress intensity values shall be as listed in Tables 1 and 1M, creep is determined to be negligible, and the following requirements are met:

- (a) Methods for evaluation of negligible creep are described in Subsection NH, para. T-1324.
- (b) Welding procedure and performance qualifications shall be conducted as prescribed in Section IX.
- (c) The design documentation shall reference this Case number.

TABLE 1
TENSILE, YIELD STRENGTH, AND DESIGN
STRESS INTENSITY VALUES
(U.S. CUSTOMARY UNITS)

For Metal Temperature Not Exceeding °F	Tensile Strength, S_u , ksi	Yield Strength, S_y , ksi	Design Stress Intensity, S_m , ksi [Note (1)]
750	67.7	31.5	21.0
800 [Note (2)]	65.4	30.5	20.3
850 [Note (2)]	61.1	29.2	19.5

NOTES:

- (1) The values of S_m do not exceed the lesser of $S_u/3$ or $2/3 S_y$ at temperature.
- (2) Upon prolonged exposure to temperatures above 800°F (425°C), the carbide phase of carbon steel may be converted to graphite.

TABLE 1M
TENSILE, YIELD STRENGTH, AND DESIGN
STRESS INTENSITY VALUES
(SI UNITS)

For Metal Temperature Not Exceeding °C	Tensile Strength, S_u , MPa	Yield Strength, S_y , MPa	Design Stress Intensity, S_m , MPa [Note (1)]
400	466	217	145
425 [Note (2)]	452	211	141
450 [Note (2)]	437	204	136
475 [Note (3)]	395	199	133

NOTES:

- (1) The values of S_m do not exceed the lesser of $S_u/3$ or $2/3 S_y$ at temperature.
- (2) Upon prolonged exposure to temperatures above 800°F (425°C), the carbide phase of carbon steel may be converted to graphite.
- (3) These values are provided for interpolation purposes only. The temperature limit is 455°C (850°F).

The Committee's function is to establish rules of safety, relating only to pressure integrity, governing the construction of boilers, pressure vessels, transport tanks and nuclear components, and inservice inspection for pressure integrity of nuclear components and transport tanks, and to interpret these rules when questions arise regarding their intent. This Code does not address other safety issues relating to the construction of boilers, pressure vessels, transport tanks and nuclear components, and the inservice inspection of nuclear components and transport tanks. The user of the Code should refer to other pertinent codes, standards, laws, regulations or other relevant documents.

PB 131818

WADC TECHNICAL REPORT 57-695
ASTIA DOCUMENT No. 151165

DETERMINATION OF THE MECHANICAL
PROPERTIES OF A HIGH PURITY LEAD AND A
0.058 % COPPER-LEAD ALLOY

THOMAS E. TIETZ

STANFORD RESEARCH INSTITUTE
MENLO PARK, CALIFORNIA

44-P
Photocopy 4160

APRIL 1958

WRIGHT AIR DEVELOPMENT CENTER

NOTICES

When Government drawings, specifications, or other data are used for any purpose other than in connection with a definitely related Government procurement operation, the United States Government thereby incurs no responsibility nor any obligation whatsoever; and the fact that the Government may have formulated, furnished, or in any way supplied the said drawings, specifications, or other data, is not to be regarded by implication or otherwise as in any manner licensing the holder or any other person or corporation, or conveying any rights or permission to manufacture, use, or sell any patented invention that may in any way be related thereto.

Qualified requesters may obtain copies of this report from the ASTIA Document Service Center, Knott Building, Dayton 2, Ohio.

This report has been released to the Office of Technical Services, U. S. Department of Commerce, Washington 25, D. C., for sale to the general public.

Copies of WADC Technical Reports and Technical Notes should not be returned to the Wright Air Development Center unless return is required by security considerations, contractual obligations, or notice on a specific document.

WADC TECHNICAL REPORT 57-695

ASTIA DOCUMENT No. 151165

DETERMINATION OF THE MECHANICAL
PROPERTIES OF A HIGH PURITY LEAD AND A
0.058% COPPER-LEAD ALLOY

THOMAS E. TIETZ

*STANFORD RESEARCH INSTITUTE
MENLO PARK, CALIFORNIA*

APRIL 1958

**MATERIALS LABORATORY
CONTRACT No. AF 33(616)-3785
PROJECT No. 2134**

**WRIGHT AIR DEVELOPMENT CENTER
AIR RESEARCH AND DEVELOPMENT COMMAND
UNITED STATES AIR FORCE
WRIGHT-PATTERSON AIR FORCE BASE, OHIO**

**Carpenter Litho & Prtg. Co., Springfield, O.
700 - May 1958**

FOREWORD

This report was prepared by Stanford Research Institute under USAF Contract No. AF 33(616)-3785. This contract was initiated under Project No. 2134, "Shielding Subsystems," Task No. 73070, "Shielding Materials." The work was administered under the direction of the Materials Laboratory, Directorate of Laboratories, Wright Air Development Center, with Mr. R. F. Klinger acting as project engineer.

This report covers work conducted from July 1956 to September 1957.

This report was prepared by T. E. Tietz of the Department of Metallurgy of Stanford Research Institute, acting as Project Leader, under the supervision of R. H. Thielmann, Chairman of the Metallurgy Department. Acknowledgment is made to Mr. A. Ruotola for his assistance throughout the testing phase of this program.

ABSTRACT

The mechanical properties of a high purity lead and a 0.058% copper-lead alloy were determined at test temperatures of 100, 175, 250, and 325°F.

Tensile properties evaluated included the ultimate strength, elongation, modulus of elasticity, proportional limit, and yield strength. Compression properties evaluated were the modulus of elasticity, proportional limit, and yield strength. Ultimate shear strength and the bearing yield strength and ultimate bearing strength were determined. Stress-creep time curves were obtained for total strain values of 0.2, 0.5, 1.0, and 2.0%, for creep times of from 1 hour to 500 hours.

The data obtained are summarized in graphical and tabular form, in the Experimental Results section of this report.

PUBLICATION REVIEW

This report has been reviewed and is approved.

FOR THE COMMANDER:



RICHARD R. KENNEDY
Chief, Metals Branch
Materials Laboratory

TABLE OF CONTENTS

<u>Section</u>	<u>Page</u>
I INTRODUCTION	1
II TEST MATERIAL	1
III TEST SPECIMENS	3
IV EXPERIMENTAL APPARATUS AND PROCEDURES	3
A. Tensile Tests	3
B. Compression Tests	7
C. Shear Tests	7
D. Bearing Tests	7
E. Creep Tests	11
1. Equipment	11
2. Test Procedure	11
V EXPERIMENTAL RESULTS	14
A. Tensile Tests	14
1. Stress-Strain Curves to Failure	14
2. Elastic Properties	16
3. Effect of Strain Rate	20
B. Compression Tests	20
C. Shear Tests	24
D. Bearing Tests	28
E. Creep Tests	32
VI SUMMARY	33

LIST OF ILLUSTRATIONS

<u>Figure</u>		<u>Page</u>
1	Dimensions of Test Specimens	4
2	Universal Testing Machine	5
3	Tensile Test Assembly	6
4	Compression Test Specimen with Compressometer	8
5	Shear Test Fixture	9
6	Bearing Test Fixture	10
7	Creep Test Units	12
8	Creep Specimen Assembly	13
9	Tensile Stress-Strain Curves to Failure	15
10	Tensile Strength and Elongation as a Function of Test Temperature.	17
11	Tensile Stress-Strain Curves to 2% Strain.	18
12	Tensile Flow Stress vs Test Temperature for Given Values of Strain	19
13	Effect of Strain Rate on the Tensile Stress- Strain Curves at 100 and 250°F.	22
14	Compression Stress-Strain Curves to 5% Strain.	23
15	Compression Flow Stress vs Test Temperature for Given Values of Strain	25
16	Shear Strength vs Test Temperature	28
17	Bearing Stress-Deformation Curves to Failure	29
18	Bearing Yield Strength and Ultimate Strength vs Test Temperature	31

LIST OF ILLUSTRATIONS (Continued)

<u>Figure</u>		<u>Page</u>
19	Total Strain vs Creep Time for High Purity Lead	34
20	Total Strain vs Creep Time for Copperized Lead	35
21	Stress vs Creep Time at Constant Strain Values of 0.2, 0.5, 1.0, and 2.0% for High Purity Lead.	36
22	Stress vs Creep Time at Constant Strain Values of 0.2, 0.5, 1.0, and 2.0% for Copperized Lead.	37

LIST OF TABLES

<u>Table</u>		<u>Page</u>
I	Chemical Composition of Test Materials.	2
II	Tensile Test Results	14
III	Tensile Data--Modulus of Elasticity, Proportional Limit, and Yield Strength.	21
IV	Compression Data--Modulus of Elasticity, Proportional Limit, and Yield Strength.	26
V	Shear Test Results	27
VI	Bearing Test Results	30

DETERMINATION OF THE MECHANICAL PROPERTIES OF A HIGH PURITY LEAD AND A 0.058% COPPER-LEAD ALLOY

I Introduction

The properties of lead make it the most practical shielding material presently available. In the design and development of nuclear-powered aircraft, the structural problem of providing effective over-all shielding with the lowest possible weight is most important, and requires that the mechanical properties of lead be sufficiently known. However, because of its low strength even at room temperature, lead has not been seriously considered as a structural material and its mechanical properties have not been adequately determined. In addition, the few studies which have been conducted on the mechanical properties of lead have been at or near room temperature.

The objective of this program was to determine the tensile, compression, shear, bearing, and creep properties of a commercially pure lead and a lead alloy, at four test temperatures up to 325°F.

II Test Material

The two materials evaluated in this program were a high purity lead (Doe Run Brand refined lead, 99.995% Pb) and a copperized lead (Copperized Doe Run Brand refined lead, 0.058% Cu), supplied by the St. Joseph Lead Company. The eutectic point in the lead-copper system occurs at approximately 0.06% copper. The chemical composition of the two test materials is given in Table I. In the case of the copperized lead, bars extruded from lot I were used for the tensile, shear, and creep specimens, and from lot II for the compression and bearing specimens. The analyses are, for all practical purposes, identical for the two lots of copperized lead.

Manuscript released by author 3 January 1958 for publication as a
WADC Technical Report.

Table I

CHEMICAL COMPOSITION OF TEST MATERIALS

Element	High Purity Lead	Copperized Lead	
		Lot I	Lot II
Pb	99.9951	99.9398	99.9404
Cu	.0001	.0577	.0577
As, Sb, Sn	.0004	.0006	.0004
Fe	.0001	.0001	.0001
Zn	.0002	.0001	.0001
Cd	.0029	.0006	.0005
Ni, Co	.0000	.0000	.0000
Bi	.0006	.0007	.0005
Ag	.0006	.0004	.0003

The lead was extruded by Morris P. Kirk and Sons, Los Angeles, into bar forms having the following cross-sections:

Type of Test	Extruded Cross Section
Tensile and Creep	1/2 x 1-1/4 inches
Compression	1/2 x 1/2 inches
Shear	1/2 inch round
Bearing	1/2 x 4 inches

The extrusion slugs were cast at 900-950°F. The slugs were 12 inches long by 4-1/2 inches in diameter, after cropping, with the exception of the bars for the bearing specimens which were extruded from a single slug, using a different extrusion press. The extrusion was done at room temperature.

III Test Specimens

The dimensions of the four types of test specimens used in this program are given in Figure 1. All test specimens were machined with their axes parallel to the extrusion direction.

All test specimens were given an annealing treatment of 2 hours in an oven at 400°F after machining and prior to testing, in order to remove any cold-work within the specimens due to machining and handling. The grain sizes of the two materials were considerably different, both in the as-received, and in the annealed conditions; the copper addition acted as a grain size refiner. The average annealed grain size of the high purity lead was about 0.55 grains per millimeter and that of the copperized lead about 18 grains per millimeter.

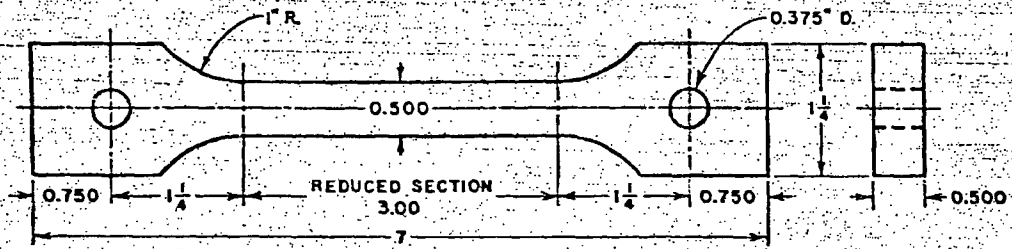
IV Experimental Apparatus and Procedures

The tensile, compression, shear, and bearing tests were conducted with a Baldwin Universal hydraulic testing machine, using a 600-pound full-scale load range. This machine, with a forced air convection furnace, is shown in Figure 2. Figure 2 also shows a dial gage mounted on the movable cross-head which was used to measure and control the cross-head travel rate during testing, and, resting on the table, a Baldwin deflectometer which was used to record the cross-head travel for tests in which cross-head travel was used as the strain measurement. The specimen was placed in the furnace approximately one hour before loading to permit the specimen to attain the test temperature. A thermocouple was attached directly to the test specimen during each test, and the test temperatures were maintained within $\pm 2^\circ\text{F}$.

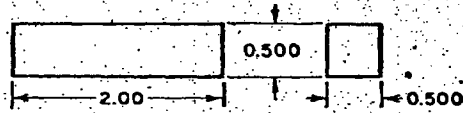
A. Tensile Tests

The tensile test specimens had a reduced cross-section of 1/2 inch x 1/2 inch x 3 inches. Figure 3 shows a tensile specimen with a Baldwin microformer extensometer in place. In this case the central 2 inches served as the gage length. This extensometer was used to evaluate the elastic properties in tension and the tensile stress-strain curve to 2% strain, at a cross-head rate of 0.015 in./min for a strain rate of 0.005 in./in./min.

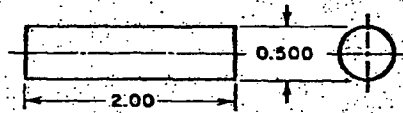
For determining the entire stress-strain curve, the strain was determined by using the deflectometer to measure cross-head travel, and in this case the entire 3-inch reduced section served as the gage length. For these tests, the cross-head rate was maintained at 0.150 in./min for a strain rate of 0.05 in./in./min.



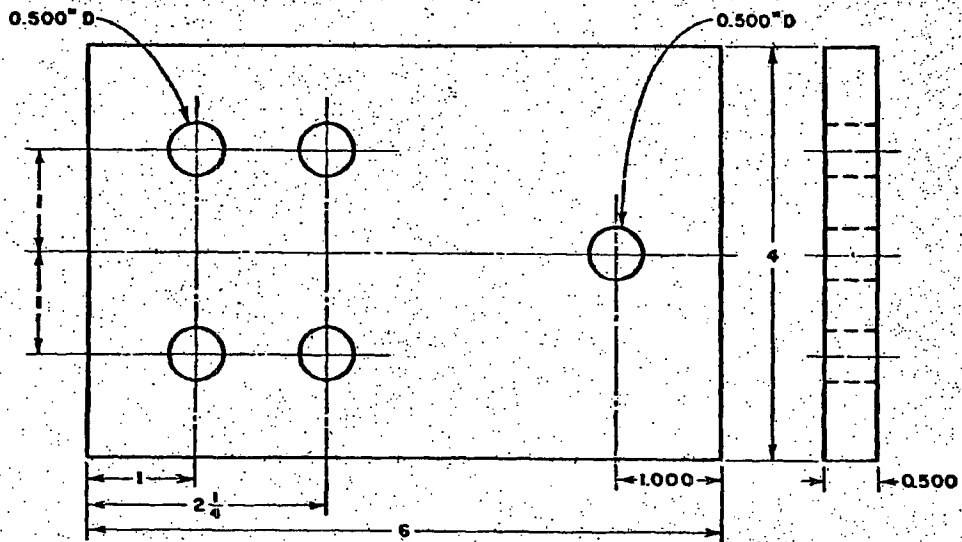
TENSILE AND CREEP SPECIMEN



COMPRESSION SPECIMEN



SHEAR SPECIMEN



BEARING SPECIMEN

8-85-F-26

FIG. 1
DIMENSIONS OF TEST SPECIMENS

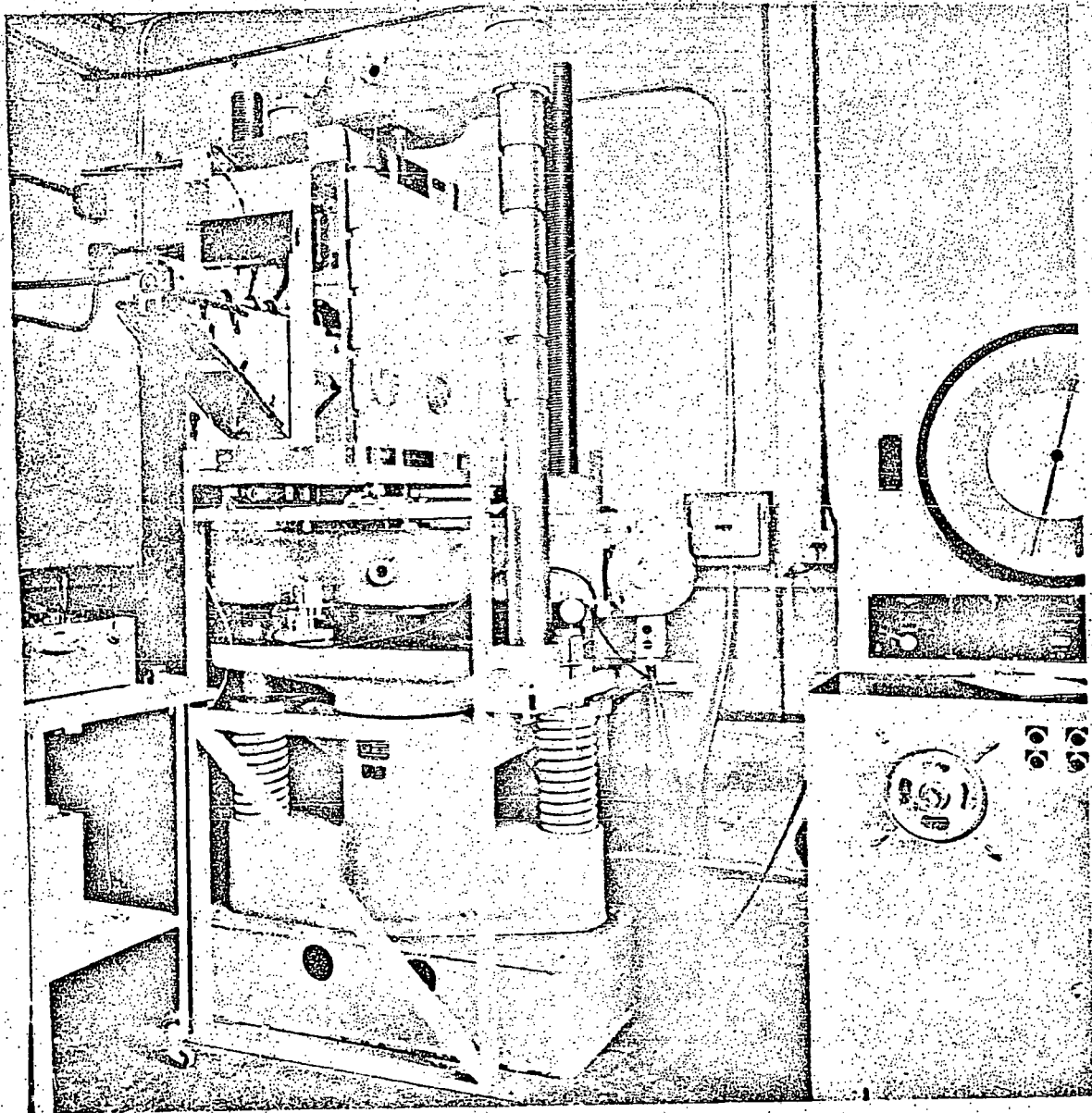


FIG. 2
UNIVERSAL TESTING MACHINE

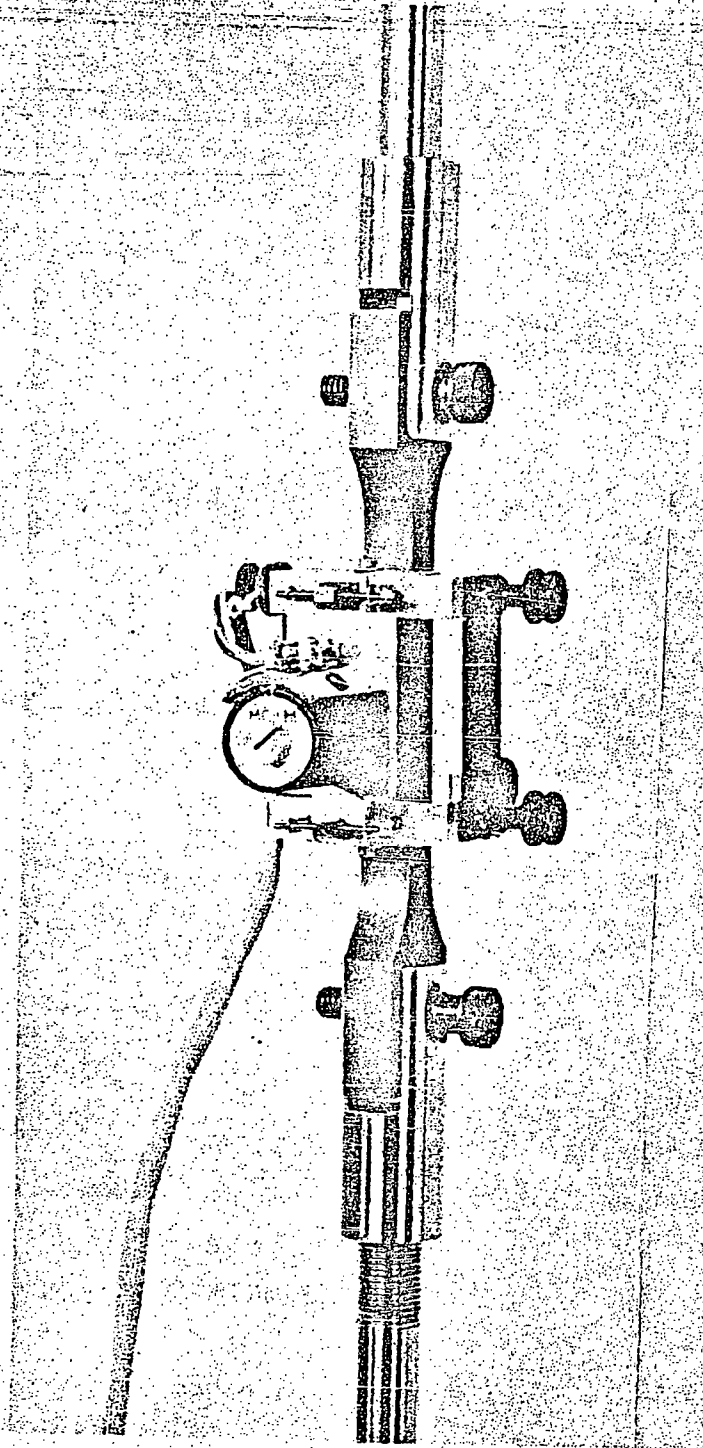


FIG. 3
TENSILE TEST ASSEMBLY

In both cases the stress-strain curves were obtained with a Baldwin stress-strain recorder.

B. Compression Tests

The compression tests were conducted on 1/2 inch x 1/2 inch x 2 inch specimens, at a cross-head travel rate of 0.010 in./min, for a strain rate of 0.005 in./in./min. Figure 4 shows the compression test specimen with a Baldwin microformer compressometer. The central 1 inch served as the gage length. This compressometer was used to evaluate the elastic properties in compression and the compression stress-strain curve to 5% strain.

Initial compression tests were conducted with a compression sub-press. At the elevated test temperatures, difficulty was encountered as a result of binding of the press. For this reason, all the compression tests were conducted without a sub-press, as indicated in Figure 4. The compressometer was also counter-balanced, with a lead block resting on a pair of support rods as indicated in the figure. A flat-ground bearing plate was placed on top of the specimen during the test.

C. Shear Tests

The shear test specimens, 1/2 inch in diameter by 2 inches long, were tested in double shear, using the fixture shown in Figure 5. A constant cross-head travel rate of 0.005 in./min was used for these tests.

D. Bearing Tests

The bearing test specimen consisted of a flat 4 inch by 6 inch by 1/2 inch plate with a 1/2-inch-diameter bearing hole whose center was 1 inch from the edge of the plate. A 1/2-inch steel pin was inserted in this hole and pulled at a constant cross-head rate of 0.005 in./min.

The yield strength, defined as 2% offset of the hole diameter, was determined by means of a small dial gage, which measured the relative pin movement and was mounted directly on the bearing test fixture, shown in Figure 6.

The stress-deformation curve to fracture was determined by measuring the cross-head movement and recording the load and deformation, using the Baldwin recorder.

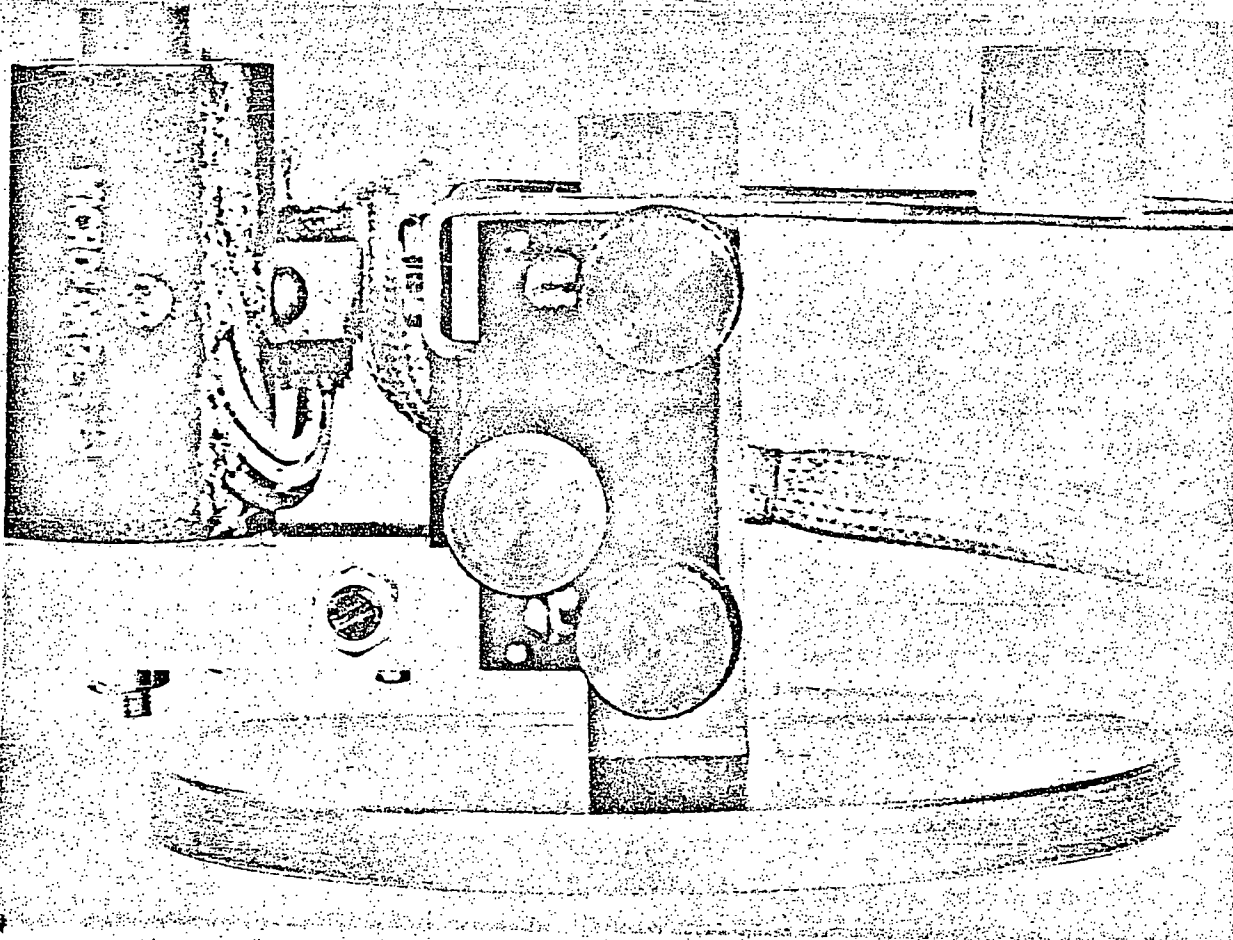


FIG. 4
COMPRESSION TEST SPECIMEN WITH COMPRESSOMETER

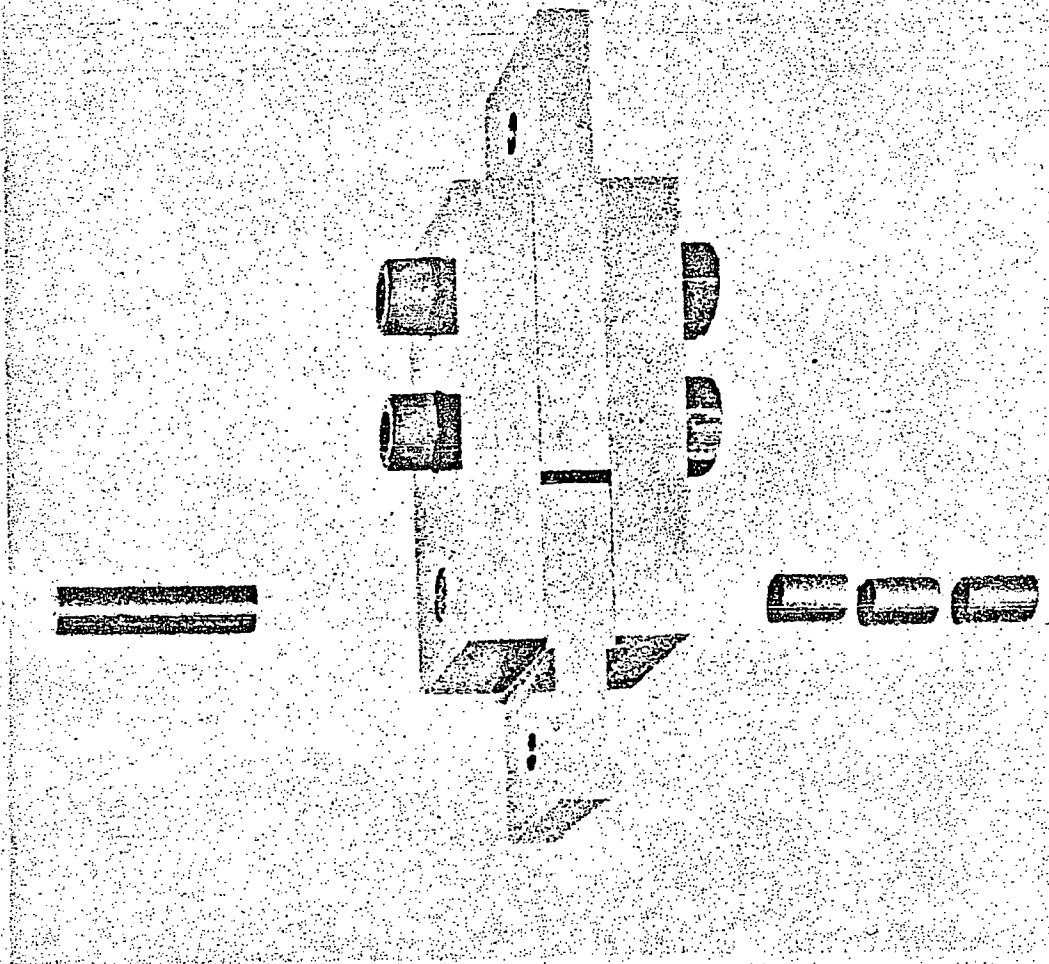


FIG. 5
SHEAR TEST FIXTURE

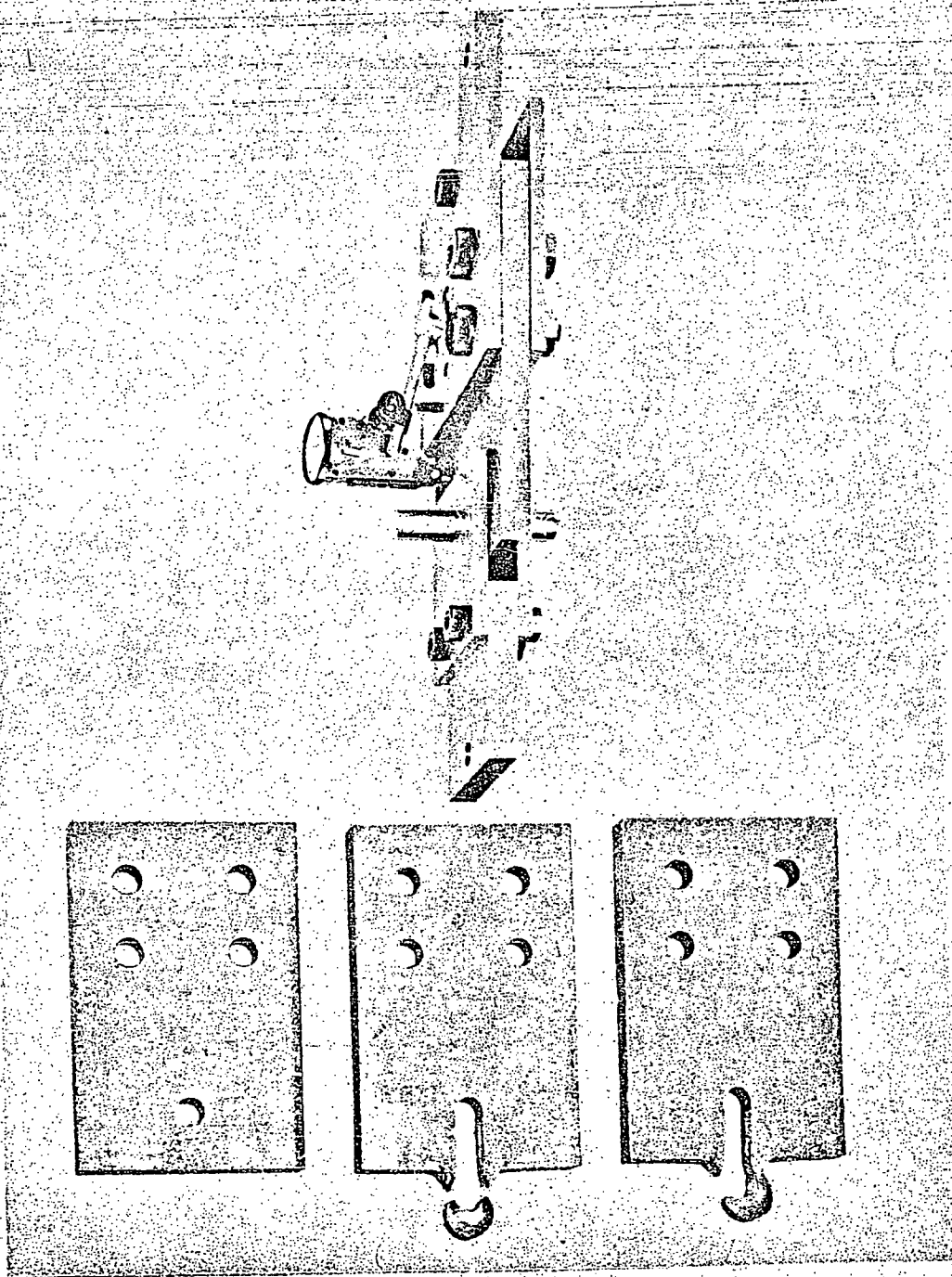


FIG. 6
BEARING TEST FIXTURE

E. Creep Tests

1. Equipment

The creep test units used for this program are shown in Figure 7. One creep unit was used for each test temperature. The furnaces for maintaining constant test temperatures consisted of cylindrical tanks 10 inches in diameter and 24 inches long, with a vertical, 2-inch-I.D. tube passing through the center of each tank. The specimens were heated and tested in an air atmosphere within the tubes. Suitable packing was used at the tube ends to prevent air convection through the tubes.

The specimens were loaded through 5 to 1 lever-arm systems in the case of the lower two test temperatures, and by dead-weight loading in the case of the upper two temperatures. The test temperatures of 100 and 175°F were maintained constant within $\pm 2^\circ\text{F}$ by water and thermostatic control; the test temperatures of 250 and 325°F were maintained constant within $\pm 1^\circ\text{F}$ by boiling glycol-water solutions and condenser systems.

An assembly of a creep specimen, pulling bars, and extensometer is shown in Figure 8. The central 2 inches of the specimen served as the gage length. The gage blocks were attached to the specimen by means of four hardened, conical points pressed into the specimen and held in place by coil springs. The relative movement of the gage blocks was transferred through two pairs of extension rods to a 0.0001-inch least-count dial gage outside the furnace. The upper guide blocks had polished surfaces which were free to move along the axis of the polished pulling bar.

2. Test Procedure

The test specimen was carefully assembled, using a special mounting board for aligning the pulling bars and extensometer. A thermocouple for temperature checks during test was tied directly to the specimen at the center of the 2-inch gage length.

A set of chromel-alumel thermocouples were calibrated, using a boiling distilled water bath which gave a calibration point midway between the four test temperatures. Four thermocouples were selected for uniformity, and one thermocouple was used for all creep tests at one test temperature.

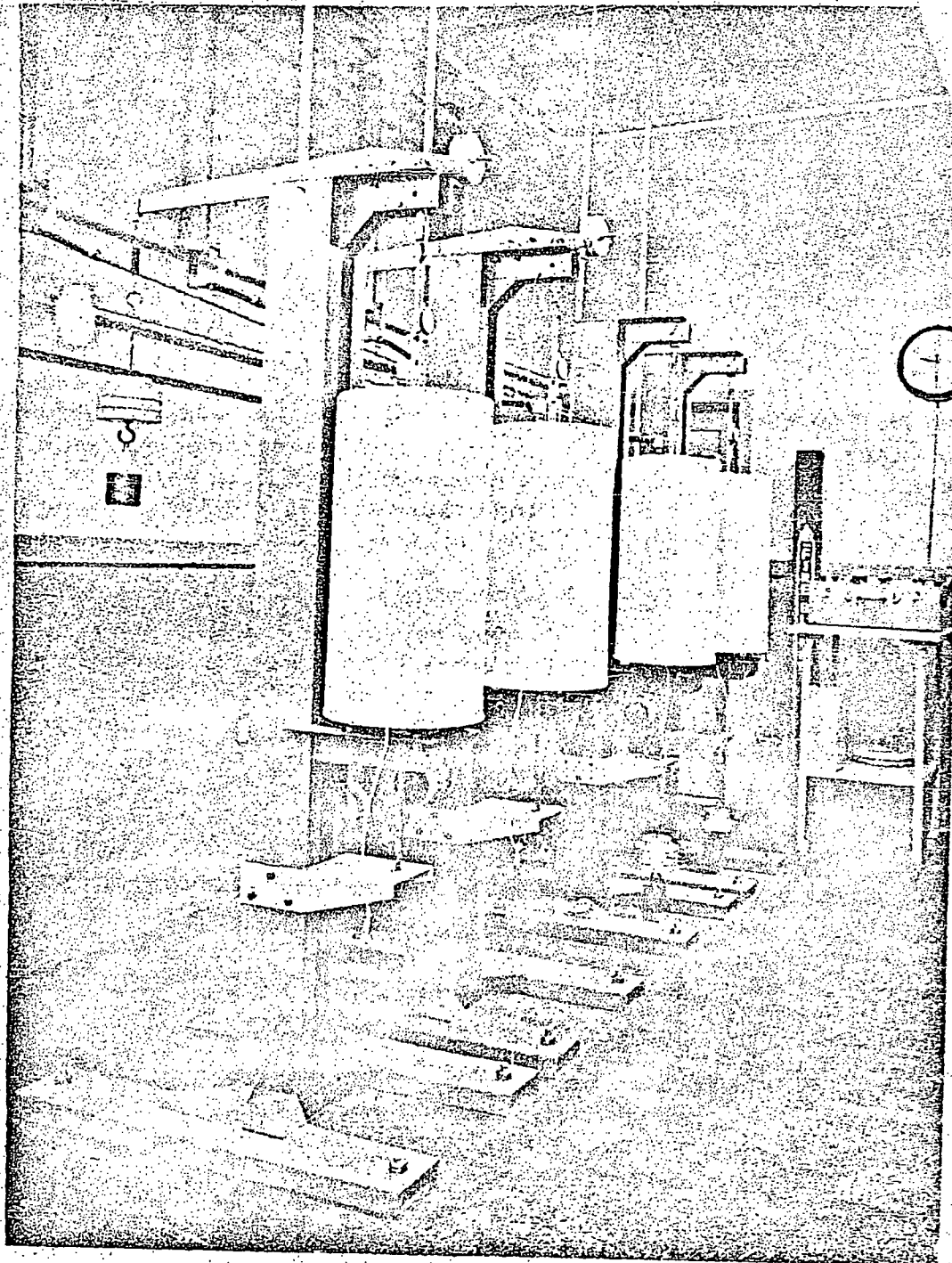


FIG. 7
CREEP TEST UNITS

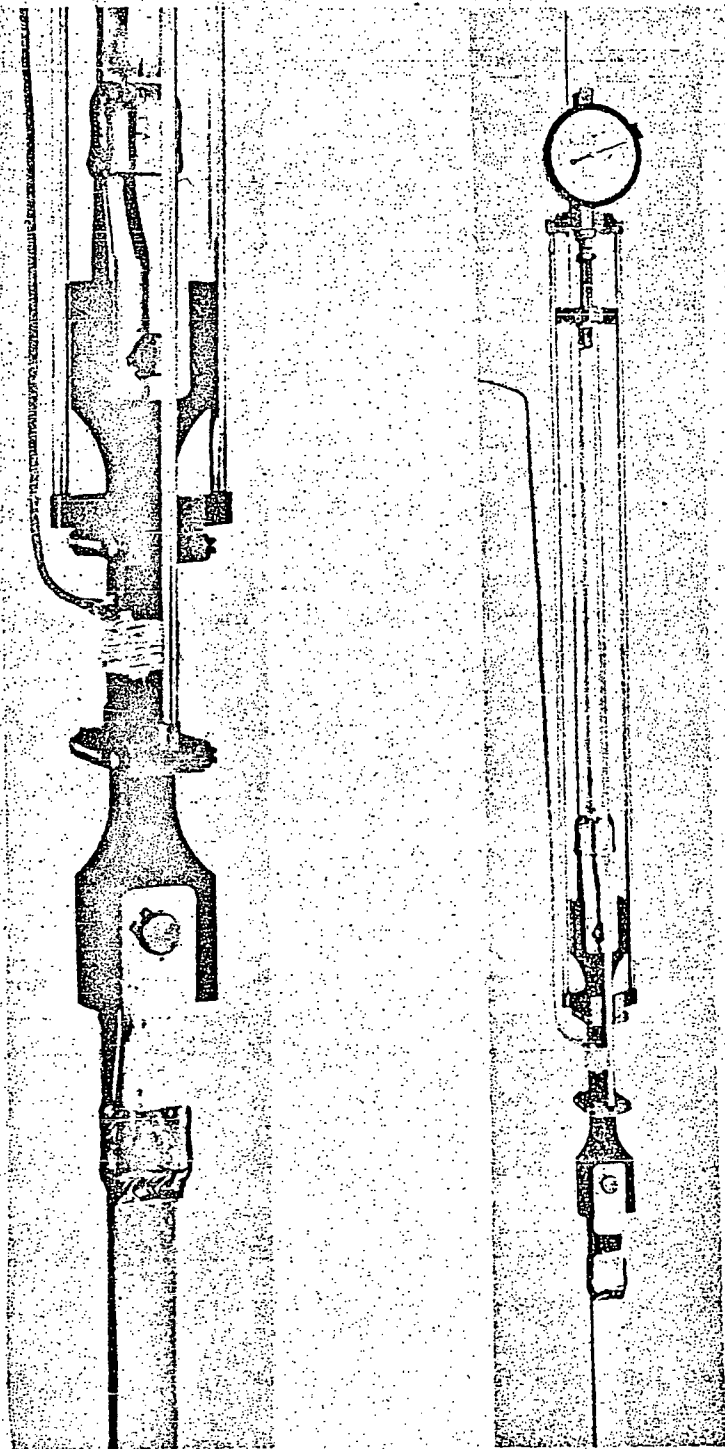


FIG. 8
CREEP SPECIMEN ASSEMBLY

The specimen assembly was inserted into the furnace two hours prior to application of the load in order to permit the specimen to attain the test temperature. The load was then gradually applied by hand over a period of about half a minute; zero time was taken when the full load was on the specimen.

V Experimental Results

A. Tensile Tests

1. Stress-Strain Curves to Failure

The stress-strain curves to failure are presented in Figure 9 for the two test materials. The tests were conducted in triplicate at each of the test temperatures: 100, 175, 250, and 325°F, and at a strain rate of 0.05 in./in./min. Data on the ultimate tensile strength and elongation are summarized in Table II. The elongation values given in the table were obtained by using gage marks originally 3.00 inches apart on the specimen.

Table II

TENSILE TEST RESULTS

Ultimate Tensile Strength (psi) and Elongation (%)
at a Strain Rate of 0.05 in./in./min

<u>Test Material</u>	<u>Test Temperature, °F</u>								
	<u>100</u>		<u>175</u>		<u>250</u>		<u>325</u>		
	<u>UTS</u>	<u>Elong.</u>	<u>UTS</u>	<u>Elong.</u>	<u>UTS</u>	<u>Elong.</u>	<u>UTS</u>	<u>Elong.</u>	
High Purity Lead	1	1828	46.0	1240	57.3	788	64.0	498	77.6
	2	1920	44.6	1196	42.6	798	50.6	488	72.0
	3	1852	40.0	1204	36.0	768	68.3	492	83.3
	Average	1867	43.5	1213	45.3	785	61.0	493	77.6
Copperized Lead	1	1580	53.6	1164	46.0	826	42.6	636	46.6
	2	1604	46.3	1148	47.0	846	50.6	638	56.0
	3	1570	53.0	1162	47.7	844	48.3	642	42.7
	Average	1585	51.0	1158	46.9	839	47.2	639	48.4

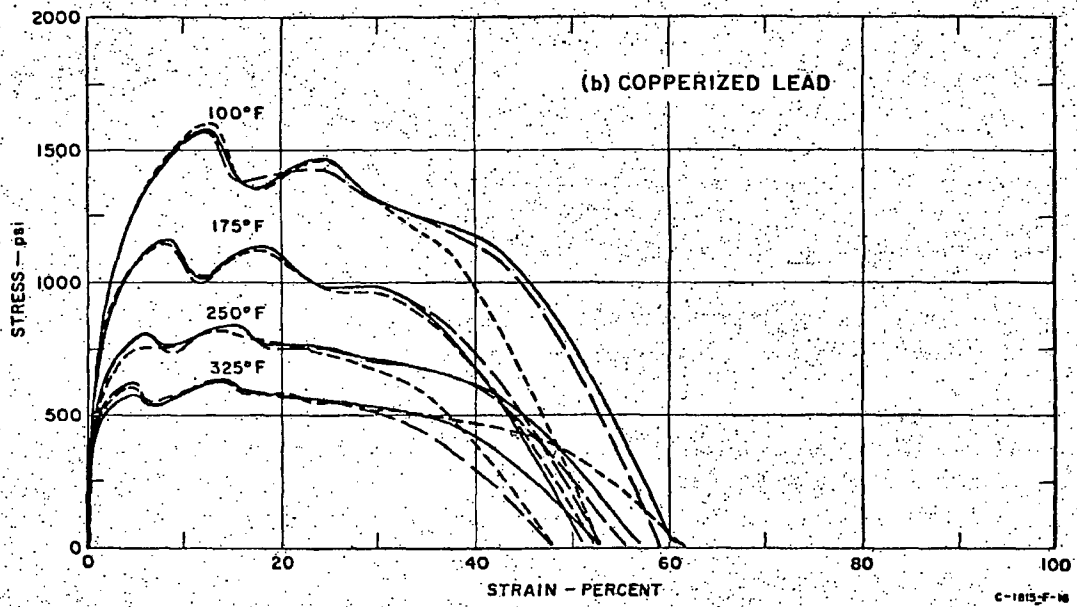
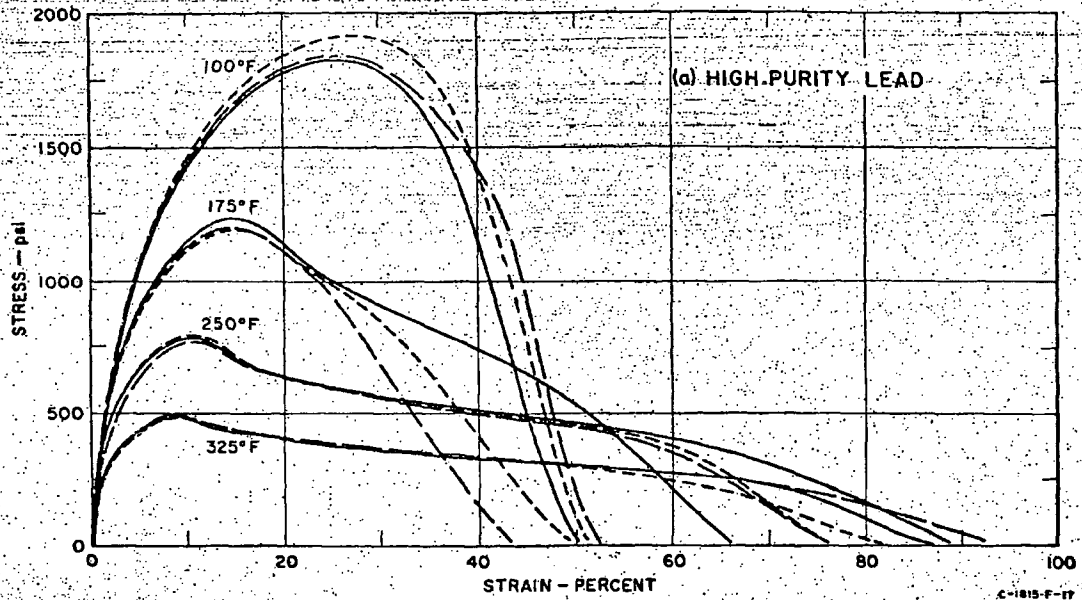


FIG. 9
TENSILE STRESS-STRAIN CURVES TO FAILURE
AT A STRAIN RATE OF 0.05 IN./IN./MIN

The triplicate tests under the same test conditions gave very similar stress-strain curves up to the point of necking. Beyond this point the curves differed considerably, due to differences in necking conditions, probably influenced by variations in grain size and grain orientation within the different specimens. The fracture strength was very nearly zero for all tests, as is indicated by the curves on Figure 9.

The stress-strain curves for the high purity lead were quite typical, each exhibiting one maximum, whereas the curves for the copperized lead all had two or more maxima. In the latter case, necking did not occur at the first maximum in the stress-strain curves; this effect was possibly associated with recrystallization of the finer-grain-size copperized lead during test.

The total elongation values shown in Figure 9 include some elongation of the specimen bearing holes, which in extreme cases amounted to about 1/16-inch per hole, whereas in most cases it was less than 1/32-inch per hole. Some elongation also occurred in the fillet areas outside the 3-inch reduced section, with the result that the indicated strain values are larger than actual. This problem was not encountered in the other tensile or compression tests, as the strain measurements were made directly on the specimen gage length.

Figure 10 presents the average values of the ultimate tensile strength and elongation as a function of test temperature. The high purity lead had a higher tensile strength at 100 and 175°F than the copperized lead and a lower value at the higher test temperatures of 250 and 325°F. It should be noted that at any one test temperature the rate of strain hardening of the copperized lead is greater than that for the high purity lead almost up to the point of the first maximum. If only the maximum associated with necking had occurred, these tests undoubtedly would have exhibited higher ultimate tensile strength values.

The percent elongation for the copperized lead was approximately constant at about 50% at all test temperatures, whereas the average elongation of the high purity lead increased from 43% to 77% over the temperature range from 100 to 325°F.

2. Elastic Properties

A second set of 24 tensile specimens was used to evaluate the elastic properties and the stress-strain curve to 2% strain. A cross-head travel rate of 0.015 in./min was used for these tests, for a strain rate of 0.005 in./in./min. The results of these tests are shown in Figure 11 for the two test materials tested at the four test temperatures. The triplicate tests at any one temperature are in good agreement. In order to show more clearly the effect of temperature, the data of Figure 11 were plotted as stress vs test temperature for constant values of total strain and are presented in Figure 12.

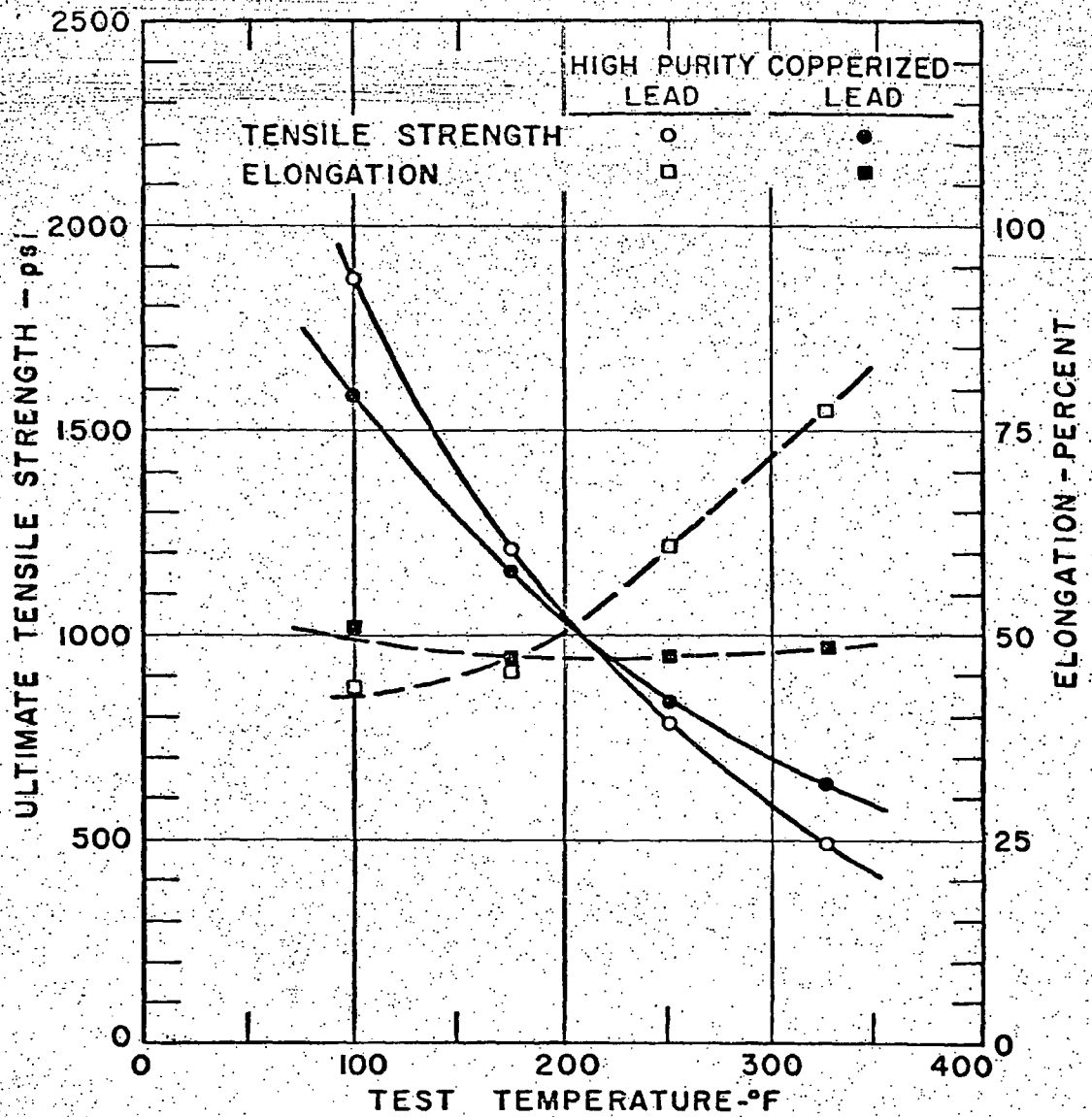


FIG. 10
 TENSILE STRENGTH AND ELONGATION AS A FUNCTION OF TEST TEMPERATURE
 AT A STRAIN RATE OF 0.05 IN./IN./MIN

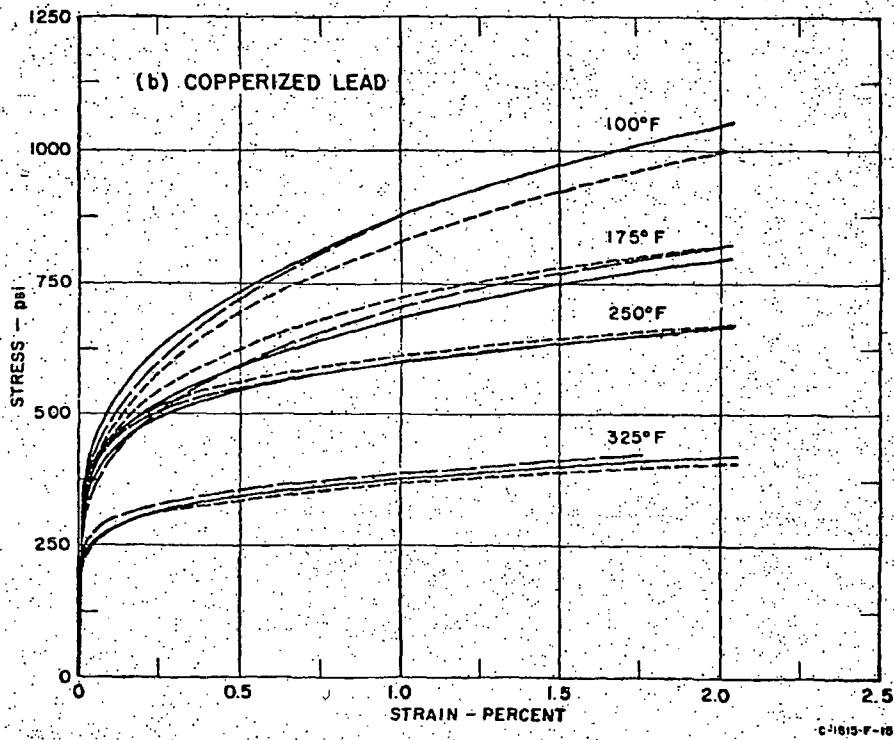
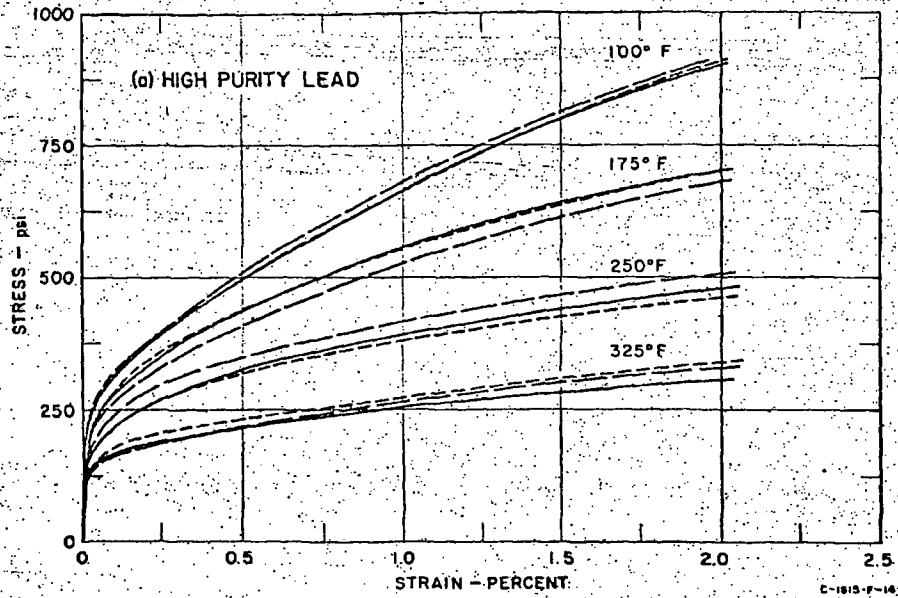


FIG. 11
TENSILE STRESS-STRAIN CURVES TO 2% STRAIN
AT A STRAIN RATE OF 0.005 IN./IN./MIN

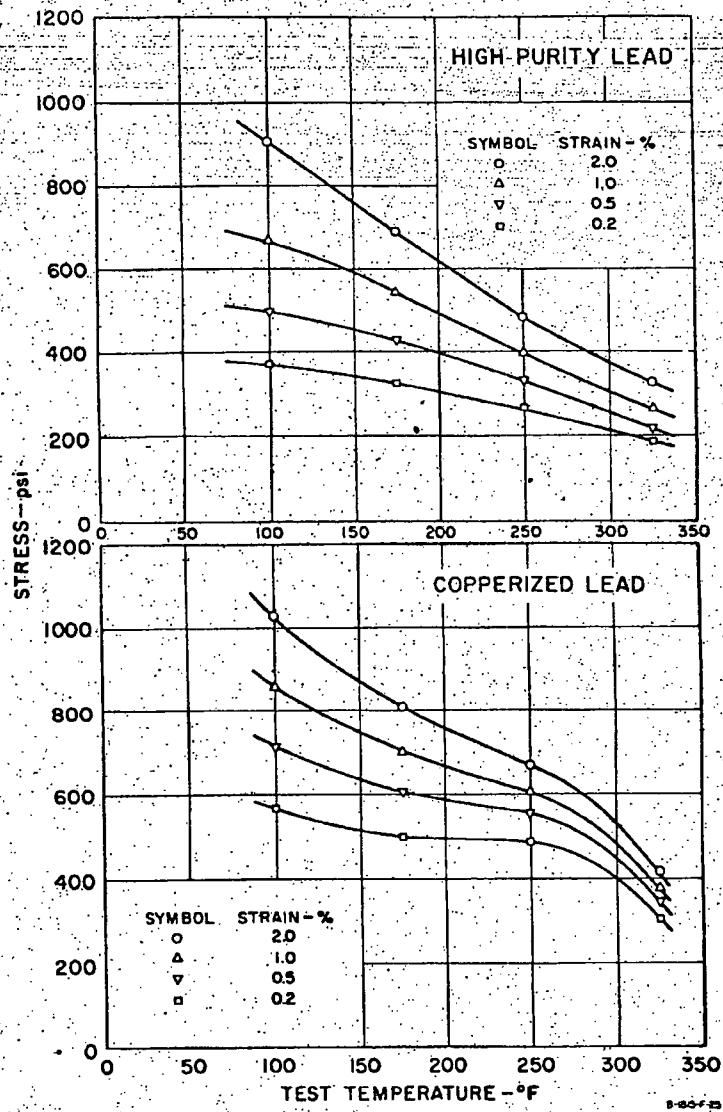


FIG. 12

TENSILE FLOW STRESS VS TEST TEMPERATURE FOR
GIVEN VALUES OF STRAIN
AT A STRAIN RATE OF 0.005 IN./IN./MIN

The elastic properties were evaluated from the recorded load-deformation charts by initially using a high strain magnification to a strain of 0.3%, 1 inch of chart being equal to 0.05% strain. The test was then completed by using a low magnification, 1 inch of chart equal to 0.2% strain, to a total strain of 2.0%. At this point the specimen was unloaded and reloaded three times, using the high strain magnification, the loading curves being used to evaluate the elastic modulus. This procedure was used to evaluate the modulus because the initial yield point was too low in most cases to make evaluation possible.

Tensile data for the modulus of elasticity, proportional limit, and yield strength are summarized in Table III. The tabulated values of the modulus of elasticity have been calculated on the basis of the reduced cross-sectional area at 2% strain. For the high purity lead, the average value of the modulus was 2.7×10^6 psi, with no apparent decrease from 100 to 250°F. Values at 325°F could not be evaluated with sufficient accuracy. The proportional limit and yield strength both show a decrease of about 50% with test temperature from 100 to 325°F. For the copperized lead the average value of the modulus was 2.2×10^6 psi with about a 10% decrease at 325°F; the proportional limit and yield strength remained practically constant from 100 to 250°F and then decreased about 35% at 325°F.

3. Effect of Strain Rate

The effect of strain on the stress-strain curve was evaluated at 100 and 250°F, for both test materials. Figure 13 presents tests conducted at a strain rate of 0.005 in./in./min, along with previous tests conducted at a rate of 0.05 in./in./min. For the high purity lead, a decrease in the strain rate from 0.05 to 0.005 in./in./min resulted in a decrease in the ultimate tensile strength of about 30% at both test temperatures, and also in a decrease in strain at the ultimate and in the total strain to fracture. For the copperized lead, the same decrease in strain rate resulted in a 15% decrease in the ultimate and a slight decrease in the elongation to fracture.

B. Compression Tests

The results of stress-strain tests in compression to 5% strain are given in Figure 14. Triplicate tests were conducted at each test temperature for both materials, using a cross-head travel rate of 0.010 in./min for a strain rate of 0.005 in./in./min. There is some overlapping in the curves for the high purity lead at small values of strain for the different test temperatures. This is most likely due to small sampling differences which initially existed from specimen to specimen. After 1% strain the curves at any one test temperature are in close agreement.

Table III

TENSILE DATA--MODULUS OF ELASTICITY
PROPORTIONAL LIMIT, AND YIELD STRENGTH

at a Strain Rate of 0.005 in./in./min

Test	Temperature, °F	Modulus of Elasticity, $\text{psi} \times 10^{-6}$				Proportional Limit, psi	Yield Strength, 0.2% Offset, psi
		E_1	E_2	E_3	$E_{\text{avg.}}$		
High Purity							
Lead							
	100	3.0	3.0	3.1	3.0	190.	372.
	100	2.6	2.6	2.7	2.6	170.	380.
	100	2.6	2.6	2.6	2.6	180.	384.
	Average				2.7	180.	379.
	175	---	---	---	---	150.	332.
	175	2.6	2.6	2.5	2.6	150.	312.
	175	2.7	2.5	2.5	2.6	---	---
	175	2.6	2.6	2.6	2.6	103.	347.
	Average				2.6	134.	330.
	250	2.4	2.9	2.4	2.6	130.	260.
	250	2.2	2.5	2.6	2.4	140.	288.
	250	3.1	2.8	3.0	3.0	130.	260.
	Average				2.7	133.	269.
	325	---	---	---	---	90.	188.
	325	---	---	---	---	72.	180.
	325	---	---	---	---	90.	200.
	Average					84.	189.
Copperized							
Lead							
	100	2.5	2.5	2.4	2.5	328.	612.
	100	2.2	2.2	2.4	2.3	200.	580.
	100	2.3	2.2	2.1	2.2	300.	560.
	Average				2.3	276.	584.
	175	1.9	2.4	2.0	2.1	350.	512.
	175	2.2	2.2	2.3	2.2	260.	488.
	175	2.4	2.3	---	2.3	270.	528.
	Average				2.2	293.	509.
	250	---	2.3	2.3	2.3	260.	488.
	250	1.8	1.8	1.9	1.8	260.	500.
	250	2.9	2.6	---	2.7	312.	504.
	Average				2.3	277.	498.
	325	2.1	2.1	2.0	2.1	200.	308.
	325	---	---	---	---	208.	320.
	325	2.0	2.0	1.9	2.0	160.	304.
	Average				2.0	189.	311.

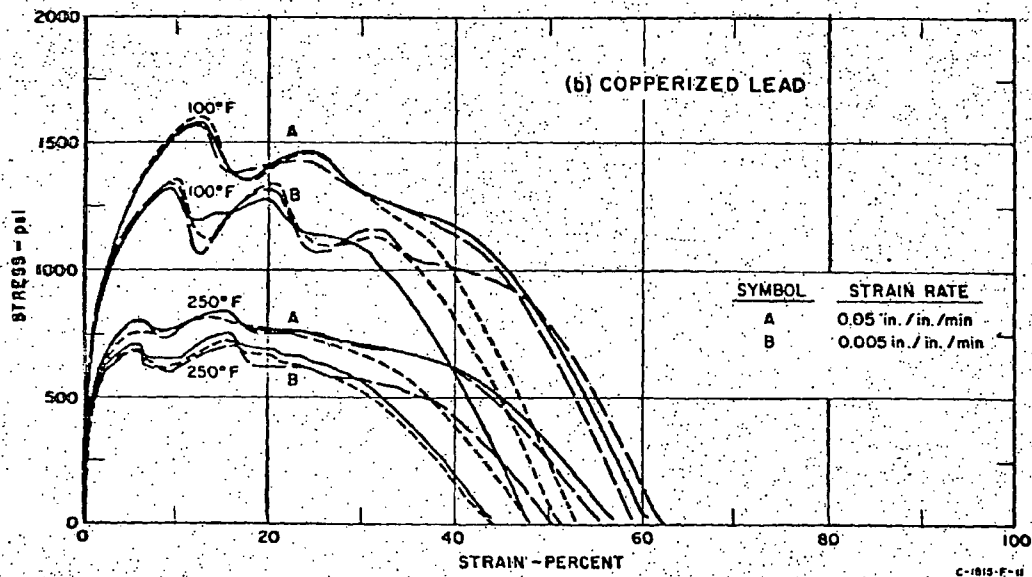
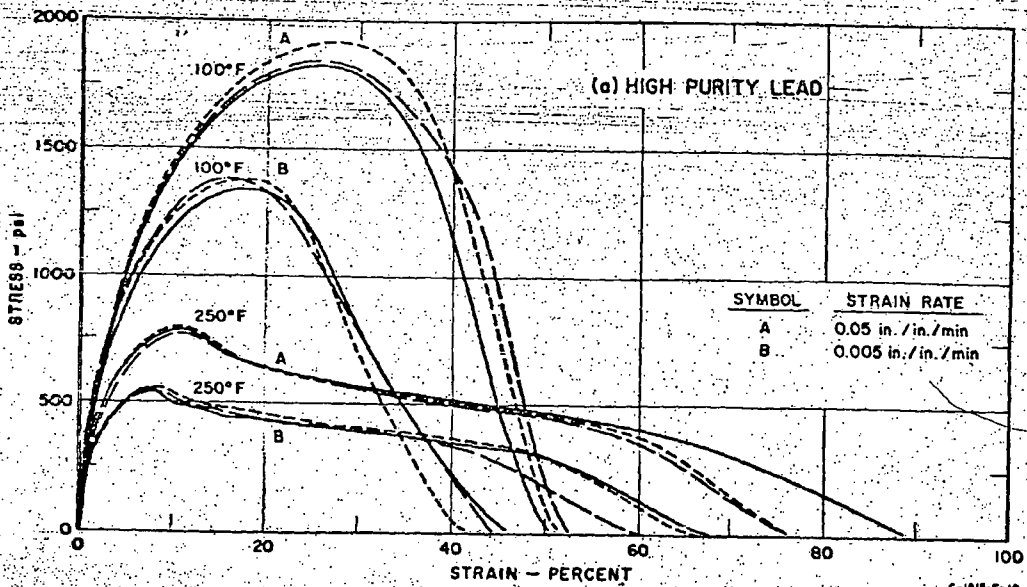


FIG. 13

EFFECT OF STRAIN RATE ON THE TENSILE STRESS-STRAIN CURVES AT 100 AND 250°F

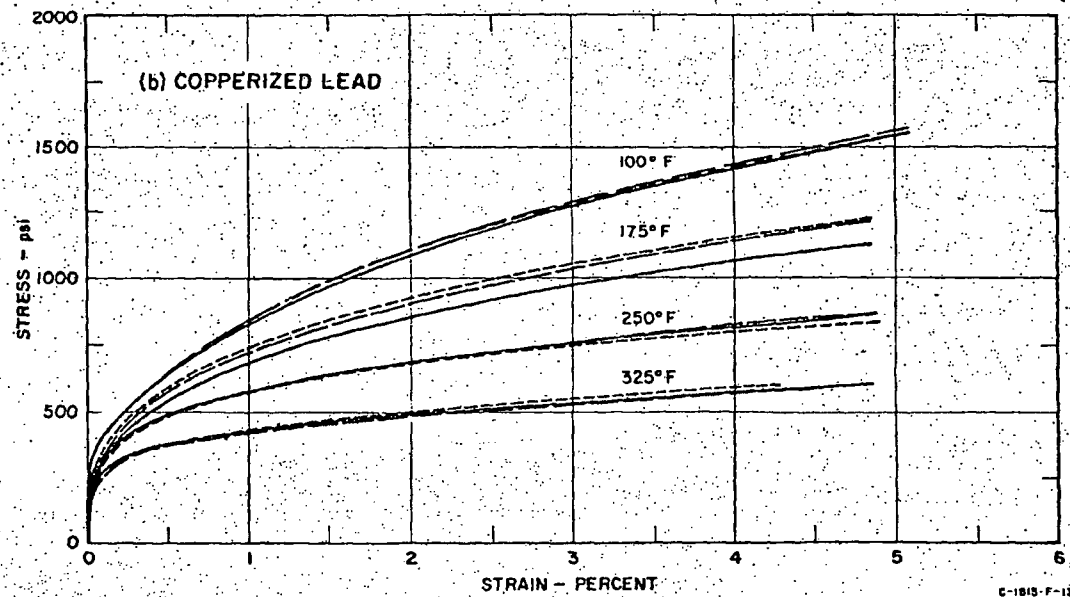
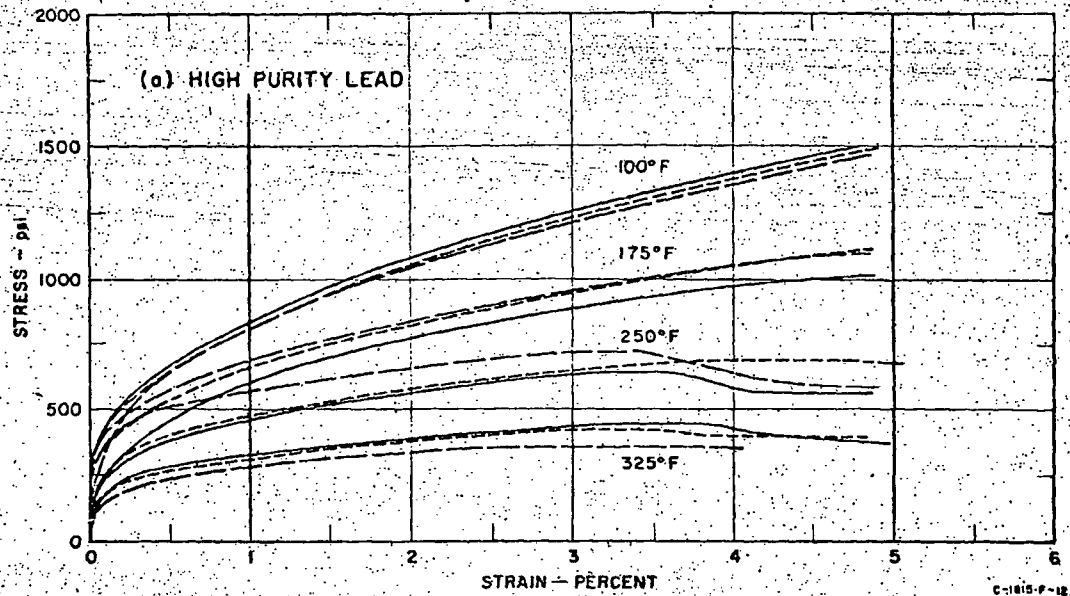


FIG. 14
 COMPRESSION STRESS-STRAIN CURVES TO 5% STRAIN
 AT A STRAIN RATE OF 0.005 IN./IN./MIN

For the high purity lead at 250 and 325°F, in some cases a decrease in the stress-strain curve occurred after 3% strain. In these cases no unusual condition was observed during test; a possible explanation is that recrystallization took place at these higher test temperatures under the particular test conditions.

The compression data are shown in Figure 15 as stress vs test temperature for various values of total strain. At the lower test temperatures the stress values for the copperized lead are only slightly higher than those for the high purity lead. At 325°F this difference becomes larger, the curves for the high purity lead decreasing more rapidly above 250°F than those for the copperized lead.

The elastic properties in compression were evaluated from the recorded load deformation charts in a manner similar to that used for the tensile tests. A high strain magnification, 1 inch of chart equal to 0.10% strain, was used to a strain of 0.3%. The test was completed at a low magnification, 1 inch of chart equal to 0.4% strain, to a strain of 5%. At this point the specimen was unloaded and reloaded three times, using the high strain magnification, the loading curves being used to evaluate the elastic modulus.

The modulus of elasticity, proportional limit, and yield strength data in compression are summarized in Table IV. The tabulated values of the modulus of elasticity have been calculated on the basis of the increased cross-sectional area at 5% strain.

The average value of the modulus was 2.6×10^6 psi for both materials, and decreased from 2.8×10^6 psi at 100°F to about 2.4×10^6 psi at 325°F. The proportional limit and yield strength values were about the same for the two leads at each of the three lower test temperatures; at 325°F the values for the copperized lead were about 50% higher than those for the high purity lead.

C. Shear Tests

The shear test results are summarized in Table V, and are presented in Figure 16 as ultimate shear strength vs test temperature. These tests were conducted by testing pins 1/2 inch in diameter by 2 inches long in double shear, using a constant cross-head travel rate of 0.005 in./min.

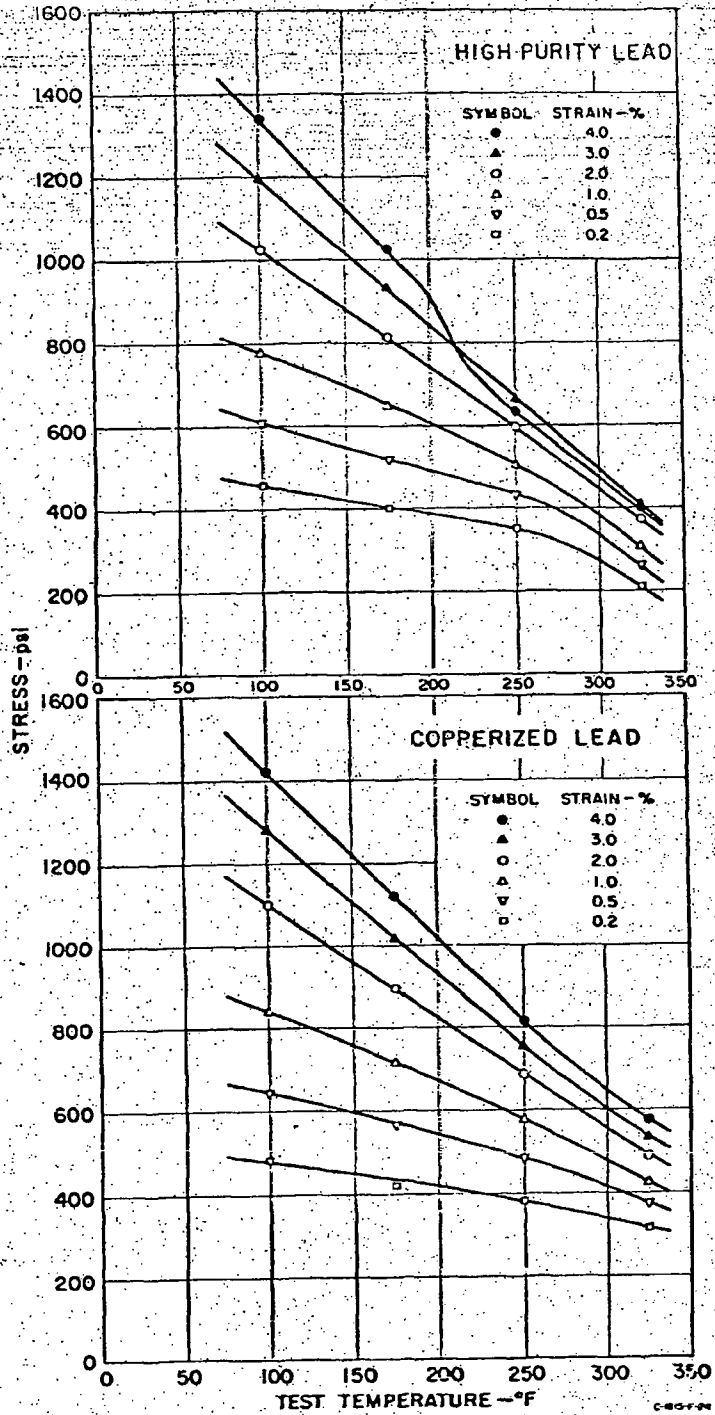


FIG. 15
 COMPRESSION FLOW STRESS VS TEST TEMPERATURE
 FOR GIVEN VALUES OF STRAIN
 AT A STRAIN RATE OF 0.005 IN./IN./MIN

Table IV

COMPRESSION DATA -- MODULUS OF ELASTICITY,
PROPORTIONAL LIMIT, AND YIELD STRENGTH

at a Strain Rate of 0.005 in./in./min

Test	Temperature, °F	Modulus of Elasticity, psi × 10 ⁻⁶				Proportional Limit, psi	Yield Strength, 0.2% Offset, psi
		E ₁	E ₂	E ₃	E _{avg.}		
High Purity Lead	100	2.8	2.8	2.8	2.8	282.	500.
	100	---	2.6	2.6	2.6	81.	440.
	100	---	3.1	3.0	<u>3.1</u>	<u>202.</u>	<u>472.</u>
	Average				<u>2.8</u>	<u>188.</u>	<u>471.</u>
	175	---	2.5	2.7	2.6	100.	328.
	175	2.8	2.3	2.6	2.6	262.	472.
	175	2.6	2.3	2.5	<u>2.5</u>	<u>202.</u>	<u>427.</u>
	Average				<u>2.6</u>	<u>188.</u>	<u>409.</u>
	250	---	3.2	2.3	2.8	80.	292.
	250	2.5	---	2.3	2.4	181.	440.
	250	2.7	---	2.1	<u>2.4</u>	<u>60.</u>	<u>322.</u>
	Average				<u>2.5</u>	<u>107.</u>	<u>351.</u>
	325	2.5	---	---	2.5	50.	228.
	325	---	---	---	---	50.	180.
	325	---	---	---	---	<u>80.</u>	<u>212.</u>
Average				<u>2.5</u>	<u>60.</u>	<u>207.</u>	
Copperized Lead	100	---	2.9	3.0	2.9	222.	492.
	100	2.9	2.9	---	2.9	222.	492.
	100	2.5	2.6	---	<u>2.6</u>	<u>201.</u>	<u>487.</u>
	Average				<u>2.8</u>	<u>215.</u>	<u>490.</u>
	175	2.8	2.8	2.6	2.7	80.	408.
	175	---	2.8	---	2.8	120.	432.
	175	3.1	3.2	3.1	<u>3.1</u>	<u>120.</u>	<u>444.</u>
	Average				<u>2.9</u>	<u>107.</u>	<u>428.</u>
	250	2.4	---	2.5	2.5	120.	396.
	250	---	2.6	2.6	2.6	120.	396.
	250	2.4	2.4	---	<u>2.4</u>	<u>80.</u>	<u>380.</u>
	Average				<u>2.5</u>	<u>107.</u>	<u>391.</u>
	325	2.4	---	---	2.4	80.	320.
	325	---	---	---	---	80.	312.
	325	---	---	---	---	<u>120.</u>	<u>328.</u>
Average				<u>2.4</u>	<u>93.</u>	<u>320.</u>	

Table V

SHEAR TEST RESULTS

Ultimate Shear Strength, psi
at a Cross-head Rate of 0.005 in./min

Test Material	Test Number	Test Temperature, °F			
		100	175	250	325
High Purity Lead	1	1167	640	415	294
	2	1130	640	412	272
	3	1107	638	415	264
	Average	<u>1135</u>	<u>639</u>	<u>414</u>	<u>277</u>
Copperized Lead	1	1012	675	513	378
	2	908	690	513	383
	3	948	660	502	385
	Average	<u>956</u>	<u>675</u>	<u>509</u>	<u>382</u>

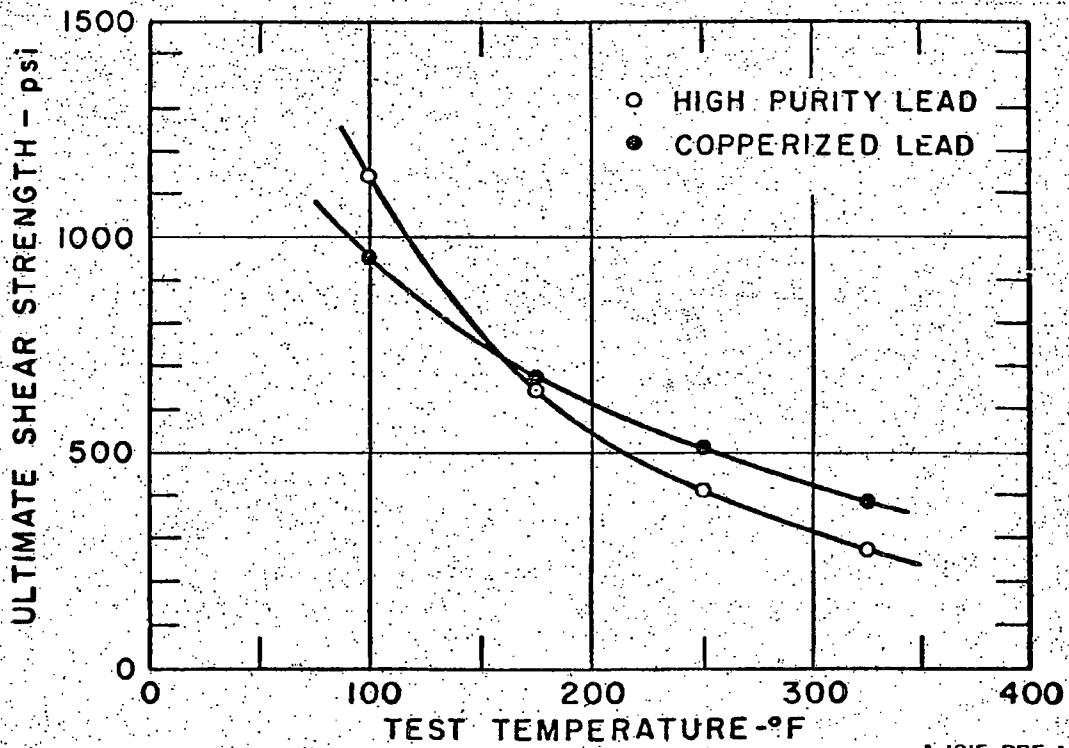
The data points in Figure 16 represent the average values for each set of triplicate tests. At 100°F the ultimate shear strength of the high purity lead was higher than that for the lead containing 0.058% copper. However, the shear strength of the high purity lead decreased more rapidly with test temperature than that of the copperized lead and was lower at temperatures above 160°F.

The shear tests on the copperized lead behaved in a similar manner to the tensile tests on the copperized lead, in that two maxima in the load occurred during each test.

D. Bearing Tests

The bearing tests were conducted at a cross-head travel rate of 0.005 in./min, and the stress-deformation curves to failure are given in Figure 17. For this purpose the stress is defined as the load divided by the bearing area, which is taken as the diameter of the bearing hole times the bearing plate thickness.

The bearing test results are given in Table VI in terms of yield strength, defined as 2% offset of the hole diameter, and ultimate bearing strength. The yield strength and ultimate strength are presented in Figure 18 as a function of temperature.



A-1815-PR5-1

FIG. 16

SHEAR STRENGTH VS TEST TEMPERATURE
 AT A CROSS-HEAD RATE OF 0.005 IN./MIN

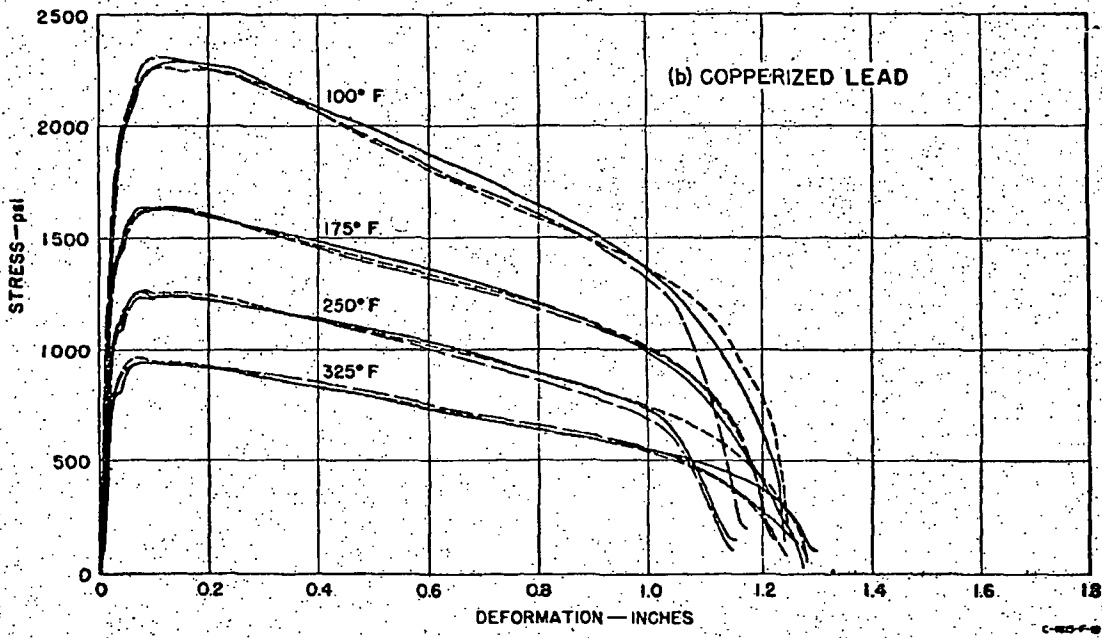
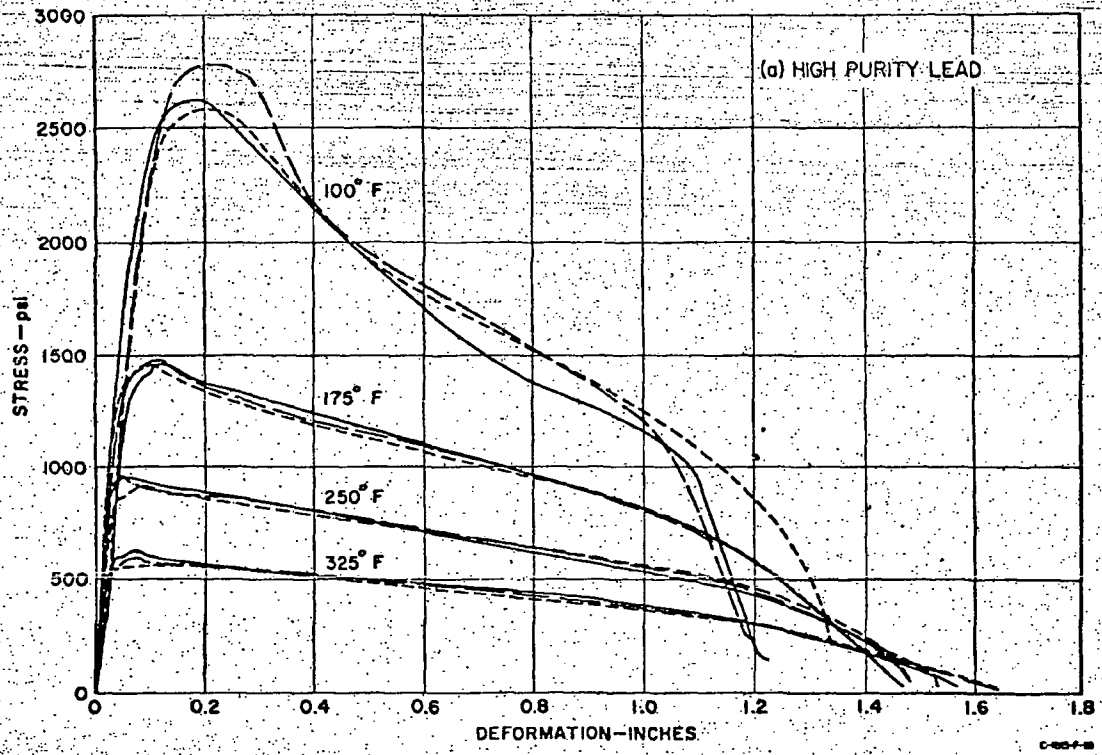


FIG. 17
 BEARING STRESS-DEFORMATION CURVES TO FAILURE
 AT A CROSS-HEAD RATE OF 0.005 IN./MIN

Table VI

BEARING TEST RESULTS

Yield Strength and Ultimate Bearing Strength
at a Cross-head Rate of 0.005 in./min

	Temperature, °F	Yield Strength, psi	Ultimate Strength, psi
High Purity Lead	100	1000.	2620.
	100	1060.	2780.
	100	1070.	2580.
	Average	1040.	2660.
	175	681.	1460.
	175	774.	1480.
	175	750.	1460.
	Average	740.	1470.
	250	629.	952.
	250	649.	963.
	250	605.	919.
	Average	630.	940.
	325	435.	629.
	325	443.	600.
	325	451.	564.
Average	440.	600.	
Copperized Lead	100	1090.	2280.
	100	1370.	2310.
	100	1150.	2260.
	Average	1200.	2280.
	175	1110.	1640.
	175	1120.	1640.
	175	1070.	1630.
	Average	1100.	1640.
	250	907.	1260.
	250	795.	1230.
	250	863.	1270.
	Average	860.	1250.
	325	710.	944.
	325	738.	947.
	325	685.	960.
Average	710.	950.	

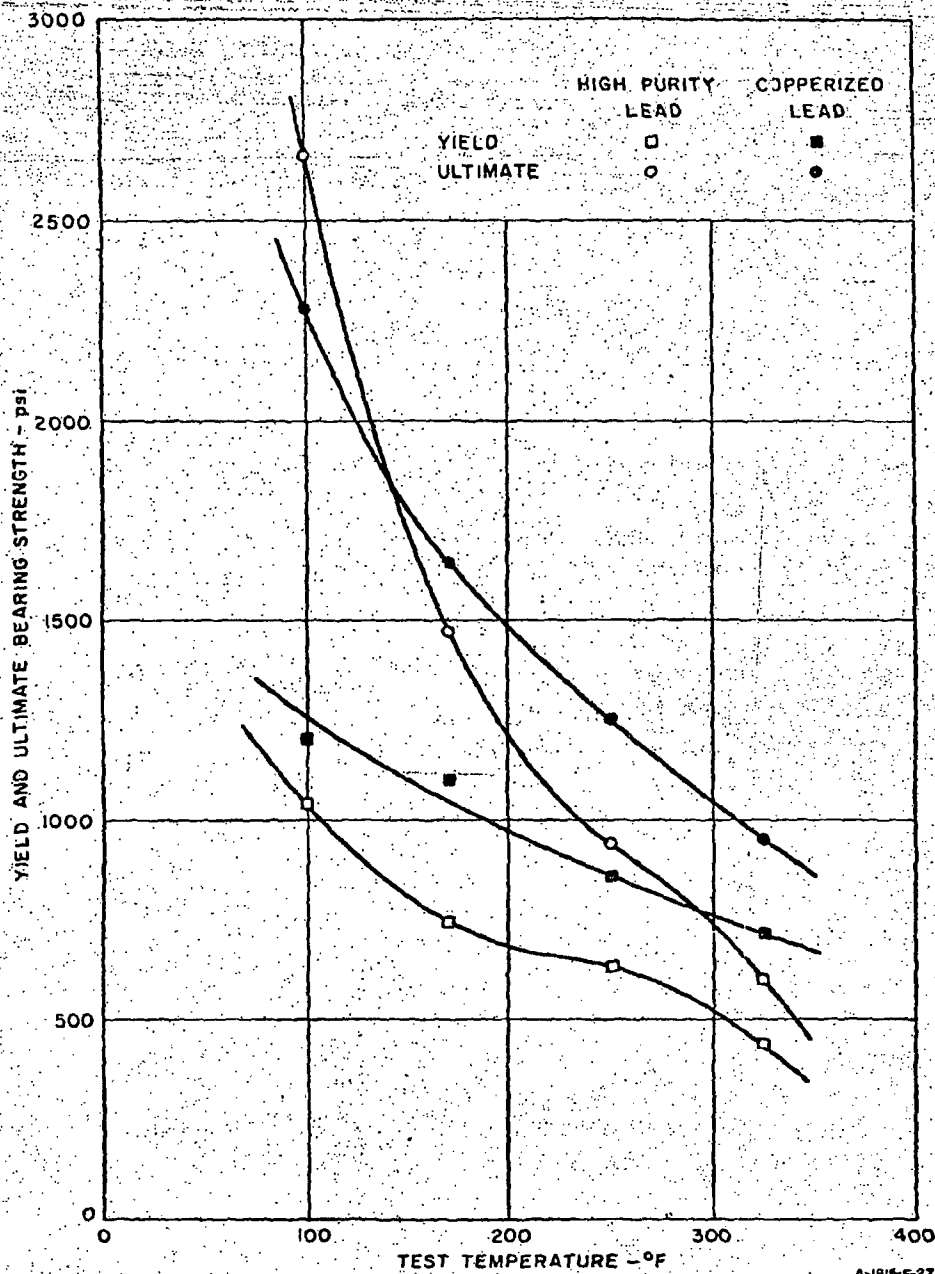


FIG. 18
BEARING YIELD STRENGTH AND ULTIMATE STRENGTH VS
TEST TEMPERATURE
AT A CROSS-HEAD RATE OF 0.005 IN./MIN

The bearing yield strength for the copperized lead is higher than that for the high purity lead at all test temperatures. The ultimate bearing strength for the high purity lead at 100°F is higher than that for the copperized, but becomes lower at temperatures above about 140°F. Inspection of the stress-deformation curves for the copperized lead shows that they exhibit a definite decrease in the rate of strain hardening, then an increase prior to the ultimate.

E. Creep Tests

The original creep data are presented as total strain vs creep time in Figure 19 for the high purity lead and in Figure 20 for the copperized lead.

Some crossing of the strain-time curves occurred at very low strain values of less than 0.0004 in./in. No fundamental significance is given to this behavior which is probably due to one or a combination of the following factors: sampling differences, slight variations in loading conditions, and possible initial lag in extensometer movement.

Greenwood and Worner,* studying the creep of lead, demonstrated that a rapid increase in the creep rate occurred when recrystallization took place during test. The longer time and higher temperature creep tests of the current study were plotted on regular coordinate paper as strain against time. All these curves showed a continually decreasing creep rate with time indicating that no recrystallization took place under the given test conditions. This was not confirmed, however, by microstructure studies.

In Figure 21 and 22 the creep results are summarized as stress-creep time curves for total strain values of 0.2, 0.5, 1.0, and 2.0% for the two test materials.

The high purity lead is less creep resistant than the copperized lead for the shorter creep times. However, for the longer creep times the high purity lead is more creep resistant than the copperized lead. This is especially true at the higher test temperatures.

It should be repeated here that these results are for the test materials in the as-received condition, annealed prior to testing only to remove any work hardening due to machining and handling. The materials were-

*Greenwood, J. Neill, and H. K. Worner, "Types of Creep Curves Obtained with Lead and Its Dilute Alloys." Jour. Inst. of Metals (1939) 64, No. 1, 135

tested in this condition in order to obtain the properties of these two materials as normally received. The grain sizes of the two materials as reported earlier were considerably different, both in the as-received and in the annealed conditions.

Several studies on the effect of grain size on the creep of metals have shown that, for any one material, a fine grain size material is in general less creep resistant than a coarser grain size material. This is attributed to the fact that the finer grain size material is generally less stable structurally.

Thus, the copperized lead, with a very fine grain size, has less creep resistance at the higher temperatures and longer creep times than it would with a coarse grain size. Under the present test conditions, this grain size effect is apparently great enough to more than counteract the alloy strengthening effect of the copper addition.

The grain size is an important factor in the creep of metals, and should be evaluated for the creep of lead at the contemplated service temperatures.

VI Summary

The tensile, compression, shear, bearing, and creep properties of a high purity lead and a 0.058% copper-lead alloy were evaluated at test temperatures of 100, 175, 250, and 325°F.

The data are summarized in graphical and tabular form in the Experimental Results section of the report.

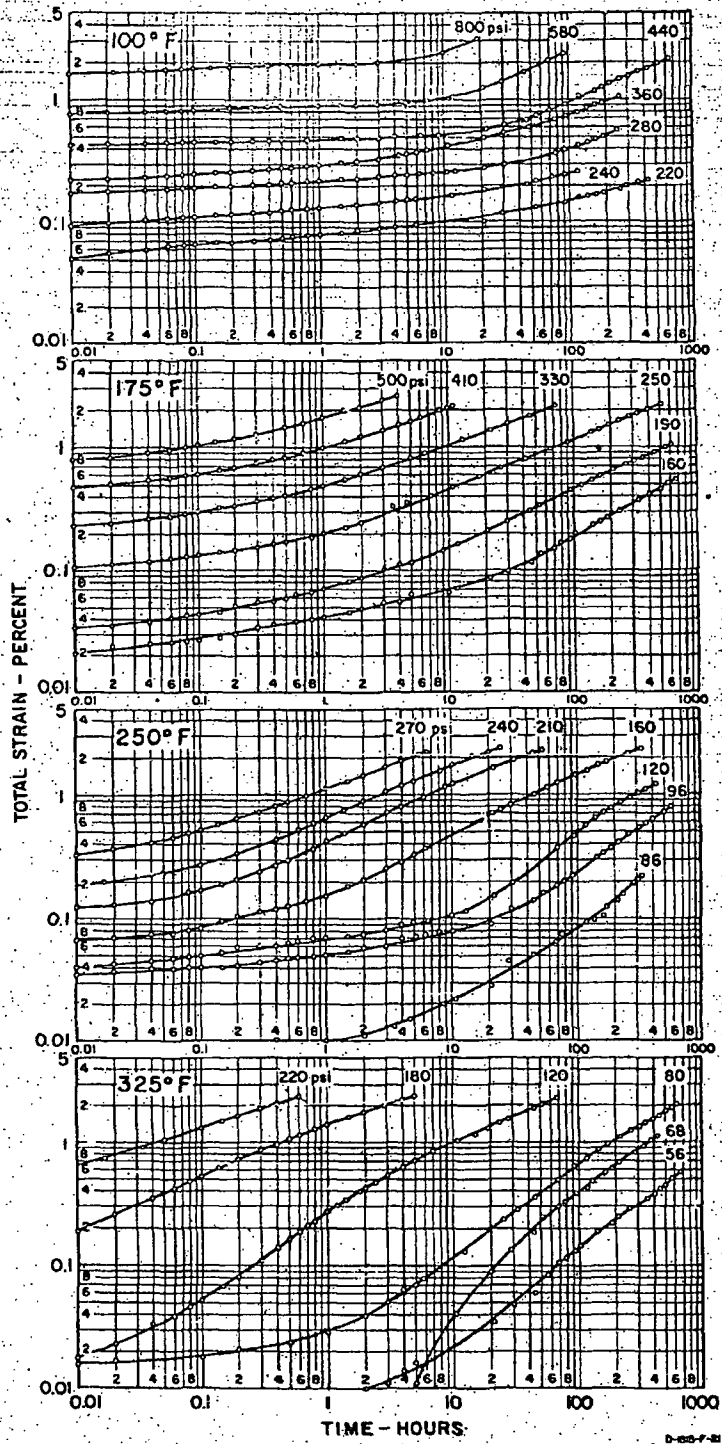


FIG. 19
TOTAL STRAIN VS CREEP TIME FOR HIGH PURITY LEAD

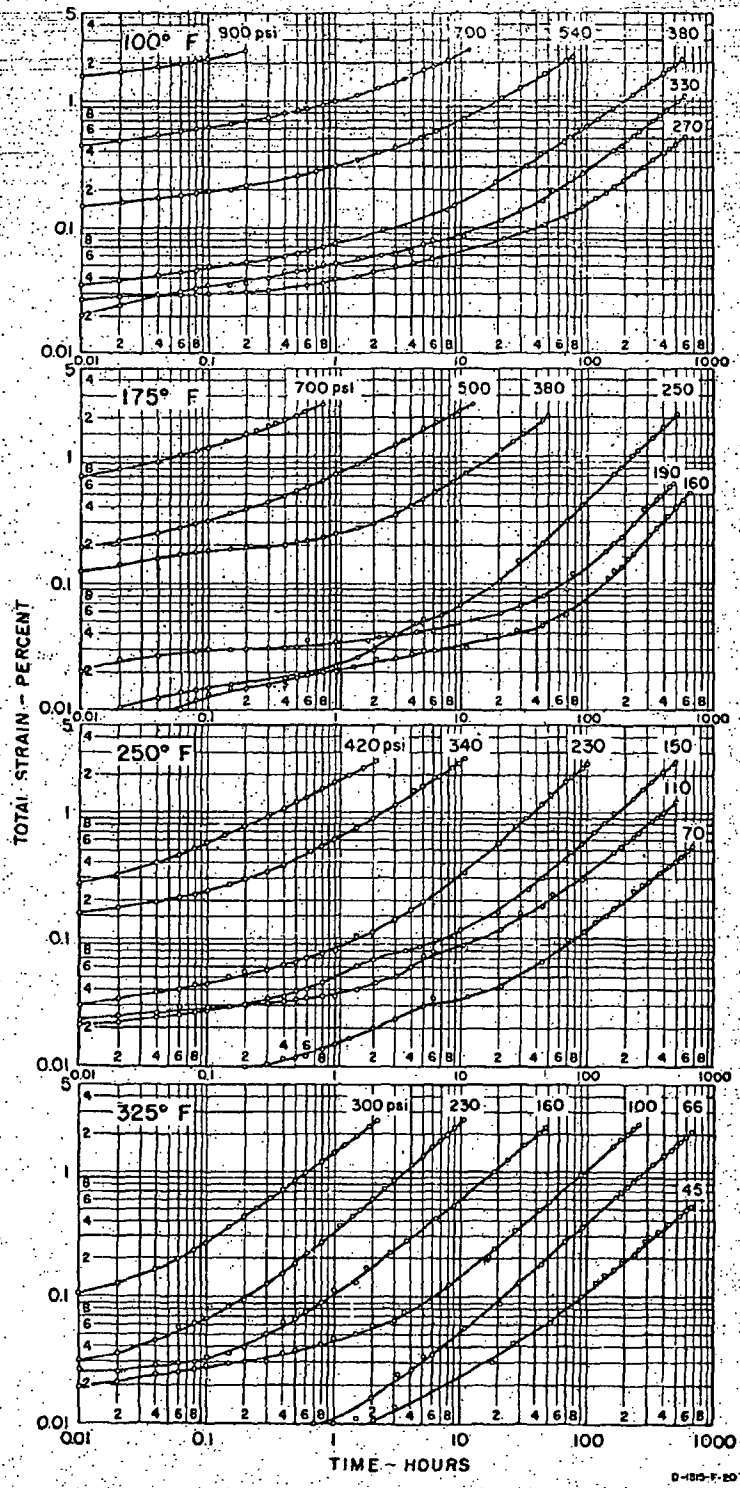


FIG. 20
TOTAL STRAIN VS CREEP TIME FOR COPPERZIED LEAD

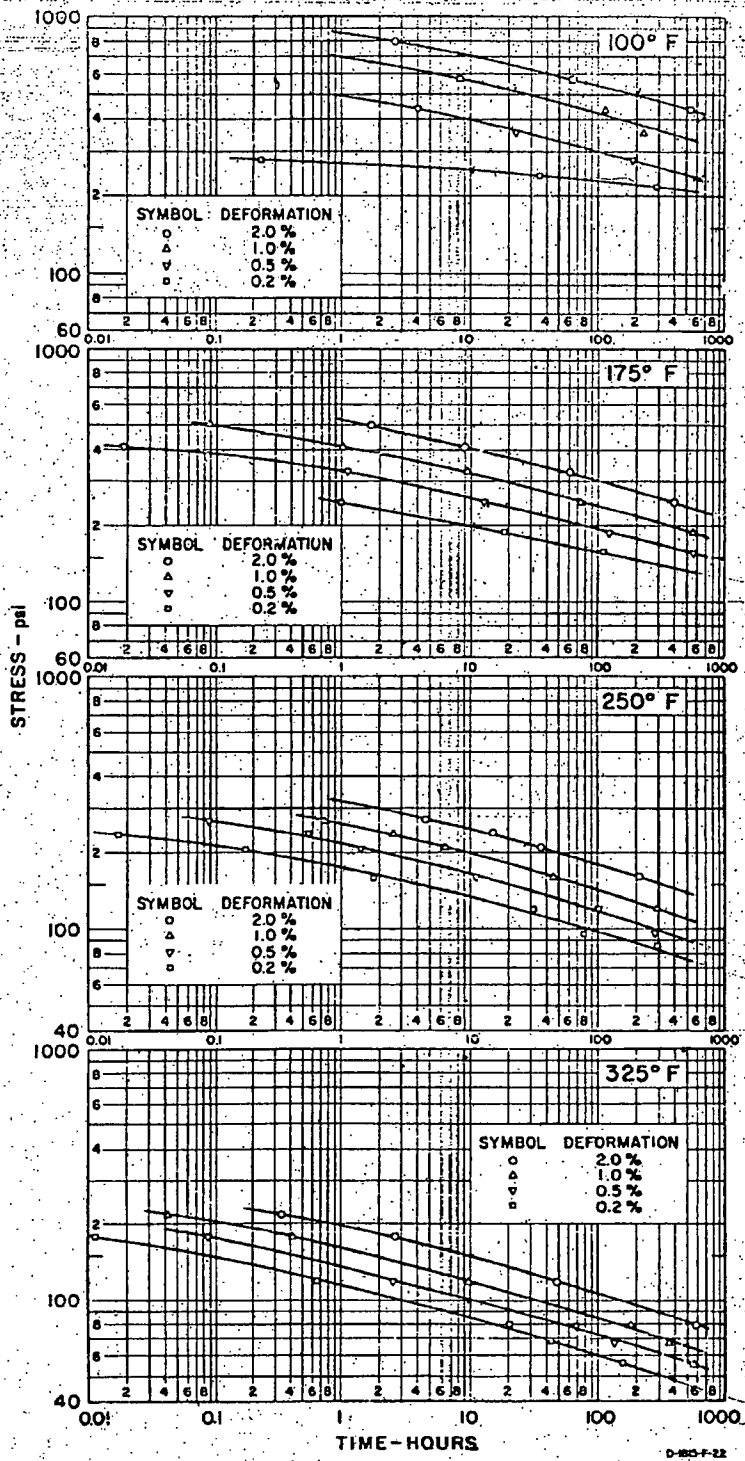


FIG. 21
 STRESS VS CREEP TIME AT CONSTANT STRAIN VALUES OF
 0.2, 0.5, 1.0, AND 2.0% FOR HIGH PURITY LEAD

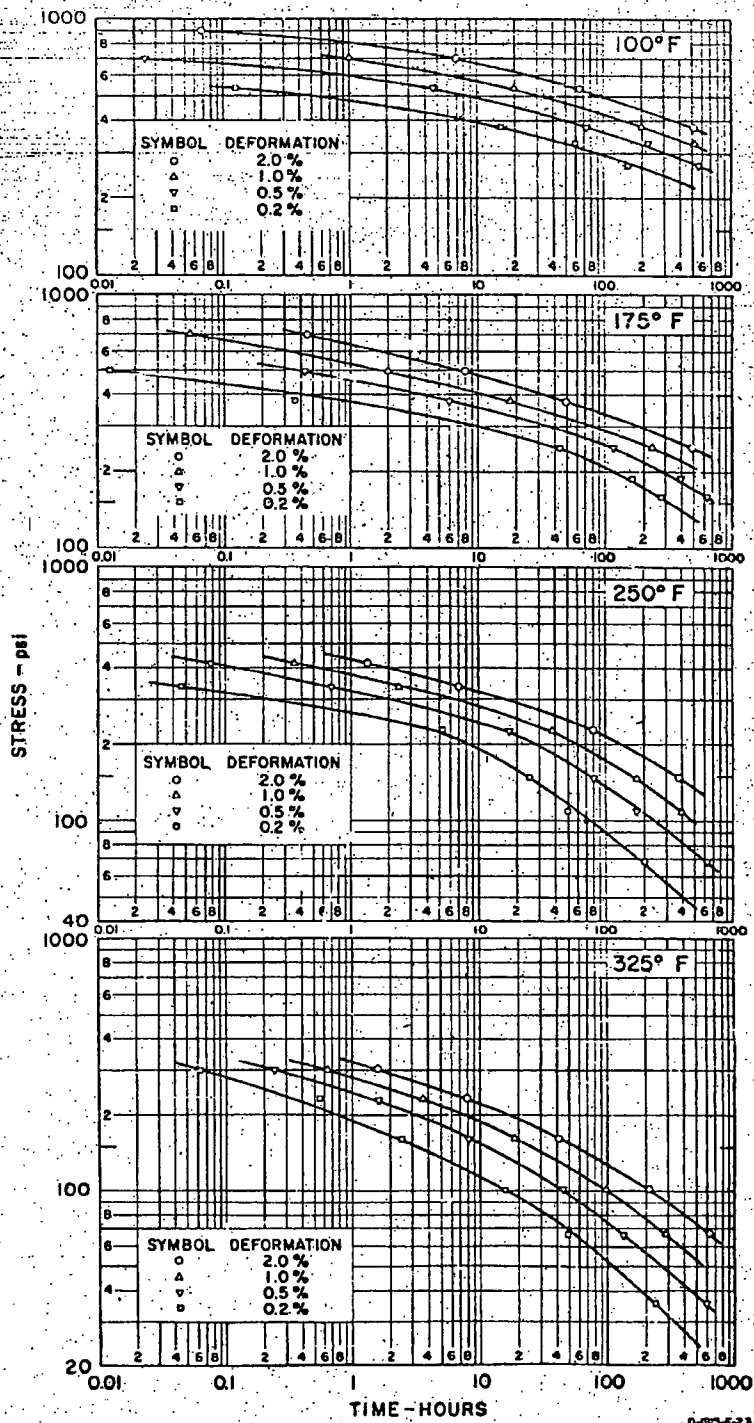


FIG. 22

STRESS VS CREEP TIME AT CONSTANT STRAIN VALUES OF 0.2, 0.5, 1.0, AND 2.0% FOR COPPERZIED LEAD

3151

NUREG/CR-0481
SAND77-1872
R-7

An Assessment of Stress-Strain Data Suitable for Finite-Element Elastic-Plastic Analysis of Shipping Containers

Henry J. Rack, Gerald A. Knorovsky



Sandia Laboratories

Prepared for

U. S. NUCLEAR REGULATORY COMMISSION

NUREG/CR-0481
SAND77-1872
R-7

AN ASSESSMENT OF STRESS-STRAIN DATA SUITABLE FOR FINITE-ELEMENT ELASTIC-PLASTIC ANALYSIS OF SHIPPING CONTAINERS

This report was prepared as an account of work sponsored by the United States Government. While the Government and the United States Department of Energy are not their employees, neither their salary or compensation, nor that of their family or immediate dependents, or either any part or condition of any intellectual, apparatus, product or process disclosed, or apparatus that by its use would not constitute patentable subject matter.

H. J. Rack
G. A. Knorovsky

Date Published: September 1978

APPROVED:

[Signature]
Manager, Nuclear Fuel Cycle Technology Development

[Signature]
Director, Nuclear Fuel Cycle Programs

Sandia Laboratories
Albuquerque, New Mexico 87185

Operated by
Sandia Corporation
for the
U. S. Department of Energy

MASTER

Prepared for
Division of Safeguards, Fuel Cycle and Environmental Research
Office of Nuclear Regulatory Research
U. S. Nuclear Regulatory Commission
Under Interagency Agreement DOE 40-550-75
NRC File No. A1045

ABSTRACT

Stress-strain data which describes the influence of strain rate and temperature on the mechanical response of materials presently being used for light water reactor shipping containers have been assembled. Selection of data has been limited to that which is suitable for use in finite-element elastic-plastic analysis of shipping containers (e.g., they must include complete material history profiles). Based on this information, recommendations have been made for further work which is required to complete the necessary data base.

CONTENTS

	<u>Page</u>
Introduction.....	11
Materials.....	12
Mechanical Properties.....	12
Austenitic Stainless Steels.....	12
Uranium.....	26
Lead.....	33
Summary and Recommendations	43
Mechanical Properties.....	44
Thermal Expansion.....	44
Elastic Properties.....	45
References.....	46
APPENDIX A - Thermal Expansion Behavior of Selected Stainless Steels, Lead, and Uranium.....	51
Stainless Steels.....	51
Uranium.....	53
Lead.....	55
APPENDIX B - Elastic Properties of Selected Stainless Steels, Uranium, and Lead.....	57
Stainless Steels.....	57
Uranium.....	65
Lead.....	66
APPENDIX C - List of Symbols.....	67
APPENDIX D - References.....	68

TABLES

<u>Number</u>		<u>Page</u>
I	Chemical Composition of LWR Shipping Cask Materials.....	13
II	Material Procurement Specifications for Light Water Reactor Shipping Casks.....	14
III	Stress-Strain Curve Availability for Selected Stainless Steels.....	16
IV	Tensile Properties of Representative Stainless Steel Alloys.....	18
V	Typical Parametric Representations Proposed for Austenitic Stainless Steels.....	25
A-I	Thermal Linear Expansion of Stainless Steel.....	52
A-II	Thermal Linear Expansion of Polycrystalline α -Uranium..	54
B-I	Effect of Temperature on the Elastic Constants of Selected Stainless Steels.....	58
B-II	Young's Modulus for Annealed 304 Stainless Steel.....	59
B-III	Shear Modulus for Annealed 304 Stainless Steel.....	59
B-IV	Poisson's Ratio for Annealed 304 Stainless Steel.....	60
B-V	Young's Modulus for Annealed 316 Stainless Steel.....	60
B-VI	Shear Modulus for Annealed 316 Stainless Steel.....	61
B-VII	Poisson's Ratio for Annealed 316 Stainless Steel.....	61
B-VIII	Probable Values for Elastic Moduli of Non-textured Polycrystalline Uranium.....	65

ILLUSTRATIONS

<u>Figure</u>		<u>Page</u>
1	Stress-strain curves for 321 stainless steel sheet at room temperature.....	17
2	Compressive stress-strain curves for 321 stainless steel sheet at room and elevated temperatures.....	17
3	Stress-strain curves for 321 stainless steel sheet at room and elevated temperatures.....	17
4	Stress-strain curves for 321 stainless steel sheet at room and elevated temperatures.....	17
5	Stress-strain curves for 347 stainless steel sheet at room and elevated temperatures.....	17
6	Stress-strain curves to failure at room and elevated temperatures for 347 stainless steel.....	17
7	Heat-to-heat variation in stress-strain diagrams for 304 stainless steel tested at (a) 297 K, (b) 366 K, (c) 477 K, and (d) 589 K.....	19
8	Heat-to-heat variation in stress-strain diagrams for 316 stainless steel at (a) 297 K, (b) 366 K, (c) 477 K, and (d) 598 K.....	20
9	Engineering stress versus engineering strain for the 301 stainless steel tested at a strain rate of $1.03 \times 10^{-3} \text{sec}^{-1}$	21
10	Tensile properties of standard grades of austenitic steel in temperature range -200 to +800°C.....	22
11	Effect of alloy stability on tensile properties of austenitic steels.....	22
12	Relationship between strain rate and temperature for serrated flow in type 330 stainless steel.....	23
13	The effect of test temperature (-200°C to 900°C) on the tensile properties and fracture of uranium.....	28
14	Ductile/brittle transition temperature versus $\log_{10}(\text{grain diameter})^{-1/2}$ for U - 300 ppm C, 50 ppm Al, 60 ppm Si, and 50 ppm Fe.....	29
15	Load-elongation curves of α -uranium (U - 140 ppm C, 30 ppm Al, 140 ppm Fe, 60 ppm Si, 40 ppm O ₂). Strain rate $2.6 \times 10^{-4} \text{sec}^{-1}$	30

ILLUSTRATIONS (cont.)

<u>Figure</u>	<u>Page</u>
16 Influence of strain rate on the true-stress versus true-strain curves of annealed polycrystalline α -uranium (110 ppm C, 35 ppm Al, 70 ppm Si, 15 ppm Cr, 8 ppm Mo, 60 ppm Fe, 40 ppm Ni, 6 ppm Cu) at 78 and 300 K.....	31
17 Stress-strain curves for alpha-extruded uranium (20 ppm C, 12 ppm N, 53 ppm Fe, 27 ppm Si, 1.3 ppm B ₂).....	32
18 Mechanical properties of uranium - 2 weight percent Mo.....	34
19 Phase diagrams for (a) copper-lead and (b) silver-lead.....	35
20 Triplicate tensile stress-strain curves to failure at a strain rate of $1 \times 10^{-3} \text{ sec}^{-1}$	37
21 Triplicate tensile stress-strain curves to 2 percent strain at a strain rate of $8.3 \times 10^{-4} \text{ sec}^{-1}$	38
22 Effect of strain rate on the tensile stress-strain curves at 311 and 393 K (triplicate curves).....	39
23 Triplicate compression stress-strain curves to 5 percent strain at a strain rate of $2.5 \times 10^{-4} \text{ sec}^{-1}$	40
24 Stress-strain curves for Pb.....	41
25 Influence of strain rate on flow stress of Pb.....	41
26 Tensile strength and elongation as a function of test temperature at a strain rate of $8.3 \times 10^{-4} \text{ sec}^{-1}$	42
27 Quasi-static true stress-strain curves for chemical lead test specimens in tension.....	42
28 Quasi-static true stress-strain curves for chemical lead test specimens in compression.....	42
29 Stress-strain curves of lead for four strain-rate ranges.....	43

ILLUSTRATIONS (cont.)

<u>Figure</u>	<u>Page</u>
A-1 Thermal expansion of 304 and 321 stainless steel.....	53
A-2 Thermal expansion behavior of α -uranium.....	54
A-3 Thermal expansion behavior of lead.....	56
B-1 Young's modulus of 304SS, annealed.....	62
B-2 Young's modulus of 316SS, annealed.....	62
B-3 Shear modulus of 304SS, annealed.....	63
B-4 Shear modulus of 316SS, annealed.....	63
B-5 Poisson's ratio of 304SS, annealed.....	64
B-6 Poisson's ratio of 316SS, annealed.....	64
B-7 Young's modulus of pure polycrystalline uranium as a function of temperature.....	65
B-8 Young's modulus of lead.....	66

AN ASSESSMENT OF STRESS-STRAIN DATA SUITABLE FOR
FINITE-ELEMENT ELASTIC-PLASTIC ANALYSIS OF SHIPPING CONTAINERS

Introduction

Recent progress in finite-element elastic-plastic analysis has brought with it a requirement for a more detailed description of a material's response to imposed mechanical and thermal loadings. Unfortunately, metallurgists have in the past typically reported the influence of such variables as temperature and strain rate only on selected properties (e.g., yield strength or tensile elongation) rather than the generalized elastic-plastic representation required for modern computer program applications.

Notwithstanding this shortcoming, a body of literature exists that can form the basis for advanced computer-aided design. The purpose of this report is to assess and compile available data, particularly those relevant to materials which are being used for light water reactor (LWR) spent fuel shipping container primary structures. Consequently, this assessment has been limited to selected stainless steels, uranium, and chemical lead. It includes, where possible, data on the stress-strain behavior of these materials over a range of strain rates (10^{-5} to 10^2 sec^{-1}) and temperatures (-40 to 320°C ; -40°F to 620°F) thought to be typical of shipping cask environments.

This survey has considered only uniaxial deformation, tensile or compressive, and does not contain any multiaxial information. In addition, fracture, creep, and cyclic loading conditions have been excluded. Since the data sources examined in

BLANK PAGE

this study generally did not cite whether the values given were average or minimum data reported are thought to be typical of the materials being examined rather than representing either average or minimum values.

This report first lists the materials used in typical shipping cask designs and their procurement specifications. It then discusses the available mechanical properties data, particularly stress-strain curves, treating each of the specific materials in separate subsections. Finally, the report recommends specific areas for further research and data acquisition.

Materials

Table I lists the chemical compositions of some of the materials presently used for LWR shipping casks. Table II lists the specific cask being considered and the material specification required for procurement of the requisite structural shapes.

Mechanical Properties

Austenitic Stainless Steels

Many investigators have examined austenitic stainless steels, because of their excellent corrosion resistance, creep resistance, and high toughness. However, their studies have tended to neglect the regime of stress/strain-rate/temperature of interest for shipping cask applications.

Probably the most extensive compilation of stress-strain data may be found in studies conducted at the Oak Ridge National

TABLE I
Chemical Composition of LWR Shipping Cask Materials
(Percentage by weight; minimum amount unless otherwise noted)

	C	Mn	Si	P	S	Cr	Mo	Ni	Fe	Other
Austenitic										
316	0.08	7.5-9.0	1.0	0.045	0.03	17.5-22.0	0.0-7.0	1.0-2.0	-	0.25/3 N
304	0.08	2.0	1.0	0.045	0.03	18.0-20.0	0.0-10.5	-	-	-
304L	0.03	2.0	1.0	0.045	0.03	18.0-20.0	0.0-12.0	-	-	-
309	0.08	2.0	1.0	0.045	0.03	19.0-21.0	0.0-12.0	3.0-4.0	-	-
317	0.08	1.5	1.5	0.045	0.04	18.0-21.0	0.0-13.0	3.0-4.0	-	-
321	0.08	2.0	1.0	0.045	0.03	17.0-19.0	0.0-13.0	-	-	0.7 Ti
347	0.08	2.0	1.0	0.045	0.03	17.0-19.0	0.0-13.0	-	-	1.1 (Cp)Ta
Ferritic										
A133 (C-1)	0.25	0.4-1.06	0.15-0.35	0.04	0.04	0.4	0.7-1.0	0.4-0.6	-	0.010-0.08 Ni/0.002/0.008 Al/0.15/0.3 Cu
A134 (C-1)	0.1-0.2	0.6-1.0	0.15-0.35	0.035	0.04	0.4	0.7-1.0	0.4-0.6	-	0.008 Al/0.15/0.3 Cu
A156 (C-55)										
1/2"	0.18	0.50-0.84	0.13-0.33	0.035	0.04	-	-	-	-	-
4"	0.12	0.50-1.25	0.13-0.33	0.035	0.04	-	-	-	-	-
8"	0.24	0.50-1.25	0.13-0.33	0.035	0.04	-	-	-	-	-
8"	0.2	0.50-1.25	0.13-0.33	0.035	0.04	-	-	-	-	-
A156 (C-70)										
1/2"	0.27	0.8-1.25	0.13-0.33	0.035	0.04	-	-	-	-	-
4"	0.26	0.8-1.25	0.13-0.33	0.035	0.04	-	-	-	-	-
4"	0.21	0.8-1.25	0.13-0.33	0.035	0.04	-	-	-	-	-
4"	0.21	0.8-1.25	0.13-0.33	0.035	0.04	-	-	-	-	-
A160										
A161	0.30-0.45	0.75-1.0	0.15-0.35	0.035	0.035	0.8-1.1	0.25	0.15-0.25	0.25 Cu	-
A163	0.40-0.45	0.75-1.0	0.15-0.35	0.035	0.035	0.8-1.1	0.25	0.15-0.25	0.25 Cu	-
A165	0.43-0.48	0.75-1.0	0.15-0.35	0.035	0.035	0.8-1.1	0.25	0.15-0.25	0.25 Cu	-
A304	0.30-0.43	0.6-0.85	0.1-0.35	0.04	0.04	0.7-0.9	1.0-2.0	0.3-0.5	-	-
Precipitation Hardening										
A167	0.5	0.5	0.5	-	-	16.5-16.8	4.25	1.0-1.5	0.25 Cu/1.5 Co	-
A168	0.08	1.25	0.5	-	-	13.5-16.8	24.0-27.0	1.0-1.5	1.0/1.25 Ti	0.25 Al/0.3 V
Precipitation										
A169	0.01	0.09	0.09	0.09	0.1	0.00-0.20	0.8-1.2	0.02	-	-
303	0.05-0.2	1.0-1.5	0.6	0.7	0.25	0.00-0.20	0.8-1.2	0.02	-	-
4401	0.15-0.7	0.15	0.4-0.8	0.7	0.1	0.1	0.45-0.9	0.15	-	-
4403	0.10	0.10	0.3-0.6	0.20	0.1	0.15-0.35	1.1-1.6	0.1	-	-
302S	0.10	0.10	0.3-0.6	0.20	0.1	0.15-0.35	1.1-1.6	0.1	-	-
Chemical Fe	0.00-0.06	-	-	0.008	0.001	-	-	-	-	0.045 (Si)Cu 0.045 (Si)Fe 0.045 (Si)Ni 0.045 (Si)Pb

TABLE II
Material Treatment Specifications for Light Water Reactor Shipping Cores

Spec.	Material	Specifications ^a	Form
WR-4, WR-5 Spent Fuel Shipping Cask	304		plate, sheet, forging
	316		bolts
	317		chiseling
	304		miniforging
	316		sheet, plate
	317		forging, fitting, sheet, plate
	316		miniforging
	317		cast form
	316		plate
	317		plate
IF 304	304		bar
	316		sheet, plate
	317		sheet, plate
	316		sheet, plate
	317		sheet, plate
	316		sheet, plate
	317		sheet, plate
	316		sheet, plate
	317		sheet, plate
	316		miniforging
HL 10/24 Ball Cask	304		sheet, plate, forging
	316		bolts
	317		pipe & fittings, tubing
	304		bolting
	316		bolting
	317		bolting
	304		miniforging
	316		miniforging
	317		miniforging
	304		miniforging
TR 6, TR 9	304		bolts
	316		plate, sheet, forgings
	317		plate
	304		plate
	316		bolting
	317		bolting
	304		miniforging
	316		miniforging
	317		miniforging
	304		miniforging

^a Refer to SAH or ASTM specification (with the exception of the HL specification for W), and include additional composition restrictions imposed by manufacturer.

Laboratory and the Hanford Engineering Development Laboratory. Since these examinations were in support of the LMPER program, they have been principally concerned with temperatures above those of concern to this program. Table III summarizes the applicable data banks presently available from these institutions. These investigators have shown that while the yield strength of 304 stainless steel at 25°C (77°F) increases by 48 MN/m² per decade increase in strain rate, the overall stress-strain behavior of the alloy does not appear to be radically altered by these rate changes.

The stress-strain curves shown in Figures 1 through 6 and Table IV should be considered only as typical of the respective alloys and product forms. Studies [3] of different product forms produced from a single heat of 304 stainless steel have demonstrated that even when chemistry variables are eliminated, variations in processing operations can cause large changes in the stress-strain response. This effect of processing variations is further complicated by the rather wide chemistry allowances shown in Table I. Combinations of these factors—different chemistry and processing—have led to considerable property variability for nominally identical alloys. Examples of this heat-to-heat variability are given in Figures 7 and 8 for 304 and 316 stainless steels, respectively.

Two additional phenomena, (i.e., the formation of deformation induced martensite and dynamic strain-aging) have been observed during tensile straining of austenitic stainless steels. The former can result in drastic changes in the stress-strain

TABLE III
Stress-Strain Curve Availability for Selected Stainless Steels*

Temperature, °C(°F)	Strain Rate (sec ⁻¹)									
	3x10 ⁻⁶	8x10 ⁻⁶	4x10 ⁻⁵	1x10 ⁻⁵	8x10 ⁻⁵	4x10 ⁻⁴	1x10 ⁻⁴	8x10 ⁻⁴	4x10 ⁻³	1x10 ⁻³
25 (77)	-	304	304	304S	304	304	304	304	304	304S
	-	-	308	-	-	308	304S	-	-	-
	-	-	308L	316	-	308CRK	316S	-	-	-
	-	-	308+	-	-	3081	316	-	-	-
	-	-	308CRZ	-	-	308CRK1	-	-	-	-
	-	-	-	-	-	304S	-	-	-	-
93 (200)	-	-	-	316	-	304	316	-	304	-
204 (400)	304	-	-	304S	304	316	-	-	304	-
	-	-	-	316	-	304	-	-	-	-
260 (500)	-	-	-	-	-	-	-	304	-	-
300 (575)	-	-	304	304S	-	-	-	-	-	-
316 (600)	304	-	308	316	304	304	316	304	304	-
	-	-	308L	-	308	-	-	-	-	-
	-	-	308L+	-	308CRZ	-	-	-	-	-
	-	-	308L+	-	-	-	-	-	-	-
	-	-	308	-	-	-	-	-	-	-

*All 308 variations are weld metal, stress-relieved.

†Aged (various treatments)

‡Weld Material

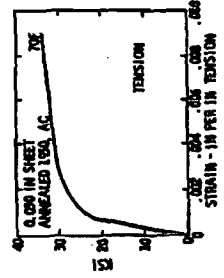


Figure 3. Stress-strain curves for 321 stainless steel sheet at room temperature [13].

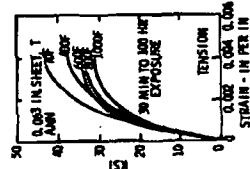


Figure 2. Compressive stress-strain curves for 321 stainless steel sheet at room and elevated temperatures [1].

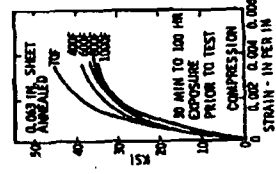


Figure 3. Stress-strain curves for 316 stainless steel sheet at room and elevated temperatures [1].

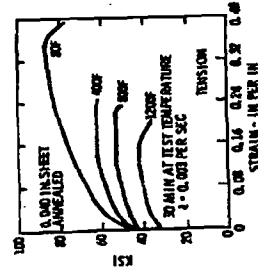


Figure 4. Stress-strain curves for 316 stainless steel sheet at room and elevated temperatures [1].

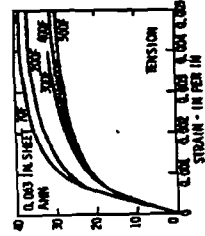


Figure 5. Stress-strain curves for 316 stainless steel sheet at room and elevated temperatures [1].

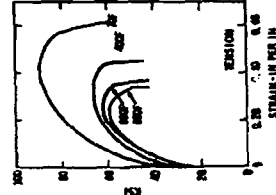


Figure 6. Stress-strain curves for 316 stainless steel sheet at room and elevated temperatures [1].

TABLE IV

Tensile Properties of Representative Stainless Steel Alloys									
Test Temperature °C		-50	-20	0	20	100	200	300	400
Tensile Strength		159.7	141.6	127.4	89.6	68.8	63.4	63.2	63.2
Stress ksi @									
Type 304	0.02% Strain	24.6	28.0	28.7	28.2	19.7	15.2	14.3	12.8
	0.05% Strain	28.7	31.4	31.8	30.0	21.5	17.9	16.6	15.5
	0.1 % Strain	33.8	33.2	33.6	31.4	22.8	19.0	17.7	16.6
	0.2 % Strain	34.3	34.9	35.2	32.7	24.2	20.2	18.8	17.5
	Elongation (%)	56.1	55.9	64.7	70.8	58.5	49.1	44.7	45.5
Reduction of Area (%)		71.0	67.0	75.0	77.4	78.5	75.2	69.6	72.0
Tensile Strength		120.7	104.8	98.6	84.7	72.1	66.8	67.2	67.6
Stress ksi @									
Type 316	0.02% Strain	37.2	33.6	30.2	28.7	22.0	18.6	17.3	16.1
	0.05% Strain	42.3	37.6	33.8	30.9	24.0	19.9	18.4	17.0
	0.1 % Strain	45.2	39.9	36.7	32.3	25.5	20.8	19.0	17.7
	0.2 % Strain	48.8	41.7	37.9	34.0	26.7	22.0	20.2	18.8
	Elongation (%)	84.0	87.3	80.1	60.7	54.1	48.2	45.5	45.6
Reduction of Area (%)		74.0	74.0	62.0	77.4	76.3	75.2	68.4	69.6
Tensile Strength		147.6	127.7	110.4	85.8	71.5	63.8	60.9	62.9
Stress ksi @									
Type 321	0.02% Strain	22.8	27.6	34.0	22.8	18.8	19.0	15.7	14.1
	0.05% Strain	26.7	30.9	39.4	25.5	23.3	20.8	17.7	16.6
	0.1 % Strain	30.0	33.2	40.5	27.3	25.1	22.2	19.3	17.7
	0.2 % Strain	34.5	36.1	41.0	29.3	26.7	23.5	20.4	20.2
	Elongation (%)	47.6	53.5	64.2	63.8	53.7	45.0	39.7	39.4
Reduction of Area (%)		70.0	71.7	75.0	7.4	78.4	72.0	72.0	67.2
Tensile Strength		165.6	127.2	111.6	94.3	75.5	66.5	64.1	64.5
Stress ksi @									
Type 347	0.02% Strain	29.3	30.7	29.8	29.8	23.1	19.3	17.9	17.5
	0.05% Strain	34.9	35.8	32.9	31.4	25.8	23.3	20.2	19.3
	0.1 % Strain	39.4	39.2	37.9	33.2	27.8	25.3	22.4	20.4
	0.2 % Strain	44.8	42.8	40.1	35.2	29.3	27.1	23.7	22.0
	0.5 % Strain	48.8	45.2	41.0	35.8	-	-	-	-
	1.0 % Strain	52.4	50.2	43.7	38.8	-	-	-	-
	Elongation (%)	49.5	56.2	65.2	54.6	48.0	41.1	41.3	39.3
Reduction of Area (%)		69.6	64.0	75.0	72.0	65.8	72.0	70.0	67.2

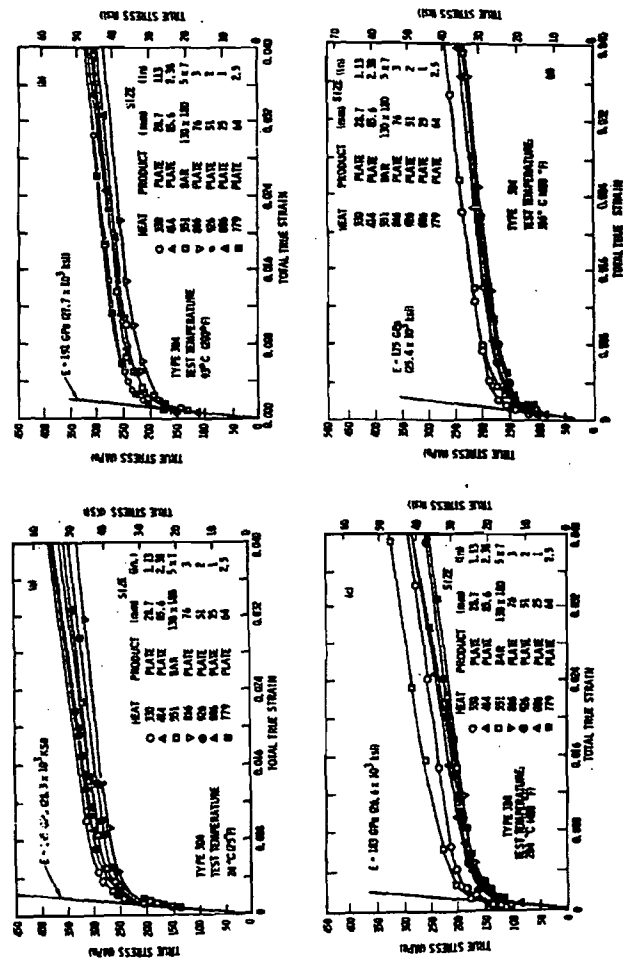


Figure 7. Heat-to-heat variation in stress-strain diagrams for 304 stainless steel tested at (a) 24°C, (b) 83°C, (c) 204°C, and (d) 318°C (41).

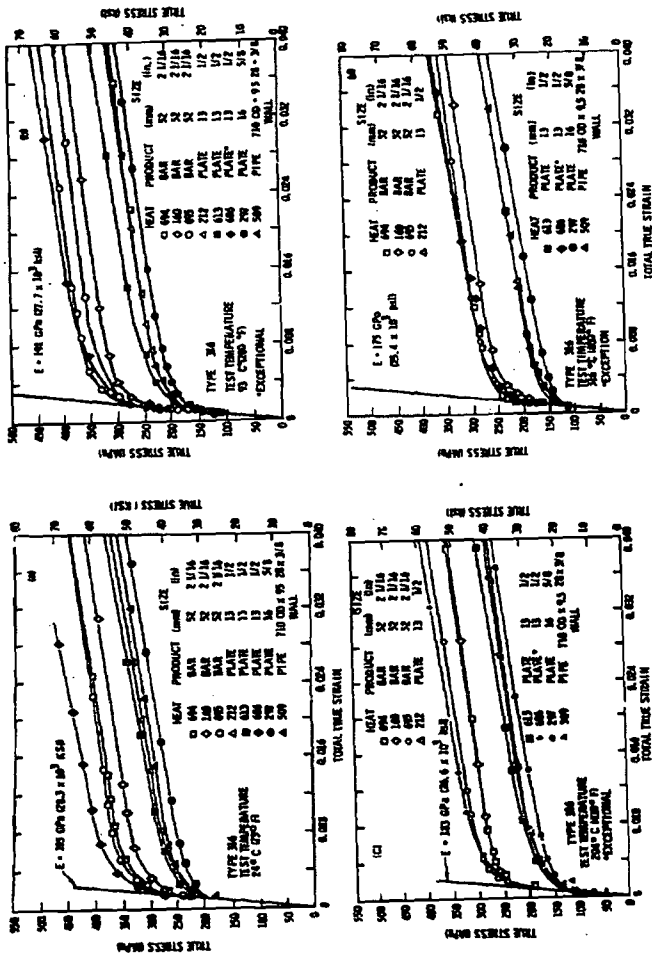


Figure 8. Heat-to-heat variation in stress-strain diagrams for 316 stainless steel at (a) 24°C, (b) 93°C, (c) 204°C, and (d) 316°C [4].

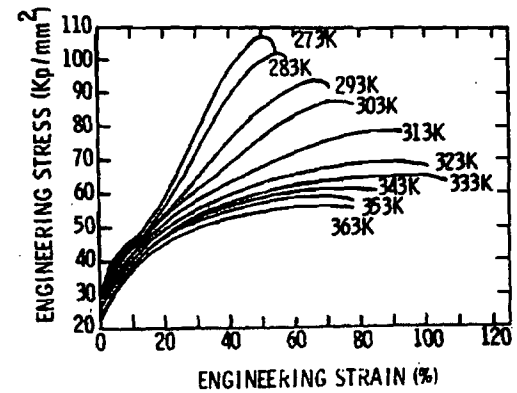


Figure 9. Engineering stress versus engineering strain for the 301 stainless steel tested at a strain rate of $1.03 \times 10^{-3} \text{sec}^{-1}$ [5].

behavior. Figure 9 shows a representative example of the effect of test temperature on the mechanical response of 301, an alloy less stable (i.e., more prone to martensite formation) than 304. Normally, stable austenitic stainless steels show an increase in yield and ultimate strengths with decreasing temperatures below ambient [2]. On the other hand, martensite-forming grades exhibit a slight decrease in yield but a rapid increase in ultimate strength. A sharp maxima in the tensile ductility also occurs (Figures 10 and 11). Although austenitic stainless steels (such as 304) which are used for LWR shipping casks are typically thought to be quite stable with respect to martensite formation, it is possible this transformation might occur in containers stressed at low temperatures. Unfortunately, the

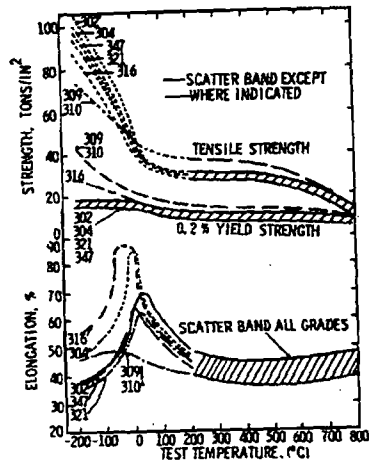


Figure 10. Tensile properties of standard grades of austenitic steel in temperature range -200 to +800°C [2].

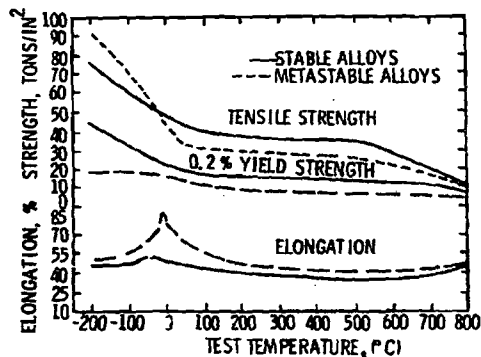


Figure 11. Effect of alloy stability on tensile properties of austenitic steels [2].

importance of this phenomenon cannot be quantitatively assessed at this time.

Dynamic strain-aging, the second phenomenon alluded to above, is usually associated with a change in the strain rate sensitivity (i.e., from an increase in flow stress with increasing strain rate to a decrease). Many consider strain-aging to be limited to bcc metals. There is evidence, however, that austenitic stainless steels may also exhibit dynamic strain-aging (serrations in the stress/strain curve) particularly in the temperature range 200 to 700°C [6]. The cross-hatched area in Figure 12 indicates the temperature and strain-rate regime within

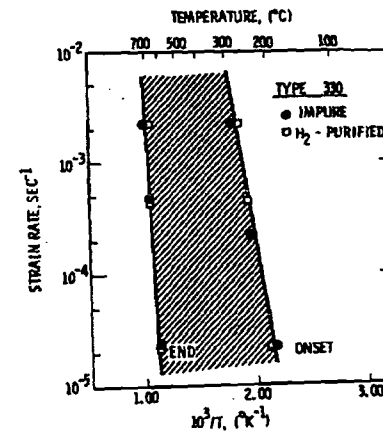


Figure 12. Relationship between strain rate and temperature for serrated flow in type 330 stainless steel [6].

which serrated flow is encountered in an AISI 330 stainless steel (Fe-15Cr-35Ni). In a more limited investigation [7], serrations have been reported in a type 316 stainless steel tested at 200°C utilizing a strain rate of $1.3 \times 10^{-2} \text{sec}^{-1}$. These conditions correspond with those predicted from the diagram for type 330 stainless steel.

The effect of strain-aging may also be important in weld regions. Current practice involves preparation of weldments with a small percentage (< 10 percent) of body-centered cubic (bcc) ferrite. This raises the possibility that not only might dynamic strain-aging take place in the face-centered cubic (fcc) parent (base) metal but also in the partially bcc weld region, perhaps under different conditions of temperature and strain-rate.

Finally, it should be recognized that it is virtually impossible to gather enough data to describe every conceivable combination of strain-rate and temperature. For this reason, procedures for interpolation and extrapolation between a more reasonable number of data points are required. Indeed, the ideal situation would be to obtain an accurate "equation of state" which might allow one to dispense with or minimize the requirements for a databank. Some progress has been made toward this goal [8-11]. These attempts involve parameterization of the stress/strain curves with the aim of reporting the influences of strain-rate, temperature, and material history on these characteristic functions. Some proposed equations are shown in Table V. However, these representations all suffer from a number of common difficulties. For example, none can predict the strain

TABLE V
Typical Parametric Representations Proposed
for Austenitic Stainless Steels

Equation	Reference
$\sigma = K_1 \dot{\epsilon}^{n_1} + \exp K_2 \exp n_2 \epsilon$	[12]
K_1, n_1, K_2, n_2 are constants	
$\sigma = (\sigma_0 - \sigma_\infty) \exp(-\epsilon/\epsilon_c) + \sigma_\infty$	[13]
$\sigma_0, \sigma_\infty, \epsilon_c$ are constants	
$\sigma - \sigma_P = \frac{C\dot{\epsilon}}{1 + P\dot{\epsilon}} + B\epsilon_P$	[14]
C, B, P are constants	
$\epsilon_L = \frac{\sigma}{E} + \left[\frac{\sigma - \sigma_P}{K} \right]^{1/m}$	[14]
K, m are constants	
See Appendix C for the definition of all other symbols.	

at fracture. Furthermore, phenomena such as strain-aging or martensite formation are not presently amenable to analysis.

Uranium

The choice of uranium or dilute uranium alloys for nuclear shielding applications is principally predicated on their high density (18.9 gm/cm^3) and atomic number. Some authors [15] suggest that these materials may be considered structurally equivalent to mild steel. However, this assumption is generally unfounded and is extremely misleading.

Pure uranium undergoes three phase changes between -40°C and its melting point. Between -40 and 633°C , the temperature region of primary interest in this examination, its crystal structure is orthorhombic. Between 663 and 700°C it has a complex tetragonal structure, and above 770°C it undergoes a transition to body centered cubic.

The orthorhombic crystal structure of the alpha (or low temperature) phase suggests that the mechanical and physical properties of uranium will be highly anisotropic. For example, Appendix A shows that the thermal expansion behavior of single crystal α -uranium, may vary by a factor of 5, depending upon the particular crystallographic direction being considered. Practically, this large anisotropy in thermal expansion results in some grains being stressed beyond yield upon cooling. Subsequent application of a load will then result in plastic flow at vanishingly small stresses [16,17].

Another complication which arises because of the anisotropic nature of α -uranium is that both its elastic and plastic properties (e.g., strain hardening behavior) are dependent upon prior processing history. Highly textured material, where nearly all of the elastically "strong" directions are aligned, shows a twofold difference in elastic modulus between the "strong" and "weak" directions (see Appendix B). Few previous investigators have measured or even considered this textural effect when discussing the plastic deformation of uranium. This fact makes direct comparisons between various studies difficult and may explain some of the scatter observed.

The mechanical properties of depleted α -uranium are also quite sensitive to temperature (Figure 13). Decreasing the test temperature from 663°C results in an increase in tensile yield and ultimate strength. This increase is accompanied (to approximately 350°C) by a decrease in tensile ductility. Between 350 and 25°C the ductility appears to be essentially independent of temperature, or may exhibit a slight minima. Finally, below 25°C the ductility decreases sharply (i.e., α -uranium undergoes a ductile-brittle transition at about 25°C). These ductility changes have been associated with fracture transitions from ductile failure, involving inclusions [18,19], to mixed ductile plus intergranular failure and, finally, to twin-matrix [19] cleavage failure at the lowest test temperature.

The ranges over which the differing temperature-ductility relationships are observed can be altered in addition by changing test conditions, α -uranium microstructure, chemistry, etc. The

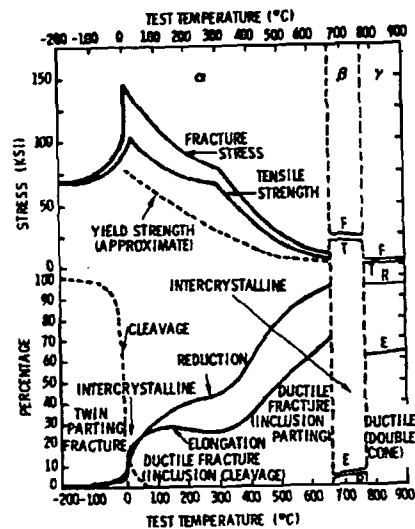


Figure 13. The effect of test temperature (-200°C to +900°C) on the tensile properties and fracture of uranium [18].

ductile-brittle transition temperature has been found to increase with increasing strain rate [21,22], grain size [17,18], grain shape irregularity [23,24], internal hydrogen content [22, 25-29], iron and aluminum content [24], residual stress level [30], humidity [31-33], and decreasing amounts of prior strain [17,34, 35]. The effect of one of these variables, grain size, on the transition temperature is shown in Figure 14. A quantitative assessment of the other variables awaits more detailed experimental studies.

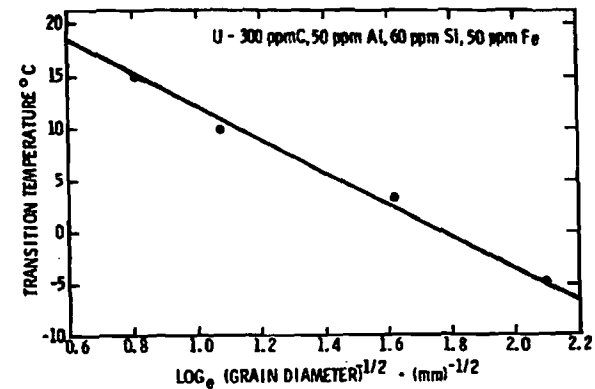


Figure 14. Ductile/brittle transition temperature versus $\log_{10}(\text{grain diameter})^{-1/2}$ for U - 300 ppm C, 50 ppm Al, 60 ppm Si, and 50 ppm Fe [3].

In a similar fashion, the ductility above the ductile-brittle transition region may be decreased by decreasing purity [36] and increasing residual stress [36,37]. Differences in residual stress level may also affect the strain hardening behavior of α -uranium. Figure 15(a) shows a family of serrated load-elongation curves of α -uranium in which the samples have had a high residual stress level induced in them by quenching from elevated temperature. If the same material had been furnace cooled, serrated yielding behavior would not have been observed (Figure 15(b)). The residual stress levels associated with these two heat treatment procedures were not reported so that our understanding of the influence of residual stress on the

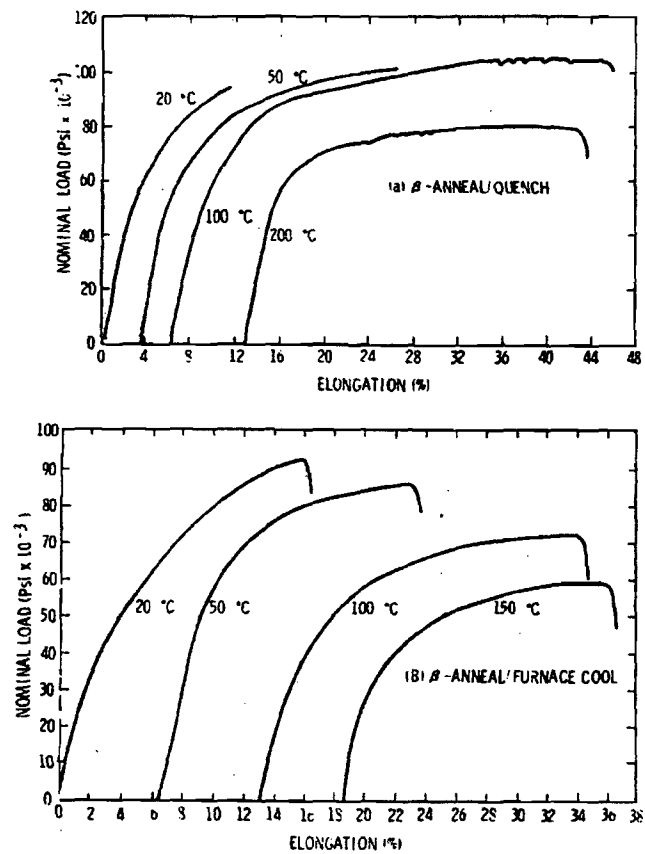


Figure 15. Load-elongation curves of α -uranium (U - 140 ppm C, 30 ppm Al, 140 ppm Fe, 60 ppm Si, 40 ppm O₂). Strain rate $2.6 \times 10^{-4} \text{sec}^{-1}$ [37].

tensile ductility in the temperature region 50 to 350°C remains qualitative. The same situation exists with regard to the impurity effects since no quantitative examination has been reported.

Finally, Figures 16 and 17 represent a summary of the presently available stress-strain curves for α -uranium. It should be recognized that neither of these series is for as-cast α -uranium; to date attempts to locate same have been unsuccessful. Notwithstanding this, it appears that the changes in strain hardening behavior that would be anticipated by increasing strain

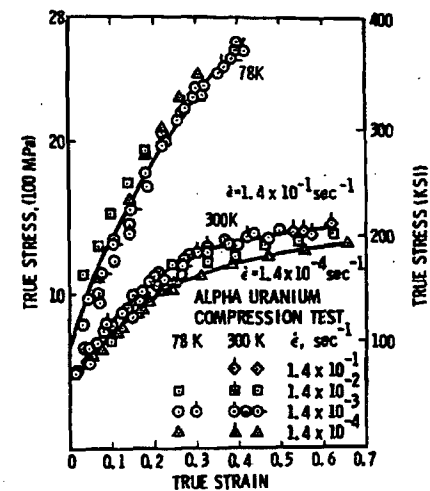


Figure 16. Influence of strain rate on the true-stress versus true-strain curves of annealed polycrystalline α -uranium (110 ppm C, 35 ppm Al, 70 ppm Si, 15 ppm Cr, 8 ppm Mo, 60 ppm Fe, 40 ppm Ni, 6 ppm Cu) at 78 and 300 K (-195 and 27°C) [38].

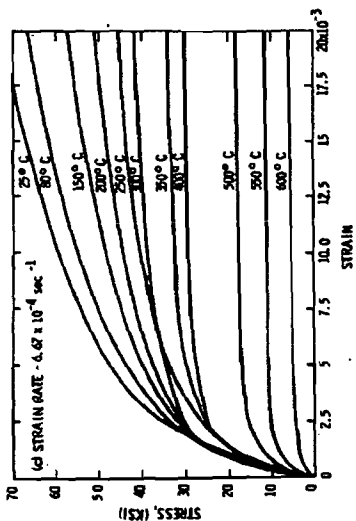
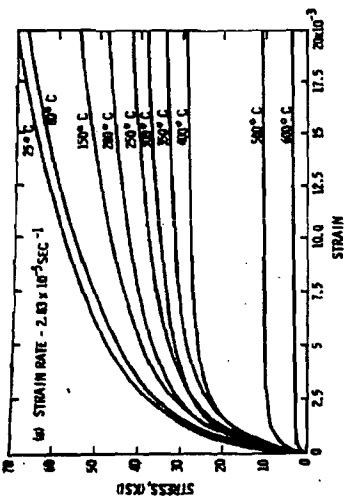
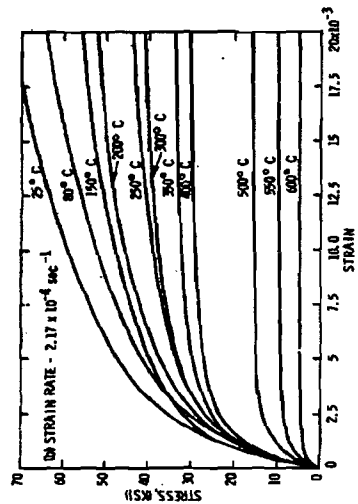


Figure 17. Stress-strain curves for alpha-uranium (20 ppm C, 15 ppm N, 5 ppm Fe, 2 ppm Si, 1.5 ppm B₂) (28).

rate appear quite small and that the changes in flow stress and strain hardening behavior with changing temperature appear to be of paramount importance.

These results all suggest that depleted α -uranium should not at present be considered as a primary structural member since it undergoes a sharp loss in ductility with decreasing temperature. However, there is some evidence which suggests that appropriately heat treated uranium alloys (e.g., U-2 wt% Mo) may have a ductile-brittle transition temperature well below that of α -uranium (compare Figures 13 and 18).

Lead

A review of those physical, chemical, and mechanical characteristics of lead which have resulted in its widespread use for nuclear shielding has been given by Stukenbroeker et al. [40]. Paramount among these is lead's high density ($\rho_{293K} = 11.35 \text{ gm/cm}^3$), low cost, and relative ease of fabrication. Although the present examination is limited to "chemical" lead, various other lead purities and alloys may be selected for nuclear applications.

The terminology "chemical" lead is generally restricted to material as specified by ASTM B29-55. Table I shows the standard chemical specification for this grade of pig lead, silver and copper being the principal impurities. Consideration of the Pb-Ag and Pb-Cu binary phase diagrams (Figure 19) suggests that while the Ag impurity concentration lies within the expected range of solid solubility, the presence of 0.04 to 0.06 weight percent copper will result in the formation of a two-phase

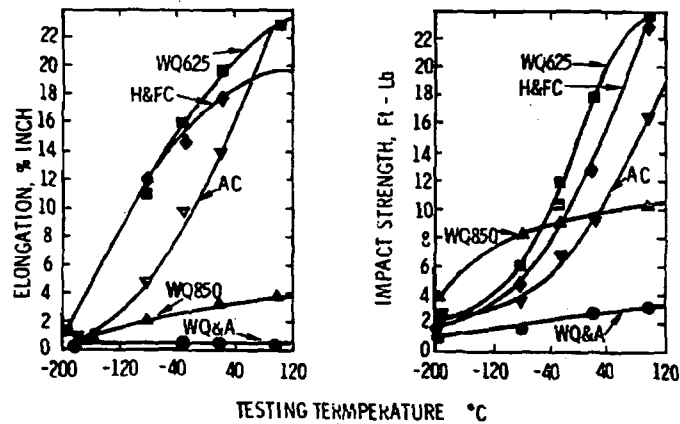
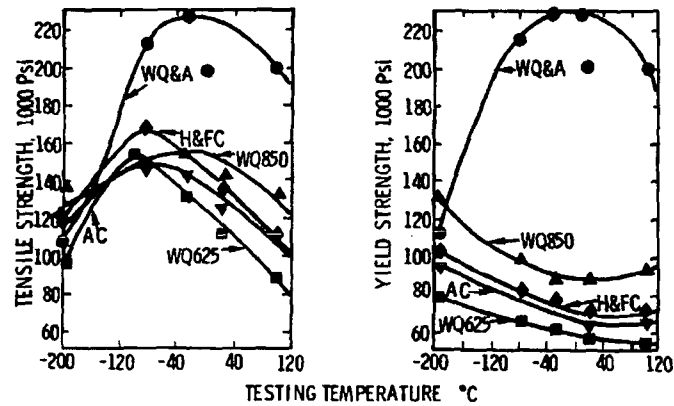


Figure 18. Mechanical properties of uranium-2 weight percent Mo (WQ&A: Water Quench and Age; H&FC: Homogenize and Furnace Cool; AC: Air Cool)[20].

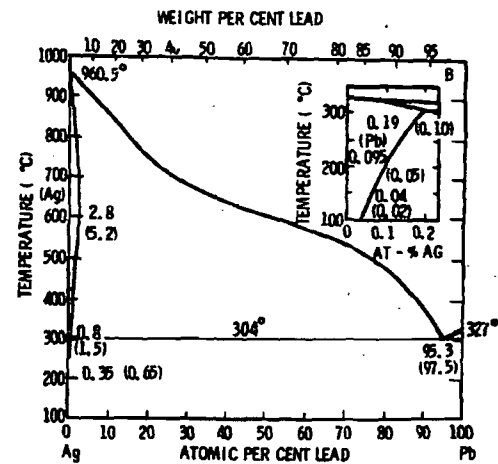
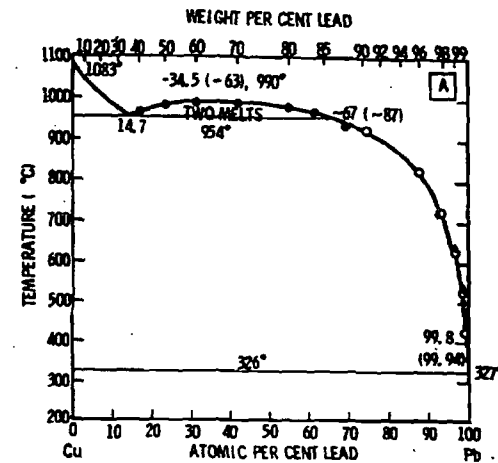


Figure 19. Phase diagrams for (a) copper-lead and (b) silver-lead [41].

(Cu+Pb) alloy. It is, therefore, not surprising that this small amount of copper has been reported to have a noticeable effect on the mechanical properties of lead.

Although there have been a number of examinations of the influence of strain-rate and temperature on the mechanical behavior of lead [42,56], application of these data to shipping cask environments is not straightforward. In general, the available data do not include a description of either the chemistry or thermomechanical condition for the material being examined. Under these circumstances probably the most complete series of experiments that have been performed to date are those of Tietz [51] (Figure 20 through 23) and Green et al. [56] (Figures 24 and 25). The former author's results demonstrate that the mechanical behavior of lead is quite sensitive to chemistry. Indeed, at low temperatures high purity (99.995 percent) lead is stronger than lead containing 0.058 weight percent Cu, contrary to what might be expected while at temperatures above 373 K (100°C), the opposite trend is observed (Figure 26). It is also interesting to note that the more recent results of Evans [45] (Figures 27 and 28) do not agree with those of Tietz. Presently, the cause of this discrepancy is undefinable, since Evans simply reported his material as "chemical" lead without giving any information as to the actual chemistry, grain structure, etc.

One final comment must be made regarding mechanical property reproducibility at high-strain rates. Generally the observed measurement errors are large and, more importantly, are unpredictable. For example, the undulations observed in the

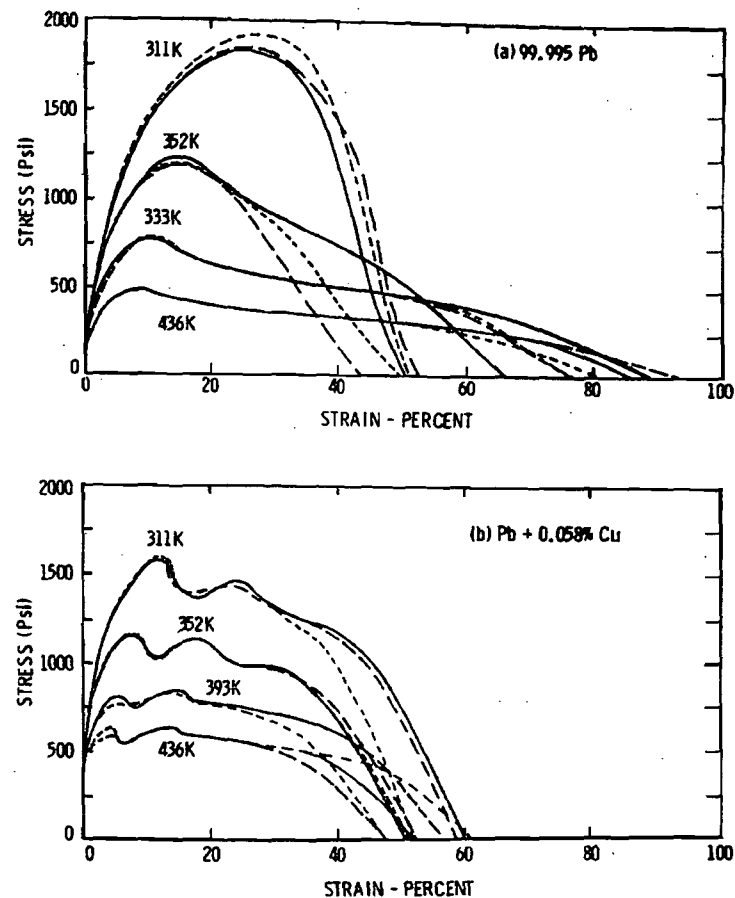


Figure 20. Triplicate tensile stress-strain curves to failure at a strain rate of $1 \times 10^{-3} \text{ sec}^{-1}$ [51].

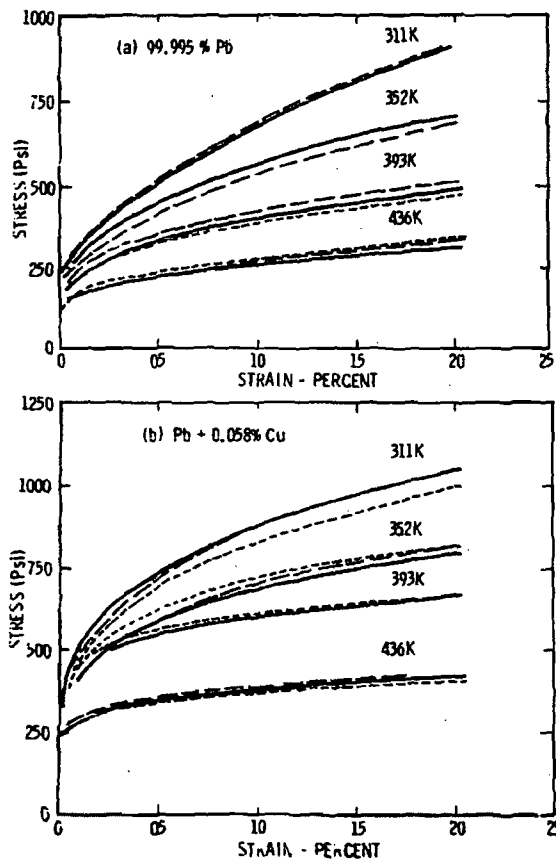


Figure 21. Triplicate tensile stress-strain curves to 2 percent strain at a strain rate of $8.3 \times 10^{-5} \text{ sec}^{-1}$ [51].

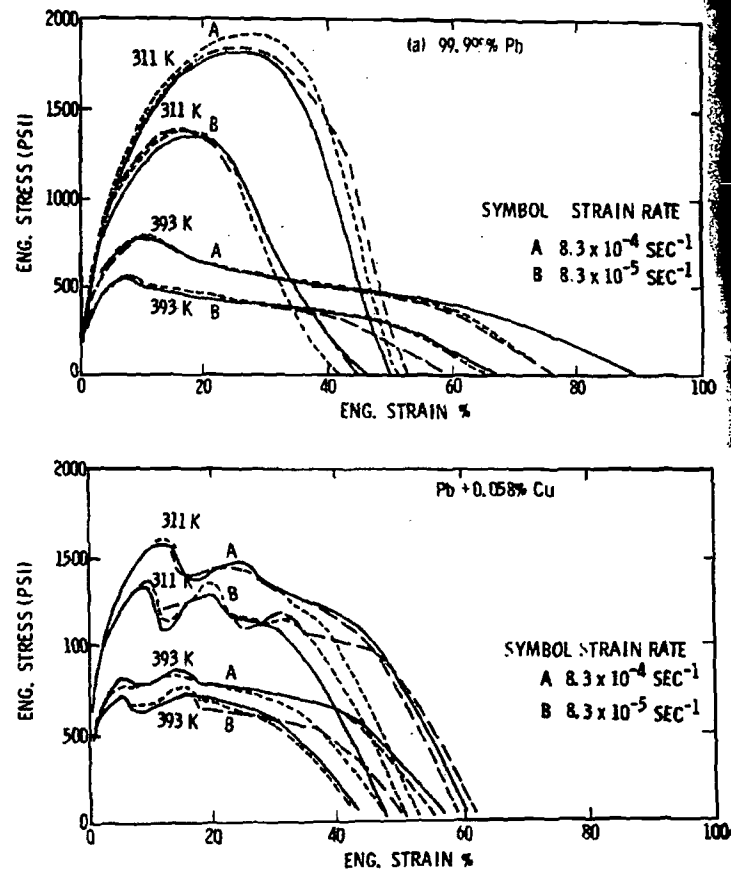


Figure 22. Effect of strain rate on the tensile stress-strain curves at 311 and 393 K (triplicate curves) [51].

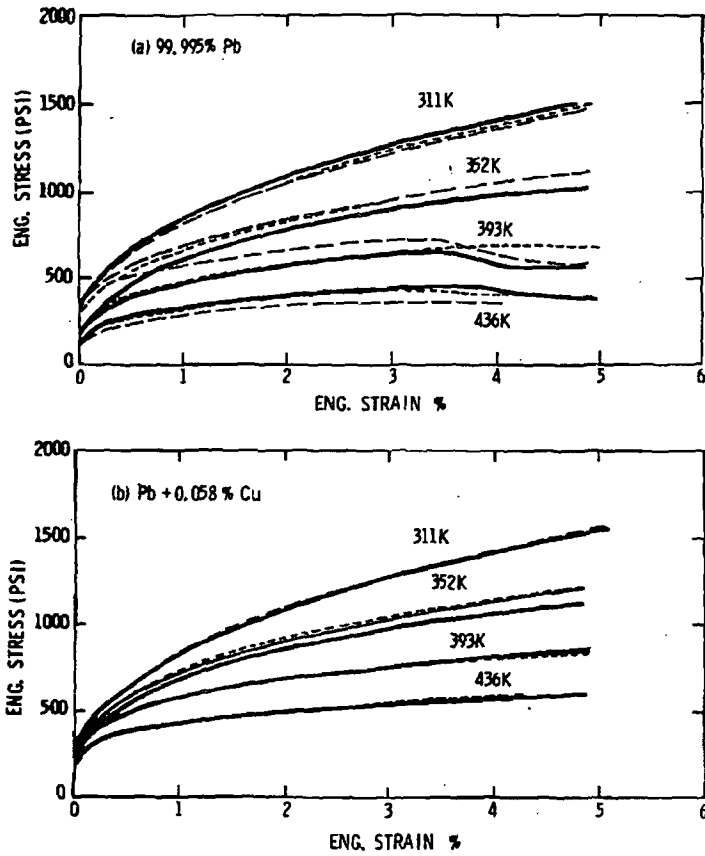


Figure 23. Triplicate compression stress-strain curves to 5 percent strain at a strain rate of $2.5 \times 10^{-4} \text{ sec}^{-1}$ [51].

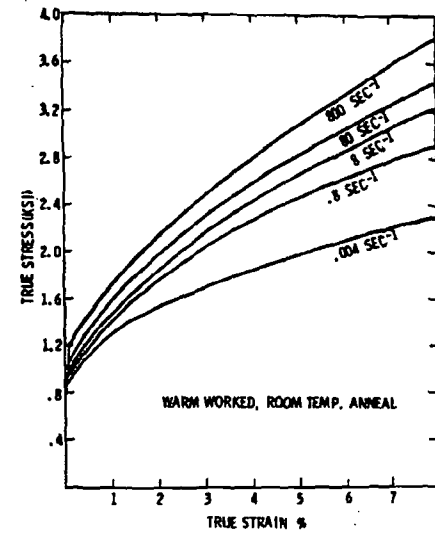


Figure 24. Stress-strain curves for Pb [56].

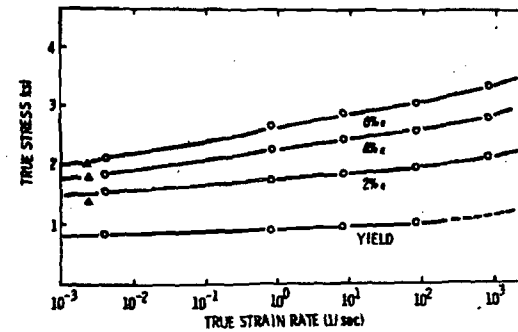


Figure 25. Influence of strain rate on flow stress of Pb [56].

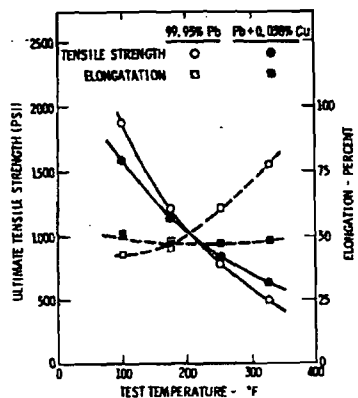


Figure 26. Tensile strength and elongation as a function of test temperature at a strain rate of $8.3 \times 10^{-4} \text{ sec}^{-1}$ [51].

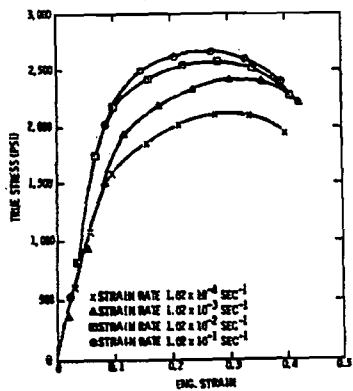


Figure 27. Quasi-static true stress-strain curves for chemical lead test specimens in tension [45].

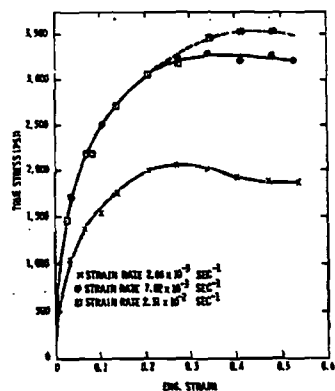


Figure 28. Quasi-static true stress-strain curves for chemical lead test specimens in compression [45].

stress-strain curves shown in Figure 29 bear little relationship to each other even though they are reported to be results of tests ostensibly carried out at different strain rates on the same lot of material. It is clear that much more care will have to be exercised in any further examination of the mechanical behavior of lead and its alloys.

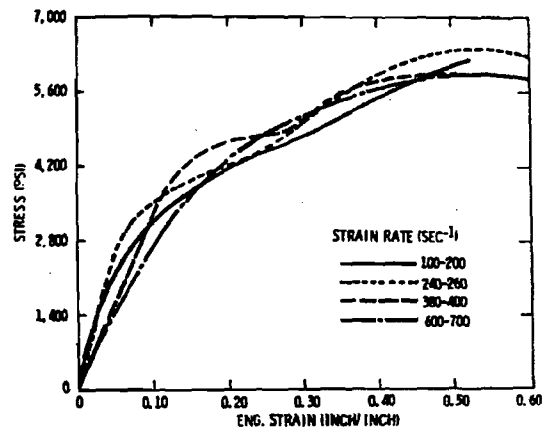


Figure 29. Stress-strain curves of lead for four strain-rate ranges [45].

Summary and Recommendations

This review of the available literature has shown that there are many areas which require further attention before an adequate data base will be established for use with increasingly sophisticated finite-element computer programs. Listed below are the

authors' recommendations of those subjects which will require further evaluation.

Mechanical Properties

1. Define the temperature, strain-rate, and strain regions for which strain-induced martensite and dynamic strain-aging will control the stress-strain behavior of the austenitic stainless steels used for LWR shipping casks.
2. Establish a data base for selected austenitic stainless steels, "chemical" lead, and as-cast α -uranium. The data base should include:
 - a. The influence of strain-rate and temperature on the tensile, compressive, and shear properties.
 - b. The influence of chemistry variation on the mechanical properties.
 - c. The influence of residual stress level and test environment on the mechanical behavior of as-cast α -uranium.
3. Develop constitutive equations to describe the stress-strain behavior of LWR shipping cask material under both normal and abnormal (due to strain aging or martensitic formation) modes of deformation.

Thermal Expansion (See Appendix A)

1. Establish the thermal expansion behavior of 216, 317, 321, and 347 stainless steel over the temperature range -40 to 320°C (-40 to 620°F).

2. Establish the thermal expansion behavior of typical product forms of α -uranium used in shipping cask applications. Particular attention should be given to the expected anisotropic orientation dependence of the thermal expansivity.

Elastic Properties (See Appendix B)

1. Extend moduli measurements for austenitic steels (304, 316, 321, 347) to the lowest operating temperatures (-40°C) associated with shipping casks.
2. Determine elastic properties of 216, 308, 317, and 347 stainless steel.
3. Determine elastic properties of selected dilute uranium alloys (e.g., U-2Mo).

The primary emphasis of all of these studies should be a systematic and quantitative assessment including pertinent microstructural information rather than the largely qualitative information available at the present time.

References

Stainless Steels

1. Aerospace Structural Metals Handbook, Vol. 2, AFML-TR-68-115, Mechanical Properties Data Center, Belfour Stulen, Inc. (1975).
2. G. P. Sanderson and D. T. Llewellyn, "Mechanical Properties of Standard Stainless Steels in the Temperature Range -196°C to +800°C," J. Iron Steel Inst. 207, 1129 (1969).
3. H. E. McCoy, Jr., and R. D. Waddell, "Mechanical Properties of Several Products from a Single Heat of Type 304 Stainless Steel," J. Eng. Mat. Tech. 97, 343 (1975).
4. J. P. Hammond and V. K. Sikka, Heat-to-Heat Variations of Total Strain (to 5%) at Discrete Stress Levels in Types 316 and 304 Stainless Steel from 24° to 316°C, ORNL/NUREG-TM-57, Oak Ridge National Laboratory, Oak Ridge, TN (November 1976).
5. A. Rosen R. Jago, and T. Kjer, "Tensile Properties of Meta-stable Stainless Steels," J. Matl. Sci. 7, 871 (1972).
6. C. F. Jenkins and G. V. Smith, "Serrated Plastic Flow in Austenitic Stainless Steel," Trans. AIME 245, 2149 (1969).
7. J. T. Barnby, "Effect of Strain Aging on the High Temperature Tensile Properties of an AISI 316 Austenitic Stainless Steel," JISI 203 392 (1965).
8. H. Yamada and Li Che-yu, "Stress-Relaxation and Mechanical Equation of State in Austenitic Stainless Steels," Met. Trans. 4, 2133 (1973).
9. R. W. Rohde and J. C. Swearingen, "A Mechanical Equation of State for Inelastic Deformation of Iron: An Analytic Description," J. Eng. Matls. Tech. 99, 59 (1977).
10. R. W. Swindeman, "Representation of the High-Temperature Tensile Behavior of Re-Annealed Type 304 Stainless Steel by the Voce Equation," J. Eng. Matls. Tech. 97B, 98 (1975).
11. J. M. Steichen, "Mathematical Description of the Elevated Temperature Flow Behavior of Type 304 Stainless Steel at High Strain Rates," J. Test. Eval. 1, 520 (1973).
12. D. C. Ludwigson, "Modified Stress-Strain Relation for FCC Metals and Alloys," Met. Trans. 2, 2825 (1971).
13. E. Voce, "The Relationship Between Stress and Strain for Homogeneous Deformation," J. Inst. Metals 74, 537 (1948).

14. Nuclear Systems Materials Handbook, Vol. 1, TID 26666, Hanford Engineering Development Laboratory, Richland, WA (1975).

Uranium

15. E. B. Blasch, G. Stukenbroeker, R. J. Lusky, C. Bonilla, and H. Berger, "The Use of Uranium as a Shielding Material," Nucl. Engr. & Design 13, 146 (1970).
16. D. Calais, G. Saada, and E. Simenel, "Influence of the Anisotropy of the Expansion Coefficient on the Elastic Properties of Uranium, Zirconium, and Zinc," Comptes Rendus 249, 1225 (1959).
17. D. M. R. Taplin and J. W. Martin, "The Effect of Grain Size and Cold Work on the Tensile Properties of Alpha Uranium," J. Less Common Metals 7, 89 (1964).
18. D. M. R. Taplin, "The Tensile Properties and Fracture of Uranium Between -200°C and 900°C," Australian Inst. Met. J. 12, 32 (1967).
19. D. M. R. Taplin and J. W. Martin, "The Metallography and Fracture of Alpha Uranium," Metallurgia 71, 83 (1965).
20. E. G. Lukas, "Properties of As-Cast and Heat Treated 2% Molybdenum-Uranium," Trans. ASM 51, 752 (1959).
21. F. Jean-Louis and P. Lacombe, "Plastic Deformation of Polycrystalline Uranium Under Tension at Various Strain Rates Between 20 and 850°C," Compt. Rend. Ser. C. 262, 316 (1966).
22. P. D. Tilburg, Impact Testing of Uranium, AWRE 0-33/66, (March 1966).
23. D. M. R. Taplin and J. W. Martin, "The Effect of Grain Shape on the Tensile Properties of Uranium," J. Nucl. Matls. 10, 134 (1963).
24. D. M. R. Taplin and J. W. Martin, "The Effect of Small Additions of Iron and Aluminum on the Tensile Properties of Alpha Uranium," J. Nucl. Matls. 12, 50 (1964).
25. W. L. Owen, "Effect of Hydrogen on Mechanical Properties of Uranium," Metallurgia 66, 3 (July 1962).
26. C. Prunier, M. Linard, and F. Giraud-Beraud, "Influence de L'hydrogen Internal sur les Proprietes Mecaniques et Structurales de L'alliage Uranium - 0.2% pds Vanadium," J. Nucl. Matls. 64, 14 (1977).

27. A. N. Hughes, S. Orman, and G. Picton, "Some Effects of Hydrogen in Uranium," Proc. Intl. Conf. on Hydrogen in Metals, Paris (1972) p. 466.
28. H. R. Gardner and J. W. Riches, "The Effect of Uranium Hydride Distribution and Recrystallization on the Tensile Properties of Uranium," Trans. ASM 52, 728 (1960).
29. G. L. Powell and J. B. Condon, "Hydrogen in Uranium Alloys," in Physical Metallurgy of Uranium Alloys, J. J. Burke, D. A. Colling, A. E. Gorum, and J. Greenspan, eds., Brook Hill Publishing Company, Chestnut Hill, MA (1976) p. 427.
30. D. M. R. Taplin and J. W. Martin, "An Effect of Thermal Cycling Upon the Ductility Transition in Alpha Uranium," J. Inst. Metals 93, 730 (1964).
31. A. N. Hughes, S. Orman, and G. Picton, "Environmental Factors Affecting the Mechanical Properties of Uranium, Part I - The Effect of Water Vapour," J. Nucl. Matls. 33, 159 (1969).
32. A. N. Hughes, S. Orman, and G. Picton, "Environmental Factors Affecting the Mechanical Properties of Uranium, Part II - The Mechanism of the Water Embrittlement of Uranium," J. Nucl. Matls. 33, 165 (1969).
33. A. N. Hughes, S. Orman, G. Picton, and M. A. Thorne, "The Effect of Humidity on the Low Temperature Tensile Properties of Uranium," J. Nucl. Matls. 33, 99 (1969).
34. P. D. Tilbury, Experiments to Improve the Mechanical Properties of Wrought Uranium, AWRB 038/68, (June 1968).
35. J. Bolton and P. D. Tilbury, "The Influence of Warm Rolling Upon the Ductile/Brittle Transition Temperature of Uranium," J. Inst. Metals 92, 95 (1963-64).
36. A. Lemogne and P. Lacombe, "Plastic Deformation in Uniaxial Tension of Monocrystals and Polycrystalline Uranium Between 20°C and 196°C," J. Nucl. Matls. 16, 129 (1965).
37. C. J. Beevers and G. T. Newman, "The Influence of Heat Treatment on the Tensile Behavior of Uranium in the Temperature Range 200-200°C," J. Less Common Metals 14, 225 (1968).
38. P. A. Loretan and G. Murphy, "The Influence of Rate of Loading and Temperature on the Tensile Properties of Normal Alpha Uranium," Proc. ASTM 64, 734 (1964).
39. J. E. Hockett, P. S. Gilman, and O. D. Sherby, "Compressive Deformation of Polycrystalline Uranium at Low Temperatures," J. Nucl. Matls. 64, 231 (1977).

Lead

40. G. L. Stukenbroeker, C. F. Bonilla, and R. W. Peterson, "The Use of Lead as a Shielding Material," Nucl. Engr. & Design 13, 3 (1970).
41. M. Hansen, Constitution of Binary Alloys, 2nd Edition, McGraw-Hill, New York (1958).
42. U. S. Lindholm, "Some Experiments with the Split Hopkinson Pressure Bar," J. Mech. Phys. Solids 12, 317 (1964).
43. J. M. Gondusky and J. Duffy, "The Dynamic Stress-Strain Relation of Lead and Its Dependence on Grain Structure," Tech. Rpt. No. 53, Brown University, Providence, RI (May 1967).
44. C. H. Mok and J. Duffy, "The Dynamic Stress-Strain Relation of Metals as Determined from Impact Tests with a Hard Ball," Intl. J. Mech. Sci. 7, 355 (1965).
45. J. H. Evans, Structural Analysis of Shipping Casks, Vol. 8, Experimental Study of the Stress-Strain Properties of Lead Under Specified Impact Conditions, ORNL-TM-1312, Oak Ridge National Laboratory, Oak Ridge, TN (August 1970).
46. L. D. Skolov, "A Systematic Study of the Dependence of Speed and Temperature of the Resistance to Deformation in One-Phase Metals," Dokl. Akad. Nauk SSSR 70, 839 (1950).
47. H. E. Cline and T. H. Alden, "Rate-Sensitive Deformation in Tin-Lead Alloys," Trans. AIME 239, 710 (1967).
48. J. A. Bailey and A. R. E. Singer, "Effect of Strain Rate and Temperature on the Resistance to Deformation of Aluminum, Two Aluminum Alloys, and Lead," J. Inst. Metals 92, 404 (1963-64).
49. L. D. Skolov, "The Effect of Temperature and Strain Velocity of the Resistance to Deformation of Metals," Russian Met. and Mining 3, 93 (1963).
50. N. Lorson and R. B. Sims, "The Yield Stress of Pure Lead in Compression," J. Mech. Phys. Solids 1, 234 (1953).
51. T. E. Tietz, "Mechanical Properties of a High-Purity Lead and a 0.058 Percent Copper-Lead Alloy at Elevated Temperatures," Proc. ASTM 59, 1052 (1959).
52. F. A. Hodierne, "A Torsion Test for Use in Metal Working Studies," J. Inst. Metals 91, 267 (1962-63).
53. H. Kolsky, "An Investigation of the Mechanical Properties of Materials at Very High Rates of Loading," Proc. Phys. Soc. 62B, 676 (1949).

54. E. R. Parker and C. Ferguson, "The Effect of Strain Rate Upon Tensile Impact Strength of Some Metals," Trans. ASM 30, 68 (1942).
55. R. F. Steidel and C. F. Makesov, "The Tensile Properties of Some Engineering Materials at Moderate Rates of Strain," ASTM Bulletin No. 247, 57 (1960).
56. S. J. Green, C. J. Maiden, S. G. Babcock, and F. L. Schierloh, The High Strain-Rate Behavior of Face Centered Cubic Metals. NBS-69-36, GM Technical Center, (October 1969).

Thermal Expansion

57. Y. S. Touloukian, R. K. Kirby, R. E. Taylor, and P. D. Desai, Thermophysical Properties of Matter, Vol. 12, Plenum Press, New York (1975).
58. D. E. Furman, "Thermal Expansion Characteristics of Stainless Steels Between -300 and 1000°F," Trans. AIME 188, 688 (1950).
59. R. D. Seibel and G. L. Mason, Thermal Properties of High Temperature Materials, WADC-TR-57-468, U.S. Air Force (1958).

Elastic Properties

60. Source Book on Stainless Steels, American Society for Metals, Metals Park, OH (1976) p. 95.
61. A. J. Goldman and W. D. Robertson, "Elastic Properties of Austenite and Martensite in Iron-Nickel Alloys," Acta Met. 12, 1265 (1964).
62. O. D. Sherby, D. L. Bly, and D. S. Wood, "Plastic Flow and Strength of Uranium and Its Alloys," in Physical Metallurgy of Uranium Alloys, J. J. Burke, D. A. Collins, A. E. Gorum, and J. Greenspan, eds., Brook Hill Publishing Company, Chestnut Hill, MA (1976) p. 311.
63. E. S. Fisher, "Temperature Dependence of the Elastic Moduli in Alpha Uranium Single Crystals, Part IV (298 to 932 K)," J. Nucl. Matls. 18, 39 (1966).
64. P. E. Armstrong, D. T. Eash, and J. E. Bockett, "Elastic Moduli of Alpha, Beta, and Gamma Polycrystalline Uranium," J. Nucl. Matls. 45, 211 (1972-73).
65. W. Koster, "Die Temperaturabhangigkeit des Elastizitätsmoduls reiner Metalle," Zeit. für Metkde 39, 1 (1948).

APPENDIX A

Thermal Expansion Behavior of Selected Stainless Steels, Uranium, and Lead

The thermal expansion behavior of stainless steel, uranium, and lead are presented below. The linear thermal expansion has been presented as $\Delta L/L_0$ where (see Appendix C for definition of symbols):

$$\Delta L = L_T - L_0$$

Stainless Steels

The thermal expansion behavior of the stainless steels presently being considered is tabulated in Table A-I and summarized in Figure A-1. The data are quite limited; none were found for 216 or 317 stainless steels. In addition, that for 321 stainless is well above the temperature range of primary interest for shipping applications. However, Figure A-1 does suggest that the thermal expansivity of many stainless steels is quite similar and that, to a first approximation, they may be represented by that of 304 stainless steel, i.e. [57],

$$\begin{aligned} \Delta L/L_0(\%) = & 0.356 + 9.471 \times 10^{-4} T + 1.031 \times 10^{-6} T^2 \\ & - 2.978 \times 10^{-10} T^3 \quad (T \text{ in } ^\circ K) \end{aligned}$$

The formation of martensite at low temperature or δ -ferrite in weldments can be expected to alter this behavior in an as yet undetermined manner.

TABLE A-I

Thermal Linear Expansion of Stainless Steel
304 Stainless (19.19 Cr, 8.49 Ni, 0.65 Mn, 0.53 Si,
0.068 C, 0.024 P, 0.007 S, balance Fe) [58]

Temperature (K)	D/L ₀ (%)	Temperature (K)	L/L ₀ (%)
233	-0.089	405	0.182
239	-0.083	411	0.191
244	-0.076	416	0.199
250	-0.071	422	0.207
255	-0.058	436	0.236
261	-0.046	450	0.259
266	-0.040	464	0.281
272	-0.029	478	0.309
278	-0.024	491	0.334
283	-0.013	505	0.358
289	-0.005	519	0.383
294	0.002	533	0.402
300	0.012	547	0.429
305	0.028	561	0.455
311	0.028	575	0.484
316	0.037	589	0.507
322	0.044	603	0.536
328	0.055	616	0.563
333	0.063	630	0.588
339	0.073	644	0.614
344	0.083	658	0.636
350	0.091	672	0.667
355	0.100	686	0.695
361	0.107	700	0.724
366	0.118	714	0.768
372	0.128	741	0.809
378	0.134	755	0.831
383	0.145	769	0.858
389	0.151	783	0.887
394	0.161	797	0.917
400	0.172	810	0.945

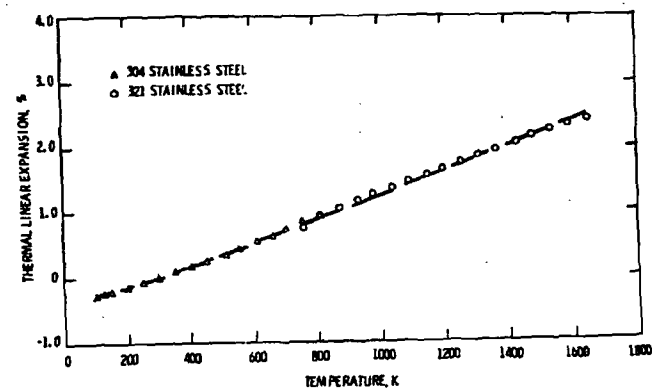


Figure A-1. Thermal expansion of 304 and 321 stainless steel.

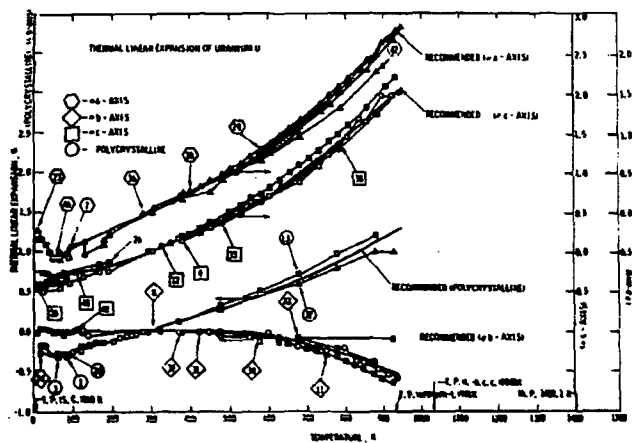
Uranium

The thermal expansion behavior of α -uranium is quite complex (see Table A-II and Figure A-2). Single crystal measurements indicate that the expansion behavior, in contrast to stainless steel or lead, is highly anisotropic and depends upon the particular crystal-lographic orientation being considered. This suggests that the thermal expansion coefficients of polycrystalline uranium will be extremely sensitive to prior processing history and are expected to be quite variable. To date there have been no investigations of the influence of thermomechanical treatment on the thermal expansivity of α -uranium so that any formalism proposed to describe its behavior must be considered as only a first approximation.

TABLE A-II

Thermal Linear Expansion of Polystalline α -Uranium

Curve 13 (99.8 U, 0.14 C, 0.03 Si)		Curve 32 ("Pure" Uranium)	
Temperature (K)	$\Delta L/L_0$ (%)	Temperature (K)	$\Delta L/L_0$ (%)
291	-0.0032	293	0.000
373	0.127	373	0.118
473	0.306	473	0.268
573	0.506	575	0.424
673	0.728	673	0.594

Figure A-2. Thermal expansion behavior of α -uranium, curve reference numbers given by Touloukian et al. [57].

Notwithstanding, Touloukian et al. [57] recommend that the thermal expansion behavior of polycrystalline α -uranium can be represented by:

$$\Delta L/L_0(\%) = -0.379 + 1.264 \times 10^{-3}T - 8.982 \times 10^{-8}T^2 + 6.844 \times 10^{-10}T^3 \quad (293 \text{ K} < T < 941 \text{ K}).$$

(T in °K)

As noted above, the error limits to be associated with this relationship must be established.

Lead

The thermal expansion behavior of lead is summarized in Figure A-3. Although the bulk of this data refers to high purity lead it appears that, in those instances where the impurity levels approach that of "chemical" lead, the expansion behavior remains relatively unaffected. Indeed, it has been proposed that all of the tabulated values can be represented to within ± 3 percent over the temperature range 100 to 600 K by the following equation [57]:

$$\Delta L/L_0(\%) = 0.786 + 2572 \times 10^{-3}T + 1.147 \times 10^{-7}T^2 + 8.770 \times 10^{-10}T^3 \quad (T \text{ in } ^\circ\text{K})$$

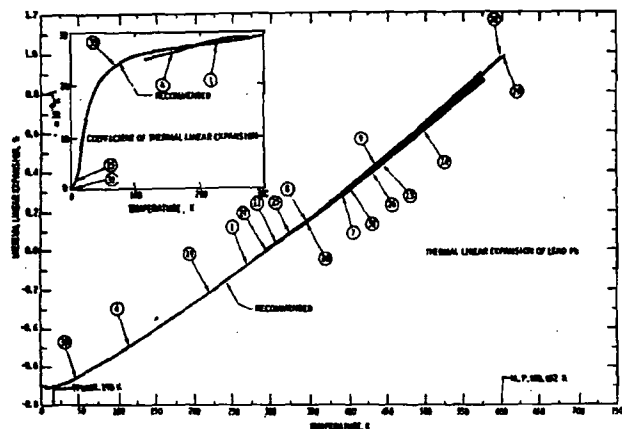


Figure A-3. Thermal expansion behavior of lead, curve reference numbers given by Touloukian et al. [57].

with the recommended values being

Temperature (K)	$\Delta L/L_0 (\%)$	$\alpha \times 10^6 (K^{-1})$
100	-0.526	25.6
200	-0.261	27.5
293	0.000	28.9
400	0.317	30.6
500	0.638	33.3
600	0.988	36.7

where

$$\alpha = (1/L_{293})dL/dT$$

APPENDIX B

Elastic Properties of Selected Stainless Steels, Uranium, and Lead

Stainless Steels

Typical values for the elastic constants of selected stainless steels are given in Tables B-I through B-VII and Figures B-1 through B-6. Examination of this data indicates that variations in chemistry within the group of austenitic stainless steels presently under consideration have little effect on their elastic properties. Furthermore, increasing temperature generally results in a gradual decrease in the Young's and shear moduli and an accompanying increase in Poisson's ratio. Again, martensite formation can be expected to cause changes. For example, the presence of martensite has been shown to lower the modulus of the parent austenite phase [61].

TABLE B-I
Effect of Temperature on the Elastic Constants of Selected Stainless Steels [60]

Type	Temperature (K)			
	297	422	533	644
Young's Modulus (10^3 ksi)				
304	29.0	27.3	26.0	24.8
316	28.4	27.2	26.4	25.6
317	27.0	26.4	25.0	-
321	28.9	27.3	25.8	24.5
347	28.9	27.5	26.1	24.8
Shear Modulus (10^3 ksi)				
304	11.2	10.4	9.8	9.3
316	11.3	10.8	10.2	9.2
317	-	-	-	-
321	11.2	10.6	9.9	9.4
347	11.4	10.7	10.1	9.5
Poisson's Ratio				
304	0.30	0.31	0.31	0.32
316	0.26	0.26	0.30	0.34
317	0.25	0.28	0.31	0.31
321	0.28	0.29	0.30	0.31
347	0.28	0.29	0.30	0.31

TABLE B-II
Young's Modulus for Annealed 304 Stainless Steel [14]

1971 ASME CODE

ASME CODE	TEMPERATURE (K)	YOUNG'S MODULUS (10^3 ksi)
SA 304	297	29.0
SA 304	422	27.3
SA 304	533	26.0
SA 304	644	24.8
SA 316	297	28.4
SA 316	422	27.2
SA 316	533	26.4
SA 316	644	25.6
SA 317	297	27.0
SA 317	422	26.4
SA 317	533	25.0
SA 317	644	-
SA 321	297	28.9
SA 321	422	27.3
SA 321	533	25.8
SA 321	644	24.5
SA 347	297	28.9
SA 347	422	27.5
SA 347	533	26.1
SA 347	644	24.8

TABLE B-III
Shear Modulus for Annealed 304 Stainless Steel [14]

1971 ASME CODE

ASME CODE	TEMPERATURE (K)	SHEAR MODULUS (10^3 ksi)
SA 304	297	11.2
SA 304	422	10.4
SA 304	533	9.8
SA 304	644	9.3
SA 316	297	11.3
SA 316	422	10.8
SA 316	533	10.2
SA 316	644	9.2
SA 317	297	-
SA 317	422	-
SA 317	533	-
SA 317	644	-
SA 321	297	11.2
SA 321	422	10.6
SA 321	533	9.9
SA 321	644	9.4
SA 347	297	11.4
SA 347	422	10.7
SA 347	533	10.1
SA 347	644	9.5

TABLE B-IV
Poisson's Ratio for
Annealed 304 Stainless Steel [14]

INTERNATIONAL SYSTEM OF UNITS (SI)		U.S. SYSTEM OF UNITS	
TEMPERATURE, DEG. CELSIUS	POISSON'S RATIO	TEMPERATURE, DEG. F.	POISSON'S RATIO
791 (1477)	2.594E-01	1421 (257)	2.694E-01
129 (252)	2.717E-01	192 (401)	2.684E-01
150 (302)	2.741E-01	289 (531)	2.711E-01
179 (347)	2.762E-01	320 (616)	2.751E-01
201 (382)	2.812E-01	350 (657)	2.785E-01
224 (425)	2.844E-01	400 (752)	2.886E-01
270 (518)	2.862E-01	500 (932)	2.931E-01
301 (572)	2.881E-01	530 (974)	2.951E-01
324 (617)	2.899E-01	550 (1021)	2.972E-01
351 (657)	2.917E-01	640 (1172)	2.992E-01
379 (717)	2.934E-01	680 (1243)	2.992E-01
421 (787)	2.952E-01	740 (1334)	2.931E-01
452 (852)	2.966E-01	750 (1361)	2.951E-01
479 (907)	2.983E-01	880 (1604)	2.970E-01
506 (952)	2.995E-01	920 (1677)	2.990E-01
529 (992)	3.017E-01	950 (1722)	3.010E-01
551 (1022)	3.032E-01	1000 (1832)	3.040E-01
579 (1067)	3.047E-01	1050 (1912)	3.060E-01
621 (1137)	3.061E-01	1150 (2072)	3.080E-01
629 (1172)	3.071E-01	1200 (2162)	3.090E-01
656 (1217)	3.082E-01	1250 (2252)	3.100E-01
679 (1247)	3.104E-01	1300 (2332)	3.110E-01
705 (1292)	3.114E-01	1400 (2512)	3.127E-01
729 (1337)	3.116E-01	1450 (2602)	3.137E-01
751 (1382)	3.119E-01	1490 (2662)	3.146E-01
779 (1427)	3.121E-01	1520 (2712)	3.150E-01

TABLE B-V
Young's Modulus for
Annealed 316 Stainless Steel [14]

INTERNATIONAL SYSTEM OF UNITS (SI)		U.S. SYSTEM OF UNITS	
TEMPERATURE, DEG. CELSIUS	YOUNG'S MODULUS, GIGAPASCALS	TEMPERATURE, DEG. F.	YOUNG'S MODULUS, KILOPOUNDS PER SQUARE INCH
791 (1477)	1.93E+11	1421 (257)	2.77E+10
129 (252)	1.93E+11	192 (401)	2.77E+10
150 (302)	1.93E+11	289 (531)	2.77E+10
179 (347)	1.93E+11	320 (616)	2.77E+10
201 (382)	1.93E+11	350 (657)	2.77E+10
224 (425)	1.93E+11	400 (752)	2.77E+10
270 (518)	1.93E+11	500 (932)	2.77E+10
301 (572)	1.93E+11	530 (974)	2.77E+10
324 (617)	1.93E+11	550 (1021)	2.77E+10
351 (657)	1.93E+11	640 (1172)	2.77E+10
379 (717)	1.93E+11	680 (1243)	2.77E+10
421 (787)	1.93E+11	740 (1334)	2.77E+10
452 (852)	1.93E+11	750 (1361)	2.77E+10
479 (907)	1.93E+11	880 (1604)	2.77E+10
506 (952)	1.93E+11	920 (1677)	2.77E+10
529 (992)	1.93E+11	950 (1722)	2.77E+10
551 (1022)	1.93E+11	1000 (1832)	2.77E+10
579 (1067)	1.93E+11	1050 (1912)	2.77E+10
621 (1137)	1.93E+11	1150 (2072)	2.77E+10
629 (1172)	1.93E+11	1200 (2162)	2.77E+10
656 (1217)	1.93E+11	1250 (2252)	2.77E+10
679 (1247)	1.93E+11	1300 (2332)	2.77E+10
705 (1292)	1.93E+11	1400 (2512)	2.77E+10
729 (1337)	1.93E+11	1450 (2602)	2.77E+10
751 (1382)	1.93E+11	1490 (2662)	2.77E+10
779 (1427)	1.93E+11	1520 (2712)	2.77E+10

TABLE B-VI
Shear Modulus for
Annealed 316 Stainless Steel [14]

INTERNATIONAL SYSTEM OF UNITS (SI)		U.S. SYSTEM OF UNITS	
TEMPERATURE, DEG. CELSIUS	SHEAR MODULUS, GIGAPASCALS	TEMPERATURE, DEG. F.	SHEAR MODULUS, KILOPOUNDS PER SQUARE INCH
791 (1477)	7.60E+10	1421 (257)	1.09E+10
129 (252)	7.60E+10	192 (401)	1.09E+10
150 (302)	7.60E+10	289 (531)	1.09E+10
179 (347)	7.60E+10	320 (616)	1.09E+10
201 (382)	7.60E+10	350 (657)	1.09E+10
224 (425)	7.60E+10	400 (752)	1.09E+10
270 (518)	7.60E+10	500 (932)	1.09E+10
301 (572)	7.60E+10	530 (974)	1.09E+10
324 (617)	7.60E+10	550 (1021)	1.09E+10
351 (657)	7.60E+10	640 (1172)	1.09E+10
379 (717)	7.60E+10	680 (1243)	1.09E+10
421 (787)	7.60E+10	740 (1334)	1.09E+10
452 (852)	7.60E+10	750 (1361)	1.09E+10
479 (907)	7.60E+10	880 (1604)	1.09E+10
506 (952)	7.60E+10	920 (1677)	1.09E+10
529 (992)	7.60E+10	950 (1722)	1.09E+10
551 (1022)	7.60E+10	1000 (1832)	1.09E+10
579 (1067)	7.60E+10	1050 (1912)	1.09E+10
621 (1137)	7.60E+10	1150 (2072)	1.09E+10
629 (1172)	7.60E+10	1200 (2162)	1.09E+10
656 (1217)	7.60E+10	1250 (2252)	1.09E+10
679 (1247)	7.60E+10	1300 (2332)	1.09E+10
705 (1292)	7.60E+10	1400 (2512)	1.09E+10
729 (1337)	7.60E+10	1450 (2602)	1.09E+10
751 (1382)	7.60E+10	1490 (2662)	1.09E+10
779 (1427)	7.60E+10	1520 (2712)	1.09E+10

TABLE B-VII
Poisson's Ratio for
Annealed 316 Stainless Steel [14]

INTERNATIONAL SYSTEM OF UNITS (SI)		U.S. SYSTEM OF UNITS	
TEMPERATURE, DEG. CELSIUS	POISSON'S RATIO	TEMPERATURE, DEG. F.	POISSON'S RATIO
791 (1477)	2.694E-01	1421 (257)	2.694E-01
129 (252)	2.717E-01	192 (401)	2.684E-01
150 (302)	2.741E-01	289 (531)	2.711E-01
179 (347)	2.762E-01	320 (616)	2.751E-01
201 (382)	2.812E-01	350 (657)	2.785E-01
224 (425)	2.844E-01	400 (752)	2.886E-01
270 (518)	2.862E-01	500 (932)	2.931E-01
301 (572)	2.881E-01	530 (974)	2.951E-01
324 (617)	2.899E-01	550 (1021)	2.972E-01
351 (657)	2.917E-01	640 (1172)	2.992E-01
379 (717)	2.934E-01	680 (1243)	2.992E-01
421 (787)	2.952E-01	740 (1334)	2.931E-01
452 (852)	2.966E-01	750 (1361)	2.951E-01
479 (907)	2.983E-01	880 (1604)	2.970E-01
506 (952)	2.995E-01	920 (1677)	2.990E-01
529 (992)	3.017E-01	950 (1722)	3.010E-01
551 (1022)	3.032E-01	1000 (1832)	3.040E-01
579 (1067)	3.047E-01	1050 (1912)	3.060E-01
621 (1137)	3.061E-01	1150 (2072)	3.080E-01
629 (1172)	3.071E-01	1200 (2162)	3.090E-01
656 (1217)	3.082E-01	1250 (2252)	3.100E-01
679 (1247)	3.104E-01	1300 (2332)	3.110E-01
705 (1292)	3.114E-01	1400 (2512)	3.127E-01
729 (1337)	3.116E-01	1450 (2602)	3.137E-01
751 (1382)	3.119E-01	1490 (2662)	3.146E-01
779 (1427)	3.121E-01	1520 (2712)	3.150E-01

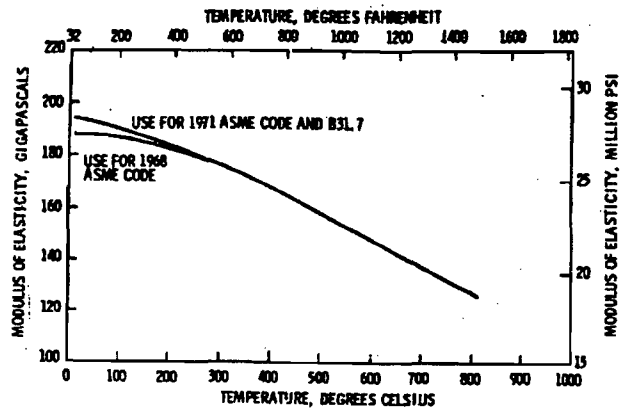


Figure B-1. Young's modulus of 30488, annealed [14].

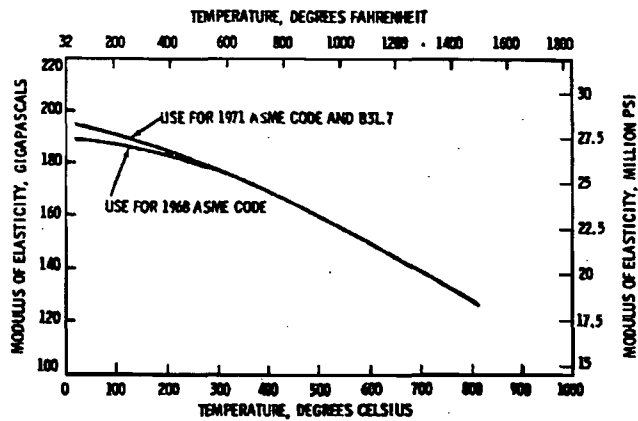


Figure B-2. Young's modulus of 31689, annealed [14].

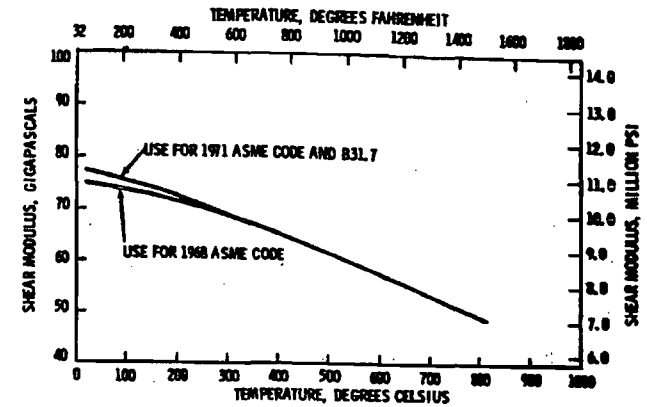


Figure B-3. Shear modulus of 30488, annealed [14].

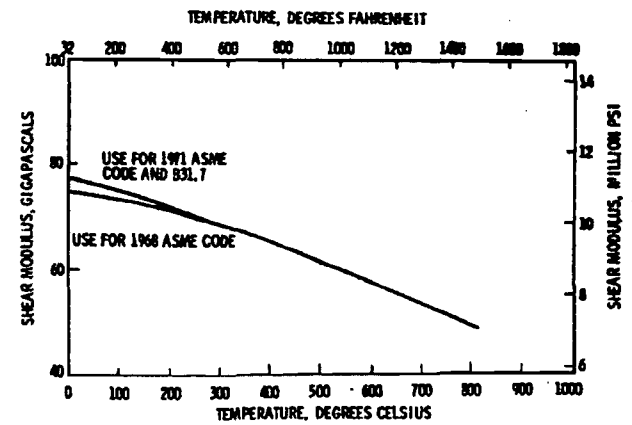


Figure B-4. Shear modulus of 31688, annealed [14].

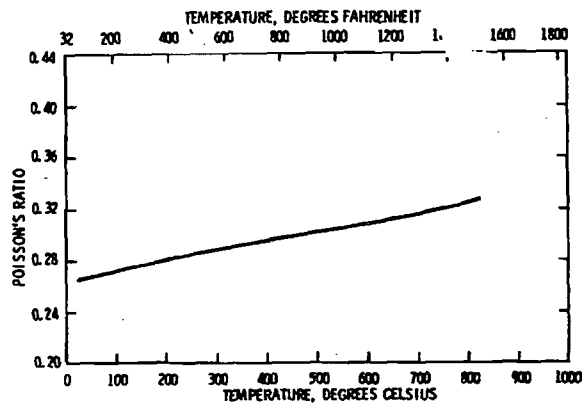


Figure B-5. Poisson's ratio of 304SS, annealed [14].

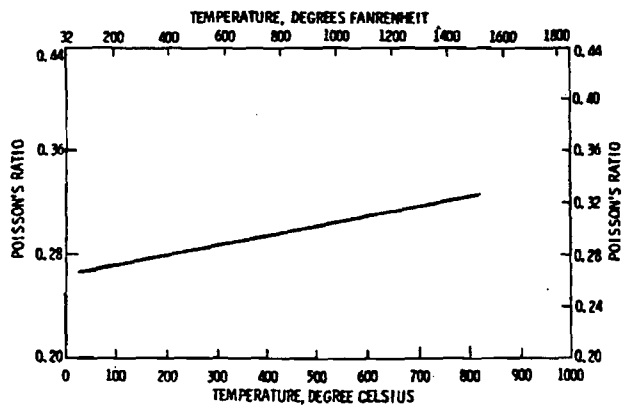


Figure B-6. Poisson's ratio of 316SS, annealed [14].

Uranium

The influence of temperature on the elastic properties of uranium are presented in Table B-VIII and Figure B-7. The solid curve in the latter refers to the modulus of random, non-textured polycrystalline uranium [62], while the minimum and maximum

TABLE B-VIII
Probable Values for Elastic Moduli
of Non-textured Polycrystalline Uranium [64]

Temperature (K)	Young's Modulus (10^6 psi)	Shear Modulus (10^6 psi)	Poisson's Ratio
200	30.5	12.50	0.22
300	29.1	11.80	0.23
400	27.6	11.20	0.23
500	26.1	10.50	0.23
600	24.3	9.70	0.25
700	22.3	8.70	0.28
800	19.7	7.60	0.30

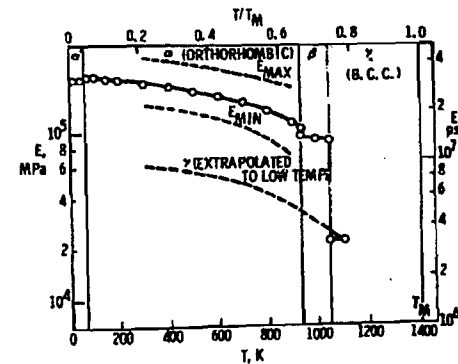


Figure B-7. Young's modulus of pure polycrystalline uranium as a function of temperature. The modulus of non-textured uranium is given by the solid line. The maximum and minimum moduli for alpha uranium from single crystal measurements are also plotted [62, 63].

values were obtained from specifically oriented uranium single crystals [63]. These results show that, whereas the modulus of non-textured polycrystalline uranium at 298 K is 29×10^6 psi, it can be as high as 41.5×10^6 psi or as low as 21.4×10^6 psi for a textured sample.

Finally, the authors were unable to obtain any reliable data on the influence of dilute alloy additions (e.g., 2 weight percent Mo) on the elastic properties of uranium.

Lead

The influence of temperature on the Young's modulus of cast high purity lead is shown in Figure B-8. Again, increasing temperature results in a gradual decrease in modulus. Attempts to locate more complete information, including values of the shear modulus and Poisson's ratio, have been unsuccessful to date.

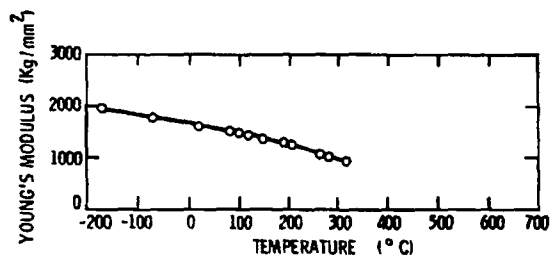


Figure B-8. Young's modulus of lead [65].

APPENDIX C List of Symbols

- σ = true stress
- σ_p = proportional limit
- ϵ = true plastic strain = $\ln(1+e)$
- e = engineering strain = $\Delta l/l_0$
- ϵ_L = total true strain
- E = Young's modulus
- $\Delta L/L_0$ = thermal linear expansion,
- L_T = length at temperature T
- L_0 = length at 293 K
- ΔL = $L_T - L_0$

DISTRIBUTION:

U.S. Nuclear Regulatory Commission (242 copies for RT)
Division of Document Control
Distribution Services Branch
7920 Norfolk Avenue
Bethesda, MD 20014

U.S. Nuclear Regulatory Commission (26)
Washington, D. C. 20555

Attn:

W. F. Anderson, OSD
C. R. Chappell, NMSS
R. G. Clary, NMSS
D. J. Guzy, NMSS
W. Sartzman, WRR
V. Hodge, NMSS
W. R. Labs, RES (10)
W. R. Lake, NMSS
C. E. MacDonald, NMSS (5)
C. R. Marotta, NMSS
J. O. Mayor, NMSS
R. H. Odegaarden, NMSS
C. R. Shieh, NMSS

4400 A. W. Snyder
Attn: D. J. McCloskey, 4410
J. V. Walker, 4420
J. A. Neuscher, 4450

4550 R. M. Jefferson
4551 R. E. Luna
4552 R. B. Pope
4552 G. C. Allen, Jr.
4552 R. G. Wakes
4551 J. M. Freedman
4553 W. A. Von Riesenmann (5)
4553 D. L. Masenberg
5500 O. E. Jones
5520 T. B. Lane
5521 S. W. Key
5521 D. W. Lobitz
5521 C. H. Stone
5522 T. G. Priddy
5800 R. S. Claassen
Attn: R. G. Kepler, 5810
R. L. Schwobel, 5820
H. Saxton, 5840

5830 H. J. Davis
Attn: W. J. Magnani, 5831
R. W. Rohde, 5832
J. L. Ledman, 5833
D. M. Maddox, 5834
C. Karnes, 5835

5832 J. W. Munford
5832 K. Eckelmeier
5832 H. J. Mack (25)
5833 G. Enorovsky (10)
8120 W. F. Altheimer
8121 A. Jones
8122 C. E. Boyle
8123 B. Sinke
8124 A. F. Baker
8310 D. Schuster
Attn: W. R. Hoover, 8314

3141 T. L. Werner (5)
3151 W. L. Garner (3)
For DOE/TIC (Unlimited Release)

3172-3 R. P. Campbell (25)
For DOE/TIC (Unlimited Release)

8266 E. A. Aas

Marks'
**Standard Handbook for
Mechanical Engineers**

Revised by a staff of specialists

EUGENE A. AVALLONE *Editor*

Consulting Engineer; Professor Emeritus of Mechanical Engineering,
The City College of the City University of New York

THEODORE BAUMEISTER III *Editor*

Retired Consultant, Information Systems Department,
E. I. du Pont de Nemours & Co.

Ninth Edition

McGRAW-HILL BOOK COMPANY

New York St. Louis San Francisco Auckland
Bogotá Hamburg London Madrid Mexico
Milan Montreal New Delhi Panama
Paris São Paulo Singapore
Sydney Tokyo Toronto

Library of Congress Cataloged The First Issue
of this title as follows:

Standard handbook for mechanical engineers. 1st-ed.;
1916-

New York, McGraw-Hill.

v. Illus. 18-24 cm.

Title varies: 1916-58: Mechanical engineers' handbook.

Editors: 1916-51, L. S. Marks.—1958- T. Baumeister.

Includes bibliographies.

I. Mechanical engineering—Handbooks, manuals, etc. I. Marks,
Lionel Simeon, 1871- ed. II. Baumeister, Theodore, 1897-
ed. III. Title: Mechanical engineers' handbook.

TJ151.S82 502.4'621 16-12915

ISBN 0-07-004127-X

Library of Congress Catalog Card Number: 87-641192

MARKS' STANDARD HANDBOOK FOR MECHANICAL ENGINEERS

Copyright © 1987, 1978, 1967, 1958 by McGraw-Hill, Inc. All Rights Reserved.

Copyright renewed 1986 by Theodore Baumeister III.

Copyright renewed 1979 by Lionel P. Marks and Alison P. Marks.

Copyright renewed 1952 by Lionel S. Marks. Copyright renewed 1969, 1958 by Lionel
Peabody Marks.

Copyright 1951, 1941, 1930, 1924, 1916 by McGraw-Hill, Inc. All Rights Reserved.

Printed in the United States of America. No part of this publication may be repro-
duced, stored in a retrieval system, or transmitted, in any form or by any means,
electronic, mechanical, photocopying, recording, or otherwise, without the prior
written permission of the publisher.

1234567890 DOC/DOC 893210987

ISBN 0-07-004127-X

First Edition	Third Edition	Fifth Edition	Seventh Edition
<i>Eleven Printings</i>	<i>Seven Printings</i>	<i>Seven Printings</i>	<i>Fifteen Printings</i>

Second Edition	Fourth Edition	Sixth Edition	Eighth Edition
<i>Seven Printings</i>	<i>Thirteen Printings</i>	<i>Eight Printings</i>	<i>Eleven Printings</i>

*The editors for this book were Betty Sun and David E. Fogarty
and the production supervisor was Teresa F. Leadon.*

It was set in Times Roman by University Graphics, Inc.

Printed and bound by R. R. Donnelley & Sons Company.

*The editors and the publishers will be grateful to readers who notify them
of any inaccuracy or important omission in this book*

Basic Properties of Several Metals
(Staff contribution)*

Material	Density, † g/cm ³	Coefficient of thermal expansion, in/(in)(°F) × 10 ⁻⁶	Thermal conductivity, Btu/(h)(ft)(°F)	Specific heat, Btu/ (lb)(°F)	Approx melting temp, °F	Modulus of elasticity lb/in ² × 10 ⁶	Poisson's ratio	Yield stress, lb/ in ² × 10 ³	Ultimate stress, lb/ in ² × 10 ³	Elongation, %
Aluminum, 2024-T3	2.77	12.6	110	0.23	940	10.6	0.33	50	70	18
Aluminum, 6061-T6	2.70	13.5	90	0.23	1080	10.6	0.33	40	45	17
Aluminum, 7079-T6	2.74	13.7	70	0.23	900	10.4	0.33	68	78	14
Beryllium, QMV	1.85	6.4-10.2	85	0.45	2340	40-44	0.024-0.030	27-38	33-51	1-3.5
Copper, pure	8.90	9.2	227	0.092	1980	17.0		See "Metals Handbook"		
Gold, pure	19.32		172	0.031	1950	10.8	0.42		18	30
Lead, pure	11.34	29.3	21.4	0.031	620	2.0	0.40-0.45	1.3	2.6	20-50
Magnesium AZ31B-H24 (sheet)	1.77	14.5	55	0.25	1100	6.5	0.35	22	37	15
Magnesium, HK31A-H24	1.79	14.0	66	0.13	1100	6.4	0.35	29	37	8
Molybdenum, wrought	10.3	3.0	83	0.07	4730	40.0	0.32	80	120-200	Small
Nickel, pure	8.9	7.2	53	0.11	2650	32.0		See "Metals Handbook"		
Platinum	21.45	5.0	40	0.031	3217	21.3	0.39		20-24	35-40
Plutonium, alpha phase	19.0-19.7	30.0	4.8	0.034	1184	14.0	0.15-0.21	40	60	Small
Silver, pure	10.5	11.0	241	0.056	1760	10-11	0.37	8	18	48
Steel, AISI C1020 (hot-worked)	7.85	6.3	27	0.10	2750	29-30	0.29	48	65	36
Steel, AISI 304 (sheet)	8.03	9.9	9.4	0.12	2600	28	0.29	39	87	65
Tantalum	16.6	3.6	31	0.03	5425	27.0	0.35		50-145	1-40
Thorium, induction melt	11.6	6.95	21.7	0.03	3200	7-10	0.27	21	32	34
Titanium, B 120VCA (aged)	4.85	5.2	4.3	0.13	3100	14.8	0.3	190	200	9
Tungsten	19.3	2.5	95	0.033	6200	50	0.28		18-600	1-3
Uranium D-38	18.97	4.0-8.0	17	0.028	2100	24	0.21	28	56	4

Room-temperature properties are given. For further information, consult the "Metals Handbook" or a manufacturer's publication.

*Compiled by Anders Lundberg, University of California, and reproduced by permission.

†To obtain the preferred density units, kg/m³, multiply these values by 1,000.

~~GESC SHIELD MATERIALS~~
~~Bisco Products~~
A Dow Corning Affiliate

100 East Devon Avenue
Grove Village, Illinois 60007-6120
TEL: 708/640-0800, FAX: 708/640-3838

GESC SHIELD MATERIALS
~~BISCO PRODUCTS~~

TECHNICAL REPORT

NO. NS-4-025

NS-4-FR WITH 0.6 WT% BORON CARBIDE FOR
CONSOLIDATED FUEL STORAGE CASK APPLICATION

GESC SHIELD MATERIALS

This shows the ASSETS that Genden Engineering Services & Construction Co. (GESC) purchased from Bisco Products (BISCO) on September 16, 1988.
BISCO in this document should be read GESC.

DATE 01/08/88

REVISION 0

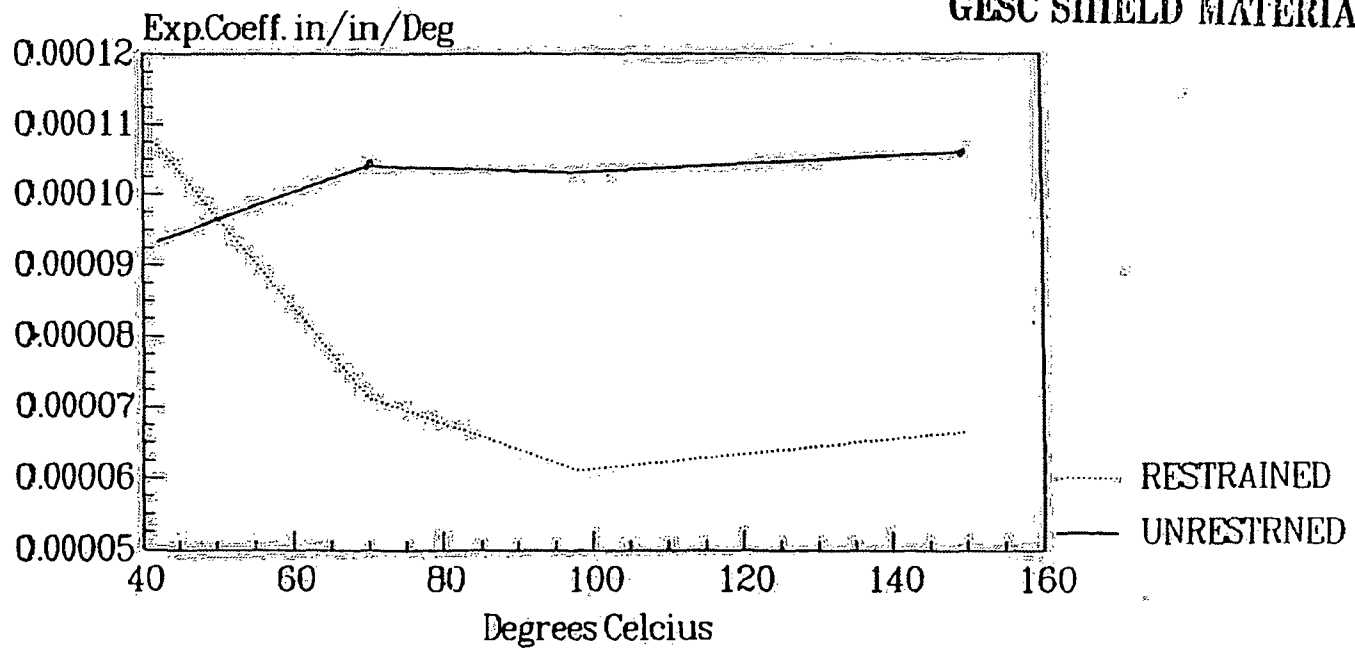
DOW CORNING

A Dow Corning Affiliate

THERMAL EXPANSION COEFFICIENT OF NS-4-FR

Figure 1

GESC SHIELD MATERIALS



R-132736

GESC

THE GENDEN ENGINEERING SERVICES & CONSTRUCTION COMPANY

GESC SHIELDING MATERIALS

License Agreement With

BISCO CONSTRUCTION

FIVE WESTBROOK CORPORATE CENTER,
SUITE 800, WESTCHESTER, ILLINOIS,
60154 U.S.A.

Subcontractors

HEC CORPORATION

TechnoPort Bldg. 2-16-2E
Minamikamata Ohta-ku, Tokyo 144, Japan
TEL (0)-3-3733-0551
(When dialing from abroad, omit the initial (0))

NOF CORPORATION

Yurakucho Bldg. 1-10-1
Chiyoda-ku, Tokyo, Japan
TEL (0)-3-3283-7206 FAX (0)-3-3283-7206
(When dialing from abroad, omit the initial (0))



**GENDEN ENGINEERING SERVICES & CONSTRUCTION
COMPANY LTD.**

HEAD OFFICE: OHEMACHI BUILDING, 1-6-1 OHEMACHI CHIYODA-KU,
TOKYO 100, JAPAN
TEL (0)-3-3216-2868 FAX (0)-3-3216-2919
(When dialing from abroad, omit the initial (0))

TECHNICAL DATA

NS-4-FR FIRE RESISTANT NEUTRON AND/OR GAMMA SHIELDING MATERIAL

property:

fluid to go
rations and
ect seals in
smoke, etc.

for almost

sed for any
d molding

clothes are

or materials

protection,
as the

NS-4-FR Fire Resistant Neutron Shielding Material is a high hydrogen structural shielding product designed for use in moderately high temperature applications. It has the unique characteristics of high strength, mechanical durability and fire resistivity. NS-4-FR may be loaded with lead and/or boron, offering excellent gamma or neutron shielding properties. NS-4-FR has been found to offer superior neutron shielding/attenuation properties over equivalently loaded polyethylene.

PROPERTIES

Color	Brown
Specific Gravity	1.68
Hydrogen	6,07E+22 atoms/cc
Maximum Continuous Operating Temperature	300°F
Radiation Resistance	Excellent
Ultimate Tensile Strength	4,250 psi
Tensile Elongation	0.65%
Ultimate Flexural Strength	7,600 psi
Ultimate Compression Strength	10,500 psi
Compression Yield Strength	8,780 psi
Compression Modulus	561,000 psi
Izod Impact Strength	2.9 ft.-lb./in.
Thermal Conductivity	4.48 BTU-in./hr.-ft. ² -°F

THEORETICAL ELEMENTAL COMPOSITION

Carbon	27.7 wt.%	Nitrogen	2.0 wt.%
Oxygen	42.8 wt.%	Aluminum	21.5 wt.%
Hydrogen	6.0 wt.%		

APPLICATIONS

Vessels, Closures, Structural Components, Doors, Bricks, Criticality Control

AVAILABILITY

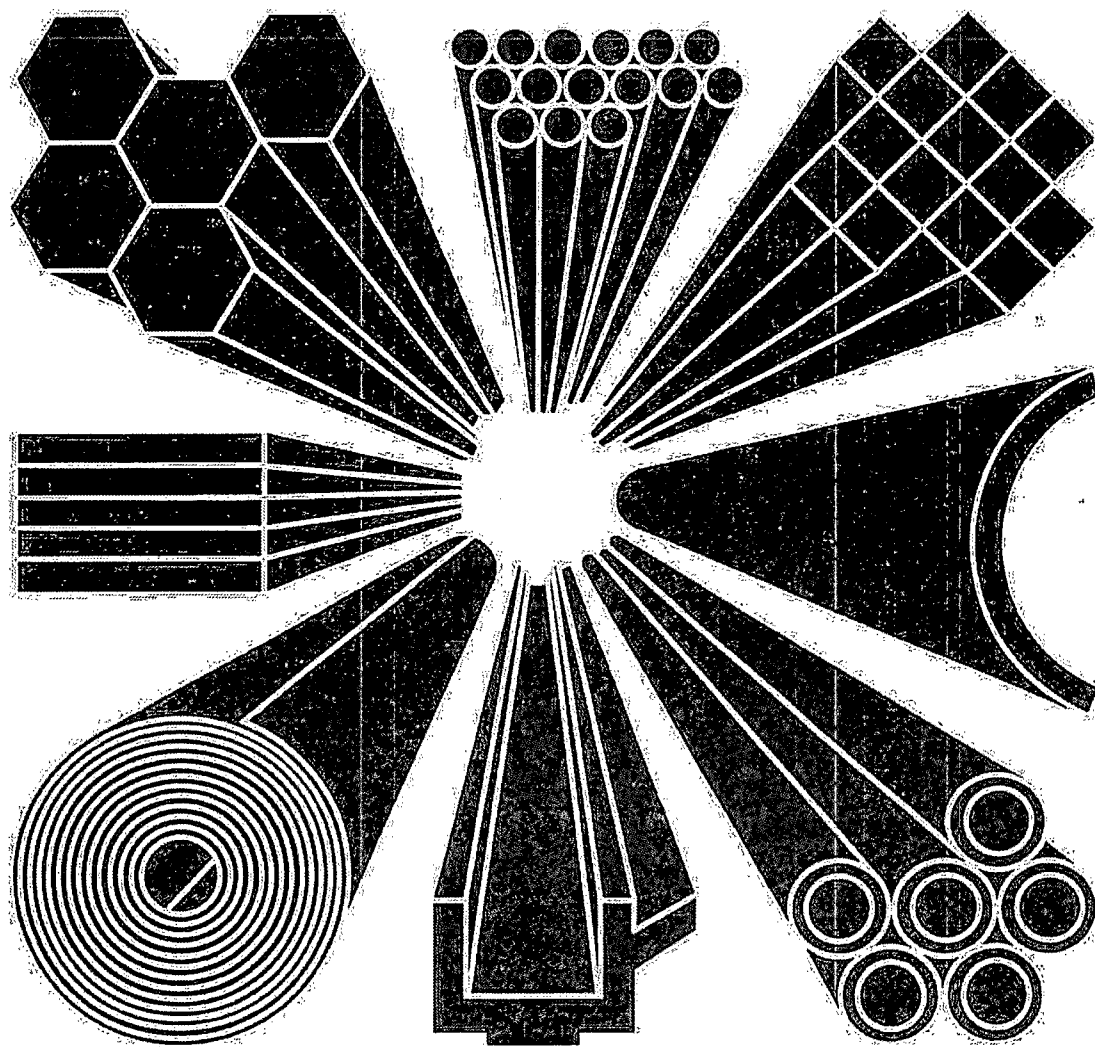
Cast Special Shapes, Plates, Rounds, Squares, Structural Shapes (vessels, tanks, etc.)

IELD and
of them.

Aluminum

● standards and data 1997

The Aluminum Association
Incorporated



The Aluminum Association
900 19th Street, N.W., Washington, D.C. 20006

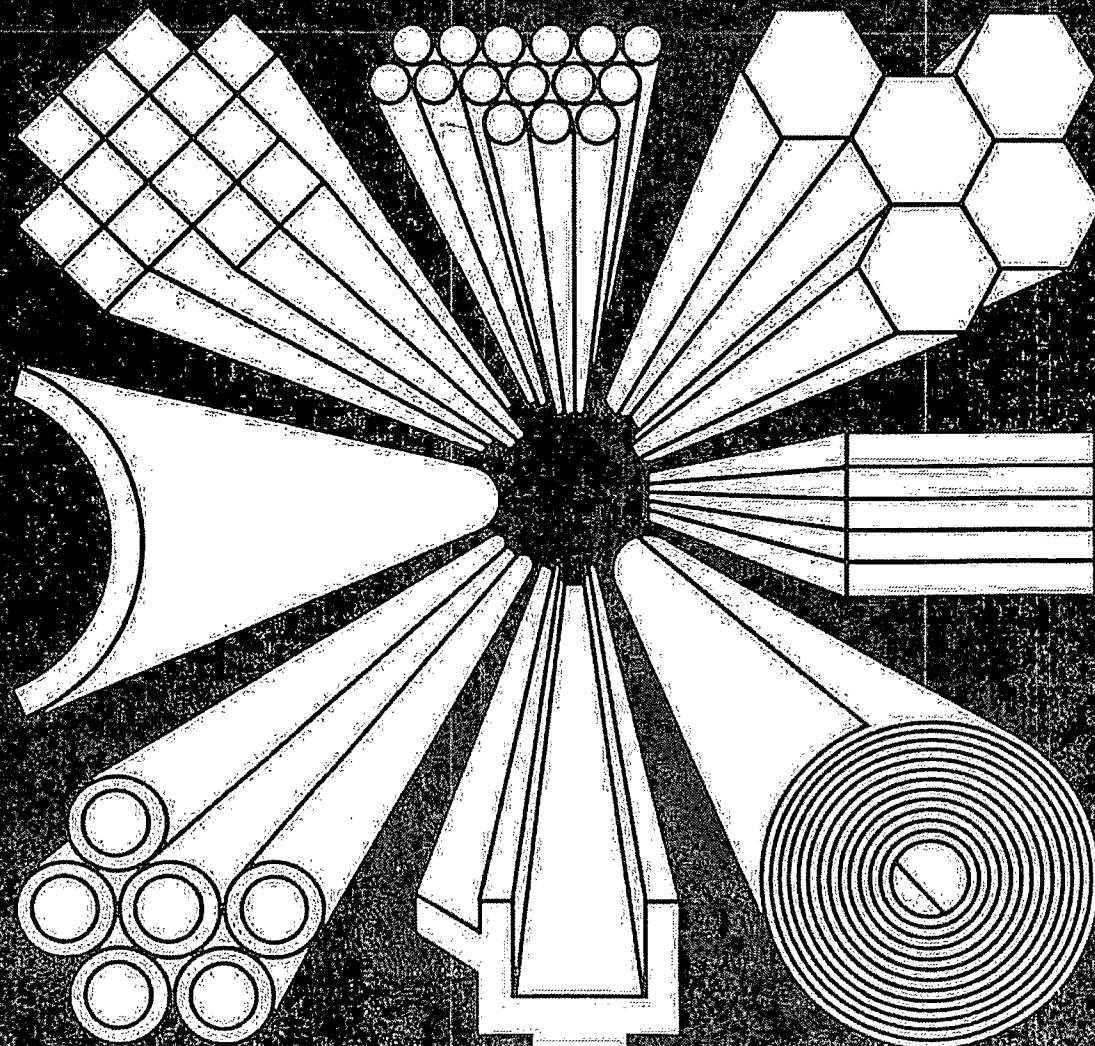


TABLE 2.2 Typical Tensile Properties at Various Temperatures ①

The following typical properties are not guaranteed, since in most cases they are averages for various sizes, product forms and methods of manufacture and may not be exactly representative of any particular product or size. These data

are intended only as a basis for comparing alloys and tempers and should not be specified as engineering requirements or used for design purposes.

ALLOY AND TEMPER	TEMP.	TENSILE STRENGTH, ksi		ELONGATION IN 2 IN., PERCENT	ALLOY AND TEMPER	TEMP.	TENSILE STRENGTH, ksi		ELONGATION IN 2 IN., PERCENT
	°F	ULTIMATE	YIELD ②			°F	ULTIMATE	YIELD ②	
1100-O	-320	25	6	50	2024-T3 (Sheet)	320	85	62	18
	-112	15	5.5	43		-112	73	52	17
	-18	14	5	40		-18	72	51	17
	75	13	5	40		75	70	50	17
	212	10	4.6	45		212	66	48	16
	300	8	4.2	55		300	55	45	11
	400	6	3.5	65		400	27	20	23
	500	4	2.6	75		500	11	9	55
	600	2.9	2	80		600	7.5	6	75
700	2.1	1.6	85	700	5	4	100		
1100-H14	-320	30	20	45	2024-T4, T351 (plate)	320	84	61	19
	-112	20	18	24		-112	71	49	19
	-18	19	17	20		-18	69	47	19
	75	18	17	20		75	68	47	19
	212	16	15	20		212	63	45	19
	300	14	12	23		300	45	36	17
	400	10	7.5	26		400	26	19	27
	500	4	2.6	75		500	11	9	55
	600	2.9	2	80		600	7.5	6	75
700	2.1	1.6	85	700	5	4	100		
1100-H18	-320	34	26	30	2024-T6, T651	320	84	68	11
	-112	26	23	16		-112	72	59	10
	-118	25	23	15		-18	70	58	10
	75	24	22	15		75	69	57	10
	212	21	19	15		212	65	54	10
	300	18	14	20		300	45	36	17
	400	6	3.5	65		400	26	19	27
	500	4	2.6	75		500	11	9	55
	600	2.9	2	80		600	7.5	6	75
700	2.1	1.6	85	700	5	4	100		
2011-T3	75	55	43	15	2024-T81, T851	320	65	78	8
	212	47	34	16		-112	74	69	7
	300	28	19	25		-18	73	68	7
	400	16	11	35		75	70	65	7
	500	6.5	3.8	45		212	66	62	8
	600	3.1	1.8	90		300	55	49	11
2014-T6, T651	700	2.3	1.4	125	400	27	20	23	
	500	11	9	55	500	11	9	55	
	600	7.5	6	75	600	7.5	6	75	
	700	5	4	100	700	5	4	100	
	-320	84	72	14	2024-T861	-320	92	85	5
	-112	74	65	13		-112	81	77	5
	-18	72	62	13		-18	78	74	5
	75	70	60	13		75	75	71	5
	212	63	57	15		212	70	67	6
300	40	35	20	300		54	48	11	
400	16	13	38	400		21	17	28	
500	9.5	7.5	52	500		11	9	55	
600	6.5	5	65	600		7.5	6	75	
700	4.3	3.5	72	700	5	4	100		
2017-T4, T451	320	80	53	28	2117-T4	-320	56	33	30
	-112	65	42	24		-112	45	25	29
	-18	64	41	23		-18	44	24	28
	75	62	40	22		75	43	24	27
	212	57	39	18		212	36	21	16
	300	40	30	15		300	30	17	20
	400	16	13	35		400	16	12	35
	500	9	7.5	45		500	7.5	5.5	55
	600	6	5	65		600	4.7	3.3	80
700	4.3	3.5	70	700	2.9	2	110		

For all numbered footnotes, see page 2-9.

tensile/typical properties

TABLE 2.2 Typical Tensile Properties at Various Temperatures ① (continued)

The following typical properties are not guaranteed, since in most cases they are averages for various sizes, product forms and methods of manufacture and may not be exactly representative of any particular product or size. These data

are intended only as a basis for comparing alloys and tempers and should not be specified as engineering requirements or used for design purposes.

ALLOY AND TEMPER	TEMP. F	TENSILE STRENGTH, ksi		ELONGATION IN 2 IN., PERCENT	ALLOY AND TEMPER	TEMP. F	TENSILE STRENGTH, ksi		ELONGATION IN 2 IN., PERCENT
		ULTIMATE	YIELD ②				ULTIMATE	YIELD ②	
2124-T851	452	102	90	10	3003-H14	320	35	25	30
	320	86	79	9		112	24	22	18
	112	76	71	8		18	22	21	16
	18	73	68	8		75	22	21	16
	75	70	64	9		212	21	19	16
	212	66	61	9		300	18	16	16
	300	54	49	13		400	14	9	20
	400	27	20	28		500	7.5	4	60
	500	11	8	60		600	4	2.4	70
	600	7.5	6	75		700	2.8	1.8	70
700	5.5	4.1	100						
2218-T61	320	72	52	15	3003-H18	320	41	33	23
	112	61	45	14		112	32	29	11
	18	59	44	13		18	30	28	10
	75	59	44	13		75	29	27	10
	212	56	42	15		212	26	21	10
	300	41	35	17		300	23	16	11
	400	22	16	30		400	14	9	18
	500	10	6	70		500	7.5	4	60
	600	5.5	3	85		600	4	2.4	70
	700	4	2.5	100		700	2.8	1.8	70
2219-T62	320	73	49	16	3004-O	320	42	13	38
	112	63	44	13		112	28	11	30
	18	60	42	12		18	26	10	26
	75	58	40	12		75	26	10	25
	212	54	37	14		212	26	10	25
	300	45	33	17		300	22	10	35
	400	34	25	20		400	14	9.5	55
	500	27	20	21		500	10	7.5	70
	600	10	8	40		600	7.5	5	80
	700	4.4	3.7	75		700	5	3	90
2219-T81, T851	320	83	61	15	3004-H34	320	52	34	26
	112	71	54	13		112	38	30	16
	18	69	52	12		18	36	29	13
	75	66	50	12		75	35	29	12
	212	60	47	15		212	34	29	13
	300	49	40	17		300	28	25	22
	400	36	29	20		400	21	15	35
	500	29	23	21		500	14	7.5	55
	600	7	8	55		600	7.5	5	80
	700	4.4	3.7	75		700	5	3	90
2618-T61	320	78	61	12	3004-H38	320	58	43	20
	112	67	55	11		112	44	38	10
	18	64	54	10		18	42	36	7
	75	64	54	10		75	41	36	6
	212	62	54	10		212	40	36	7
	300	50	44	14		300	31	27	15
	400	32	26	24		400	22	15	30
	500	13	9	50		500	12	7.5	50
	600	7.5	4.5	80		600	7.5	5	80
	700	5	3.5	120		700	5	3	90
3003-O	320	33	8.5	46	4032-T6	320	66	48	11
	112	20	7	42		112	58	46	10
	18	17	6.5	41		18	56	46	9
	75	16	6	40		75	55	46	9
	212	13	5.5	43		212	50	44	9
	300	11	5	47		300	37	33	9
	400	8.5	4.3	60		400	13	9	30
	500	6	3.4	65		500	8	5.5	50
	600	4	2.4	70		600	5	3.2	70
	700	2.8	1.8	70		700	3.4	2	90

For all numbered footnotes, see page 2-9.

TABLE 2.2 Typical Tensile Properties at Various Temperatures ^① (continued)

The following typical properties are not guaranteed, since in most cases they are averages for various sizes, product forms and methods of manufacture and may not be exactly representative of any particular product or size. These data

are intended only as a basis for comparing alloys and tempers and should not be specified as engineering requirements or used for design purposes.

ALLOY AND TEMPER	TEMP. °F	TENSILE STRENGTH, ksi		ELONGATION IN 2 IN., PERCENT	ALLOY AND TEMPER	TEMP. °F	TENSILE STRENGTH, ksi		ELONGATION IN 2 IN., PERCENT
		ULTIMATE	YIELD ^②				ULTIMATE	YIELD ^②	
5050-O	320	37	10	...	5083-O	320	59	24	36
	-112	22	8.5	...		-112	43	21	30
	-18	21	8	...		-18	42	21	27
	75	21	8	...		75	42	21	25
	212	21	8	...		212	40	21	36
	300	19	8	...		300	31	19	50
	400	14	7.5	...		400	22	17	60
	500	9	6	...		500	17	11	80
	600	6	4.2	...		600	11	7.5	110
700	3.9	2.6	...	700	6	4.2	130		
5050-H34	-320	44	30	...	5086-O	320	55	19	46
	-112	30	25	...		-112	39	17	35
	-18	28	24	...		-18	38	17	32
	75	28	24	...		75	38	17	30
	212	28	24	...		212	38	17	36
	300	25	22	...		300	29	16	50
	400	14	7.5	...		400	22	15	60
	500	9	6	...		500	17	11	80
	600	6	4.2	...		600	11	7.5	110
700	3.9	2.6	...	700	6	4.2	130		
5050-H38	-320	46	36	...	5154-O	320	52	19	46
	-112	34	30	...		-112	36	17	35
	-18	32	29	...		-18	35	17	32
	75	32	29	...		75	35	17	30
	212	31	29	...		212	35	17	36
	300	27	25	...		300	29	16	50
	400	14	7.5	...		400	22	15	60
	500	9	6	...		500	17	11	80
	600	6	4.2	...		600	11	7.5	110
700	3.9	2.6	...	700	6	4.2	130		
5052-O	-320	44	16	46	5254-O	320	52	19	46
	-112	29	13	35		-112	36	17	35
	-18	28	13	32		-18	35	17	32
	75	28	13	30		75	35	17	30
	212	28	13	36		212	35	17	36
	300	23	13	50		300	29	16	50
	400	17	11	60		400	22	15	60
	500	12	7.5	80		500	17	11	80
	600	7.5	5.5	110		600	11	7.5	110
700	5	3.1	130	700	6	4.2	130		
5052-H34	-320	55	36	28	5454-O	320	54	19	39
	-112	40	32	21		-112	37	17	30
	-18	38	31	18		-18	36	17	27
	75	38	31	16		75	36	17	25
	212	38	31	18		212	36	17	31
	300	30	27	27		300	29	16	50
	400	24	15	45		400	22	15	60
	500	12	7.5	80		500	17	11	80
	600	7.5	5.5	110		600	11	7.5	110
700	5	3.1	130	700	6	4.2	130		
5052-H38	-320	60	44	25	5454-H32	320	59	36	32
	-112	44	38	18		-112	42	31	23
	-18	42	37	15		-18	41	30	20
	75	42	37	14		75	40	30	18
	212	40	36	16		212	39	29	20
	300	34	28	24		300	32	26	37
	400	25	15	45		400	25	19	45
	500	12	7.5	80		500	17	11	80
	600	7.5	5.5	110		600	11	7.5	110
700	5	3.1	130	700	6	4.2	130		

For all numbered footnotes, see page 2-9.

tensile/typical properties

TABLE 2.2 Typical Tensile Properties at Various Temperatures ^① (continued)

The following typical properties are not guaranteed, since in most cases they are averages for various sizes, product forms and methods of manufacture and may not be exactly representative of any particular product or size. These data

are intended only as a basis for comparing alloys and tempers and should not be specified as engineering requirements or used for design purposes.

ALLOY AND TEMPER	TEMP. F	TENSILE STRENGTH, ksi		ELONGATION IN 2 IN., PERCENT	ALLOY AND TEMPER	TEMP. F	TENSILE STRENGTH, ksi		ELONGATION IN 2 IN., PERCENT
		ULTIMATE	YIELD ^②				ULTIMATE	YIELD ^②	
5454-H34	320	63	41	30	6061-T6, T651	320	60	47	22
	112	46	36	21		112	49	42	18
	18	44	35	18		18	47	41	17
	75	44	35	16		75	45	40	17
	212	43	34	18		212	42	38	18
	300	34	28	32		300	34	31	20
	400	26	19	45		400	19	15	28
	500	17	11	80		500	7.5	5	60
	600	11	7.5	110		600	4.6	2.7	85
700	6	4.2	130	700	3	1.8	95		
5456-O	320	62	26	32	6063-T1	320	34	16	44
	112	46	23	25		112	26	15	36
	18	45	23	22		18	24	14	34
	75	45	23	20		75	22	13	33
	212	42	22	31		212	22	14	18
	300	31	20	50		300	21	15	20
	400	22	17	60		400	9	6.5	40
	500	17	11	80		500	4.5	3.5	75
	600	11	7.5	110		600	3.2	2.5	80
700	6	4.2	130	700	2.3	2	105		
5652-O	320	44	16	46	6063-T5	320	37	24	28
	112	29	13	35		112	29	22	24
	18	28	13	32		18	28	22	23
	75	28	13	30		75	27	21	22
	212	28	13	30		212	24	20	18
	300	23	13	50		300	20	18	20
	400	17	11	60		400	9	6.5	40
	500	12	7.5	80		500	4.5	3.5	75
	600	7.5	5.5	110		600	3.2	2.5	80
700	5	3.1	130	700	2.3	2	105		
5652-H34	320	55	36	28	6063-T6	320	47	36	24
	112	40	32	21		112	38	33	20
	18	38	31	18		18	36	32	19
	75	38	31	16		75	35	31	18
	212	38	31	18		212	31	28	15
	300	30	27	27		300	21	20	20
	400	24	15	45		400	9	6.5	40
	500	12	7.5	80		500	4.5	3.5	75
	600	7.5	5.5	110		600	3.3	2.5	80
700	5	3.1	130	700	2.3	2	105		
5652-H38	320	60	44	25	6101-T6	320	43	33	24
	112	44	38	18		112	36	30	20
	18	42	37	16		18	34	29	19
	75	42	37	14		75	32	28	19
	212	40	36	16		212	28	25	20
	300	34	28	24		300	21	19	20
	400	25	15	45		400	10	7	40
	500	12	7.5	80		500	4.8	3.3	80
	600	7.5	5.5	110		600	3	2.3	100
700	5	3.1	130	700	2.5	1.8	105		
6053-T6, T651	75	37	32	13	6151-T6	320	57	50	20
	212	32	28	13		112	50	46	17
	300	25	24	13		18	49	45	17
	400	13	12	25		75	48	43	17
	500	5.5	4	70		212	43	40	17
	600	4	2.7	80		300	28	27	20
	700	2.9	2	90		400	14	12	30
					500	6.5	5	50	
					600	5	3.9	43	
					700	4	3.2	35	

For all numbered footnotes, see page 2-9.

TABLE 2.2 Typical Tensile Properties at Various Temperatures ^① (concluded)

The following typical properties are not guaranteed, since in most cases they are averages for various sizes, product forms and methods of manufacture and may not be exactly representative of any particular product or size. These data

are intended only as a basis for comparing alloys and tempers and should not be specified as engineering requirements or used for design purposes.

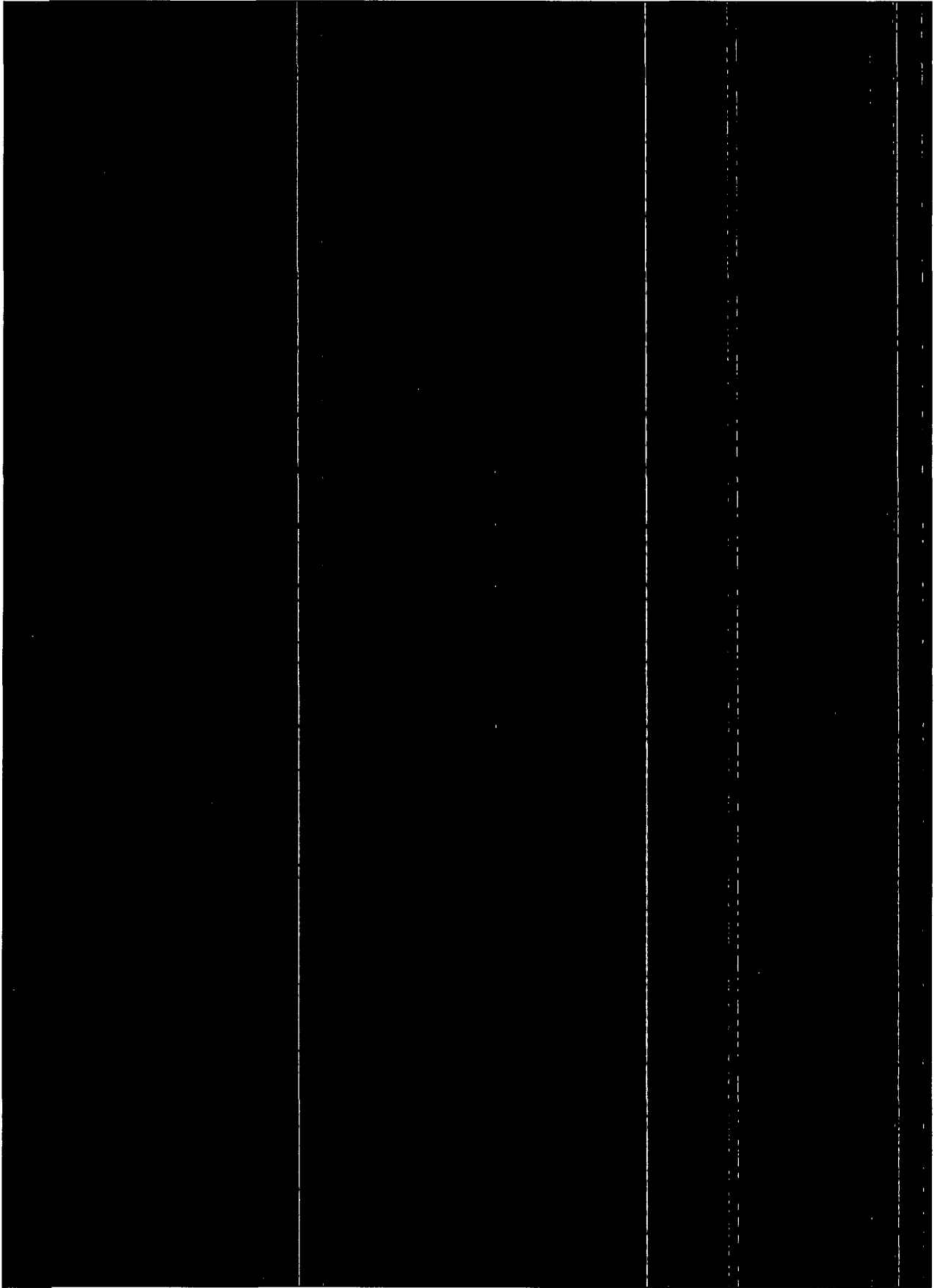
ALLOY AND TEMPER	TEMP. °F	TENSILE STRENGTH, ksi		ELONGATION IN 2 IN., PERCENT	ALLOY AND TEMPER	TEMP. °F	TENSILE STRENGTH, ksi		ELONGATION IN 2 IN., PERCENT
		ULTIMATE	YIELD ^②				ULTIMATE	YIELD ^②	
6262-T651	320	60	47	22	7178-T6, T651	-320	106	94	5
	112	49	42	18		-112	94	84	8
	-18	47	41	17		-18	91	81	9
	75	45	40	17		75	88	78	11
	212	42	38	18		212	73	68	14
	300	34	31	20		300	31	27	40
6262-T9	320	74	67	14	400	15	12	70	
	-112	62	58	10	500	11	9	76	
	-18	60	56	10	600	8.5	7	80	
	75	58	55	10	700	6.5	5.5	80	
	212	53	52	10	7178-T76, T7651	-320	106	89	10
	300	38	37	14		-112	91	78	10
	400	15	13	34		-18	88	76	10
	500	8.5	6	48		75	83	73	11
600	4.6	2.7	85	212		69	64	17	
700	3	1.8	95	300		31	27	40	
7075-T6, T651	320	102	92	9	400	15	12	70	
	112	90	79	11	500	11	9	76	
	-18	86	75	11	600	8.5	7	80	
	75	83	73	11	700	6.5	5.5	80	
	212	70	65	14	7475-T61 Sheet	320	99	87	10
	300	31	27	30		112	88	79	12
	400	16	13	55		18	84	75	12
	500	11	9	65		75	80	72	12
600	8	6.5	70	212		70	65	14	
700	6	4.6	70	300		30	26	28	
7075-T73, T7351	320	92	72	14	400	14	11	55	
	112	79	67	14	500	9.5	7	70	
	-18	76	65	13	600	6.5	5.5	80	
	75	73	63	13	700	5	3.8	85	
	212	63	58	15	7475-T761 Sheet	-320	95	82	11
	300	31	27	30		-112	84	73	12
	400	16	13	55		-18	80	70	12
	500	11	9	65		75	76	67	12
600	8	6.5	70	212		64	61	14	
700	6	4.6	70	300		30	26	38	
7175-T74	320	106	99	13	400	14	11	55	
	112	90	83	14	500	9.5	7	70	
	18	87	80	16	600	6.5	5.5	80	
	75	80	73	14	700	5	3.8	85	
	212	72	69	17	7475-T761 Sheet	-320	95	82	11
	300	35	31	30		-112	84	73	12
	400	18	13	65		-18	80	70	12
						75	76	67	12
				212		64	61	14	
				300		30	26	38	

^① These data are based on a limited amount of testing and represent the lowest strength during 10,000 hours of exposure at testing temperature under no load; stress applied at 5,000 psi/min to yield strength and then at strain rate of 0.05 in./in./min to failure. Under some conditions of temperature and

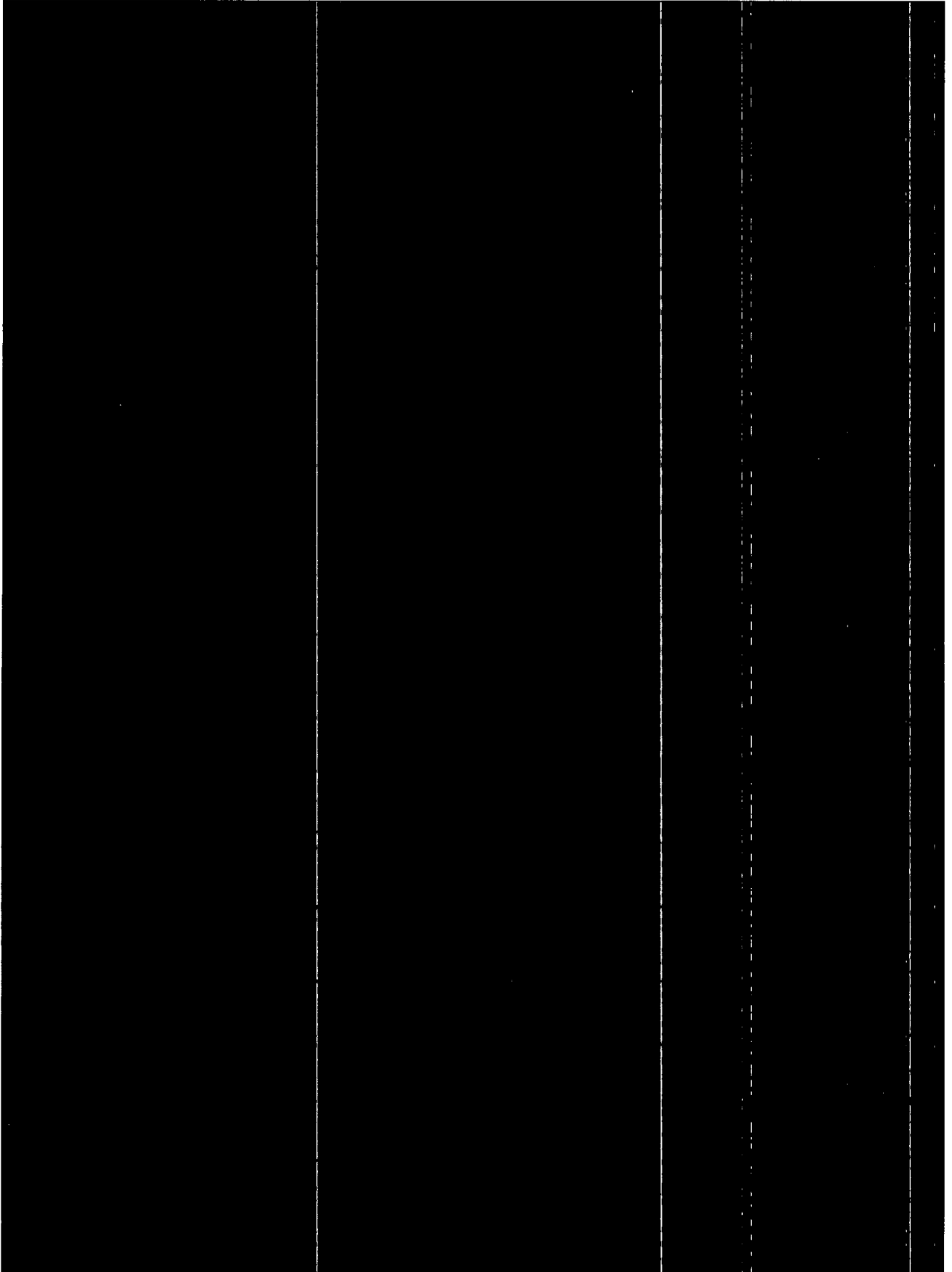
time, the application of heat will adversely affect certain other properties of some alloys.

^② Offset equals 0.2 percent.

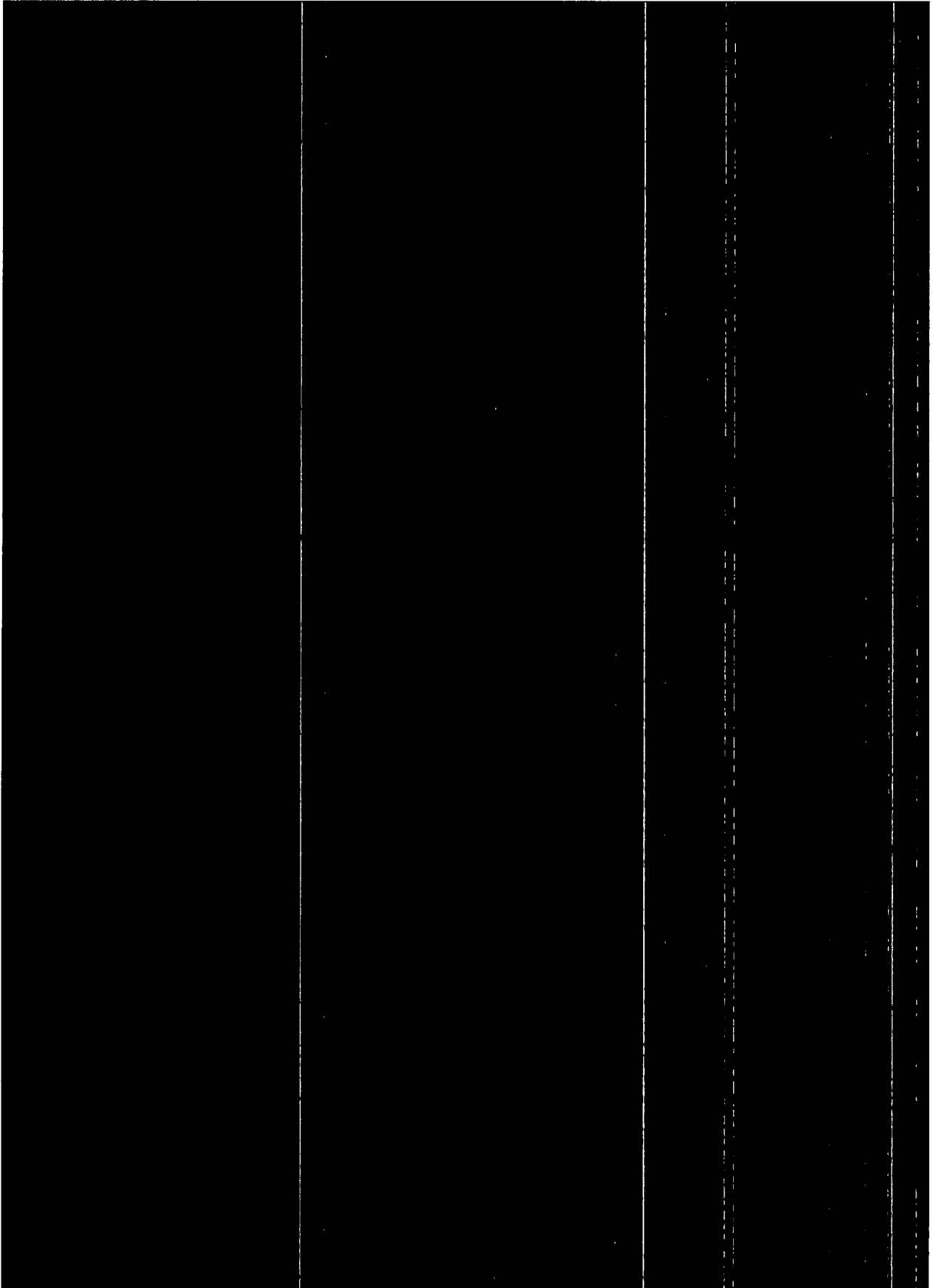
"NAC PROPRIETARY INFORMATION REMOVED"



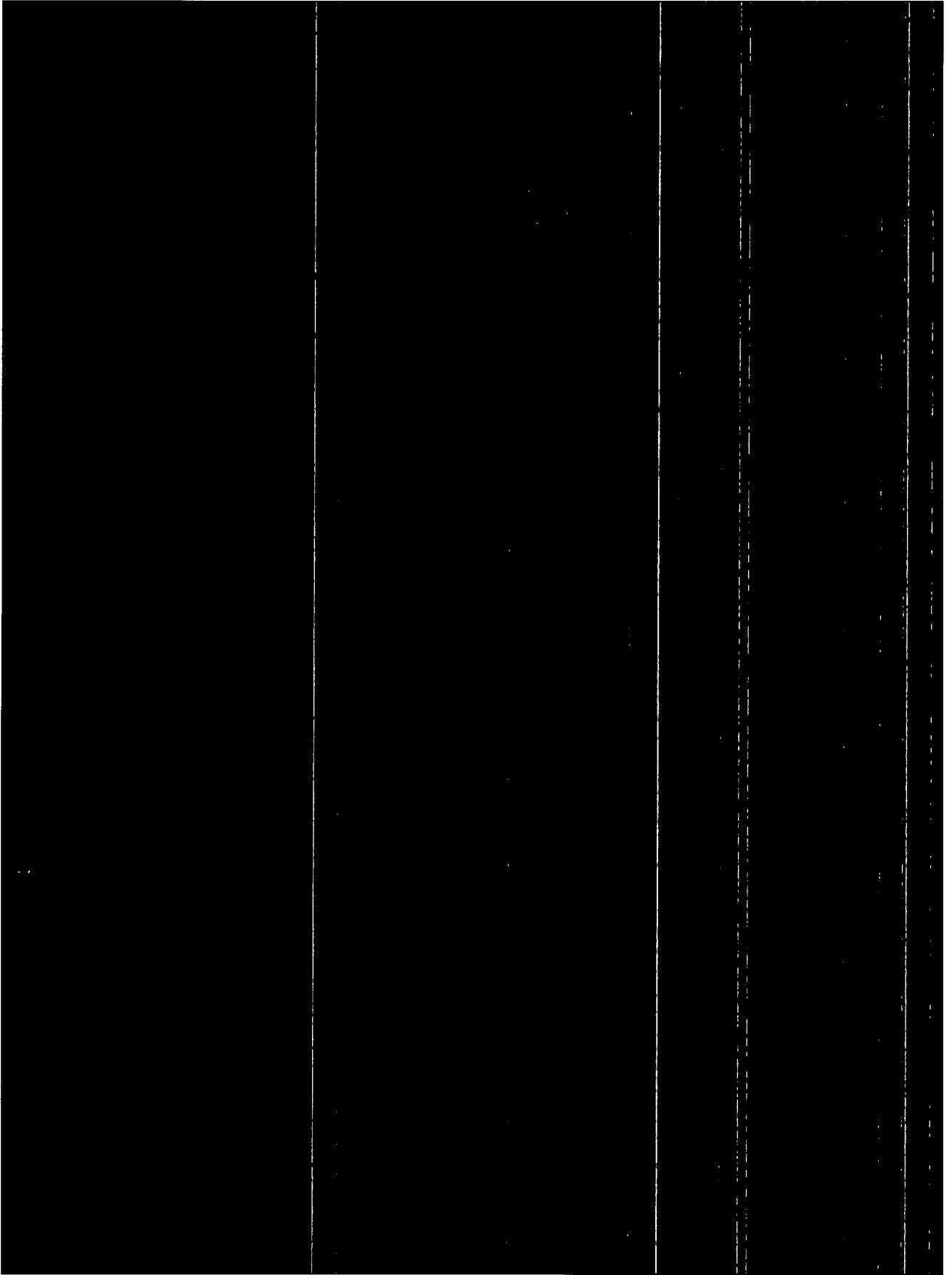
"NAC PROPRIETARY INFORMATION REMOVED"



"NAC PROPRIETARY INFORMATION REMOVED"



"NAC PROPRIETARY INFORMATION REMOVED"





Experimental Studies on Long-term Thermal Degradation of Enclosed Neutron Shielding Resin

Ryoji ASANO¹, Nagao NIOMURA²

¹Hitachi Zosen Corporation, Japan

²Ocean Cask Lease Co., Ltd, Japan

INTRODUCTION

Resins which have high Hydrogen atom content are effective for Neutron shielding and are recently used for neutron shielding material of spent fuel shipping casks. As the resins themselves are easily burned at relatively low temperature, which could be the problem during the fire test condition, mixture of resin and fire retardant which main component is a hydroxide compound is usually used as shielding material. The fire retardant prevents resin from burning by decomposing of the hydroxide compound under fire test condition.

When these resins are used for neutron shielding material of cask, their temperature rises during the transportation by decay heat of spent fuel. Therefore, thermal degradation of resin (hereafter called as "heat weight loss") at the operating temperature should be paid attention.

Furthermore, when the resin is used for neutron shielding material, there are two cases. One is to put it on the outside surface of the cask and the other is to enclose it between two layers. In former case, the heat weight loss occurs in air of which study report can be obtained. On the other hand, the latter is the reaction in the enclosed environment which study report can be seldom obtained. Therefore, the study of the heat weight loss in the enclosed environment was carried out for long term period assuming the operating time of the real cask .

TEST MATERIAL

Test material is NS-4-FR supplied by BISCO CO. LTD, U.S.A. Raw materials are epoxi resin, hardener and fire retardant. They are mixed together and hardened according to the manu-

facturing manual supplied by BISCO. NS-4-FR is the neutron shielding material which contains about 60% of aluminium hydroxide as fire retardant.

TEST

Tests were carried out in order of basic material test, open test, enclosed test and long term cyclic test which simulates the operation term of cask. The test results are explained as follows.

Basic material test

TG tests which can be performed comparatively easily were carried out in order to study basic thermal characteristics of the test material. The test conditions are as follows.

<u>Condition</u>	<u>Case 1</u>	<u>Case 2</u>
Atmospheric gas	Air&N ₂	Air&N ₂
Gas Flow Rate(cc/min)	150	200
Temp. Rising Rate(°C/min)	3	10
Max. Temperature(°C)	220	530

Heat weight loss could not be detected in the Case 1. The results of Case 2 are as follows.

- (1) The weight loss of the test specimen in nitrogen gas was much smaller than that in air between 300°C and 380°C which were shown in Fig 1. It indicates that the test materials are decomposed and loose its weight by oxygen in air and by heat within the temperature range.
- (2) Comparing the results between test material and NS-4- FR without fire retardant, the weight loss of latter is less than that of former until 360°C as shown in Fig. 2. It indicates that the weight loss of former is mainly due to the decomposition of aluminium hydroxide as fire retardant. This result means that the decomposition of aluminium hydroxide is important for the weight loss during low temperature. And it is necessary to select a suitable grade of aluminium hydroxide, as the decomposition temperature depends on the purity and grain size of aluminium hydroxide.

TG test results can not be used directly for long term degradation data because the test specimen was pulverized to very small size, and reaction and diffusion is very rapid, but they can be good reference information.

Open test

Open tests were performed varying the shape of test specimen and temperature to study heat weight loss in air. The results are as follows.

(1) Effect of shape of test specimen

To study the effect of the shape, cubic and cylindrical test specimens with nearly equal weight were tested. It was observed that the heat weight loss of latter which had larger surface area was always larger than that of the former. It indicates that effects of surface oxidation and surface diffusion are important factors for the heat weight loss.

(2) Effect of temperature

The heat weight loss at 125°C, 150°C, 175°C and 200°C are shown in Fig.3 as a function of time. The increase of the heat weight loss is observed in 200°C test after 1000 hr. It is supposed that generation of continues crack inside of the test specimen makes it easy to diffuse the decomposed resin component and water.

Enclosed test

Supposing that the neutron shielding material is filled in the enclosures tests were conducted to study the effects of enclosed condition to the heat weight loss. The tests were performed on test specimen in the sealed stainless steel container with Ar atmosphere.

(1) Sealed stainless steel container

Seal container is shown in Fig. 4, of which lid is welded to seal the cavity of the container perfectly. Enough height of container cavity is provided to avoid the effect of welding heat to the test specimen. Ar gas seal hole is seal-welded and cooled immediately by water after replacing air with Ar gas.

(2) Test Condition

Continuous test and cyclic test of 110 hr heating and 58 hr cooling which simulated the actual operating condition of cask were performed at 125°C, 150°C and 175°C. The test duration was from 8 to 16 weeks.

(3) Test Results

Test results are shown also in Fig.3. Main results are as follows.

(a) Test Results at 125°C

The heat weight loss at 1512 hr continuous test and that at 1760 hr cyclic test were negligible. The heat weight loss at this temperature is regarded as insignificant.

(b) Test Results at 150°C

The heat weight losses at both 1224 hr continuous tests, 990 hr cyclic test and 1760 hr cyclic test were almost 1/3 of that of open test.

(c) Test Results at 175°C

The heat weight losses at both 1600 hr continuous test, 1210 hr cyclic test and 1760 hr cyclic test were almost half of that of open test.

(d) Due to the few test specimens and short test period, data scattering was observed in the test results. However, heat weight loss of enclosed test is clearly less than that of open test except those at 125°C when no heat weight loss was observed.

Long term cyclic test at 150°C

In order to avoid scatter in test results and to estimate heat weight loss during long term use of cask, long term cyclic tests at 150°C were conducted, where temperature supposed was the maximum working temperature of neutron shielding material during transportation. The results are shown in Fig. 5. Total test specimens were 18 and maximum test period was 56 weeks. One cycle is composed of 110 hr heating and 58 hr cooling which is same as the enclosed test above. The heat weight loss for 56 weeks was about 1.1%.

DISCUSSION

The relation between heat weight loss $W(\%)$ and test period $D(\text{day})$ is given from Fig. 5, as follow.

$$W=100.63-0.218x\log D$$

Using this equation the heat weight loss for 20 years $W_{20}(\%)$ can be estimated as follow.

$$\begin{aligned} W_{20} &= 100.63 - 0.218 \times \log(20 \times 365) \\ &= 1.87(\%) \end{aligned}$$

From the calculation above it is enough to have the cask design margins of 2.0% heat weight loss even if the scattering in the test results are taken into account.

Water drops were observed on inside surface of sealed container when the lid was cut off to open and to take out the test specimen from the container after test. It is considered that these drops prevented the temperature rise of test specimen by evaporating during the test and reduced the heat weight loss of the specimen.

From the results, it is concluded that NS-4-FR is effective as neutron shielding material of cask, especially when it is used in enclosed condition.

BISCO (150°C HEATED)

TG	<Sample>	<Comment>	<Temp.program (C)	(C/min)	(min)>
	9.652mg	10°C/min	1# 20.0-500.0	10.00	0.00
<Date>	(9.652mg)		<Gas>		
90/04/10 16:51	<Reference>		N ₂ AND AIR	150.0ml/min	0.0ml/min

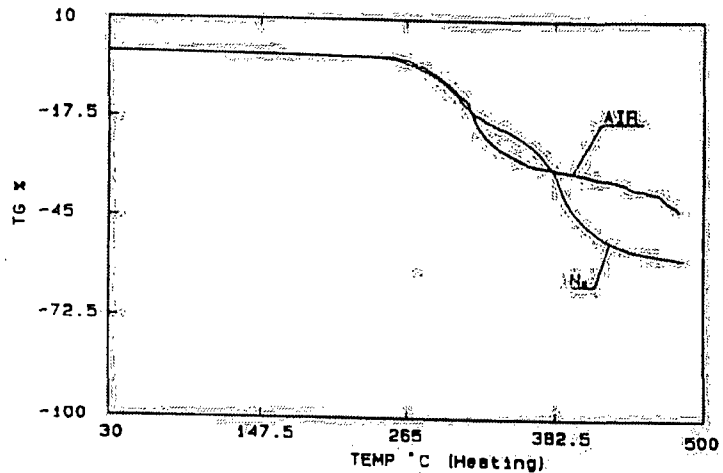


Fig 1 TG OF NS-4-FR IN AIR AND NITROGEN

BISCO

TG	<Sample>	<Comment>	<Temp.program (C)	(C/min)	(min)>
	RESIN AND NS-4-FR		1# 25.0-500.0	10.00	0.00
	7.965mg		<Gas>		
<Date>	(7.965mg)		N ₂	200.0ml/min	0.0ml/min
90/04/26 14:00	<Reference>				
	Al2O3				

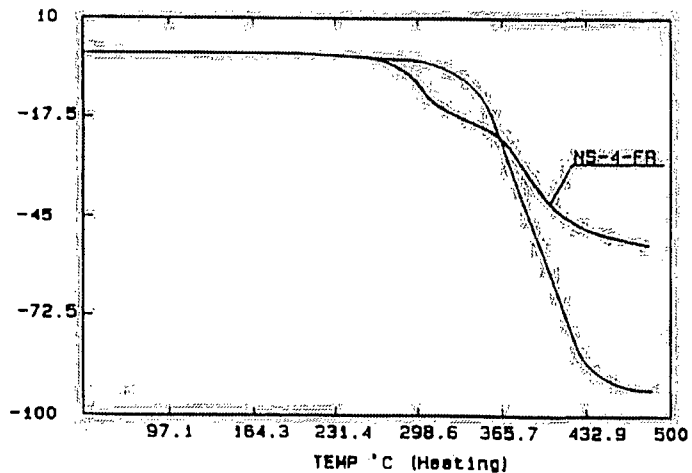


Fig 2 TG OF NS-4-FR W/O FIRE RETARDANT

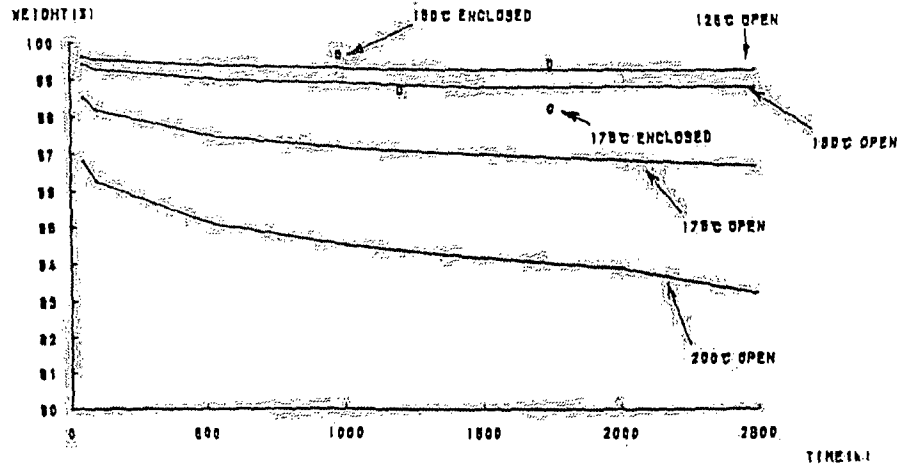


Fig. 3 WEIGHT LOSS BY OPEN AND ENCLOSED TEST

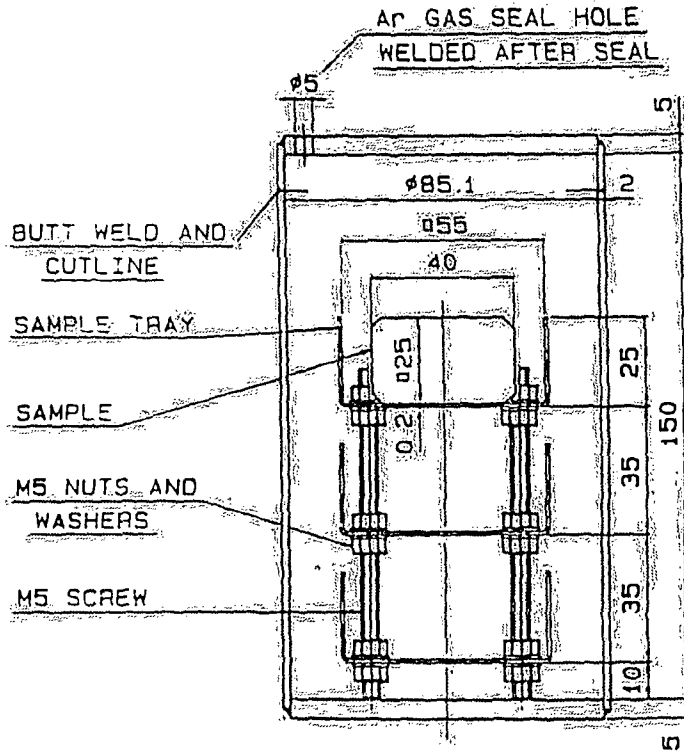


Fig 4 SEALED STAINLESS STEEL CONTAINER

HEAT WEIGHT LOSS (%)

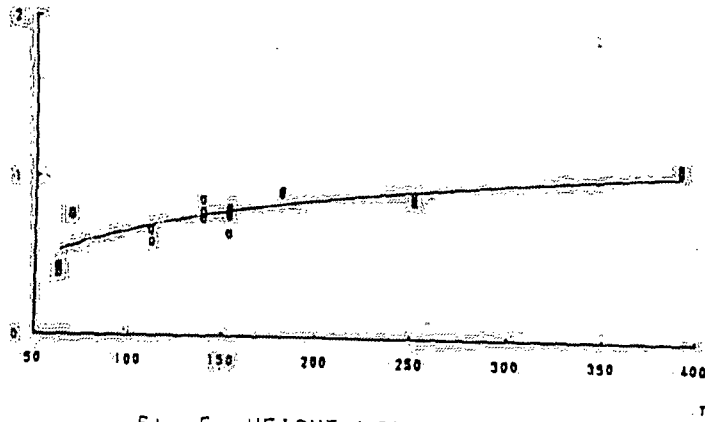


Fig. 5. WEIGHT LOSS OF LONG TERM CYCLIC TEST

EVALUATION TEST ON THE THERMAL STABILITY OF RESIN AS NEUTRON SHIELDING MATERIAL FOR SPENT FUEL TRANSPORT CASK

Y.Momma(1), M.Matsumoto(1), M.Takani(2), S.Shirai(2), O.Umegaki(2),
Y.Irisa(3), K.Maruoka(3), K.Sakai(4), H.Nishioka(4) and O.Kadota(5)

- (1) Tokyo Electric Power Company (TEPCO), 1-1-3 Uchisarwai-cho, Chiyoda-ku, Tokyo, Japan
- (2) Nuclear Fuel Transport Corporation. Ltd.(NFT),1-1-3, Shiba Daimon, Minato-ku,Tokyo Japan
- (3) Mitsubishi Heavy Industries Ltd.(MHI), 1-1-1 Wadasaki-machi, Hyogo-ku, Kobe, Japan
- (4) Genden Engineering Services & Construction Comp.(GESC), 1-6-1, Ohtemachi, Chiyada-ku, Tokyo, Japan
- (5) NOF Corporation. 4-20-3. Ebisu, Shibuya-ku, Tokyo, Japan

SUMMARY

Epoxy-resin based neutron shielding material, NS-4-FR, is used for spent fuel transport and/or storage cask. In this paper the outline of thermal aging test performed to evaluate the heating effect on this neutron shielding material, NS-4-FR, is introduced. The test is consisted of two kinds of thermal aging test, one is "Basic Test" and the other is "Block Heating Test". The former is cooperatively performed by ten Japanese Electrical Power Companies, and the latter is done by GESC and NOF Corporation.

Outline of Basic Test

In order to obtain the basic data for evaluation of heating effect on the neutron shielding efficiency of NS-4-FR, weight of isothermally heated sample was measured and composition of gaseous compounds released from sample were analyzed. Each NS-4-FR sample was sealed in a stainless steel tube with end plugs and heated isothermally at 150~190°C in thermostats.

Based on the results of this "Basic Test", it was confirmed that the heating under 170°C in the closed system gives little effect on the shielding efficiency of NS-4-FR from the view-point of cask design.

Outline of Block Heating Test

Temperature of neutron shielding material in the actual cask is not uniform. To aid to evaluate the effect of temperature gradient on the shielding efficiency, thermal aging test using test blocks was performed.

Cylindrical test block covered by thermal insulation was set upright on the electrically heated hot

plates, and the bottom of the test block was kept at 170°C in the air. Along the axis of the blocks, temperature distribution during heating was measured, the density and chemical element distribution were measured after the heating.

Based on the measured density distribution in the block, it was confirmed that it is sufficiently conservative to evaluate the weight change of NS-4FR in the actual cask by using isothermal heating data.

BASIC TEST

Test Conditions

"Basic Test" was performed with a view to obtaining the data for evaluation of heating effect on the properties of NS-4FR, especially on its shielding efficiency. In this test the external appearances of samples were observed, their weights and composition of gaseous compounds released from samples were measured after isothermal heating over 150°C.

Thermal aging conditions were determined in conformity to the international guide for the thermal evaluation and classification of electrical insulation (IEC Pub.216) and German specification on the thermal evaluation of plastics (DIN53 446).

Thermal aging conditions such as heating temperature, heating time, sample size, sample number, etc., are shown in Table 1-1.

Sample Preparation

Samples were prepared by GESC through the same process by using dedicated mixing machine for the actual installation so that they have just the same properties as NS-4FR in actual cask. GESC is the company concerning in installation of NS-4FR into the actual casks.

Test Procedure

Each one of cylindrical sample was inserted into a stainless steel tube (sample tube) and sealed with end plugs so that each sample could be heated in closed atmosphere. Sample for gas analysis was sealed in sample tube by end plugs with valve. Before sealing air contained in sample tube was replaced with nitrogen-oxygen mixed gas with appointed composition. Samples were heated in several thermostats at appointed temperature for appointed period shown in Table 1-1. Each temperature of these thermostats was controlled within $\pm 0.5^\circ\text{C}$.

After achieving of each heating period, sample tube was pulled out from thermostats and cooled down to room temperature. External appearances of samples were observed and their photographs were taken. Each sample was weighed by direct reading balance. A constituent of gas collected from sample tube was analyzed by gas chromatography-mass spectrograph (GC-MS) and its composition was determined by gas chromatography (GC).

Test Results

External Appearance of Heated Samples

All the samples were observed before and after heating. While they showed a slight change in color, no deformations nor cracks which affect neutron shielding efficiency was observed in heated samples.

Weight Change of Heated Samples

All the samples showed some weight loss after heating. Weight change at each heating temperature is shown in Figure 1-1. It is noticeable that weight loss has a tendency to saturate in the early stage of heating period, especially earlier than 1000hr. The portion of weight loss after 1000hr was extremely small. Each weight loss at all the temperatures except at 190°C was relatively small, and those after 5000hr at 150°C, 160°C, 170°C and 180°C were 1.4wt%, 2.3wt%, 2.9wt% and 3.9wt%, respectively. The weight loss at 190°C exceeded 4wt% only after 200hr, thermal aging at this temperature was completed at 200hr.

The averaged rate of weight loss during each heating period ($\Delta W/\Delta t$) can be estimated based on this result. Figure 1-2 shows this estimated average rate of weight loss during each heating period. From this figure, it can be confirmed that weight loss rate decreases rapidly with heating period. For instance, the averaged rate of weight loss at 170°C between 1000~2000hr⁽¹⁾ becomes smaller than 1/60 of that between 0~100hr⁽¹⁾, and 1/10 of that between 100~200hr⁽¹⁾.

Composition of Gas released from Heated Sample

The result of analysis on the composition of gaseous compounds released from sample is shown in Figure 1-3. From this result it is confirmed that over 90wt% of gaseous compounds is consisted of water (vapor). Therefore it could be considered that the weight loss is mainly caused by release of water from NS-4-FR and that the source of water is that absorbed in NS-4-FR and/or crystal water in aluminum hydroxide added in NS-4-FR as flame retarder.

BLOCK HEATING TEST

Test Method

In order to simulate the temperature distribution of the shielding material in the actual cask under its working condition, cylindrical test blocks of NS-4-FR were continuously heated at its bottom side over a hot plate at 170°C for 300hr and 2,000hr in the air. Test blocks were covered with thermal insulation, and the temperature distribution in test blocks was measured during heating. Figure 2-1 shows the shape and size of the test blocks. After the heating, the test blocks were cut off vertically along its central axis to observe the appearance of cross section and to measure the density and chemical composition in several points.

Test Result

Appearance of Heated Test Blocks

In both test blocks heated for 300hr and 2000hr, slight change of the color was observed in the range of about 50mm above the bottom. However, neither deformations nor cracks was observed in the samples. The range where the color changed did not expand further regardless of heating time, showing its dependence only on temperature.

Note(1) : Averaged rates of weight loss between 0~100hr, 100~200hr and 1000~2000hr are plotted at the points of 100hr, 200hr and 2000hr, respectively

77
24
312
15/6
1872

Weight Loss Due to Heating

Figure 2-2 shows the relation between the temperature distribution and weight loss estimated from measured density change in the test block heated for 2000hr. While some weight loss was observed it was comparatively small. The weight loss of NS-4-FR in the cask heated under the condition of temperature gradient can be estimated by using this result. Assuming the temperature of NS-4-FR in the cask is between 100°C and 170°C, the average weight loss of this sample in the region of this temperature range can be estimated to be less than 1%. This value is considerably small, compared with the weight loss in the "Basic Test" for 2000hr heating at 170°C.

CONCLUSIONS

The thermal aging test on epoxy-resin based neutron shielding material, NS-4-FR, was performed. The following conclusions are led, and it was confirmed that NS-4-FR sufficiently keeps its neutron shielding efficiency under heating up to 170°C in closed system from the view point of cask design ;

- No deformation nor crack which may affect the shielding efficiency was observed in the heated sample,
- Large portion of weight change (weight loss) at 150~180°C occurred in early stage of heating, earlier than 1000hr, weight loss after this was very small,
- Weight loss under 180°C in closed system was small. Those at 180°C / 5000hr and 170°C / 5000hr were < 4wt% and < 3wt%, respectively,
- The main component of released gas from sample was water (vapor),
- Weight loss due to heating under the condition of temperature gradient was much smaller than that isothermally heated sample. Therefore it is conservative to evaluate a thermal aging effect on the neutron shielding efficiency of NS-4-FR in actual cask based on the result of isothermal heating test.

REFERENCES

- DIN53 446 : "Deutsche Normen : Bestimmung von Temperatur-Zeit-Grenzen", (1962)
- IEC Pub.216-1.2 : "Guide for the Determination of Thermal Endurance Properties of Electrical Insulating Materials : Part 1 and Part 2"

Table 1-1 Thermal Aging Condition in Basic Test

Item	Test Condition in this test and suggested in DIN and/or IEC		
	This Test	DIN or IEC Pub.216 ⁽¹⁾	Remarks
Number of temp. condition	5 conditions	≥ 3 conditions	satisfied
Temp. interval	10°C	10~25°C 20°C (≥ 10°C)*	satisfied
Heating temp.	150,160,170,180 and 190°C	lowest test temp. ≥ temp. which gives longer life than 5000hr * highest test temp. ≥ temp. which gives longer life than 100hr *	satisfied
Heating condition	continuous heating	continuous (or cyclic*) heating	satisfied
Heating period	100,200,500,1000, 2000, 3600 and 5000hr	1, 2, 4, 8, 16 and 32 weeks	satisfied
Sample size	6mm φ x 60mm	120mm x 15mm x 10mm (same size for measurement of Brinell hardness, etc.)	conservative from the view-point of weight change evaluation because of larger S/V ratio
Sample number	5 samples for weight meas. 1 sample for gas analysis	5 samples not specified	satisfied
Atmosphere	closed condition	to consider actual working condition*	satisfied

(note 1)

*mark : based on IEC Pub.216-1,2
no marks : based on DIN53 446

Japan $\frac{S}{V}$ NAC $\frac{S}{V}$

Japan $S = \cancel{24} \pi r h + (2\pi r^2) = 2\pi (3)(60) + (2\pi (3)^2) =$
 $V = \pi r^2 h$

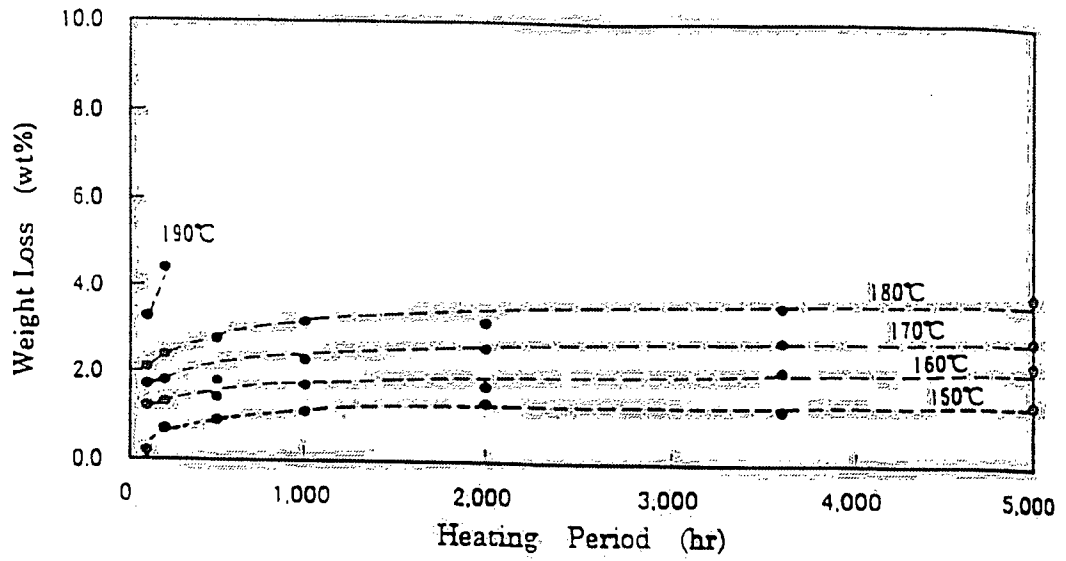


Figure 1-1 Weight Loss of NS-4 FR by Heating in Closed System

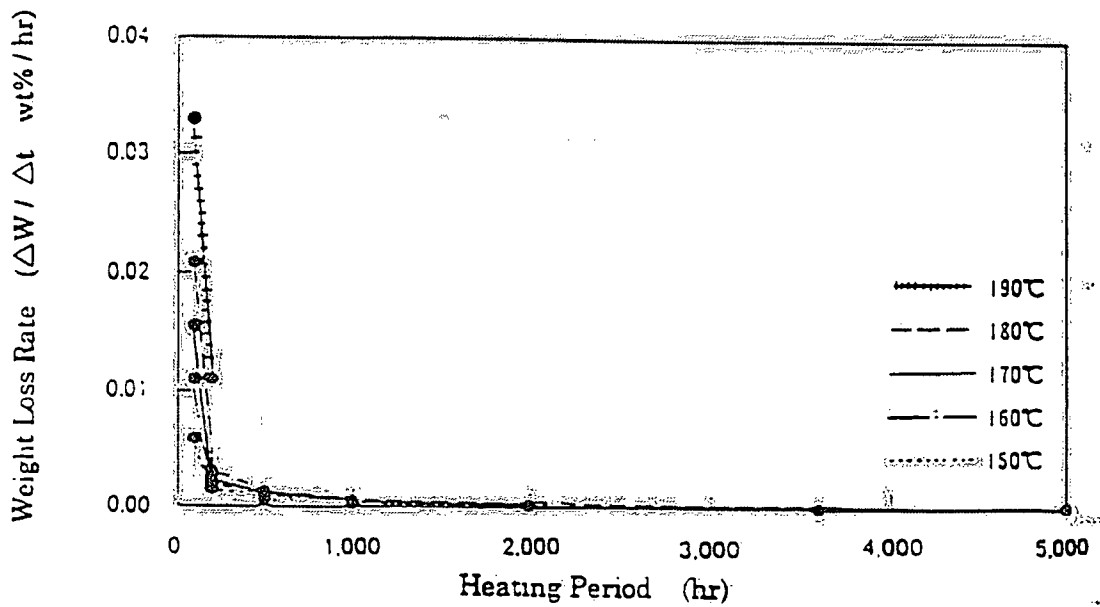


Figure 1-2 Change of Weight Loss Rate

Averaged weight loss rate between t_{n-1} and t_n : $\Delta W / \Delta t = (\Delta W_n - \Delta W_{n-1}) / (t_n - t_{n-1})$

here $\Delta W / \Delta t$ is plotted at the point of time t_n

ΔW : weight loss between t_{n-1} and t_n

Δt : time interval between t_{n-1} and t_n

ΔW_n : weight loss at $t_n = (W - W_n) / W$

ΔW_{n-1} : weight loss at $t_{n-1} = (W - W_{n-1}) / W$

W : sample weight before heating

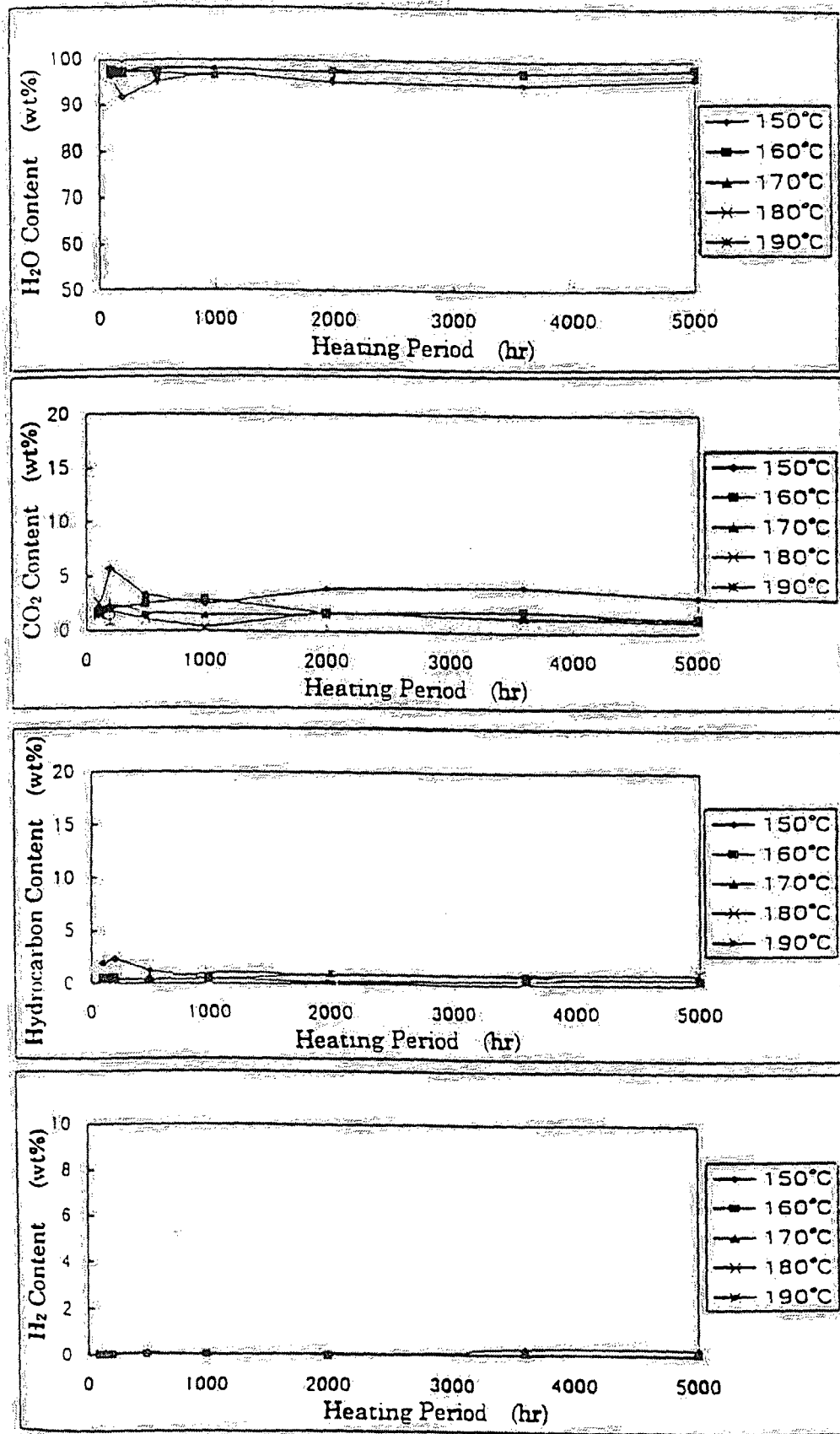


Figure 1-3 Content of Gaseous Compound released by Heating

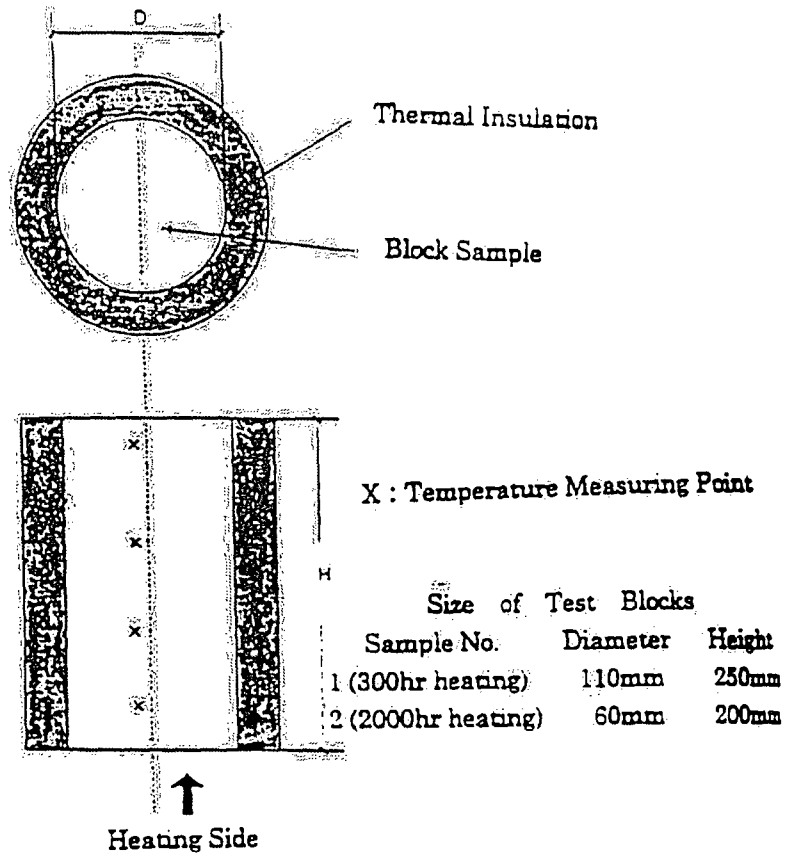


Figure 2-1 Shape and Size of Test Blocks for Block Heating Test.

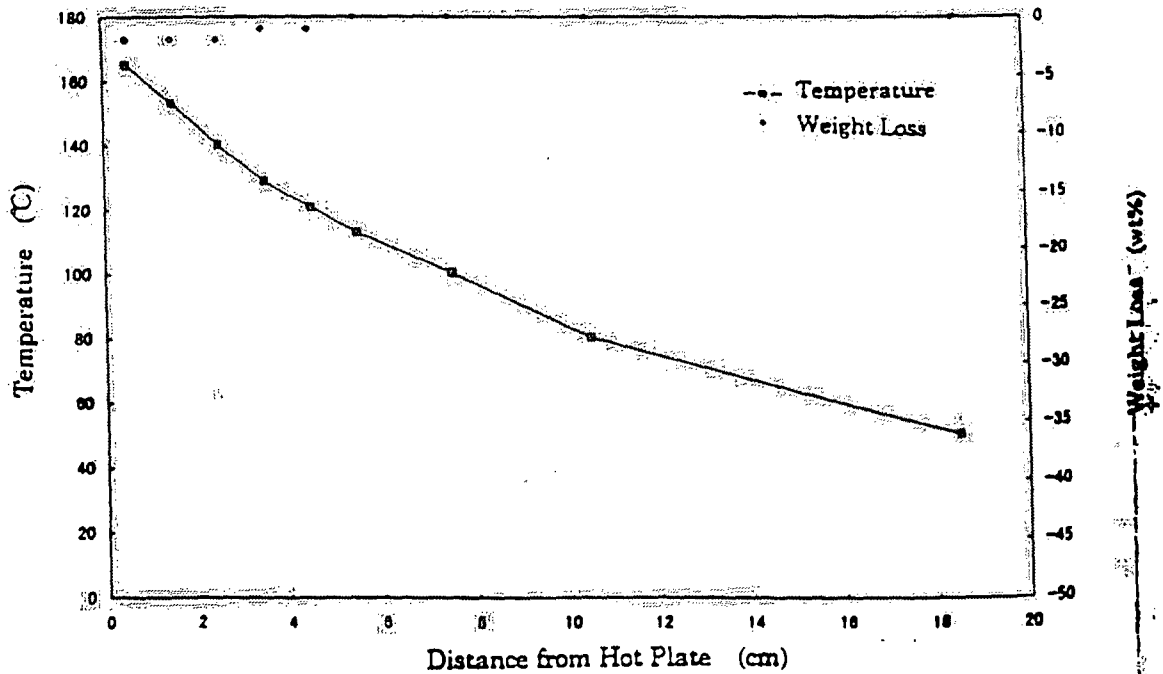


Figure 2-2 Temperature Distribution and Weight Loss of Block Heating Test Sample after 2000hr

NAC Proprietary Calculations in Support of the MAGNATRAN Application

1. Calculation No. 71160-2007, Structural Evaluation of the Neutron Absorber Retainer, Revision 3
2. Calculation No. 71160-2035, Structural Evaluation of PWR Fuel Assembly Spacer for Transportation, Revision 2
3. Calculation No. 71160-2101, Structural and Thermal Material Properties – MAGNASTOR/MAGNATRAN Cask System, Revision 6
4. Calculation No. 71160-2108, Transport Cask Structural Evaluation, Revision 2
5. Calculation No. 71160-2110, MAGNATRAN Transport Cask Lifting Trunnion Structural Analysis, Revision 1
6. Calculation No. 71160-2113, Transport Cask Neutron Shielding Structural Evaluation, Revision 2
7. Calculation No. 71160-2116, Structural Evaluation of MAGNATRAN Canister, Revision 1
8. Calculation No. 71160-2117, PWR Basket Structural Evaluation – Transport, Revision 1
9. Calculation No. 71160-2118, BWR Basket Structural Evaluation – Transport, Revision 1
10. Calculation No. 71160-2119, BWR Basket Stability Evaluation – Transport, Revision 1
11. Calculation No. 71160-2120, Canister Spacer Structural Evaluation – Transport, Revision 1
12. Calculation No. 71160-2126, Fuel Rod Accident Evaluation, Revision 1
13. Calculation No. 71160-2127, PWR DFC Basket Structural Evaluation – Transport, Revision 1
14. Calculation No. 71160-2132, Structural Evaluation of MAGNATRAN TSC3 and TSC4, Revision 1
15. Calculation No. 71160-2138, MAGNATRAN Balsa-Redwood Impact Limiter Free Drop Structural Evaluation, Revision 3
16. Calculation No. 71160-2145, PWR Basket Stability Evaluation – Transport, Revision 5
17. Calculation No. 71160-2155, BWR Fuel Assembly Impact Calculation, Revision 0
18. Calculation No. 71160-3011, Effective Property Calculation of PWR/BWR Fuel Assembly and Poison Plate for Transport Condition of the NAC MAGNATRAN System, Revision 0
19. Calculation No. 71160-3013, Thermal Evaluation of MAGNATRAN Transport Cask/BWR Canister, Revision 0
20. Calculation No. 71160-3014, Thermal Evaluation of NEWGEN Transport Cask/PWR Canister, Revision 2
21. Calculation No. 71160-3015, MAGNATRAN PWR/BWR Cask/Basket Hypothetical Fire Accident Analyses, Revision 1
22. Calculation No. 71160-3045, Evaluation of the Convection Film Coefficient for the MAGNATRAN Cask Surface, Revision 0
23. Calculation No. 630073-2140, Structural Evaluation of MAGNATRAN GTCC TSC, Revision 2
24. MAGNATRAN Shielding Sample Data Files, CD Disk 1 of 1
25. MAGNATRAN Criticality Sample Data Files, CD Disc 1 of 1

Proprietary Calculations withheld per 10 CFR 2.390